The Role of Amino Acids and the Threonine-SAM Pathway in the Development of Bovine Inner Cell Mass and Pluripotency

A thesis submitted in partial fulfilment of the requirements for the degree of

Doctor of Philosophy

in

Biological Sciences

at

The University of Waikato

by

Vahid Najafzadeh

THE UNIVERSITY OF WAIKATO
Te Whare Wānanga o Waikato

March 2018

Abstract

Pluripotent stem cells (PSCs) are the foundation of all cell types in the body including functional gametes. They are derived either from the inner cell mass (ICM) of preimplantation mouse and rat embryos, known as embryonic pluripotent stem cells (ePSCs) or embryonic stem cells (ESCs) or via reprogramming of somatic cells to their pluripotent state, known as induced pluripotent stem cells (iPSCs). PSCs are excellent tools for gene editing and accelerated breeding in livestock animals. So far, germline-competent PSCs have only been isolated in mice and rats. Bovine ESCs are yet to be isolated due to the inadequate understanding of the mechanisms involved in bovine pluripotency. This study aimed to investigate the metabolic aspects of bovine ICM development and pluripotency.

In this study, amino acids were screened via a targeted depletion approach to determine if any amino acid was critical for bovine ICM development and pluripotency. Experiments were conducted on *in vitro* fertilised day (D) 5 preimplantation bovine embryos, individually cultured in chemically-defined, protein- and glutamine-free synthetic oviduct fluid with variations of essential (E) and non-essential (NE) amino acids (AAs) until D8. Depleting (Δ) one (threonine, methionine), two (threonine_methionine, cysteine_methionine, cysteine_threonine, isoleucine_leucine, isoleucine_lysine, leucine_lysine), three (cysteine_methionine_threonine, isoleucine_leucine_lysine) or six (histidine_phenylalanine_arginine_valine_tryptophan_tyrosine) EAAs did not affect ICM formation, even when NEAAs were also removed from Δthreonine and Δmethionine groups. However, depleting another six (cysteine_isoleucine_lysine_leucine_methionine_threonine), nine (+cysteine_methionine_threonine, +isoleucine_leucine_lysine), eleven EAAs (+threonine, +methionine) or all twelve EAAs impaired blastocyst development. *In vitro* fertilised D1 preimplantation mouse embryos cultured from D1-4 were also not affected by a Δthreonine culture condition.

The role of the threonine dehydrogenase (TDH)-mediated threonine-s-adenosylmethionine (SAM) pathway in bovine ICM development and pluripotency in bovine embryos and cells was also investigated. This metabolic pathway has been shown to play a critical role in sustaining mouse pluripotency. TDH expression was probed at mRNA and protein levels, and its activity was knocked down using chemical inhibitors quinazolinecarboxamide (Qc1) and 3-hydroxynorvaline (3-HNV). The effect of TDH inhibition on embryo development, cell numbers, lineage-specific marker gene expression, histone trimethylation and autophagy was studied.

Abstract

TDH was present in trophectoderm (TE), ICM and 6 day old (D6) ICM outgrowths but absent in D6 TE primary cultures. In bovine embryos, Qc1 reduced blastocyst grade 1-3 (B^{1-3}) and B^{1-2} embryo development 1.5- and 2-fold, respectively, compared to the dimethyl sulfoxide (DMSO) controls. Qc1 also reduced ICM and TE cell numbers ~2-fold. This cell loss was due to increased autophagy. Qc1-treated ICM and TE nuclei were explicitly hypermethylated at histone (H)3 lysine (K)4 trimethylation (me3), while H3K9me3 and H3K27me3 were not affected. Hypoblast (PDGRFα), pluripotency-associated epiblast (NANOG, FGF4, and SOX2) and TE (CDX2) markers were not altered in the Qc1 group compared to DMSO controls. Qc1 also severely compromised mouse embryos cultured from day 1-4. In bovine cells, Qc1 compromised fresh ICM, D6 ICM outgrowths and fresh TE cells but failed to impair D6 TE primary cultures. 3-HNV severely compromised bovine embryo development, D1 ICM outgrowths, D6 TE primary cultures and bovine embryonic fibroblast (BEF) cells. However, it unexpectedly severely impaired TDH-free skin fibroblasts in a Δthreonine culture condition.

The results indicate that the effect of amino acid starvation on embryos is different from that on individual cells. The findings also suggest that TDH is vital for bovine embryonic development via regulating H3K4me3 levels. Moreover, the results denote that TDH becomes restricted to cultured ICM cells and disappears from TE primary cultures. This may indicate that TDH is essential for maintaining bovine pluripotency. 3-HNV was claimed to be a specific TDH enzyme inhibitor; However, this study showed that it compromises TDH-free cells in a Δthreonine culture condition, suggesting that it does not specifically impair cells and embryos via the TDH-mediated threonine-SAM pathway.

Acknowledgements

Dr Ryan Martinus, I sincerely and humbly thank you for your immense support and help, especially over the past year whenever I was hopeless and frustrated you were always there for me helping me out through those difficult times. Finishing this tough journey would not have been possible without you. It was a great honour for me to be your student.

I would also like to thank **Dr Björn Oback** for all the support he has given me over these past five years. Especially over the last year helping me the thesis and giving me his critical comments. Your mannerism, calmness, passion for doing a good and factual science, openness to criticism, and believing in the capabilities of your students should be exemplary to any junior scientist stepping in this path. Thanks for EVERYTHING!

I would also like to say a sincere "thank you" to **Pavla Turner**, **Andria Green**, **Fleur Oback**, **Jan Oliver**, **and Lindsay McGowan** for mentoring and helping me with my experiments. Thanks for your infinite wisdom and patience.

A special thanks to **Dr Jing Wei Wei** for his incredibly enormous help and support with producing mouse embryos and other lab works. You are awesome!

Dr Stephan Wanger, I am grateful to you for mentoring me with the transfection experiments. Thanks for your patience and optimism. You are also a great football teammate as well!

Zach Mclean, you were a great help when I first started my work in the lab. You are a real scientific role model with a brilliant mind. Thank you for mentoring and helping me when in need. I wish you all the very best with your PhD journey.

I would also like to thank **Dr Sara Edwards** for her immense support and her scientific comments on my thesis. It is sincerely appreciated.

I would also like to express my gratitude to the University of Waikato and AgResearch Limited for providing me with this fantastic opportunity to build and improve my scientific and academic capacity.

Finally, a special thanks to my lovely family, **my mother**, **my father**, my sisters, **Vajiheh and Vida**, and my brother **Amir**. Thank you for your never-ending and unconditional love and support.

Table of Contents

List of Figures

List of Tables

List of Equations

List of Abbreviations

G

H

I

J

K

L

M

N

P

Q

R

S

T

U

W

List of Publications and Conference Contributions

I. **Vahid Najafzadeh**, Ryan Martinus, Björn Oback. The role of amino acid metabolism in bovine inner cell mass development and pluripotency. (Manuscript in preparation).

II. **Vahid Najafzadeh**, Ryan Martinus, Björn Oback. The role of threonine dehydrogenase in bovine ICM development and pluripotency. (Manuscript in preparation).

III. **Vahid Najafzadeh**, Ryan Martinus, Björn Oback. The role of amino acid metabolism in bovine inner cell mass development and pluripotency. (Poster presentation at 33rd Annual Meeting of ESHRE Conference, Geneva, Switzerland, July 2017.)

IV. **Vahid Najafzadeh**, Ryan Martinus, Björn Oback. The role of amino acid metabolism in bovine inner cell mass development and pluripotency. (Oral Presentation at Biology Conference, Waikato University, October 2016.)

V. **Vahid Najafzadeh**, Ryan Martinus, Björn Oback. Targeted screen for amino acids that regulate bovine inner cell mass development. (42nd IETS Annual Conference, Kentucky, USA, January 2016)

Chapter 1

1. Chapter One: Literature review

1.1. Introduction

The discovery of mouse (m) embryonic (e) pluripotent stem cells (PSCs) or embryonic stem cells (ESCs) in 1981 revolutionized biological and medical fields [1; 2]. PSCs have changed our understanding of mammalian gene function and are molecularly and functionally regarded as one of the best-defined cell types [3]. Bona fide ePSCs have been isolated only from mice [4] and rats [5]. Despite three decades of endeavour, livestock ePSCs have not yet been isolated. Livestock PSCs have several potential applications and benefits to agricultural industries. These cells are relatively highly efficient tools for genetic manipulation [6], enabling the production of more productive livestock, improving their reproducibility and health and making them more environment-friendly [7]. Genomically engineered livestock PSCs also have applications in biopharming, using cattle as bioreactor through which large-scale biopharmaceutical proteins are produced [3]. Moreover, they could also be used for generating large animal models for studying human disease [3].

The aim of studying bovine inner cell mass (ICM) development and PSC-like cells was to: i) probe the role of amino acid metabolism in bovine ICM development and pluripotency via targeted amino acid (AA) screening and ii) investigate the role of the TDH-mediated threonine (Thr)-S-adenosylmethionine (SAM) chemical pathway in these cells. The essential amino acid (EAA) threonine has been shown to play a vital role in maintaining mouse pluripotency, without which the mouse ePSCs stopped proliferating and did not form colonies [8]. Methionine (M) likewise sustained human pluripotency, and in its absence, undifferentiated cells underwent apoptosis [9]. Studies have also shown that mouse ePSCs rely on the TDH-mediated Thr-SAM pathway [8; 10]. Blocking this pathway via threonine depletion from the media or pharmacological inhibition lead to mouse ePS cell death [10; 11]. It is hoped that the findings of this study will help us further our understanding of bovine ICM development and regulation. Uncovering mechanisms regulating bovine pluripotency will eventually lead us to culture bovine ePSCs in vitro.

The literature review chapter will discuss the biology of PSCs and their characteristics. A history of how PSCs were discovered, and the process leading to the definition of a fully-defined culture medium for bona fide PSCs. Amino acid requirements of PSCs and the role of the threonine-SAM metabolic pathway in mouse pluripotency will also be discussed in a separate section. Progress so far made in other species, in particular cattle, with regard to their pluripotency state will also be covered.

1.2. Biology of pluripotent stem cells

1.2.1. Defining pluripotent stem cells

1.2.1.1. Pluripotency

The term 'pluripotent stem cell' refers to the ability of a cell to differentiate into all the body cell types (including functional gametes) and proliferate *in vitro* indefinitely [12] (Figure 1). PSCs originate from two sources: one, by culturing ICM cells of embryos produced via parthenogenetic activation (PG), natural mating, nuclear transfer (NT), or *in vitro* fertilization (IVF). These cells are known as embryonic PSCs or embryonic stem cells. In the mouse, oocyte fertilization leads to the formation of a single cell termed the zygote. This zygote has the capacity to form an entire animal plus all the supportive extraembryonic tissues; Hence, it is described as totipotent [13]. The zygote goes through the first cleavage after 28-30 hours (h), splitting in half to make a 2-cell embryo [14]. This is the start of a series of cell divisions in which each cell divides in half while the embryo size remains the same as the original oocyte. Each of these cells now is called a blastomere. This phenomenon happens as the embryo makes its way through the oviduct to the uterus. The embryo then transforms from the 8-cell stage into the morula, which is a tight ball of cells. By increasing the morula cell number, cell polarity and accompanying signalling events, the first wave of lineage segregation separates blastomeres into an outer trophectoderm (TE) and inner ICM, thus indicating the end of totipotency (Figure 1 & Figure 2) [15]. This leads to the formation of a cavity (known as the blastocoel) by secretion of fluid into the morula. The second lineage deviation commences during the blastocyst stage where the ICM cells segregate into an apical cell layer with underlying cells, becoming the hypoblast and epiblast, respectively (Figure 1 & Figure 2) [16].

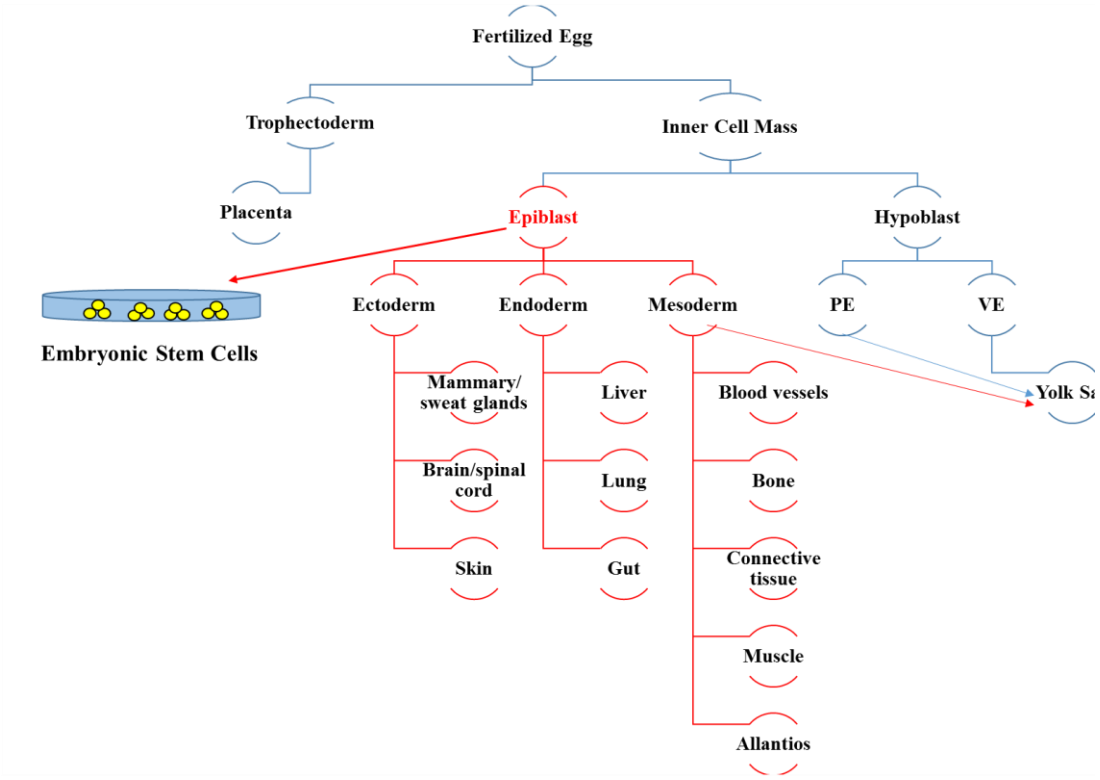

Figure 1. Pluripotency in mouse ePSCs
Mouse ePSCs are derived from 3.5 day-old blastocysts. They give rise to all cells in an adult body, including functional gametes.

These three distinct cell types have different functional and molecular characteristics. The trophectoderm forms the outer layer of the embryo with tight junctions [17]. Further along the implantation process, it will attach to the uterus and undergo differentiation into giant cells to become part of the placenta, serving as a connection between the mother and the embryo. This provides nutrients and other on-demand signals for proper embryo growth during gestation. These cells are molecularly characterized by expression of caudal type homeobox 2 (CDX2) and keratin 8 (KRT8). The hypoblast consists of an apical layer of cells between the epiblast and blastocoel, expressing molecular markers including GATA binding protein 4 (GATA4) and GATA binding protein 6 (GATA6). This will later form the yolk sac. The epiblast consists of a cell population that will eventually form the entire animal. All cells in the body, including gametes, derive from this part of the embryo. These cells are one source of PSCs (Figure 1 & Figure 2).

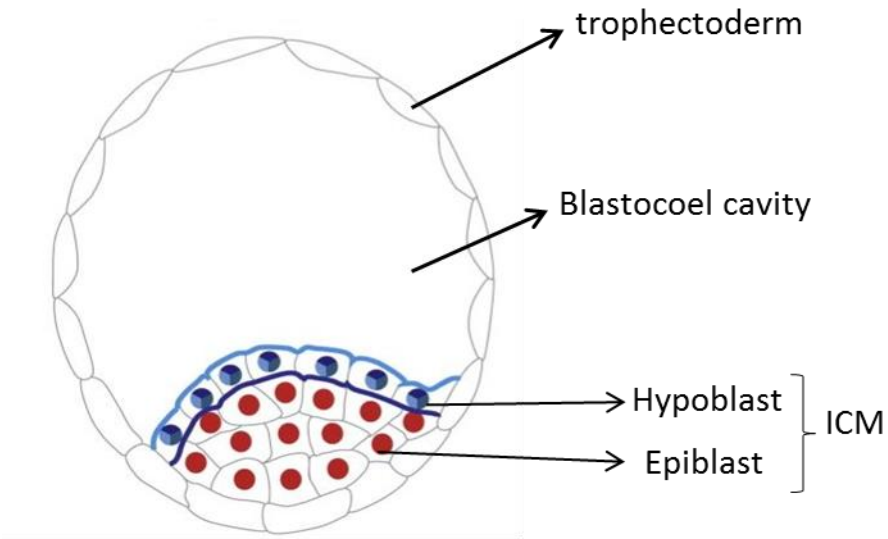

Figure 2. A mammalian blastocyst
Three cell lineages have formed after the second wave of lineage segregation: the trophectoderm, hypoblast and epiblast. (Adapted from Artus J *et al.* 2011.)

Development of the bovine embryo proceeds in the same chronological order as a mouse, but over an extended time. The gestation period in the mouse is only 20 days (D) and therefore once the blastocyst comes out of its zona pellucida shell, the hatched embryos start attaching to the uterine wall through trophoblast invasion [16]. However, the hatched ungulate (including bovine) blastocyst does not attach to the uterus and initiates a fast trophoblast development and elongation, from sphere to filamentous phase, which consequently transitions the blastocyst morphology prior to implantation. In the cow, this elongation starts about gestational day 12 and the ovoid to filamentous transition phase is complete around day 18 of gestation [18; 19]. This lengthening and expansion allow for more placental surface resulting in maternal-conceptus cross-talk and nutrient exchange [20]. Elongation happens at the same period with gastrulation [18; 21; 22], which is another crucial difference between the mouse and bovine [23]. Implantation is permitted only after gastrulation is complete, occurring around days 18-20 [24]. This extra phase of development before implantation existing in the cattle species may explain why bovine ePSCs have not yet been isolated [25].

Another alternative way of producing PSCs is through reprogramming technology, by introducing the expression of four classical genes (Yamanaka factors), namely POU class 5 homeobox 1 (Oct4), SRY-box 2 (Sox2), Kruppel-like factor 4 (Klf4), and c-MYC proto-oncogene (c-Myc), encoding pluripotency-associated transcription factors

into a terminally-differentiated cell and resetting it to its pluripotent state, which then is called induced pluripotent stem cell (iPSC) [26]. Once induced, they fulfil all the criteria of pluripotency: the ability to differentiate to all body cell types including gametes, self-renewal, molecular characteristics and chimera contribution [27]. Other than in mice, iPSCs have also been successfully generated in humans [28-30], rat [31] and rhesus monkeys [32] using Yamanaka factors.

1.2.1.2. Self-renewal

While maintaining their undifferentiated state, PSCs multiply their number *in vitro* indefinitely and in a symmetrical manner [33]. The dividing speed in some PSC types is too short, at only 5 h [8]. This is due to having no G1 or G2 checkpoints and spending most of their time in S phase, replicating their deoxyribonucleic acid (DNA) [8]. Theoretically, ePSCs are considered immortal, however, when cultured for a long time, random genetic mutations occur within them [34]. They measure less than 10 µM in diameter, while somatic cells measure between 10-30 µM [35]. These relatively small ePSCs also possess very little cytoplasm as most of the volume is occupied by the nucleus. Mouse ePSCs form tight, dome-shaped colonies [36].

1.2.1.3. Molecular characteristics of PSCs

PSCs are distinguishable by specific molecular markers. NANOG, SOX2 and OCT4 are the main transcriptional factors in the pluripotency regulatory network and, in combination, define pluripotency. OCT4 is a POU domain transcription factor expressed in epiblast and hypoblast cells [37] and is vital for the development of ICM [38] as well as for the self-renewal of PSC [39]. OCT4 functions as a heterodimer with SOX2, thus placing SOX2 among the core regulators [40]. SOX2, a member of the SOXB1 transcription factor family, is an important transcription factor in pluripotent stem cells. NANOG is a transcription factor indispensably involved in self-renewal and maintenance of PSCs [41; 42]. NANOG is crucial for ICM development and predominantly co-localizes with OCT4 and SOX2 in mouse and human PSCs. Other pluripotency transcription factors include KLF4, KLF2, estrogen-related receptor beta (ESRRB), transcription factor CP2 like 1 (TFCP2L1), TBX3 and gastrulation brain homeobox 2 (GBX2) [43]. In bovine however, *OCT4* is expressed in both the hypoblast and trophectoderm until it becomes restricted to the epiblast after hatching [24; 44]. The first expression of *NANOG* is initiated in a subset of ICM cells, which subsequently

becomes exclusive to epiblast with the hypoblast marker GATA6 in day 8 blastocysts [45]. Likewise, ICM and epiblast increasingly express SOX2 [46]. Other epiblast markers, including developmental pluripotency-associated protein 3 (DPPA3) and KLF4, have not been studied in bovine in depth; however, their expression levels between porcine ICM and epiblast show discrepancies [47].

1.2.1.4. Chimera contribution

In science, a single organism composed of cells from different embryos is called a chimera [48]. This was first devised by Richard Gardner and Ralph Brinster [49]. By combining chimera and ePSC technology, making a whole animal from a single cell has become possible. This means that ePSCs contribute to all tissue types in the animal, including the transmitting germline [50]. Germline contribution is the most definitive proof of pluripotency. If a PSC gene is manipulated and that cell contributes to a chimeric animal, all the cells in the body, including germline cells, carry the same genetic modification made in the original cell. This technology allows scientists to investigate biological functions of a gene of interest.

When ICM cells of a diploid blastocyst are used to make the chimera through morula or blastocyst injection or aggregation with eight-cell diploid embryos, they contribute only to the epiblast and primitive endoderm and not to the extraembryonic tissues due to more restricted lineage potency of ICM cells [51]. PSCs likewise behave more like epiblast cells; they contribute only to germ layers that give rise to all embryonic tissues and some extraembryonic tissues, including the amnion, the mesoderm of the yolk sac, the allantois and the embryo-derived blood vessels in the placenta [52]. Tetraploid complementation is the most stringent assay for proving pluripotency through making chimeras. In this technique, tetraploid embryos, which are 4n in their DNA content, are made, then 2n ePSCs are injected into the embryo [53]. Even though tetraploid blastocysts can be made, postimplantation survival is poor because of the lack of epiblast cells and embryos fail to survive beyond mid-gestation [54]. When using tetraploid embryos in conjunction with PSCs, tetraploid cells rarely contribute to the ICM, through which the embryo itself forms; however, they mostly contribute to the primitive endoderm and trophectoderm [55]. Therefore, the resultant embryo will comprise the PSC-derived conceptus and extraembryonic mesoderm while the

trophectoderm and primitive endoderm are derivatives of the tetraploid host embryo [53].

1.2.2. Derivation of first mouse embryonic pluripotent stem cell line

The discovery of the first mouse ePSCs was sparked by the study of mouse embryonic carcinoma (EC) cells derived from germ cell tumours. In the mid-1960s Kleinsmith and colleagues observed that EC cells were able to both renew indefinitely and differentiate into other tissue types [56]. Despite having similar morphology and potency to ePSCs in early discovery, EC cells carry genetic aberrations and abnormal karyotypes that make them inappropriate for producing chimeric mice [57]. Interestingly, when used to generate chimeric mice, their contribution was very limited and did not give rise to many cell types [58]. The first derivation of ePSCs was made from ICM of preimplantation mouse embryos (the 129/Sv strain) by two independent groups [1; 2] where they grew ePSCs in a culture system having mitotically inactivated mouse embryonic fibroblast (MEF) cells as well as serum. These cells could differentiate *in vitro* into a variety of cell types. Moreover, upon injection into the mouse blastocysts, they produced cell types in all three germ layers.

It has been shown that mouse strains differed in their efficiency when producing ePSCs. The 129/Sv mouse strain used in the first studies is the one that most ePSC lines are derived from. Mouse strains such as BALB/c, BXSB/MpJ-Yaa and MRL/Mp-lpr/lpr did not yield any PSC lines in the first standard culture medium [59] and ePSCs derived from C57BL/6 needed a modified culture regime [60].

1.2.3. Paths to reaching a fully defined medium

1.2.3.1. Feeder replacement

Primary derivation of ePSCs from preimplantation mouse embryos was dependant on both feeder cells and serum to prevent differentiation. In the late 1980s, two independent groups identified a cytokine which could substitute for feeder cells [61; 62]. This cytokine known as leukaemia inhibitory factor (LIF) was a significant breakthrough since when mouse ePSCs were cultured in a feeder-free medium containing LIF plus serum, they could propagate and form pure and homogeneous colonies that contributed to germline-competent chimeric mice [63]. Efforts aimed at finding the signalling pathway associated with cytokine LIF led to the discovery of the Janus kinase (JAK)/ Signal Transducer and Activator of Transcription (STAT) pathway

[64]. This pathway has three main components: a cell surface receptor (gp130 receptor), a Janus kinase, and a Signal Transducer and Activator of Transcription protein. LIF binding activates the receptor-associated JAK, and then recruits and phosphorylates STAT3 transcription factors, which dimerize and translocate to the nucleus, leading to transcriptional activation of pluripotency-associated genes. Some other JAK/STAT3-promoting cytokines such as interleukin-6 (IL6) have also been discovered which can retain pluripotency and proliferation *in vitro* [65]. Despite the identification of LIF, culture remained reliant on the use of serum for mouse ESC maintenance.

1.2.3.2. Serum replacement

It has been demonstrated that LIF the cytokine in addition to serum, could retain mouse ePSCs in a state of pluripotency [61; 62]. However, after removal of serum only, ePSCs began to differentiate into neural precursors. This raised the question of what could substitute for the serum to sustain mouse pluripotency in conjunction with cytokine LIF. Previously it had been discovered that neural differentiation was initiated by fibroblast growth factor (FGF) functioning through the extracellular signal-regulated kinases (ERK) pathway [66]. On the other hand, bone morphogenetic proteins (BMPs), members of the Transforming growth factor (TGF)-β superfamily, were shown to have anti-neural effects [67]. Therefore, it was hypothesized that if the ERK pathway was blocked, it could sustain pluripotency. This was shown to be the case and BMPs in conjunction with LIF cytokine maintained pluripotency, with no need for serum [68]. However, applying BMP alone drove mouse ePSCs towards epithelial cell commitment [69]. Regarding the mechanism, BMP acts through the SMAD-Id pathway by activating Id genes which promote expression of pluripotency-associated transcription factors [68].

1.2.3.3. Maintaining pluripotency through inhibition of differentiating signalling pathways

While LIF and BMP were sufficient for sustaining mouse pluripotency, not all mouse ePSC lines were able to propagate and maintain their pluripotency in this fully defined medium. Knowing that FGF helps neural differentiation through the mitogen-activated protein kinases (MAPK)/ extracellular signal-regulated kinases (ERK) pathway, a study showed that by using small inhibitory molecules targeting FGF receptor tyrosine kinase and subsequently the downstream ERK pathway, they could successfully propagate

ePSC colonies. However, there was still a high rate of cell death and slow growth [69]. Complementing the culture medium with another small molecule inhibiting glycogen synthase kinase 3 (GSK3) [70], downstream of the Wnt pathway, however, supported growth and proliferation of mouse germline-competent ePSCs in the absence of LIF and BMP [69]. This culture, known as "2i" regime, even allowed the expansion and growth of germline-competent ePSCs from all mouse strains tested to date [69; 71-73]. This suggested that ePSCs have an innate programme for self-renewal so that they do not require exogenous stimuli, which may be the reason for their latent tumorigenicity [69].

1.2.4. Naïve vs. primed pluripotent state

While mouse ePSCs rely on inhibition of ERK-Gsk3 pathways to maintain their pluripotency state, human ePSCs are dependent on FGF2/activin A (or TGFβ1) as core governors of pluripotency signalling networks [74]. This discrepancy arises from the fundamental differences between two different pluripotency states: naïve and primed. The term naïve refers to the state that ePSCs are in when captured from preimplantation mouse blastocysts (days 3.5-4.5 in the mouse). When maintained in serum/LIF (or LIF/BMP, or 2i/LIF) culture conditions, these ePSCs express naïve markers such as KLF5, TFCP2L1, and DPPA3, hold high clonogenicity, have both X chromosomes active in the female cell lines, and can contribute to germline-competent chimeras [69; 75]. In contrast, primed ePSCs, which are captured right after implantation (days 4.5-5.75 in the mouse) when the epiblast transforms into a cup-shaped epithelium [76], are not dependent on the LIF/Stat3 pathway, and instead, rely on FGF2/activin A (or TGFβ1) pathway. They do not express the aforementioned naïve markers, have one X chromosome inactivated, and cannot contribute to germline-competent chimeras [77; 78]. So far, human ePSCs and post-implantation mouse epiblast PSCs (epiPSCs) have proven to be in the primed state, and pre-implantation mouse PSCs hold a naïve state [76].

1.3. Metabolic requirements of pluripotency

Metabolism is the sum of all the chemical reactions occurring in a cell (including both catabolic and anabolic processes). These chemical reactions make it possible for cells to grow, reproduce, and respond to their environment in a sustainable manner [79]. Every cell type has its own metabolic signature by which the cell is identified, and PSCs

are no exception to this. Their population doubling feature and unique pluripotency state require them to hold a metabolic profile exclusive to them.

Wang and colleagues in 2009 mapped a different route to pluripotency through a chemical pathway which involved EAA threonine being catabolised by threonine dehydrogenase (TDH) [8]. This pathway is called one-carbon metabolism or threonine-SAM pathway and is crucial for mouse ESCs to sustain their pluripotency state. It begins with TDH enzyme converting threonine into acetyl-CoA and glycine. Acetyl-CoA is utilised in the tricarboxylic acid (TCA) cycle, whereas glycine joins the folate cycle contributing to SAM production. SAM provides methyl groups for trimethylation of histone proteins in mouse ePSCs [10]. Using mass spectrometry, Wang and colleagues observed relative changes in threonine and acetyl-CoA levels in opposite directions upon ePSC differentiation. Thr levels trended upwards upon differentiation, whereas acetyl-CoA declined. This finding raised the possibility of TDH being involved in mouse pluripotency [8].

In the mitochondria of mouse PSCs, TDH and glycine C-acetyltransferase (Gcat), also called 2-amino-3-ketobutyrate-CoA ligase, form a stable complex in which TDH produces transient 2-amino-3-ketobutyrate through NAD^+-dependent oxidation of Thr. TDH channels this molecule to the Gcat enzyme wherein it is catabolized into glycine and acetyl-CoA [80] (Figure 3 & Figure 4). The gcat expression is universal and is found in all cell types.

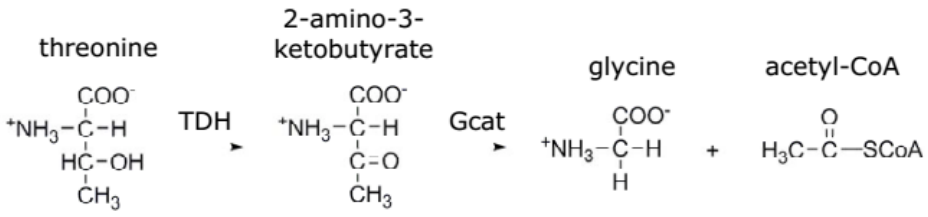

Figure 3. Threonine is catabolised into glycine and acetyl-CoA via threonine dehydrogenase (TDH).
In mitochondria, TDH catabolises threonine into transient 2-amino-3-ketobutyrate. Gcat, which is universally expressed in mice, pairs with TDH which leads to the production of glycine and acetyl-CoA from threonine (Dale 1978, Srere 1987).

Using quantitative polymerase chain reaction (qPCR), the messenger ribonucleic acid (mRNA) levels of 15 enzymes were measured, including TDH which is actively involved in the one-carbon metabolism pathway in ES cells and other mouse adult tissues including brain, liver, lung, heart, kidney, intestine, testis. This revealed that TDH mRNA level in ES cells was roughly 1000 times higher than any of the other 7 tissues [8]. Co-localisation of the TDH signal (by immunofluorescence assay) with mitochondrial staining also further confirmed its existence in the mitochondria of mouse ePSCs and its loss upon differentiation. Additionally, Western blot results showed the disappearance of TDH protein once mouse ePSCs started differentiating [8].

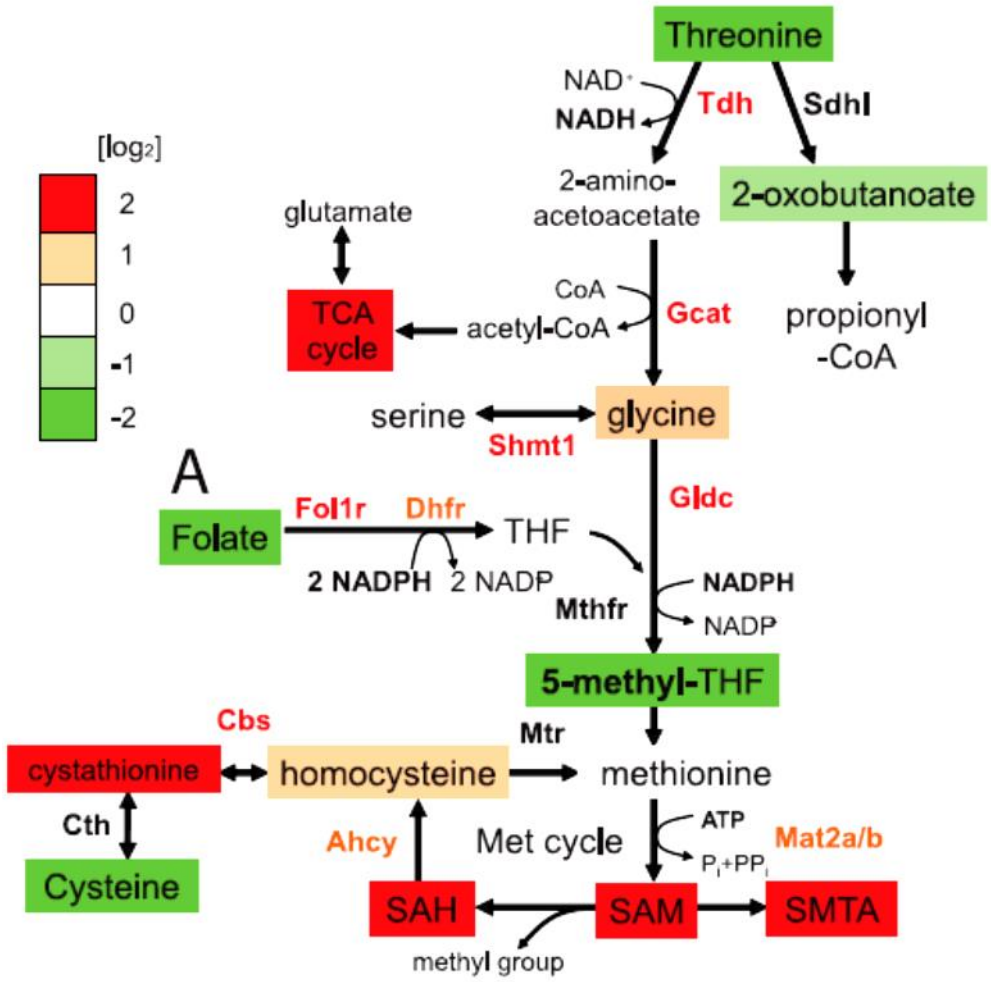

Figure 4. Schematic of threonine fate in mitochondria of mouse ePSCs.
Threonine is converted into 2-amino-acetoacetate by TDH. This intermediate product is then broken down into glycine and acetyl-CoA. (adapted from Shyh-Chang N *et al.* 2013)

To practically investigate Thr metabolism role in the mouse ePSC state, Wang and colleagues next explored individual AA dropout for all 20 AAs wherein each culture medium one AA was absent. All the mouse ePSCs were growing as normal in their single AA-free culture medium after 36 h except for the Thr-free one in which they stopped proliferating and forming colonies (Figure 2-8). Single AA deprivation conducted on MEF cells and the mouse NIH 3T3 cell line did not show any sensitivity to Thr [8].

Assuming Thr metabolism was involved in pluripotency through its catabolism into glycine and acetyl-CoA, further experiments supplemented Thr-free culture medium

with increased concentration of glycine. Glycine generated in the mitochondria via the one-carbon metabolism pathway is used to charge tetrahydrofolate (THF), a key intermediate of the one-carbon metabolism pathway necessary for producing methionine, via glycine cleavage system [81]. Glycine supplementation in the absence of Thr, however, did not support ESC pluripotency any better than Thr-free culture medium. This led to speculation that external glycine cannot be delivered to the mitochondria of ePSCs. Furthermore, it was hypothesized that acetyl-CoA might be as crucial as glycine as it declines in abundance upon ePSC differentiation. To test this assumption, a synthetic variant of threonine containing an extra carbon atom called 3-hydroxynorvaline (3-HNV) was used as a substitute for Thr. Once channelled through TDH, 3-HNV is catabolized into glycine and propionyl-CoA. 3-HNV not only failed to compensate for the absence of Thr but instead, it compromised ePSC colony formation even in the presence of Thr. No inhibitory effect of 3-HNV on HeLa, MEF and 3T3 cells was observed either, consistent with the interpretation that TDH-catabolized glycine and acetyl-CoA production is critical for mouse ePSC survival [8].

In situ hybridization and immunofluorescence staining techniques showed that TDH protein and mRNA, respectively, were exclusively expressed in the ICM of four-day-old mouse embryos. Thus, given that ICM is an *in vivo* representative of ePSCs in culture, it was suggested that 3-HNV would inhibit mouse embryo development. Indeed, 300 µM 3-HNV administration to mouse morula impaired embryo development. However, the mouse embryos proceeded with normal development when 4 mM threonine was administered along with as much as 1 mM 3-HNV, concluding that ICM cells are also dependent on TDH-mediated Thr catabolism for their survival [8].

The same group in 2011 revealed another inhibitor of TDH enzyme [11]. After unbiased chemical screening of around 200,000 drugs, they discovered a class of quinazolinecarboxamide (Qc) compounds that affected TDH enzyme activity. Six chemicals from the Qc family emerged from the chemical screening and were chosen for further investigation. Qc1 proved to be highly efficient (IC_{50}=0.5 µM) at blocking TDH enzyme activity as well as impeding mouse ePSCs. While 50 µM Qc1 impaired mouse ePSC colony formation and more prolonged exposure led to cell death, differentiating embryoid bodies (aggregations of differentiating pluripotent stem cells) looked normal in growth and morphology even at 90 µM Qc1 administration after 24

h. The process leading to cell death, however, was not apoptosis but autophagy. Autophagy (self-eating) is the process by which bulk cytoplasmic proteins and organelles become encapsulated in lysosomes for degradation [82]. This process is vital when cells undergo starvation, thus by doing so, they can scavenge the nutrients needed for sustaining more vital processes [11; 82].

Another study in 2013 investigated Thr downstream metabolites and the pathway through which Thr exerts its effect using [U-^{14}C]Thr in mouse ePSCs with high-performance liquid chromatography (HPLC). The fate of Thr was monitored and showed, again, threonine breakdown into glycine and acetyl-CoA [10]. [U-^{13}C]Thr provided ~20% of the citrate through acetyl-CoA, while the amount of citrate from [U-^{13}C] glucose was ~35%. [U-^{13}C]Thr-derived glycine, on the other hand, donated its ^{13}C-methyl group for making 5-methyltetrahydrofolate (5mTHF) and its end product SAM. In contrast, MEFs incubated with [U-^{14}C] Thr did not show any dependence on Thr catabolism [10]. SAM is a universal methyl donor that by donating methyl groups, it is converted to S-adenosylhomocysteine (SAH) via the methyltransferase enzyme [83]. In cells, the SAM/SAH ratio plays a crucial role in regulating protein methylation, where increased SAH has an inhibitory effect on methyltransferases [84] (Fig. 3). Thr-dependent changes in the SAM/SAH ratio correlated with global trimethylation (me3) of histone (H) 3 lysine (K) 4. Thr restriction resulted in reduced H3K4me3, thus revealing a possible mechanistic link between cellular metabolism and the epigenetic state. Epigenetic plasticity depends on the euchromatin state of the ePSCs. Knowing that global H3K4me3 and H3 acetylation (ac) is vital for sustaining that state [85-88], using western blotting, the hypothesis of H3K4me3 and H3ac dependence on Thr catabolism in mouse ePSCs was tested. It was found that Thr restriction caused decreased H3K4me3 level after 48 h, whereas H3ac did not show any change. In contrast, MEFs did not experience either H3K4me3 or H3ac fluctuation upon Thr restriction [10]. Next, methylations of H3 K (4, 9, 27, 36, and 79) upon depriving mouse ePSCs of a variety of individual candidate AAs (Thr, glycine (Gly), Met, serine (Ser), leucine (Leu)) were conducted [10]. Upon its restriction, Thr was the only AA that negatively affected only H3K4me3 and H3K4me2, and not the other ones. Using qPCR, it was shown that upon Thr restriction on mouse ePSC and subsequent TDH ablation, there was a decrease in gene expression of pluripotency markers, *Oct4*, *Sox2*, *Nanog*,

Rex1, and PR/SET domain 1 (*Blimp1*), while differentiation factors, including forkhead box A2 (*Foxa2*) and SRY-box 17 (*Sox17*), increased [10].

Since *TDH* is a pseudogene in human and produces a truncated protein, which is non-functional (Figure 14), another study speculated that human ePSCs should rely on another amino acid than threonine. Human ePSCs seeded in culture media for 48 h each missing one amino acid identified that omission of methionine from the culture medium had the most effect on human ePSC survival [9]. Tryptophan, lysine, and leucine omission similarly decreased human ePSC survival. However, only methionine metabolism was investigated further. Met deprivation led to decreased SAM level, reduced H3K4me3 and NANOG expression levels, accompanied by differentiation of human ePSCs/iPSCs. Unlike mouse ePSCs, long-term Met deprivation of human ePSCs resulted in the activation of p53-p38 signalling pathway and consequently cell death [9].

Overall, these findings suggest a link between cellular metabolism and the epigenetic state in the mouse and human species, which begins from Thr and Met catabolism, respectively, and ends with regulating SAM levels for adjusting the H3K4me3 level.

1.4. Pluripotent stem cells in other species

1.4.1. Rat

With the first fully defined culture medium, LIF/BMP, ePSCs were only permissive in the mouse species. Finally, dual inhibition (2i) regime made it possible to crack the lock of pluripotency in the rat as well. Rat ePSCs express pluripotency markers, retain the capacity to differentiate into derivatives of all three germ layers, and most importantly, they can pass their genetic content onto their descendants through germline contribution [5; 89]. Establishment of germline-competent rat ePSCs makes genetic modification possible to produce models for the study of human diseases [89]

1.4.2. Human

The first *in vitro* cultured human ePSCs were derived from preimplantation human embryos in 1998 [90]. However, these cells have different characteristics and media requirements in comparison to their mouse counterpart, thus are considered primed ePSCs [78]. Based on this definition, these cells are dependent on FGF2/activin A (or TGFβ1) culture conditions, and not the LIF/Stat3 pathway, do not express naïve markers such as KLF5, TFCP2L1, DPPA3, have one active X chromosome in female

cell lines, and are not able to contribute to germline-competent chimeras. However, the last criterion has not been tested due to ethical issues involving the use of human embryos.

The first human naïve ePSCs were claimed to have been captured in 2013 [91]. Using culture conditions that necessitate complete elimination of MAPK/ERK signalling pathway, these naïve ePS cell lines can be derived from human preimplantation embryos, de novo iPS cell lines, or from pre-existing primed ePSCs/iPSCs. The culture conditions include 2i/LIF together with P38i, JNKi, aPKCi, ROCKi, low doses of FGF2 and TGFβ1 (or Activin A). The authors claimed this condition renders human ePSCs more similar, but not identical, to murine naïve PSC. Since chimeric analysis using human embryos is ethically and legally not allowed, these human naïve ePSCs were microinjected into mouse morulae and contributed to the embryos with low efficiency up to day 17.5 [91]. The following year another group revealed two different culture conditions depending on the state of human ePSCs [92]. The recipe for pre-existing primed human ePSC lines was pre-culturing with butyrate and suberoylanilide hydroxamic acid (histone deacetylase inhibitors), followed by culture in MAPK/ERK and GSK3 inhibitors (2i) with FGF2. For direct derivation of human ePSCs from human embryos, the culture comprised the 2i regime with the addition of FGF2. It was claimed that human naïve ePSCs resemble their naïve counterparts in mouse regarding growth characteristics, pluripotency gene expression profile, X-inactivation profile, mitochondrial morphology, miRNA profile, and development in the context of teratomas. Nonetheless, the robustness of naïve human ePSCs was shown in the context of differentiation to all three germ layers with underscoring robust endoderm derivation which had not been seen in primed human ePSCs previously [92]. However, these cells do not resemble *in vivo* epiblast cells at the methylome level [93].

1.4.3. Cattle

Since ePSCs can replicate indefinitely and form all three germ layer cells as well as functional gametes, they are considered a valuable tool for genetic selection and modification. It becomes even more imperative in livestock especially cows as commercial animals which deliver invaluable nutrients and profits to human beings including biopharming, improved production traits such as milk and meat quality, and a more sustainable environment by reducing land degradation and air and water pollution [94].

Ever since the first mouse naïve ePSCs were discovered, the effort to unveil their counterparts in farm animals was initiated. Despite numerous efforts, all attempts to generate self-renewing and stable ePSC lines in cattle have so far failed [95-105]. The first report of generation of bovine ePSCs was in 1991. These putative bovine ePS cells carrying a normal karyotype could last only four passages [106]. Subsequently, these cells were examined for *in vitro* differentiation potential. However, chromosomal aberrations appeared in early passages. In 1992, using superovulation, a study claimed the establishment of bovine ePSC primary cultures from day 7 bisected blastocysts. The medium used for this study was a modified minimum essential medium (MEM)-Alpha with 10% FCS, mercaptoethanol, glucose, LIF and HEPES-buffer. However, the cells were not able to expand further than four passages. Nonetheless, the cells were used for NT, and a few embryos were able to reach the 8 to 16 stage [95]. In 1993, Sims and colleagues first developed a suspension culture system for low number of cells from bovine. The medium used was CR1 containing selenium, insulin, transferrin, and FCS. A minimum of three blastocysts was cultured to establish one primary culture [107]. Using them as donor cells for NT, it was shown that these ePS-like cells could yield calves as efficiently as somatic cells [108; 109]. In 1996, Stice and colleagues reported isolation of bovine ePSCs from morulae and early blastocysts, using a growth medium consisting of alpha-MEM supplemented with 10% FCS and 0.1 mM 2-Mercaptoethanol. H=this enabled them to multiply their population up to fifty passages in over a year. As NT donors, they were able to establish pregnancy. However, all these pregnancies failed before day 60 due to defects in placenta development. Early passages of bovine ePSCs (less than 10 passages) also contributed to chimeric animals, but the conceptuses showed cotyledon abnormalities [110]. In 1998, Cibelli and colleagues produced chimeric calves using bovine ePSCs (The culture medium was MEM-Alpha with 10% FCS, mercaptoethanol, glucose, L-glutamine, and tylosin tartrate) by two approaches: i) using galactosidase-Neomycin-transfected (under the control of a CMV promoter) fibroblasts for NT followed by the isolation of bovine ePSCs from the resulting blastocysts; and ii) isolating bovine ePSCs from IVF blastocysts followed by transfection with the same construct. In the first approach, 85% of offspring and in the second one 60% had bovine ePSCs contributing to at least one organ tissue [111]. However, both approaches failed to show any germline contribution. In 2000, Iwasaki and colleagues produced chimeric calves with feeder-free bovine ePSCs in a mixture of DMEM and TCM 199 (1:1), 10% FBS, L-glutamine, nonessential amino acid, and

LIF. However, the cells had gained a fibroblast-like morphology and, following injection, only two of 6 calves were recognised chimeric with bovine ePSC contribution limited only to liver and hair follicles [112]. In 2001, a group reported long-term *in vitro* culture of bovine ePSCs with over 150 passages. ePSCs were cultured in alpha-MEM medium supplemented with 10% FBS, b-mercaptoethanol, L-glutamine, penicillin, streptomycin, and amphotericin B. Human and mouse embryonic markers (stage-specific embryonic antigen (SSEA)-1, SSEA-3, SSEA-4 and c-Kit receptor) were positive in this cell line and they could differentiate into embryoid bodies. However, following some passages, they showed chromosomal instability and failed to form any teratomas in immunocompromised mice [113]. In 2003, Saito`s group reported four ePS-like cell lines passaged over 20 times with intact karyotypes. The cells were cultured in an alpha-MEM medium supplemented with 10% FBS, 2-mercaptoethanol, LIF, human epidermal growth factor (EGF), penicillin, and streptomycin. Morphologically, these cell lines resembled mouse ePSCs and were positive for SSEA-1, STAT3, OCT4 and alkaline phosphatase (AP) as well as having the ability to contribute to chimeras but not germline [98]. In summary, these findings over the past 3 decades indicate that the progress in isolating cattle PSCs has been gradual but promising. Nowadays, optimising pluripotency culture conditions has been strikingly improving. With better understanding of mouse pluripotency, and following the discovery of the '2i regime', pluripotency has become accessible even in other refractory species. The given example is other strains of mouse embryos and rat which were captured using this medium [4; 69; 114]. The effect in bovine species, however, has not been as dramatic. Studies from our laboratory have probed the existence of a pluripotent ground state in cattle embryos [115], short-term ePSC [116] and finite iPSC cultures [117] benefiting from this regime. We have further developed the 2i method by adjusting pluripotency-promoting small molecules. This improved the *in vitro* bovine embryo development ratio and quality. This known as $2i^+$ regime further improved *in vitro* embryo development and quality. Based on comprehensive transcriptional profiling, $2i^+$ also increased pluripotency-associated gene expression profile [118]. This regime, moreover, yields more SOX2 positive ICM outgrowths, however, the colonies remain the same size (unpublished data).

1.5. Protein overexpression as a genetic tool

Functional studies are used to determine the function of a gene of interest in a given context [119]. The goal of such experiments is to evaluate any phenotypic change associated with changing the expression level of the gene, in this case, overexpression [120].

When a gene is not expressed, or its expression is at a very low level, overexpression of that particular gene becomes a handy tool to study its function and, thus, the phenotype conferred to the cell or organism. Using transgenic plasmids is one way of multiplying the quantity of protein of interest. Once introduced into the cell, the transcription and translation machinery of the host cell will help the transgene plasmid produce the protein of interest at detectable levels. This could be a transient state and the plasmid DNA of interest becomes degraded after a short period. However, to express the gene stably and continuously, the plasmid DNA needs to incorporate within an active site of the genome content. For a high-efficiency rate of transgene integration in the genome of the host cell, choosing a good gene delivery system that does less harm to the host cell is very crucial. The piggyBac (PB) system, derived from the cabbage looper moth Trichoplusiani, represents an efficient way for gene delivery into mammalian cells [121]. The PB transposon is a movable genetic element that efficiently transposes between vectors and chromosomes through a “cut-and-paste” mechanism. During transposition, the PB transposase recognizes transposon-specific inverted terminal repeats (ITRs) sequences located on both ends of the transposon vector, and efficiently moves the contents from its original position and efficiently integrates them into TTAA chromosomal sites [122]. As many as 15 copies of the plasmid can be randomly incorporated throughout the genome within one cell [123].

Recently a highly efficient PB system has been developed by which protein production becomes inducible [124]. The system has two transposon-containing piggyBac plasmids and integration is mediated through the piggyBac transposase (PBase) plasmid, pCyL43. While the first plasmid contains the target and puromycin resistance genes (a tetracycline response element (TRE) promoter control both), the second plasmid carries the reverse tetracycline transactivator (rtTA) inducer which is under constitutive expression controlled by a Cytomegalovirus (CMV) promoter. Once exposed to the antibiotic doxycycline (Dox), the rtTA structure changes allowing it to dock with TRE promoter on the first plasmid and turn on the expression of both target

and resistance genes. In the absence of doxycycline, the rtTA cannot adopt conformation changes any longer, and therefore there will be no expression of downstream genes (Figure 5). Hence, antibiotic Dox is a determinant element in turning a gene on or off in this system.

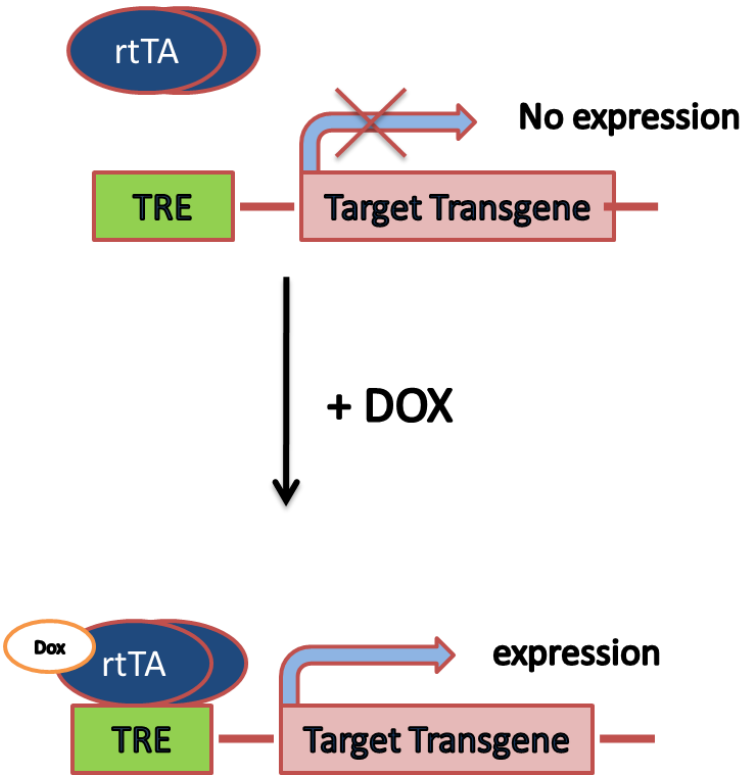

Figure 5. A reverse tetracycline transactivator (rtTA) driving a gene from TRE promoter.
When Dox is available, it transforms the rtTA structure which allows for pairing with the TRE promoter. This will then turn on the expression of target and resistance genes.

1.6. Aim of this study

It has been suggested that there is a species-specific connection between amino acid metabolism and epigenetics for sustaining pluripotency. Mouse ePSCs are critically dependent on threonine which is catabolised via the TDH-mediated threonine-SAM pathway, resulting in regulating SAM and subsequently H3K4me3 levels [8; 10]. In contrast, methionine omission from human ePSC culture medium leads to decreased levels of SAM and subsequently H3K4me3, which then down-regulate NANOG expression level [9]. Building upon these findings, the objectives of this study were to:

i. Undertake a targeted amino acid screen to identify amino acid(s) whose metabolism might be involved in the regulation of bovine ICM formation and pluripotency.

ii. Investigate the role of the TDH-mediated threonine-SAM pathway in bovine ICM development and pluripotency.

Chapter 2

2. Chapter Two: materials and methods

2.1. General materials

All materials, equipment, recipes, reagents, culture media, and cell lines used in this study are listed in the Appendix.

2.2. *In vitro* production of bovine embryos

By default, all media and buffer requirements for embryo work were pre-warmed to 38.5°C, unless otherwise mentioned.

2.2.1. *In vitro* maturation

In vitro matured non-activated metaphase II (MII)-arrested oocytes were derived as described previously [125]:

A. Ruakura (Hamilton, NZ) abattoir ovaries were collected from mature cows, placed into saline (30°C), and transferred to the laboratory within 2-4 h.
B. Cumulus-oocyte complexes (COCs) were collected in H199 (AgResearch, New Zealand) medium supplemented with 925 IU/ millilitre (ml) heparin (Sigma-Aldrich) and 20 µl/ml 20% (w/v) albumin (Sigma-Aldrich) concentrate by aspirating 3-12 mm follicles into a 15 ml Falcon tube using an 18-gauge needle and negative pressure (40-50 mm Hg).
C. Only COCs that had an unexpanded cumulus mass with 5 or more continues layers and with homogenous ooplasm were selected for *in vitro* maturation (IVM).
D. COCs were washed twice with H199-10% fetal calf serum (FCS) (Invitrogen, USA).
E. COCs were then washed once in B199-10% FCS.
F. Ten COCs in B199 (AgResearch, New Zealand)-10% FCS were transferred in a volume of 10 µl into a 40 µl drop of IVM medium in 65 mm dishes overlaid with paraffin oil.
G. Dishes were placed in an incubator humidified with 5% CO_2 at 38.5°C for 20-22 h.

2.2.2. *In vitro* fertilisation

After IVM for 20-22 h, *in vitro* matured oocytes with expanded cumulus cells were subjected to *in vitro* fertilization as described previously [126]:

A. One hour before insemination, an Ambreed Friesian 05-255 101604 Reeds Chee or Deacon straw (LIC, New Zealand) containing semen from a proven fertile bull was taken from liquid nitrogen and thawed in a 30-35°C water bath for 30 seconds.
B. The contents of one 0.25 ml straw containing 1 x 10^8 spermatozoa were emptied into a 5 ml falcon tube.

C. Using a sterile Pasteur pipette, the entire contents of the falcon tube was layered upon a Percoll (45%:90%) (Sigma-Aldrich) or BoviPure & BoviDilute (40%:80%) (Nidacon, Sweden) gradient and centrifuged at 700× g for 20 min or at 300 × g for 15 min, respectively, at room temperature (RT).

Meanwhile, oocytes were prepared as described in steps D to G.

D. Oocytes were removed from IVM drops using a 200 µl pipettor and transferred into a 35 mm Petri dish containing HEPES (H) buffered synthetic oviductal fluid (SOF) (HSOF) (AgResearch, New Zealand).
E. Cumulus cells were loosened gently by pipetting the COCs up and down 2-3 times. Extra care was taken to not strip the cumulus cells but to only relax the compact layers.
F. Oocytes were washed once with HSOF and then transferred into a Petri dish containing IVF medium.
G. The oocytes were then transferred to equilibrated (38.5°C, 5% CO_2) 30 µl droplets of IVF medium in 10 µl IVF medium.
H. IVF plates were returned to the incubator (Sanyo incubator, Japan) (38.5°C, 5% CO_2).
I. The motile sperm fraction was aspirated from the bottom of the tube immediately following centrifugation (Heraeus, Germany) of the sperm-gradient mix (step C) and was slowly added to a tube containing 1 ml HSOF and mixed gently.
J. The tube was then centrifuged at 200× g (if percoll gradient used) or 300× g (if BoviPure & BoviDilute gradient used) for 5 min at RT.
K. The supernatant was immediately removed and the sperm pellet was resuspended slowly in 200 µl of equilibrated (38.5°C, 5% CO_2) IVF medium (AgResearch, New Zealand).
L. Ten µl of the sperm preparation was used for counting the sperm using a Neubauer haemocytometer (Sigma-Aldrich).
M. Sperm concentration was diluted to $1x10^6$ /ml in the equilibrated (38.5°C, 5% CO_2) IVF medium.
N. Fertilization was achieved by adding 10 µl of diluted sperm to the 40 µl drop containing oocytes prepared as in step G.
O. IVF plates were then incubated in a 38.5°C, 5% CO_2 conditioned incubator for 22-24 h.

2.2.3. *In vitro* culture

At 22-24 h post-fertilization, *in vitro* culturing was performed as follows:

A. After 22-24 h post-fertilization, presumptive zygotes were washed in prewarmed HSOF.

B. To dislodge the cumulus cells, they were then treated with hyaluronidase (1 mg/ml) (Sigma-Aldrich) for 3 min while being shaken on the mini-shaker (ThermoFisher Scientific).
C. Once washed in HSOF medium, presumptive zygotes were transferred to pre-equilibrated fresh early SOF (ESOF) (AgResearch, New Zealand) droplets (pre-equilibrated for two hours prior to zygote transfer) overlaid with mineral oil (Vitrolife, Sweden) and incubated (10 zygotes per 20 µl droplet) in a humidified modular incubation chamber gassed with 5% CO_2, 7% O_2, and 88% N_2.
D. On D5, embryos were transferred to fresh drops of late SOF (LSOF) medium (AgResearch, New Zealand) (pre-equilibrated for two hours prior to embryo transfer) overlaid with mineral oil and incubated in a humidified modular incubation chamber gassed with 5% CO_2, 7% O_2, and 88% N_2.
E. Embryos were graded on D8 post-fertilization. Morphological grading was applied according to international embryo transfer society (IETS) standards (E).

2.3. *In vitro* production of mouse embryos

To generate *in vitro* produced mouse embryos (the protocol has been adjusted based on paper [127]):

A. 8-12 week old female (B6C3 or Swiss strain) mice were intraperitoneally (IP) injected with 10 international unit (IU) of pregnant mare serum (PMS) (Sigma-Aldrich) on day zero at 5:00 pm.
B. The second IP injection was of human chorionic gonadotropin (HCG), 10 IU/ml (Sigma-Aldrich) administrated 48 hours later, at 5:00 pm.
C. 14-17 h later, mice were euthanized, and abdominal skin and peritoneum were cut open with scissors.
D. After visualising the oviduct, its length was tracked until the ovaries were observed.
E. The ovaries were then excised using scissors and placed onto recovery medium (HCZB and 0.1% PVP) (Sigma-Aldrich).
F. Once all ovaries were removed, under Nikon SMZ800 stereomicroscope (Nikon, Japan) the ampulla was ruptured to release the oocytes.
G. Oocytes were then placed into pre-warmed 0.1% hyaluronidase (Sigma, New Zealand) for 15 min to dislodge cumulus cells.

H. Subsequently, they were transferred to an M16 medium (Sigma-Aldrich) and after two washes in the wash drops, they were distributed across the culture drops and incubated at 5% CO_2 and 37°C.
I. After 5 h, they were transferred to PG culture medium (AgResearch, New Zealand) drops and placed back into the incubator for another 6 h.
J. They were then transferred to designed treatment groups according to the requirements of the experiment.

2.4. Amino acid dropout experiments

The AA dropout experiments were conducted in bovine and mouse embryos as follows.

2.4.1. Bovine embryos

A. D5 post-IVF embryos were first graded into three groups; i) less than 8 cells, ii) more than 8 cells, iii) one cell.
B. Group i and ii were then equally distributed across the desired number of treatment groups.
C. Subsequently, each group was thoroughly washed in pre-warmed phosphate-buffered saline (PBS) (Sigma-Aldrich) - Poly (vinyl alcohol) (PVA) (Sigma-Aldrich) to avoid any protein/AA carry over from ESOF medium.
D. Embryos were then transferred into treatment groups. An LSOF medium without Eagle's essential- and non-essential- AAs (Sigma-Aldrich), bovine serum albumin (BSA) (Sigma-Aldrich), and Glutamax (Gln) (Invitrogen) was chosen as base medium and called base SOF (bSOF) medium. Treatment groups were generated by adding AAs and BSA (if needed) back to the bSOF and embryos were individually cultured in them until D8. For individual embryo culture, 20-30 5-µl culture drops were made in 6 cm dishes.
E. On D8, embryos were categorized as early (EB), mid blastocyst (MB), expanded blastocyst (XB) or hatched blastocyst (HB), and graded according to IETS standards as described in appendix E and further analysed if needed.

2.4.2. Mouse embryos

A. D1 presumptive PG-activated zygotes produced in section 2.3 were inspected carefully and any zygote containing dark cytoplasm was discarded.
B. Zygotes were then randomly grouped according to the designed treatments.
C. Subsequently, they were thoroughly washed in a prewarmed PBS-PVA buffer.

D. They were then transferred to their respective treatment groups. An M16-based home-made medium without all AAs (for concentrations see [128]) and BSA, was used as a base medium and called base M16 (bM16) (Table 22 except for BSA). Treatment groups were made by adding AAs and BSA back to bM16. The embryos were individually cultured onto 5 µl culture drops until D4. They were then visualised and graded under microscope.

2.5. Cell culture procedures

By default, all media, buffers, and additives were pre-warmed at 37°C water bath for cell culture. The techniques were adopted from [129].

2.5.1. Thawing cells

A. Vials containing approximately 1 ml of cells with variations in cell number were taken out of liquid nitrogen storage and transferred to a 37°C water bath.
B. Vials were removed from the water bath when the vials were approximately 80% thawed and wiped with 70% ethanol.
C. Cells were then transferred into a tube containing 5 ml of Dulbecco's Modified Eagle's Medium (DMEM)/F12 (ThermoFisher Scientific) + 1× GlutaMAX™ (ThermoFisher Scientific) and FCS (DMEM/F12-10% FCS) and centrifuged at 1000 × g for 3 minutes (min).
D. The medium was removed carefully, and the pellet was resuspended in an appropriate medium, according to the cell type.
E. Cells were counted using a Neubauer haemocytometer.

2.5.2. Cell culture

Cells were diluted and seeded in culture dishes at a specified density based on Table 21 and incubated under 5% CO_2 at 38.5°C or 37°C depending on the cell type.

2.5.3. Passaging

A. Upon reaching 70-90% confluence, cells were washed twice with PBS.
B. 0.25% trypsin- Ethylenediaminetetraacetic acid (EDTA) (Sigma-Aldrich) was added at amount of 20 µl/cm^2 for two min.
C. Once almost all cells detached from the culture dish, a 5-fold excess of culture media was added to neutralise the trypsin effect.
D. Cells were transferred to a 15 ml conical tube and centrifuged at 1000 × g for 3 min.
E. The medium was then removed carefully.

F. The pellet was resuspended in an appropriate pre-warmed culture medium.
G. Cells were counted using a Neubauer haemocytometer.
H. They were then passaged and seeded at a specified density according to the culture dishes used.

2.5.4. Freezing

Once cells reached 70-90% confluent, cells were ready to be frozen for storage.

A. Cells were lifted with trypsin as described in section 2.5.3.
B. They were transferred to a 15 ml conical tube and centrifuged for 3-5 min at 1000× g.
C. While the cells were being centrifuged, the cryopreservation solution (20% dimethyl sulfoxide (DMSO) (Invitrogen) in FCS) was freshly prepared.
D. After centrifugation, the supernatant was removed and a culture medium according to cell type was added to the cell pellet at a volume equal to 50% of total volume required. This is usually 1 ml, which means 0.5 ml of the total volume would be culture medium and the remaining 0.5 ml was the cryopreservation medium which was added dropwise and mixed gently.
E. Required densities of cells were then aliquoted in 1 ml volumes per cryovial and placed in a freezing box (Mr Frosty) in a -80°C freezer.
F. After 24 h, vials were transferred into liquid nitrogen for long-term storage.

2.6. Transfection of mammalian cells

Transfection is the process by which a plasmid is introduced into eukaryotic cells. The majority of the plasmid DNA will remain within the cytoplasm and will only be expressed for a few days before being degraded or diluted by cell division [130]. However, a small percentage of plasmids will incorporate into the host genome allowing stable expression, assuming it has integrated into a transcriptionally active region [131]. There are a number of different transfection strategies and the one used in this study is as below which was adopted from [129] with slight modifications:

2.6.1. Lipofectamine® LTX

Lipofectamine® LTX (Invitrogen) is a lipid-based transfection protocol that can achieve relatively high transfection efficiencies while also being gentle on the cells. The cationic lipid reagent LTX supplied by the kit spontaneously forms condensed lipid complexes with DNA by binding to the negatively charged phosphate backbone. The complexes are then believed to

interact with the cell membrane allowing for endocytosis and subsequent release within the cytoplasm [132].

Based on the requirements of the experiment, different culture dishes were used which accommodate different cell numbers (Table 1). Therefore, different cell densities require different Lipofectamine® reagents which have been stated in Table 1.

Table 1. Quantities of Lipofectamine® LTX components according to different sizes of culture dishes.

Culture dish type	96-well (per well)	4-well (per well)	12-well (per well)	3 cm	6 cm	10 cm
Adherent cells	1×10^4	1×10^5	2×10^5	5×10^5	2×10^6	4×10^6
Opti-MEM medium	17.5 µl	100 µl	200 µl	500 µl	1 ml	3 ml
Plasmid DNA	0.1 µg	0.5 µg	1 µg	2.5 µg	5 µg	15 µg
PLUS™ Reagent	0.1 µl	0.5 µl	1 µl	2.5 µl	5 µl	15 µl
Lipofectamine® LTX	0.3 µl	1.25 µl	2.5 µl	6.25 µl	12.5 µl	37.5 µl
pCyL43 (transposase plasmid)	-	-	-	0.7 µl	-	3 µl

The following is the procedure for Lipofectamine® LTX transfection:

A. BEF cells were seeded onto the required number of culture dishes for each experiment, one or two days before transfection to reach 60-80% confluence.

B. On the day of transfection, DMEM/F12-10% FCS media was refreshed at least two hours before transfection. Since the TRE3G promoter was Dox-inducible, 2 µg/ml of Dox was also added to the fresh medium.
C. For transfection mix, the required amount of plasmid DNA was added to opti-MEM reduced serum medium (ThermoFisher Scientific) in a 1.5 ml Eppendorf tube in order to form lipid complexes.
D. The diluted DNA solution was then gently mixed with the PLUS™ reagent (ThermoFisher Scientific) in order to boost transfection efficiency, and the mix was left to incubate for 5 min at RT.
E. Subsequently, the specified volume of LTX reagent (ThermoFisher Scientific) was added to the solution and incubated for 30 min at RT to form DNA-lipid complexes.
F. The DNA-lipid complexes were then added dropwise to the culture dishes, swirled gently and placed back into the incubator for 48 h.

2.6.2. Types of transfection

2.6.2.1. Transient transfection

Transient transfection results in cells expressing the foreign gene of interest for a short period, but they do not incorporate it into their genome. Therefore, the new gene will not be replicated and the foreign gene disappears by the next cell division. Transient transfection is a convenient tool for analysis of the gene of interest allowing rapid assessment of whether the plasmid is functional and expresses the gene of interest shortly after transfection. Usually 48 h posttransfection, cells can be used for a quick analysis such as immunofluorescence.

2.6.2.2. Generation of mammalian stable cell line

In contrast to transient transfection, in which foreign DNA disappears after a short period, in stable transfection the introduced DNA is incorporated into the host genome. Stably transfected cells pass the introduced DNA to their daughter cells. To produce stably transfected cells, DMEM/F12-10% FCS media was refreshed 48 h after transfection and appropriate amounts of puromycin (2 µg/ml) (Sigma-Aldrich) and doxycycline (Dox) (2 µg/ml) (Sigma-Aldrich) was added to the culture dishes. The medium was refreshed every 48 h. A non-transfected and a – Dox dish were also included as controls. Once 80-90% confluence was reached, cells were passaged while still being under puromycin and Dox selection. At this point, cells were harvested for characterisation of transgene expression or freezing.

2.7. Staining protocols

2.7.1. Standard immunofluorescence protocols

Immunofluorescence (IF) was used to detect proteins on a single cell level. Unless otherwise stated, all embryo immunostaining was performed using the following protocols.

2.7.1.1. Immunofluorescence on embryos

IF for D8 bovine IVF-produced embryos was performed in 96 well plates using a fine glass Pasteur pipette to transfer them across different wells by mouth pipetting.

A. In a 96-well culture dish, embryos were fixed with 60 µl of 65°C depolymerized 4% paraformaldehyde (PFA) (Sigma-Aldrich) (w/v) /4% (w/v) sucrose (Sigma-Aldrich) solution in PBS/PVA for 15 min at RT.
B. Embryos were washed once with 60 µl PBS-PVA at RT.
C. Embryos were then quenched with 60 µl of 50 mM ammonium chloride (NH_4Cl) in PBS-PVA for 10 min at RT.
D. Embryos were washed once with 60 µl of PBS/PVA at RT.
E. Embryos were then permeabilized in 0.1% Triton X-100 (TX) (Invitrogen) for 10 min.
F. Embryos were subsequently blocked with 5% serum (subject to change depending on what animal the secondary antibody was raised in) or 3% BSA and incubated for 90 min at RT.
G. Embryos were then incubated with 60 µl of appropriate concentrations of primary antibodies (Table 2) and left overnight on a slowly shaking platform at 4°C.
H. Embryos were washed twice with 60 µl PBS/PVA for 15 min each.
I. Embryos were subsequently incubated with 60 µl of appropriate concentrations of secondary antibodies (Table 2) and 5 µg/ml of H33342 (Invitrogen) and incubated for 30 min at 37°C.
J. Embryos were washed twice with 60 µl PBS/PVA for 15 min each time.
K. Finally, embryos were mounted in 3 µl of either DAKO fluorescent mounting medium (Agilent Technologies, USA) or ProLong™ antifade mountant (ThermoFisher Scientific) on a clean glass slide and overlaid with a coverslip.
L. Image acquisition was performed using either a Wide-field epifluorescence (Olympus Corporation, Japan) or confocal laser scanning microscope (Olympus Corporation, Japan) as described in part 2.7.6

2.7.1.2. Immunofluorescence on cells

All antibody staining of cells or primary cell cultures was performed using the following protocol unless otherwise specified.

A. Cells cultured in 8-well dishes were fixed with 4% PFA solution for 15 min at RT.
B. Cells were then washed three times each time 5 min in PBS.
C. Cells were then incubated in quenching solution NH_4Cl for 10 min to minimise autofluorescence.
D. Cells were subsequently washed two times each time 5 min in PBS.
E. Cells were then permeabilized in 0.1% TX (Invitrogen) for 10 min.
F. Cells were washed two times each time 5 min in PBS.
G. Cells were incubated in the appropriate blocking solution (5% serum or 3% BSA) for 90 min.
H. Subsequently, the required amount of primary antibody dilution (Table 2) was prepared using blocking solution as the diluent and 150 µl was pipetted into each well before incubating at 4°C overnight. A no primary antibody group was also included as negative control.
I. Cells were then washed with PBS twice, for 5 min each, to remove any unbound primary antibody.
J. Secondary antibodies were diluted in blocking solution according to Table 2, mixed with the Hoechst 33342 nuclear stain to a working concentration of 5 µg/ml. 150 µl of the secondary/Hoechst dilution was added to each well including the negative control well before incubating for 30 min at 37°C in the dark.
K. Cells were followed by two times wash each time 15 min in PBS.
L. Coverslips were then mounted on the 8-well chamber using 5 µl of ProLong® Diamond antifade mounting medium and left to set at 4°C for at least 30 min.
M. Image acquisition was performed using either a Wide-field epifluorescence or confocal laser scanning microscope as described in part 2.7.6.

Table 2. Primary and secondary antibodies used for IF & western blot.

Primary antibodies	WB dilution	IF Dilution	Source	Catalogue #
Goat anti-SOX2		1:30	R&D Systems	AF2018
mouse anti-CDX2		1:200	Biogenex	AM392-5M

Rat anti-Troma-1 (KRT8)		1:10	DSHB	
Rabbit anti-TDH	1:5000	1:500	Dr Steven L. McKnight*	
rabbit anti-H3	1:5000		Abcam	ab1791
Mouse anti-H3K4me3		1:100	Abcam	ab1012
mouse anti-H3K9me3		1:1000	Diagenode	c15200146
Rabbit anti-H3K27me3		1:500	Diagenode	c15410069
AF6-anti-SAM 2a		1:30	Arthus Biosystems	MAF00202-50
AF488-anti-SAH 2a		1:30	Arthus Biosystems	MAF00302-50
Secondary antibodies				
AlexaFluor® 568 donkey anti-mouse		1:2000	Invitrogen (USA)	
AlexaFluor® 488 donkey anti-mouse		1:2000	Invitrogen (USA)	
AlexaFluor® 568 donkey anti-goat		1:2000	Invitrogen (USA)	
AlexaFluor® 488 donkey anti-goat		1:2000	Invitrogen (USA)	
AlexaFluor® 568 goat anti-rat		1:2000	Invitrogen (USA)	
AlexaFluor® 488 goat anti-rat		1:2000	Invitrogen (USA)	
AlexaFluor® 568 goat anti-rabbit		1:2000	Invitrogen (USA)	
AlexaFluor® 488 goat anti-rabbit		1:2000	Invitrogen (USA)	
Polyclonal Goat Anti-Rabbit immunoglobulins, conjugated with HRP	1:5000		DAKO (Agilent Technologies, USA)	

*University of Texas

2.7.2. Immunofluorescence protocol for histone methylation antibodies

2.7.2.1. IF on embryos

The same procedure was followed as detailed in 2.7.1.1 except that the embryos were permeabilized and fixed with 3.6% PFA/ 1% TX simultaneously for 15 min at RT.

2.7.3. IF protocol for SAM/SAH antibodies

A. When cells were ready to be stained, the medium was removed from wells and washed with 1 ml 1X PBS 3 times.
B. 200 µl 80% frozen cold acetone (-20°C) was added to fix the cells under -20°C for 30 min.
C. Cells were washed with 1ml 1X PBS 3 times.
D. AF-488-anti-SAH and PE-anti-SAM antibodies (Table 2) were added to the staining buffer (PBS/1% BSA) to the final concentration of 60 µg/ml and incubated at 4°C for 1 h.
E. Hoechst 33342 nuclear stain was diluted to the final concentration of 5 µg/ml using staining buffer and then incubated for 20 min.
F. Cells were washed with 1 ml PBS three times.
G. Coverslips were then mounted onto the 8-well chambers using 5 µl of ProLong® Diamond antifade mounting medium. The slides were now ready for microscopy and imaging.

2.7.4. Mitochondrial staining

2.7.4.1. Mitochondrial staining of embryos

A. Embryos were washed three times in 3% prewarmed BSA-PBS for 5 min each time.
B. They were then incubated for 30 min in the same buffer containing 250 nM Mitotracker Red CMXRos (Molecular Probes M-7512, Oregon, USA) under 5% CO_2 at 38.5°C.
C. After incubation, embryos were washed three times in pre-warmed PBS and fixed with 4% PFA fixative for 30 min at RT.
D. They were then processed for TDH antibody staining with the standard protocol.

2.7.4.2. Mitochondrial staining of cells

A. The media was removed from cells grown in 8-well dishes.
B. 200 µl prewarmed (37°C) staining buffer (only DMEM/F12 without serum) containing 250 nM Mitotracker Red CMXRos (Molecular Probes M-7512, Oregon, USA) was added to each well and incubated for 30 min under growth conditions.
C. After incubation, the staining buffer was replaced with fresh prewarmed full media/buffer, and cells were observed under a fluorescent microscope.
D. To fix cells, medium/buffer was replaced with pre-warmed 4% PFA and incubated for 30 min.

E. Cells were then washed once with PBS.
F. They were subsequently processed for TDH antibody staining with the standard protocol.

2.7.5. Differential staining and cell quantification

2.7.5.1. Differential staining of embryos

The protocol was adopted from [133] as follows:

A. 150 µL PBS/PVA was added to 50 µL Anti-Bovine Serum developed in Rabbit (RαB) (Sigma B3759 Missouri, USA) and centrifuged for 10 min at 2000 revolutions per minute (rpm) before use.
B. 134 µl PBS/PVA, 8µl H33342 stock and 8µl Propidium iodide (PI) stock (ThermoFisher Scientific) (1.0 mg/ml in water) were added to 50 µL Guinea Pig (GP) Compliment Serum (Sigma S1639 Missouri, USA) and centrifuged for 10 min at 2000 rpm before use.
C. RαB and GP working solutions were prepared in two separate 6 cm Petri dishes. 2x40 µl wash drops and 6x20 µL culture drops of RαB and GP were made and covered with warm mineral oil. They were then placed on a warm stage and protected from light.
D. The zona pellucida of the selected embryos were dislodged by transferring them to a 30-50 µL pronase (5 mg/ml) (Sigma-Aldrich) drop. As soon as the zona started to look expanded/relaxed, the embryos were transferred to a dish containing PBS/ PVA (0.1 mg/ml) to stop the pronase digestion and the zona was completely removed using a Pasteur pipette.
E. 5-10 embryos were transferred at a time with as little buffer as possible to an RαB drop, washed 3x in this drop to remove PBS/PVA.
F. The washing was repeated in a second drop.
G. The embryos were then spread out in the culture drop for 30 min on a warm stage (38°C) while being protected from light. Antibodies bind to the outer TE cells but are prevented by the zonular tight junctions between these cells from penetrating the blastocoel and binding to the ICM cells.
H. The embryos were then transferred to a 3 cm dish containing PBS/PVA and washed three times.
I. 5-10 embryos at a time, with as little buffer as possible, were then moved to a GP drop and washed 3x in this drop to remove PBS/PVA.
J. The washing was repeated in a second drop.

K. The embryos were then spread out in the culture drop for 30 min on a warm stage, being protected from light.
L. Subsequently, the individual embryos were transferred to a dish of prewarmed PBS/PVA for a gentle wash.
M. They were then mounted on a clean slide using 3 µl ProLong® Diamond Antifade mounting medium.
N. The embryos were gently covered by a coverslip (22x22) to spread over the embryos. The samples were now ready for imaging.

2.7.5.2. Differential staining of cells

8µl H33342 stock and 8µl PI stock were added to the existing 184 µl culture medium and incubated for 25 min in the incubator. The samples were now ready for imaging. The live cells will stain only blue, whereas the compromised cells will stain both blue and red, thus appearing as pink under microscope. The following equation was used to quantify the percentage of compromised cells. ImageJ software was used to quantify the cells of interest (blue or pink) were counted and normalized to the total cell number (blue+ pink) for the given sample.

Equation 1. The equation for calculating the percentage of compromised cells

% of compromised cells= no. pink cells/ total number of pink and blue cells x 100

2.7.6. Measuring autophagy

The following protocol was provided with the Autophagy Detection Kit (ab139484) and was optimised for use with embryos:

A. LSOF medium was removed and the embryos were washed with 1x Assay buffer provided with the kit. For every 1 mL of 1x Assay Buffer or complete cell growth medium, 2 µL of Green Detection Reagent and 1 µL of Nuclear Stain was added.
B. The embryos were then incubated with the detection reagent for 30 min at 38.5°C in the dark.
C. They were subsequently washed with 100 µL of 1x Assay Buffer.
D. The buffer was then removed and the embryos were transferred onto a glass slide with 5 µl of ProLong® Diamond antifade mounting medium, and a coverslip was then placed on top.
E. The stained embryos were then analysed by wide-field fluorescence microscope.

2.8. Image acquisition

2.8.1. Wide-field epifluorescence microscopy

Slides were viewed with an Olympus BX50 microscope (Olympus Corporation, Japan) at either 200X or 400X magnification. The Hoechst stain was visualized by excitation at 405 nm (the blue channel), while red and green fluorophore-conjugated antibodies were visualised at 568 nm and 488 nm (red and green channel, respectively). After adjusting exposure times using the Spot Basic software (Spot Imaging Solutions, USA), either black and white or coloured photographs were acquired by the inbuilt Spot RT3 camera. Black and white images were later pseudo-coloured using ImageJ software (National Institute of Health, USA).

2.8.2. Immunofluorescence quantification

The following is the method used to measure pixel intensities using IF photographs:

A. The image was viewed using ImageJ software. The "area" and "mean grey value" boxes from the analyse bar were selected.
B. One IF image was selected and using the Freehand Selection tool a line was drawn around its area and measured by applying "measure" (or Ctrl+M) from the Analyse bar. All desired values ticked off in section A appeared in a new box.
C. To subtract background, 5 random circles were drawn for each IF image adjacent to the nuclei and measured as above.
D. All values were copied into a prepared table in an Excel spreadsheet with all formulas and parameters required.
E. The background was subtracted from the actual pixel intensities.
F. The new values of IF images of the same treatment group were averaged and the values were plotted.

2.9. Western blotting

Western blot was performed according to [134] with some slight modifications.

2.9.1. Cell lysis and protein extraction

To lyse cells and extract proteins, radioimmunoprecipitation assay (RIPA) buffer (ThermoFisher Scientific) was prepared using the recipe in Table 13

A. After removing samples from storage in liquid nitrogen, or having performed section 2.5.3 (B-E), the cells were treated with 100 µl RIPA buffer per $1x10^6$ cells and incubated on ice for 30 min.
B. The cells were then centrifuged immediately for 20 min at 4°C.

C. Subsequently, the supernatant was removed and transferred to a new Eppendorf tube and stored at -80°C.

2.9.2. SDS-PAGE

A. A pre-cast 4-12% Bis-Tris gradient polyacrylamide gel (ThermoFisher Scientific), containing a stacking and a running gel, was loaded onto an electrophoresis chamber.
B. The chamber was filled with NuPAGE running buffer (ThermoFisher Scientific).
C. A total volume of 24 µl (18 µl sample, and 6 µl loading dye) was loaded into each well of the gel along with 6-10 µl of ladder.
D. The SDS-PAGE (Bio-Rad, USA) ran at 120 volts for 60-90 min depending on the size of the protein of interest.

2.9.3. Electroblotting

A. Two absorbent pads, four pieces of pad-sized filter papers, and one nitrocellulose membrane (ThermoFisher Scientific) were soaked in transfer buffer (see the recipe in section Table 13).
B. The SDS-PAGE gel was carefully removed from the tray and placed into a tray containing transfer buffer.
C. Subsequently, the blot was placed within a sandwich using a cassette containing the following (Figure 6):

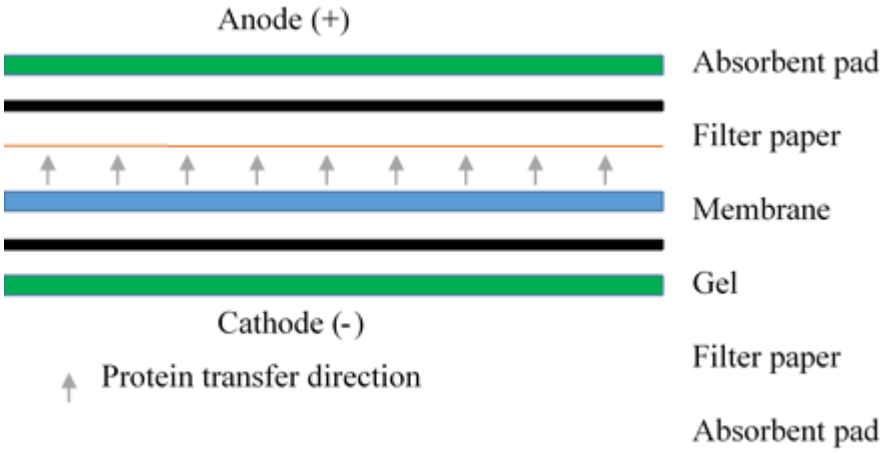

Figure 6. Layers of a western blot sandwich.

D. The blot sandwich was then placed into an electro-blot chamber (Bio-Rad, USA) containing fresh transfer buffer, and placed on a stirring platform.
E. The power supply was set to 30 volts to run overnight.

2.9.4. Ponceau S staining

A. The following morning the blot sandwich was disassembled.
B. The nitrocellulose membrane was placed into a plastic dish and covered with Ponceau S (Sigma-Aldrich) for 5 min at RT. This was to confirm that any protein had been transferred onto the membrane.
C. The membrane was washed with Milli-Q water until the excessive Ponceau S was washed out and protein bands became distinct and visible.
D. A photocopy was taken before removing the staining using Tris-buffered saline plus tween 20 (TBST) buffer.

2.9.5. Immunostaining

A. The blot was blocked in 5% skim milk (dissolved in TBST) for 60 min.
B. Then it was placed into primary antibody solution (Table 2) at 4°C shaking overnight.
C. The following morning the blot was washed three times each time 10 min with TBST.
D. Subsequently, secondary antibody solution (Table 2) was applied at RT for 60 min on a slow shaking platform.
E. The blot was again washed three times for 10 min each time with TBST.

2.9.6. Band detection

Antibody detection took place by applying Western Lightning Plus ECL kit (Perkin Elmer, USA). The reagents were mixed 1:1 and applied to the blot for 1 min. After excess reagent removal, the blot was then placed inside the ImageQuant LAS 4000 (GE Healthcare Life Sciences, UK) platform. The exposure time varied depending on the type of antigen and antibody. However, the starting point could be a fraction of a second.

2.10. Polymerase chain reaction (PCR)

2.10.1. RNA extraction and complementary DNA synthesis

The ZyGEM RNA extraction kit (New Zealand), was used to isolate total RNA from mammalian cell cultures and bovine embryos as follows:

A. Mammalian cells were harvested and resuspended in 50 µl of RNAGEM master mix solution composed of 1 µl RNAGEM, 5 µl SILVER buffer and 44 µl of Diethylpyrocarbonate (DEPC)-treated water. For bovine embryos, this solution was 0.5 µl RNAGEM, 1 µl SILVER buffer and 8.5 µl of DEPC-treated water.
B. The solution was then transferred to a 1.5 ml Eppendorf tube, vortexed briefly and spun down in a mini-centrifuge.

C. The reaction was then incubated for 10 minutes at 75°C to activate the enzyme, RNAGEM.
D. The tube was then placed back on ice and 2 µl of DNase in 5 µl of DNase buffer was added to the reaction, vortexed briefly and spun down. For bovine embryos, this was 1.0 µl of DNase buffer and 0.4 µl of DNase.
E. The reaction was next incubated at 37ºC for 5 minutes followed by 5 minutes at 75ºC to deactivate the enzyme.
F. After placing back onto ice, 5.7 µl of TE buffer was added to the reaction and spun down. For bovine embryos, this was 1.4 µl.
G. For complementary DNA (cDNA) synthesis, the reaction was prepared by adding 1 µl of deoxynucleotide Triphosphates (dNTP) mix (Invitrogen) and 0.5 µl of random hexamer primers (Invitrogen) to 9 µl of the RNA extract.
H. The reaction was then incubated at 65ºC for 5 minutes to denature secondary RNA structures before plunging into ice for 1 minute to allow the random hexamer primers to bind.
I. Meanwhile, a cDNA master mix was prepared which was composed of 4 µl First-Strand 5x buffer (Invitrogen), 4 µl of $MgCl_2$ (Invitrogen), 1 µl of RNaseOUT^{TM} (Invitrogen), and 1 µl of SuperScript^{TM} III reverse transcriptase (Invitrogen).
J. The cDNA master mix was then added to the reaction mix, vortexed briefly and spun down. A reverse transcriptase negative reaction was also prepared in which 1 µl of DEPC-treated water was added in place of SuperScript^{TM} III reverse transcriptase.
K. The reactions were then placed into the Eppendorf Mastercycler Gradient PCR machine (Bio-Rad, USA) and run on the cDNA synthesis program (25ºC, 10 min; 50ºC, 50 min; 80ºC, 5 min; hold at 4ºC).
L. Once complete, cDNA samples were stored at -20ºC.

2.10.2. Primer design

The NCBI nucleotide database was used to design primers for amplifying genes of interest (Table 3). The default criteria for primer design were: i) product length between 170–230 nucleotides, ii) a melting temperature (Tm) between 57 and 63ºC, iii) primer spans exon-exon junctions, IV) primer pair must be separated by at least one intron on the corresponding genomic DNA. However, there were some exceptions that didn't match all criteria above such as *TDH*. Selected oligonucleotides were purchased from Integrated DNA Technologies and delivered in a lyophilized state at RT. Primers were resuspended in DEPC-treated water to a

stock concentration of 1mM. For use, the primer stock was diluted with DEPC-treated water to 10 μM. Diluted primers were stored at -20ºC and primer stocks were stored at -80ºC.

Table 3. List of primers used in this study.

PCR primers	Sequence (5'-3')	Tm (°C)	Amplicon Size (bp)	Reference
Bovine primers				
18S	F:GACTCATTGGCCCTGTAATTGGAATGAGTC R: GCTGCTGGCACCAGACTTG	80	87	[135]
NANOG	F: CACCCATGCCTGAAGAAAGT R: TGCATTTGCTGGAGACTGAG	83	295	[136]
FGF4	F:TACGGCTCGCCTTTCTTCAC R:TTCTTGGCCTTGCCGTTCTT	88	131	[117]
SOX2	F:GTAGTTTGCTGCCTCTTTAAGAC R:CGCTTCCCTCCTCTTCTG	90	152	[117]
CDX2	F:AGACAAATACCGGGTCGTGTACA R:TTTGCTCTGCGGTTCTGAA	87	162	[137]
KRT8	F:GGACCCCTGGCTTCAACT R:CCCTGCACAGCTCCATCT	89	199	[138]
TDH	F: TGAGTCCTGGGTGGCTGT R: GAAGGGCTACCACCAAACC	84.5	187	This study
SOX17	F:ATGCTGGGCAAGTCGTGG R:CTTTAGCCGCTTCACCTGCTT	91.8	147	[118]

PDGFRα	F: CCCCGACGTGGAAATCAGAA R: CATCTGGGTCTGGCACGTAG	79	87.5	[118]
Mouse primers				
Gapdh	F: CCCACTAACATCAAATGGGG R: CCTTCCACAATGCCAAAGTT	88		[139]
Tdh	F: CGATTGGAGCCTTTGGACCT R: CGGCGTAGTCAGTTGTTCCT	86	213	This study

2.10.3. Standard curve generation

A standard curve was used to aid quantification of mRNA copy number of the gene of interest in a given sample. This was done as follows:

A. A series of log dilutions (1 to $1/1x10^6$) was prepared using a purified PCR product of the gene of interest.
B. A qPCR reaction was prepared and run as described in section 2.10.4 using 1 µl of the serial dilution as template. The lower dilutions (1/10 to $1/1x10^3$) were run in duplicate while the higher dilutions ($1/1x10^4$ to $1/11x10^6$) were run in triplicate.
C. Standard curve data was subsequently exported and graphed in Microsoft Excel. If a standard curve had an amplification efficiency between 1.8 and 2, it was used for quantification equations.

2.10.4. Quantitative PCR

qPCR is a useful tool to amplify and quantify nucleic acids (mRNA or DNA). In this study, it was used to quantify mRNA of the gene of interest. All qPCR-associated work was performed under RNase-free conditions. Reactions were prepared in LightCycler® glass capillaries (Roche, Germany) in a total volume of 10 µl. The following was the instructions used:

A. The required number of capillaries were organized in a capillary box using sterile tweezers and placed at 4°C while the reaction master mix was prepared.
B. All reagents including primers, DEPC-treated water, master mix, and templates were thawed on ice and spun down briefly using a mini-centrifuge. The Takara Bio SYBR®

Ex Taq qPCR master mix (Clontech Laboratories) was used for mRNA quantification and included fluorescent DNA intercalating reagent, SYBR® Green I.

C. Each sample contained: i) 5 µl of Takara master mix, ii) 0.8 µl of combined forward & reverse primer (10µM), iii) 3.2 µl of DEPC-treated water.
D. After a short vortex and a brief spin down, 9 µl of reaction master mix was added to each pre-chilled glass capillary (on ice) followed by 1 µl of the respective cDNA sample. Alongside the cDNA samples, a positive and a negative template control (PTC and NTC, respectively) were also included to account for reaction efficiency and contamination, respectively. The NTC contained 1 µl of DEPC-treated water instead of cDNA, while the PTC contained a 1/100 dilution of a purified PCR product of the gene of interest. Additionally, a reverse transcriptase negative group was also included in each run to ensure there was no genomic DNA contamination from the cDNA synthesis reaction.
E. The capillaries were then sealed carefully using the capping tool.
F. The reaction capillaries were subsequently placed into a capillary carousel and spun down using the LC Carousel Centrifuge 2.0 (3,000g, 10 sec) (Roche, Germany). Using LightCycler® software, the reaction template described in Table 4 was selected.

Table 4. LightCycler® reaction template for qPCR.

Status	Temperature (°C)	Duration	Cycle
Denaturation	95	10 min	1
Annealing	95	20 sec	45
	60	20 sec	
	72	20 sec	
Melting Curve	95	2 min	1
Cooling	4	Hold	1

G. Once reactions completed, results were analysed using LightCycler® software (Roche, Germany). Product identity and authenticity were verified by performing a melting curve analysis. Different primers result in different PCR products with different sizes which vary in GC content and hence have a specific melting temperature. The no template control (NTC) should not show any melting peak as it does not have any cDNA template. If it did produce a specific melting peak, the results were not reliable and were subsequently discarded.

H. Depending on the abundance of the targeted mRNA, each sample crossed the threshold level of fluorescence at a specific point which is called crossing point (CP) value and corresponds to the cycling number. CP values were then transferred to Microsoft Excel and relative concentrations were calculated using Equation 2.

I. The value from this equation was divided by the relative concentration of the internal control (*18s* for bovine and glyceraldehyde 3-phosphate dehydrogenase (*Gapdh*) for mouse cells) to give the relative ratio.

Equation 2. Calculating the relative concentration of the gene of interest based on the standard curve.

$$\text{Relative concentration} = e^{(-(\text{CP value} - \text{slope})/\text{y intercept})}$$

For log calculations, the equation below was implemented.

Equation 3. $\log_{10}$ equation conversion.

$$\text{Log}_{10} = \text{power } (x-10)$$

2.11. TDH overexpression

2.11.1. Generation of the PB-TRE-TDH plasmid

2.11.1.1. TDH fragment design

The bovine TDH mRNA sequence was acquired from the NCBI database, purchased from GeneArt Strings™ DNA fragments (Life Technologies, USA), and upon delivery resuspended in DEPC-treated water to a final DNA concentration of 20 ng/µl, and then stored at -20ºC. To help with cloning, the TDH coding sequence was flanked by a 5' SalI and 3' NotI restriction enzymes (Clontech, USA), and three 'stuffer' nucleotides were added to either side (Table 17). The entire sequence (1178 base pair (bp)) was cloned into the PB-TRE plasmid.

2.11.1.2. Polyadenylation

Polyadenylation is the addition of multiple adenosine (A) monophosphates (poly (A) tail) to the 3' terminus of target cloned RNA. This tail is crucial for nuclear export, translation, and stability of mRNA in mammalian cells [140].

The following is the instructions for polyadenylation:

A. A mix of :
   i. 0.5 µl 10x buffer (Sigma-Aldrich)
   ii. 0.5 µl FastStart Taq DNA polymerase (Sigma-Aldrich)
   iii. 0.25 µl PCR Nucleotides mix (dNTPs) (Sigma-Aldrich)
   iv. 0.75 µl Milli-Q H_2O
   v. 3 µl TDH fragment

to the total volume reaction of 5 µl was made in a 0.5 ml Eppendorf tube.

B. The tube was subsequently placed into PCR machine (Roche, Germany), and the reaction conditions described in Table 5 were run.

Table 5. Reaction conditions for Polyadenylation.

Status	Temperature (ºC)	Duration
Denaturation	94	3 min
Annealing	55	30 s
	72	30 min
Cooling	4	1 h

2.11.1.3. pGEM®-T Easy plasmid ligation

In order to add sticky ends to the TDH fragment, it was inserted into a pGEM®-T Easy plasmid (Promega, USA). Below were the instructions for ligation.

A. A 10 µl ligation reaction was prepared by mixing:
   i. 5 µl 2x rapid ligation buffer
   ii. 1 µl pGEM®-T Easy plasmid
   iii. 1 µl T4 DNA Ligase (Promega, USA)
   iv. 3 µl TDH fragment in a 0.5 ml Eppendorf tube.
B. The ligation reaction was incubated at RT for 2 h.

2.11.1.4. Bacterial transformation

To multiply copy numbers, plasmids were introduced into bacteria. This phenomenon is called transformation and was performed as follows:

A. Bacterial stocks containing 50 µl of One Shot® TOP10 competent Escherichia coli (Invitrogen) were removed from -80ºC freezer and thawed on ice.
B. 5 µl of the ligation reaction was then added to the vial Escherichia coli and incubated on ice for 20-30 min.
C. The transformation tube was subsequently heat shocked in a 42ºC water bath for 30-60 seconds.
D. The tube was then placed back on ice and incubated for two min.
E. 250 µl of SOC bacterial medium was then added to the transformation mixture and left in a 37ºC water bath or shaking incubator for 45 min.
F. The transformed bacteria were then spread across a Luria-Bertani (LB) (ThermoFisher Scientific) agar plate, containing 50 µg/ml ampicillin and incubated upside down at 37ºC overnight.

2.11.1.5. Bacterial colony selection

The following day transformed bacterial plates were taken out of the incubator. To confirm that the bacterial colonies have taken up the target plasmid:

A. Three blue colonies were randomly circled.
B. Using a pipette tip, they were then picked and transferred individually to a tube containing 5 ml of LB broth plus the 50 µg/ml ampicillin antibiotic.
C. The cultures were then incubated at 37ºC with shaking overnight (18-22 h) to produce enough bacteria for miniprep (2.11.1.6).

2.11.1.6. Miniprep

Miniprep is the term for small-scale plasmid isolation (10 µg). The PureLink® Quick Plasmid DNA Miniprep Kit (Invitrogen) was used according to the manufacturer's instructions as follows:

A. The bacterial culture was centrifuged at 4,000 × g, for 10 min.
B. The supernatant was discarded and the bacterial pellet was resuspended in 250 µl of resuspension buffer containing RNase A.

C. The bacteria were subsequently lysed by adding 250 µl of lysis buffer and mixed thoroughly by inverting 5 times.
D. The reaction was then neutralised with 350 µl of precipitation buffer. This buffer precipitates the denatured chromosomal DNA and proteins.
E. The lysate reaction was then centrifuged at 12,000 × g, for 10 min.
F. The supernatant, which contained the plasmid of interest, was gently removed and transferred to a spin column within a wash tube.
G. The spin column was centrifuged at 12,000 × g, for 1 min and the flow through discarded. The plasmid DNA now adhered to the silica membrane.
H. The column was washed with 700 µl of wash buffer containing ethanol and centrifuged at 12,000 × g, for 1 min, and the flow through was discarded.
I. The spin column was then transferred into a sterile 1.5 ml recovery tube.
J. 75 µl of TE buffer or Milli-Q water was added to the column membrane and incubated for 1 min.
K. The tube was centrifuged at 12,000 × g, for 2 min to elute the plasmid DNA.
L. The concentration of the plasmid was measured using Nanodrop Spectrophotometer ND-1000 (ThermoFisher Scientific, USA) as described in 2.11.1.7.
M. Plasmid DNA was stored at 4ºC (short-term), or -20ºC (long-term).

2.11.1.7. Plasmid quantification

Following plasmid DNA isolation, the Nanodrop Spectrophotometer ND-1000 (ThermoFisher Scientific) was used to measure its concentration. The following was the instruction for measuring the plasmid concentration:

A. The machine was first calibrated with water and then blanked with Milli-Q water.
B. One µl of plasmid DNA was then loaded and measured by light absorbance (A) at 260 nm which is converted to ng/µl. The purity of the DNA was evaluated by dividing its A value at 260 nm over its A value at 280 nm (A260/A280). An A260/A280 ratio between 1.8 and 2.0 meant that the plasmid DNA was of appropriate purity.

2.11.1.8. Restriction digestion

This was performed to ensure that the plasmid DNA contained the TDH fragment. The plasmid was digested with the restriction enzymes detailed in Table 6. All restriction enzymes and buffers were supplied by New England BioLabs (USA).

A. The digestion reaction consisted of:

i. One µg of DNA
ii. One unit of each restriction enzyme
iii. 10x cut smart buffer (ThermoFisher Scientific).

B. The reaction was incubated at 37ºC for 30 min.
C. It was then loaded onto a 0.8% agarose gel made according to section 2.11.1.9.

Table 6. Restriction enzymes and buffers Restriction Enzyme.

Restriction enzyme	Digest Buffer	Cut Site
NotI (HF)	10x cut smart buffer	GC^GGCCGC
SalI (HF)	10x cut smart buffer	G^TCGAC

2.11.1.9. Gel electrophoresis

Agarose gel electrophoresis is a frequently used technique to separate fragments of DNA by size. Then, the separated bands are visualised and analysed under UV. To separate fragments, a 0.8% agarose gel was made. The following was the instruction for gel electrophoresis:

A. 100 ml of 1x TAE buffer was poured into a tray containing 0.8 g of UltraPure™ agarose powder (ThermoFisher Scientific). It was then heated in the microwave for approximately 1-2 min until completely dissolved and no crystal structures were visualised.
B. Once the solution cooled down, 8 µl of SYBR® Safe (ThermoFisher Scientific) was added and mixed well, making it possible to visualise the DNA fragments under UV light.
C. A taped gel cast with an appropriate comb was prepared and the solution was subsequently poured into it and left to solidify.
D. The gel was then placed into an electrophoresis tank containing 1x TAE buffer and the comb removed.
E. Eight µl of 1 kb+ DNA ladder was loaded into the first well. This was to identify the molecular size of the DNA fragments.
F. Two µl of 5x Takara DNA loading dye was added to 8 µl of DNA sample, mixed and loaded into the adjacent wells.
G. The electrophoresis chamber was then connected to the power supply and run at 90V for 40 min.

H. The gel was then visualised on the BioRad Gel Doc UV Imager (BioRad, USA) and analysed using Quantity One software (BioRad, USA).
I. The gel containing the TDH fragment was subsequently cut and excised under UV light and used for assembly with PB-TRE3G plasmid as described in part 2.11.1.10.

2.11.1.10. Gel extraction and purification

The Wizard® SV Gel and PCR Clean-Up System Kit (Promega, USA) was used to extract and purify DNA from an agarose gel containing the DNA fragment of interest. The following was the instruction for DNA purification:

A. The gel containing the target DNA fragment was placed on an ultraviolet (UV) lightbox and exposed briefly to the light to visualise the target band.
B. Once visualised, it was then quickly cut and excised.
C. The isolated gel slice was then placed into a 1.5 ml Eppendorf tube and weighed.
D. An equal amount of membrane binding solution was poured into the tube which followed by placing on a 60ºC thermomixer until the gel thoroughly dissolved.
E. Once dissolved, the solution was transferred into an SV mini column and left at RT to incubate for 1 min, so that the DNA had enough time to bind to the column membrane.
F. The minicolumn was subsequently spun down on a mini centrifuge at 14,000 × g, for 1 min, followed by discarding the flow through.
G. The column was then washed with 700 µl of wash buffer and centrifuged at 14,000 × g for 1 minute.
H. Next, the column was centrifuged at 14,000 × g, for 1 min to dry.
I. To elute DNA fragments, the column was placed in a nuclease-free 1.5 ml Eppendorf tube, followed by the addition of 50 µl of nuclease-free water and left for 1 min before spinning down at 14,000 × g, for 1 min.
J. The flow-through solution contained the purified DNA of interest which was then measured by the Nanodrop Spectrophotometer ND-1000 (ThermoFisher Scientific) and stored at -20ºC or used for the next step.

2.11.1.11. PiggyBac Plasmid Ligation

A. A 20 µl ligation reaction was prepared by mixing:
    i. 100 ng of linearized inducible PiggyBac plasmid PB-TRE3G (6.6 kb) (Addgene, USA).
    ii. 60 ng of ‘sticky ends’ TDH fragment (1178 bp).

iii. 2 µl of 5x DNA ligation buffer (Invitrogen)
iv. 1 µl of T4 DNA ligase (Invitrogen)
v. Nuclease-free water up to 20 µl.

A negative ligation control reaction was also prepared which contained water instead of TDH fragment.

B. The ligation reactions were mixed gently and incubated at RT for 2 h.
C. Subsequently, a bacterial transformation was performed as described in section 2.11.1.4. However, Top10 bacteria (ThermoFisher Scientific) were replaced with DH5α (ThermoFisher).
D. Sections 2.11.1.5, 2.11.1.6, 2.11.1.7, 2.11.1.8, and 2.11.1.9 were repeated with this plasmid DNA accordingly.
E. A sample of the purified plasmid DNA was also used for sequencing (section 2.11.1.12) to make sure there were no mutations in the TDH fragment.

2.11.1.12. DNA sequencing

2.11.1.13. Sequencing preparation

Sequencing was performed by Massey Genome Service, New Zealand in a 20 µl reaction volume containing 300-600 ng of plasmid DNA and 4 pmol/L of sequencing primer (Table 7).

Table 7. Primers used for DNA sequencing.

Plasmid	Target DNA	Primer name	Primer (5'-3')
PB-TRE	plasmid	PB-TRE	F: GTACGGTGGGCGCCTATAAA R: GACCTTGCATTCCTTTGGCGAGAG
pGEM	plasmid	M13	F: CCCAGTCACGACGTTGTAAAACG R: AGCGGATAACAATTTCACACAGG

2.11.1.14. Sequencing analysis

The bioinformatics software Geneious, version 8.1 (Biomatter Ltd, New Zealand) was used to analyse sequencing results. Any plasmid containing a mutation was considered unacceptable for further use and therefore discarded. If there was no mutation in the inserted TDH fragment, the colony was used for transfection as follows in section 2.11.1.15.

2.11.1.15. Maxiprep

For transfection of cells, a large quantity of targeted plasmid DNA was required. To produce this amount, large-scale plasmid isolation (600 µg), using the PureLink® Quick Plasmid DNA Maxiprep Kit (Invitrogen, USA) was performed.

A. The day before, bacteria having the plasmid of interest were cultured in a beaker containing 200 ml of LB medium plus 50 µg/ml ampicillin and incubated in a shaker incubator at 37ºC overnight.
B. The following morning, the beaker was removed from the shaker and the bacterial culture was pelleted by centrifugation at 4,000 g for 10 min.
C. The supernatant was removed and the bacterial pellet was resuspended in 10 ml of resuspension buffer containing RNase.
D. The bacteria were then lysed with 10 ml lysis buffer and gently inverted until homogenous.
E. The tube was then incubated for 5 min at RT.
F. 10 ml of precipitation buffer was added to neutralise the lysis reaction and the sample was mixed by gentle inversion.
G. The reaction was subsequently transferred to a HiPure filter maxi column containing a filtration cartridge that had been equilibrated with 30 ml of equilibration buffer.
H. The lysate was allowed to drain by gravity flow, after which the column was washed with 50 ml of wash buffer.
I. The column was then transferred to a 50 ml polypropylene centrifuge tube.
J. 15 ml of elution buffer was added to the column to elute the plasmid DNA through gravitation.
K. 10.5 ml of isopropanol was added to precipitate the DNA, mixed well, then was centrifuged at 20,000 × g, 30 min, 4ºC.
L. After discarding the supernatant, the DNA pellet was washed with 5 ml of 70% ethanol.
M. The tube was then centrifuged at 20,000 × g, for 10 min at 4ºC.
N. Ethanol was decanted and the DNA pellet was left at RT to air-dry for 10 min.
O. The pellet was then resuspended in 200 µl of TE buffer.
P. Subsequently, the plasmid DNA solution was transferred to a sterile 1.5 ml Eppendorf tube and upon measuring the concentration, it was stored at -20ºC.

2.11.1.16. Long-term storage of bacterial clones

Bacterial clones that contained a validated target plasmid DNA were stored long term by freezing in the presence of glycerol. To do this 200 µl of 100% glycerol was added to 200 µl of the bacterial culture containing the plasmid DNA of interest and stored at -80ºC.

2.12. ICM isolation techniques

2.12.1. Triton X-100-based ICM isolation

TX (Sigma-Aldrich)-based ICM isolation is a much faster and inexpensive method for isolating bovine ICM than the current conventional method which uses antibodies against the TE. To isolate intact ICM using TX detergent [141]:

A. Blastocysts were washed in a PBS/PVA solution.
B. Blastocysts were then transferred to pronase (working concentration: 5 mg/ml) solution and incubated for 1 min, resulting in dislodging the zona pellucida.
C. Blastocysts were then placed back into PBS/PVA buffer and washed to neutralize the pronase effect.
D. To remove the zona pellucida, the embryos were gently pipetted up and down.
E. Blastocysts were incubated with 0.2% TX for approximately 3 seconds and then transferred back to PBS/PVA buffer.
F. Blastocysts were pipetted up and down to dislodge TE cells, leaving the ICM intact.

2.12.2. Immunosurgery-based ICM isolation

The technique [142] is the same as differential staining as described in section 2.7.5.1. However, Hoechst and PI stains were not added to the GP complement. In addition, once the embryos were taken out of GP complement, they were put into the PBS/PVA buffer and gently pipetted up and down until all TE cells dislodged.

2.12.3. Primary ICM outgrowth culture procedure

A. The desired number of 8-well chambers were coated with 1% gelatin (Sigma-Aldrich).
B. The coated 8-well chambers containing 200 µL N2B27 culture medium (see Appendix E) were incubated in a humidified modular incubation chamber gassed with 5% CO_2, 7% O_2, and 88% N_2 for 2 h.
C. ICM isolation was then performed by either immunosurgery (IS) or TX-based techniques.
D. Once isolated, the ICMs were transferred into the equilibrated 8-well chambers under the sterile laminar hood.

E. Finally, they were transferred to a humidified modular incubation chamber gassed with 5% CO_2, 7% O_2, and 88% N_2 for 6 days, without refreshing the medium.
F. After 6 days, the ICM outgrowths were ready for further analysis.

2.13. Mechanical isolation of trophectoderm cells

A. A 100 µl drop of HSOF medium without BSA was made in a 3 cm culture dish. This would help embryos stick to the bottom of the dish.
B. D8 bovine blastocysts were placed onto the drop and aligned against the microblade (Bioniche, Animal Health, USA), installed on a bright-field Olympus microscope (Olympus, Japan).
C. The microblade was used to cut the embryo into two pieces consisting of TE and TE+ICM.
D. The TE slice was then picked and used for further analysis.

2.14. Primary trophectoderm culture procedure

The protocol was adopted from [143] with slight modifications as follows:

A. The desired number of 8-well chambers were coated with Geltrex™ (ThermoFisher Scientific) for 30 min prior to culturing.
B. Using pronase, embryos were stripped of their zona pellucida (as described in section 2.12.1) and transferred to DMEM/F12 medium containing 10% FCS, 50 µM 2-Mercaptoethanol (2ME) (Sigma-Aldrich) and 10 µl/ml penicillin/streptomycin (Sigma-Aldrich).
C. They were then cultured in a humidified modular incubation chamber gassed with 5% CO_2, 7% O_2, and 88% N_2 for 6 days, without refreshing the medium.

2.15. Incubation protocol for pharmacological drugs

Pharmacological drugs used in this study were 50 µM Qc1 (Sigma-Aldrich) [11] and 300 µM-4 mM 3-HNV (Sigma-Aldrich) [8] which have been shown to have inhibitory effects on the TDH-mediated threonine-SAM pathway. 3-HNV is a synthetic form of threonine with an extra carbon atom in its molecular structure. When hydrolysed by TDH, instead of producing glycine and acetyl-CoA, it is broken down to glycine and propionyl-CoA.

2.15.1. Bovine embryo treatment

A. LSOF culture dishes containing the desired chemicals were prepared and pre-equilibrated for at least 2 h before transferring embryos.

B. D5 post-IVF embryos were graded and categorised as more than 8 cells, less than 8 cells and one cell and were equally distributed across treatment groups. One cell embryos were discarded.
C. The culture dishes were subsequently placed back into a humidified modular incubation chamber gassed with 5% CO_2, 7% O_2, and 88% N_2 until D8.
D. On D8, the embryos were graded according to the IETS standards described in Appendix E and used for further analysis.

2.15.2. Cell treatment

A. Cells were seeded into dishes as described in section 2.5.2.
B. They were then treated with the inhibitors, followed by placing them back into 38°C incubator for 24 and 48 h, for Qc1 and 3-HNV, respectively.
C. After the incubation time completed, the cells were analysed for the effects of the inhibitors.

2.16. Statistical analysis

Statistical significance was accepted at $P<0.05$ and determined using Fisher's exact test for IVP development and 2-tailed Student′s t-tests for average cell numbers, gene expression, pixel intensity measurements. All bars represent standard error of the mean (SEM).

Chapter 3

3. Chapter Three: Results- role of amino acid metabolism in bovine ICM development and pluripotency

3.1. Targeted amino acid screening on bovine embryos

Amino acid dropout experiments were performed (see section 2.4.1) to determine if bovine ICM development and pluripotency rely on the metabolism of a particular amino acid(s) as it has been shown that mouse and human ESCs depend on threonine and methionine metabolism, respectively [8; 9]. A prerequisite was to optimise the system including determining the best period for amino acid dropout, group vs. single embryo culture, and any critical steps to avoid any amino acid/protein carry-over across treatment groups. The final criteria for performing an efficient amino acid deprivation included culturing bovine embryos from day 5 to day 8, individual embryo culture, washing embryos in PBS/PVA on day 5 change-over, before transferring to the treatment groups. A list of amino acids and BSA concentrations, along with their abbreviations [128] used in this study is provided in Table 8.

Table 8. List of amino acids, abbreviations and concentrations used in this study.

Amino acid	3-letter abbreviation	1-letter abbreviation	Concentrations (µM)
Cysteine	Cys	C	100
Isoleucine	Ile	I	400
Leucine	Leu	L	400
Lysine	Lys	K	400
Methionine	Met	M	100
Phenylalanine	Phe	F	200
Serine	Ser	S	100
Threonine	Thr	T	400
Tryptophan	Trp	W	50
Tyrosine	Tyr	Y	200

Valine	Val	V	400
Bovine albumin serum	BSA	-	8 mg/ml
Glutamax™	Gln		1 mM

3.1.1. Essential amino acids are vital for bovine embryo development

IVF-produced embryos were put into their treatment groups on D5 and graded on D8. All AA dropouts were performed in bSOF (which is an LSOF medium without Gln, BSA, and AAs, explained in section 2.4.1) and depending on the treatment purposes, the targeted AAs were dropped out and the rest added back to the medium. Once BSA was dropped out of the bSOF-BSA-AAs group, Blastocyst (B) grade 1-3 (B^{1-3}) development was not affected ($P>0.05$). However, B^{1-2} development was significantly reduced from 24% in the bSOF_BSA_AAs group to 9% in the bSOF_AAs group ($P<0.05$) (Figure 7). Since AA dropouts were performed in the absence of BSA, the control group is considered bSOF_AAs and all the treatment groups were compared to it. When NEAAs were removed from bSOF_AAs, B^{1-3} development rate did not change ($P<0.05$), However, B^{1-2} development was reduced from 9% to 1% ($P<0.005$). Upon removing EAAs from bSOF_AAs, both B^{1-3} and B^{1-2} embryo developments decreased by 17% and 6%, respectively ($P<0.005$). When the embryos were cultured in bSOF, B^{1-3} development declined from 25% to 6% ($P<0.005$). B^{1-2} embryo development was also significantly reduced from 9% to 0% in the control group ($P<0.005$) (Figure 7).

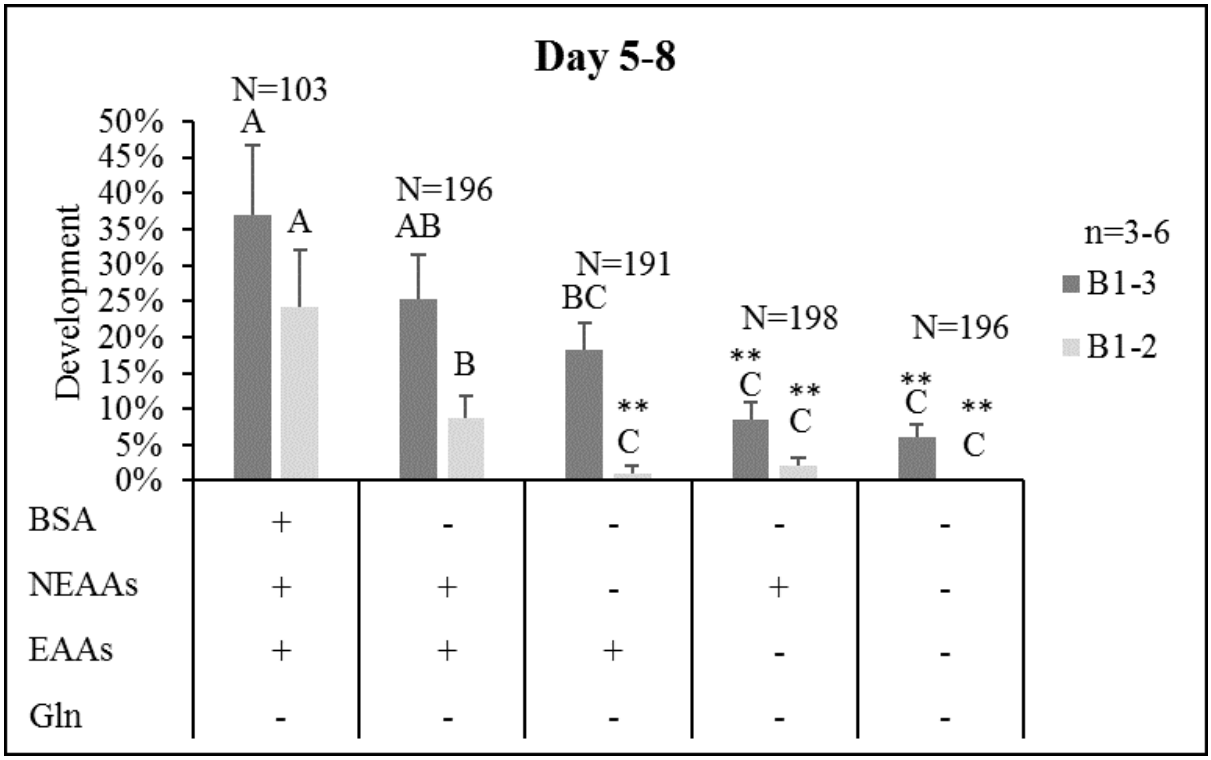

Figure 7. Variations of BSA, glutamax, group EAA and NEAA starvation effects on bovine embryo development cultured individually from D5-8. Before transferring to the treatment groups on day 5, embryos were washed in PBS/PVA buffer to avoid any protein/AAs carry-over into the culture condition-defined treatment groups. N= no. of fertilized embryos placed into IVC. n = no. of independent IVF experiments. The medium was used for this experiment and the following experiments in section 3.1 was base (b) SOF, which is an LSOF medium without Gln, BSA and AAs, explained in section 2.4.1). Error bars = SEM. Fisher's exact test was used to measure significance.** = Groups differ P<0.005 from the bSOF-AAs control group. Means with different letters are significantly different (P<0.05). Grading criteria from Appendix F. BSA= bovine serum albumin, NEAAs= non-essential amino acids, EAAs= essential amino acids, Gln= glutamax.

3.1.2. Threonine starvation/provision does not impact bovine embryo development

Threonine dropout during preimplantation bovine embryo development, from day 5 to 8 was investigated based on a study in 2009 [8] which showed that absence of this essential amino acid from the culture medium of mouse ePSCs led to ceasing colony formation. Bovine embryos were cultured in their treatment groups including bSOF_AAs, bSOF_AAs_ΔThr, bSOF_EAAs_ΔThr, bSOF_NEAAs_Thr, bSOF_Thr, and bSOF_NEAAs. B^{1-3} and B^{1-2} developments in bSOF_AAs_ΔThr and bSOF_EAAs_ΔThr were not different from the bSOF_AAs control group (P>0.05). On the other hand, Thr provision (in the absence of the other 11 EAAs) did not enhance B^{1-3} and B^{1-2} embryo development, with or without NEAAs inclusion, with respect to the bSOF_AAs group (P<0.05) (Figure 8). In summary, Thr deprivation or provision does not affect early bovine embryo development.

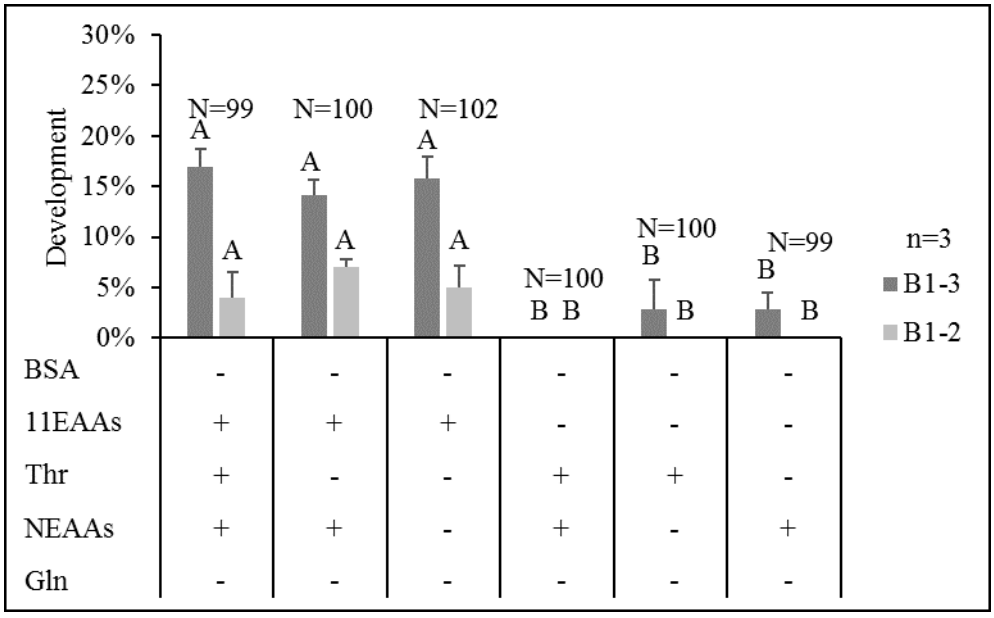

Figure 8. Threonine starvation/provision effect on bovine embryo development cultured individually from D5-8.
N= no. of fertilized embryos placed into IVC. n = no. of independent IVF experiments. Grading criteria from Appendix E. Error bars = SEM. Means with different letters are significantly different, determined by Fisher's exact test ($P<0.05$). BSA= bovine serum albumin, EAA= essential amino acids, NEAAs= non-essential amino acids, Gln= glutamax.

3.1.3. Methionine starvation/provision does not impact bovine embryo development

Methionine metabolism has been shown to be essential for human ESC and in its absence cells stop proliferating [9]. Bovine embryos were cultured in their respective treatment groups including bSOF_AAs, bSOF_AAs_ΔMet, bSOF_EAAs_ΔMet, bSOF_NEAAs_Met, bSOF_Met, and bSOF_NEAAs from day 5 and graded on day 8. With regards to Met dropout in the presence or absence of NEAAs, B^{1-3} development was not statistically different from the bSOF_AAs control group ($P>0.05$). Removing Met from bSOF_AAs did not affect B^{1-2} development, however, when NEAAs and Met were both removed from bSOF_AAs, B^{1-2} development decreased ($P<0.005$). This suggests that this reduction is due to the absence of NEAAs and not Met. On the other hand, supplementing bSOF with Met in the presence or absence of NEAAs did not enhance B^{1-3} and B^{1-2} development ($P>0.05$) (Figure 9). In summary, Met starvation or provision does not affect early bovine embryo development.

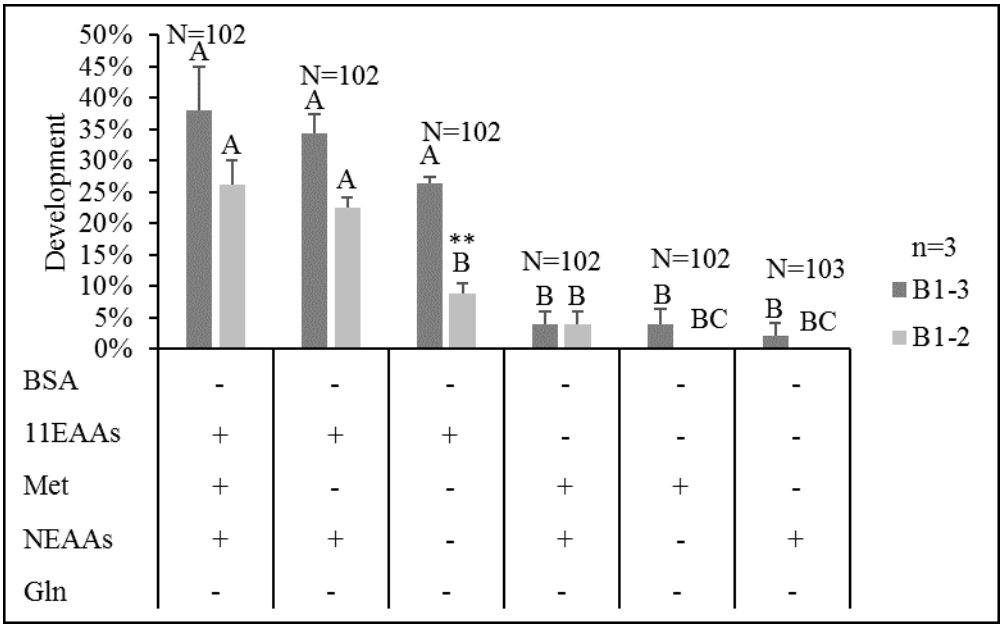

Figure 9. Methionine starvation/provision effect on bovine embryo development cultured individually from D5-8.
N= no. of fertilized embryos placed into IVC. n = no. of independent IVF experiments. Grading criteria from Appendix E. Error bars = SEM. Fisher's exact test was used to measure significance. ** = Groups differ P<0.005, from the bSOF_AAs control group. Means with different letters are significantly different, (P<0.05). BSA= bovine albumin serum, EAAs= essential amino acids, NEAAs= non-essential amino acids, Gln= glutamax.

3.1.4. Dropping out TMCILK group has a more negative impact on embryo development than VYWHFA group

Since Thr and Met absence from the culture medium did not affect bovine embryo development, we aimed to study the effect of other amino acids in a broader scope. Therefore, the EAAs were divided into two groups to examine whether the absence of either of these groups would impair embryo development. It had been already shown that removal of Threonine (in mouse) [8], and methionine, lysine, and leucine (in human) [9] impaired PSC development. Adding isoleucine and cysteine (plays a part in the one-carbon metabolism pathway) to this group (TMCILK), and putting the other 6 including tryptophan, valine, tyrosine, phenylalanine, histidine, and arginine (VYWHFA) in the other group, the effect of group EAAs starvation on the bovine embryos was investigated. When group VYWHFA was omitted from the bSOF_AAs medium, B^{1-3} and B^{1-2} development were not affected significantly compared to the bSOF_AAs control group (P>0.05). Upon omission of TMCILK from bSOF_AAs, B^{1-3} development reduced from 28% to 14% (P<0.005). For B^{1-2} development, there was also a significant reduction from 15% in the bSOF_AAs control group to 5% in the bSOF_AAs_TMCILK group (P<0.05) (Figure 10).

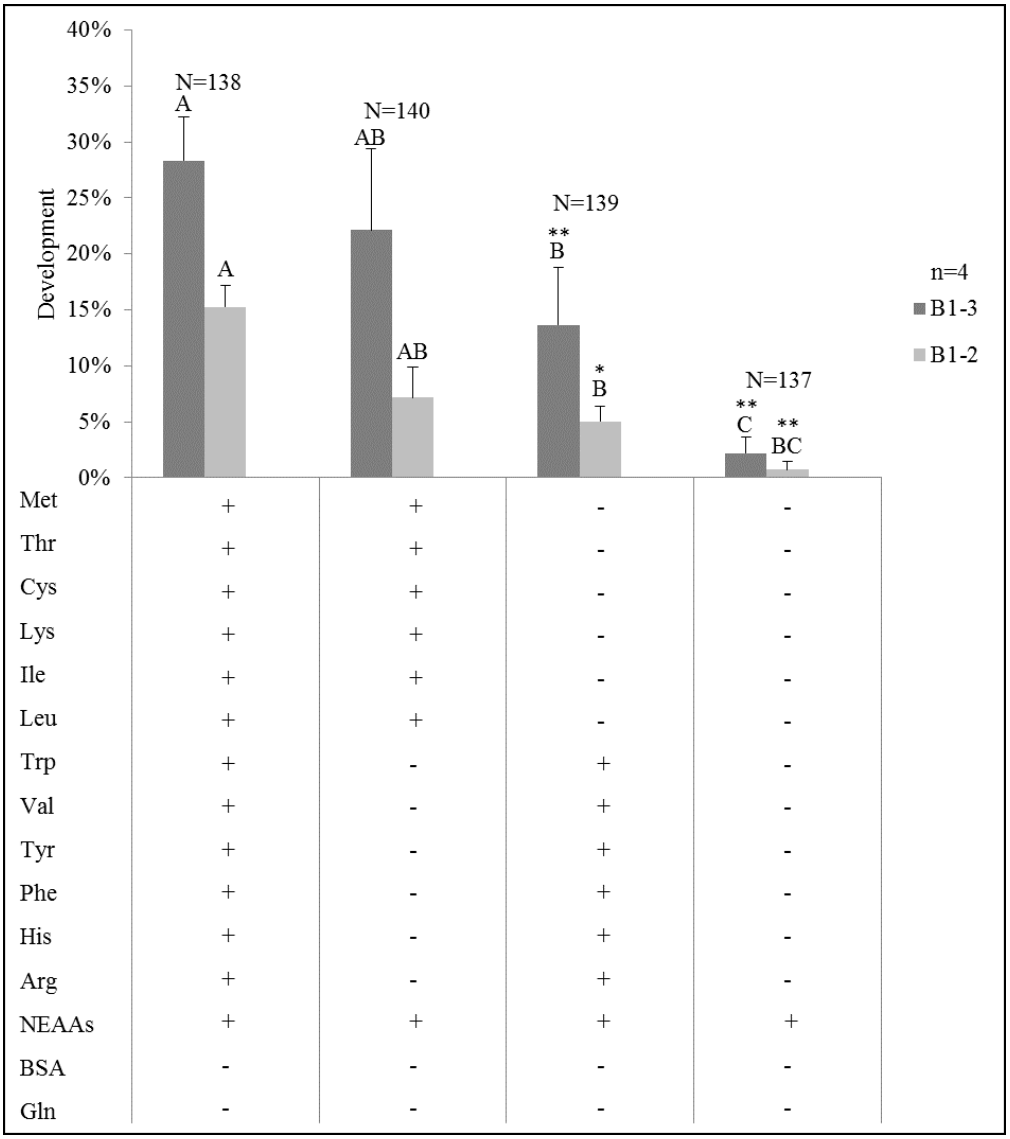

Figure 10. TMCILK omission from the LSOF_AAs medium reduces embryo development significantly.
Bovine embryos were cultured individually from D5-8 in their respective treatment groups.N= no. of fertilized embryos placed into IVC. n = no. of independent IVF experiments. Grading criteria from Appendix E. Error bars = SEM. Fisher's exact test was used to measure significance. *, ** = Groups differ $P<0.05$ and $P<0.005$, respectively, from the bSOF_AAs control group. Means with different letters are statistically different ($P<0.05$). Gln= glutamax.

Since the absence of TMCILK group from the LSOF_AAs culture medium had a more significant impact on embryo development than the removal of VYWHFA group, the TMCILK group was further investigated to see if any pairs or triplets of EAAs would emerge impairing embryo development in their absence.

3.1.5. Pairs and triplets amino acid starvation in the TMCILK group do not impact bovine embryo development

IVF-produced embryos were cultured in their respective treatment groups as indicated in Figure 11. When TM were removed from bSOF_AAs, B^{1-3} and B^{1-2} development did not significantly change ($P>0.05$) (Figure 11). Omitting TC from bSOF_AAs did not affect $B1^{-3}$ and B^{1-2} development relative to the bSOF_AAs control group ($P>0.05$). Culture of embryos in a bSOF_AAs medium without MC did not reduce B^{1-3} and B^{1-2} development compared to the bSOF_AAs control group ($P>0.05$). When TMC amino acids were removed from the bSOF_AAs medium, B^{1-3} and B^{1-2} development were not affected with respect to the bSOF_AAs control group ($P>0.05$). In the bSOF_AAs_ΔLI medium, there was no reduction in B^{1-3} and B^{1-2} development when comparing to the bSOF_AAs control group ($P>0.05$). when LK were removed from bSOF_AAs, B^{1-3} and B^{1-2} development was not reduced relative to the bSOF_AAs control group ($P>0.05$). bSOF_AAs_ΔIK culture did not affect B^{1-3} and B^{1-2} embryo development compared to the bSOF_AAs control group ($P>0.05$). Furthermore, Removing LIK amino acids from the bSOF_AAs medium did not compromise B^{1-3} and B^{1-2} embryo development ($P>0.05$). Supplementing bSOF_NEAAs with TMC amino acids did not stimulate B^{1-3} and B^{1-2} embryo development relative to the bSOF_NEAAs control group ($P<0.005$). The development of B^{1-3} and B^{1-2} was not enhanced in a bSOF_NEAAs medium supplemented with LIK amino acids compared to the bSOF_NEAAs control group ($P<0.05$).

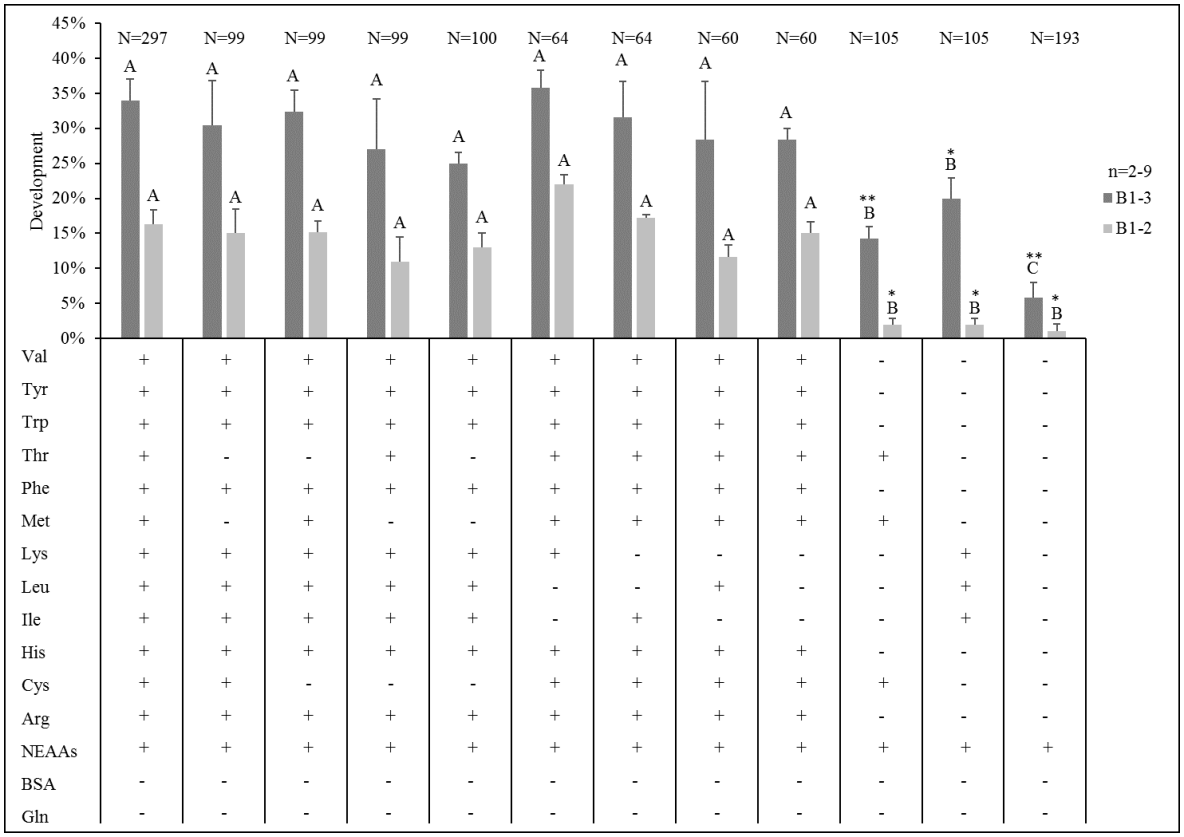

Figure 11. pairs and triplets of EAAs (within TMCLIK group) omission effect on bovine embryo development cultured individually from D5-8. N= no. of fertilized embryos placed into IVC. n = no. of independent IVF experiments. Grading criteria from Appendix E. Error bars = SEM. Fisher's exact test was used to measure significance. *, ** = Groups differ P<0.05 and P<0.005, respectively, from the bSOF_AAs control group. Means with different letters are significantly different (P<0.05).

Overall, the amino acid starvation results show that the omission of any individual, paired, or even triplet AAs did not lead to a significant reduction in bovine embryo development.

3.2. Threonine starvation does not affect mouse embryo development

Since there was no published data regarding the effect of threonine starvation on ICM development in mouse embryos, the validity of the experimental approach adopted during these studies was assessed by carrying out a complementary study using mouse embryos. Mouse zygotes were cultured in their respective treatment groups including commercial M16 (first bar in Figure 12), homemade M16 (bM16_BSA; second bar in Figure 12), bM16_AAs (third bar in Figure 12), bM16_AAs_ΔThr (fourth bar in Figure 12), and bM16_NEAAs (fifth bar in Figure 12). The results showed 46% mouse embryo development in the bM16_BSA medium, which is as good as commercial m16 with 51% mouse embryo development (Figure 12). When BSA in the bM16_BSA was replaced with AAs (bM16_AAs), mouse embryo development reduced by 28% which was significant (P<0.005). This group (the third bar) acted as the

control. When Thr was omitted from the bM16_AAs group, it did not affect mouse embryo development (P>0.05). Depriving mouse embryos of BSA and EAAs resulted in no development (P<0.05).

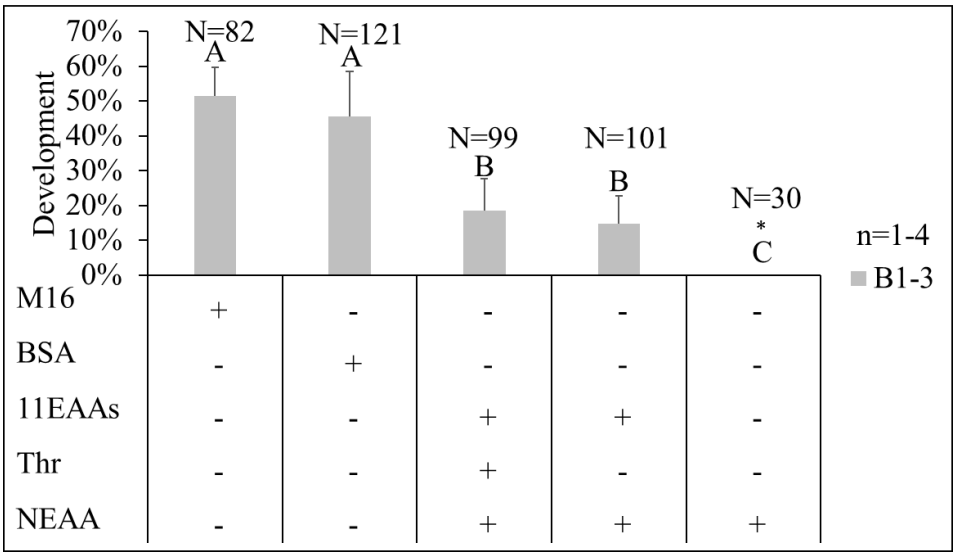

Figure 12. The effect of threonine starvation on mouse embryo development cultured individually from D1-4.
N= no. of fertilized embryos placed into IVC. n = no. of independent IVF experiments. M16 indicates the commercial one. Error bars = SEM. Fisher's exact test was used to measure significance. * = Groups differ P<0.05 from the bM16_AAs control group (the third bar). Means with different letters are significantly different (P<0.05). BSA= bovine albumin serum, EAAs= essential amino acids, NEAAs= non-essential amino acids Thr=threonine.

In summary, single (ΔT, ΔM), pair (ΔTM, ΔTC, and ΔMC), triplets (ΔTMC, ΔLIK), group (ΔVYWHFA) amino acid dropout did not affect bovine embryo development. Only ΔTMCILK culture medium compromised embryo development. This suggests that embryos compensate lack of these essential in other ways. These findings also indicate that starving mouse embryos of threonine does not affect their development. This is in contrast with the findings on the effect of threonine on mouse ePSCs [8]. However, it is in agreement with the findings of this study that threonine absence did not affect bovine embryo development. This may indicate that embryos do not respond to amino acid starvation conditions in the way that PSCs do.

Chapter 4

4. Chapter Four: Results- role of the threonine-SAM metabolic pathway in bovine ICM development and pluripotency (threonine dehydrogenase detection)

4.1. Investigation of threonine dehydrogenase presence in bovine embryos and cells

Previous chapter demonstrated that amino acid dropout on embryos was not the best approach for determining ICM dependence on any amino acid. Because it was observed that mouse embryos, which express TDH were not reversely affected by the mission of threonine. However, it was intriguing to see if the downstream pathway (the threonine-SAM pathway) would be operating in bovine embryos and ICMs. It has been shown that the TDH-mediated threonine-SAM pathway is involved in mouse pluripotency [8]. Acetyl-CoA and glycine are the products of threonine catabolism, in which acetyl-CoA contributes to the TCA cycle while glycine contributes to the production of SAM and subsequent trimethylation of the H3K4 epigenetic marker. This epigenetic change eventually activates genes associated with mouse pluripotency [10]. Blocking this pathway leads to mouse ePSC death [11]. In this section, the presence of TDH enzyme in bovine cells and tissues was investigated.

4.1.1. TDH protein overexpression

Since the rabbit polyclonal anti-TDH antibody available to be used in this study was raised against mouse TDH peptides [8], it was necessary to confirm if it cross-reacts with bovine species as mouse and bovine TDH proteins are not identical (Figure 14). Aligning the sequences of 2 mouse peptides (epitopes), used for generating the TDH antibody [8], against bovine TDH protein sequence indicated that epitope 1 had 2 amino acid mismatches, whereas epitope 2 had 4 mismatches (Figure 13). Therefore, it was necessary to determine if this mouse polyclonal TDH antibody was able to recognize the bovine TDH protein. This was achieved by overexpression of the bovine TDH protein in a suitable expression vector, which is described in the following sections.

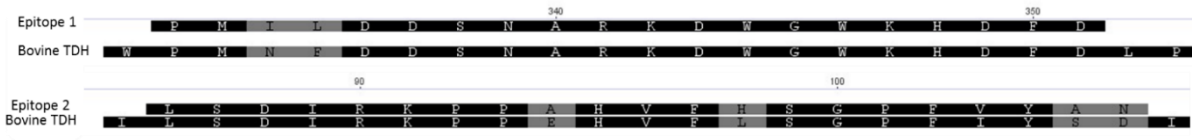

Figure 13. Mouse epitope sequences, used to produce rabbit anti-TDH polyclonal antibody, are aligned against the bovine TDH sequence.
Black boxes indicate amino acid agreements and grey boxes indicate disagreements against the bovine TDH protein (NP_001039569). Antibody peptides sequences are from [8]. Ab= antibody.

4.1.1.1. Protein sequencing

TDH is a nuclear-encoded mitochondrial enzyme. This protein is synthesised in the cytoplasm and imported into mitochondria [144]. Using the NCBI database, mouse and bovine TDH proteins were aligned and, as shown in Figure 14A, blast [145] shows 82% identity between these two proteins. Using Geneious software, TDH protein sequences of mouse, bovine and human were aligned for protein sites to be depicted (Figure 14B). The figure shows highly conserved protein sites of bovine against the mouse species, whereas, in the human, most of the protein sites have disappeared leaving a truncated protein which is non-functional [146].

A.

Score	Expect	Method	Identities	Positives	Gaps
613 bits(1580)	0.0	Compositional matrix adjust.	305/373(82%)	328/373(87%)	0/373(0%)

```
Query  1    MPVVRVLRRVACWMLQSPACGCRAPVLPSRFLGTSPRQIPMDANFHSTSFSEADQQRVLI  60
            M  + +L++V     QS A  CR  VLP +FLGTS  +IP DANFHSTS SEA+  RVLI
Sbjct  1    MLFLGMLKQVVNGTAQSKASSCRKLVLPLKFLGTSQHRIPADANFHSTSISEAEPPRVLI  60

Query  61   TGGLGQLGVGLASFLRKRFGKDNVILSDIRKPPEHVFLSGPFIYSDILDYKNLREIVVNN  120
            TGGLGQLGVGLA+ LRKRFGKDNVILSDIRKPP HVF SGPF+Y++ILDYK+LREIVVN+
Sbjct  61   TGGLGQLGVGLANLLRKRFGKDNVILSDIRKPPAHVFHSGPFVYANILDYKSLREIVVNH  120

Query  121  RITWLFHYSALLSAVGEANVSLARAVNITGLHNVLDVAAEHGLRLFVPSTIGAFGPTSPR  180
            RI+WLFHYSALLSAVGEANVSLAR VNITGLHNVLDVAAE+ +RLFVPSTIGAFGPTSPR
Sbjct  121  RISWLFHYSALLSAVGEANVSLARDVNITGLHNVLDVAAEYNVRLFVPSTIGAFGPTSPR  180

Query  181  NPTPDLCIQRPRTIYGVSKVHAELMGEYYYYRYGLDFRCLRYPGIISADSQPGGGTTDYA  240
            NP PDLCIQRPRTIYGVSKVH ELMGEYYYYRYGLDFRCLRYPGIISADSQPGGGTTDYA
Sbjct  181  NPAPDLCIQRPRTIYGVSKVHTELMGEYYYYRYGLDFRCLRYPGIISADSQPGGGTTDYA  240

Query  241  VQIFHEAVKNGRFECNLKPDTRLPMMYIDDCLRATLEVMEAPAESLSMRTYNISAMSFTP  300
            VQIFH A KNG FECNL+  TRLPMMYI DCLRATLEVMEAPAE LSMRTYNISAMSFTP
Sbjct  241  VQIFHAAAKNGTFECNLEAGTRLPMMYISDCLRATLEVMEAPAERLSMRTYNISAMSFTP  300

Query  301  EELAQEVLKHVPELQVTYNVDPVRQAIADSWPMNFDDSNARKDWGWKHDFDLPELVTTML  360
            EELAQ + KH P+ Q+TY VDP+RQAIA+SWPM  DDSNARKDWGWKHDFDLPELV TML
Sbjct  301  EELAQALRKHAPDFQITYCVDPLRQAIAESWPMILDDSNARKDWGWKHDFDLPELVATML  360

Query  361  NFHGSESRVAQAN  373
            NFHG  +RVAQ N
Sbjct  361  NFHGVSTRVAQVN  373
```

B.

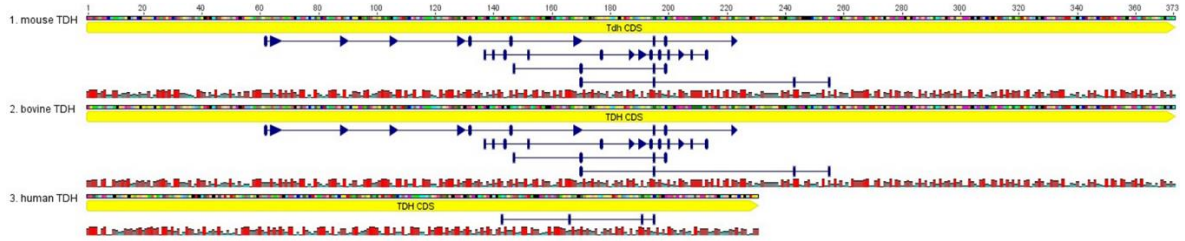

Figure 14. TDH protein sequences in mouse, bovine and human species. **A**) Comparison of mouse and Bovine TDH protein sequences shows 82% similarity. Query= mouse, subject= bovine. **B**) Unlike human gene which produces a truncated and non-functional TDH protein, mouse and bovine show more similarity in their TDH protein structure. Yellow bars= coding DNA sequence (CDS), blue arrows= protein sites, coloured columns= hydrophobicity of each amino acid.

4.1.1.2. Generation of inducible TDH expression plasmids

4.1.1.2.1. pGEM®-TDH plasmid cloning

To add sticky ends to the TDH fragment (see section 2.11.1.1), it was first cloned into an intermediary plasmid pGEM®, before cloning into the main plasmid PB-TRE (Figure 15A). Once cloned and purified as described in section 2.11, the pGEM-TDH plasmids were digested with restriction enzymes (Figure 15A), and the bands were visualised by gel electrophoresis. Following digestion, two DNA fragments were identified: i) one at 3 kb for pGEM backbone, ii) one at 1.2 kb for TDH fragment (Figure 15B). As depicted in Figure 15b, of 6 colonies, 5 showed the expected band sizes. To identify any point mutations in the TDH fragment, the plasmid DNA was sequenced (see section 2.11.1.14) using M13 forward and reverse primers (Table 7). Sequencing results confirmed that the cloned TDH fragment remained unchanged and free from any mutations in all tested clones. Therefore, clone #6 was randomly selected for making PB-TRE-TDH plasmid (Data not shown).

A.

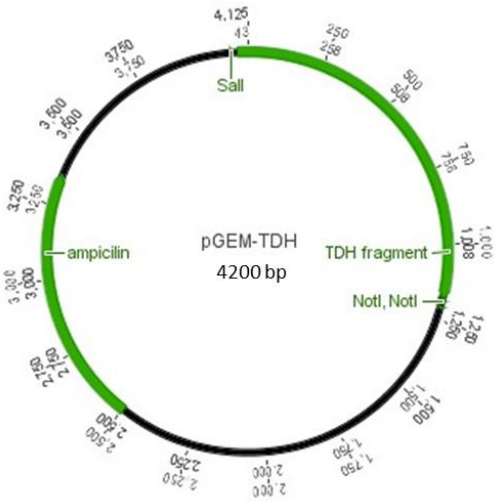

B.

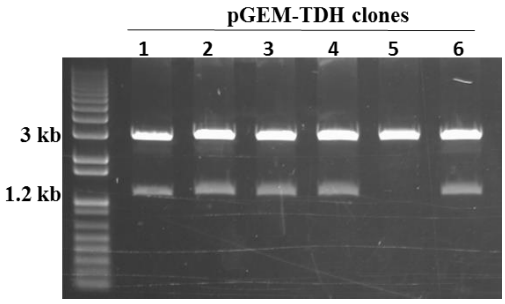

pGEM plasmid= 3kb

TDH fragment= 1.2 kb

Figure 15. SalI/NotI restriction digestion of the pGEM-TDH plasmid.
A) Schematic of the pGEM-TDH plasmid showing the approximate positions of the SalI and NotI restriction enzyme cut sites. **B**) an agarose gel of a SalI/NotI restriction digestion showing that all bacterial pGEM-TDH clones (3 kb) correctly ligated the TDH fragment (1.2 kb) except for #5 that did not show any TDH fragment. TDH fragment from clone #6 was randomly chosen for cloning into PB-TRE plasmid.

4.1.1.2.2. PB-TRE-TDH plasmid cloning and validation

Following the sequencing results, the confirmed #6 TDH fragment was excised and used for cloning into the inducible PB-TRE plasmid (section 2.11). Plasmid validation was subsequently performed by digesting the PB-TRE-TDH plasmids with appropriate restriction enzymes as shown in Figure 16A. The expected bands in the clones were; i) 6.6 kb for PB-TRE backbone and ii) 1.2 kb for TDH fragment. Of the 6 plasmid clones, 5 had the desired bands and one had an incorrect band size (Figure 16B). To confirm that no point mutations had been introduced, these 5 plasmids were sequenced (see section 2.11.1.14) using the primers listed in Table 7. As shown in Figure 16C, colony #5 showed no mutations. Therefore, colony #5 was used for cell transfection in the subsequent experiments.

A.

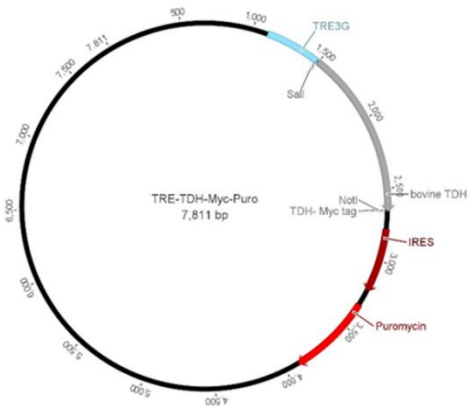

B.

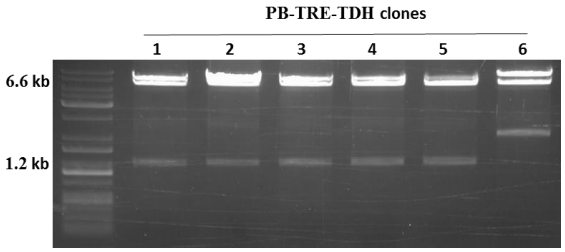

PB-TRE plasmid= 6.6 kb

TDH fragment= 1.2 kb

C.

Figure 16. SalI/NotI restriction digestion of the PB-TRE-TDH plasmid. **A**) Schematic of the PB-TRE-TDH plasmid showing the approximate position of the SalI and NotI restriction enzyme cut sites. **B**) An agarose gel of a SalI/NotI restriction digestion on PB-TRE-TDH bacterial clones. 5 out of 6 bacterial clones gave rise to two bands, one at 6.6 kb (PB-TRE backbone) and one at 1.2 bp (TDH fragment). **C**) Electropherogram of TDH fragment of clone #5 showing no point mutations in the sequence. This clone was selected for mammalian cell transfection.

4.1.1.2.3. Transfection of EF5-TET cells with PB-TRE-TDH

4.1.1.2.3.1. Transient transfection

For PB-TRE-TDH transfection, the bovine EF5-TET line was chosen since it already contained the rtTA transgene required for inducible expression. Two groups including a group with no Dox (-Dox) and one non-transfected EF5-TET cells were included as controls. After 48 h, the cells were stained with the rabbit polyclonal TDH antibody. As it is shown in Figure 17, IF showed an strong signal of TDH enzyme in the +Dox group. This was co-localised with a Myc-tag that was attached to the C-terminus of the TDH fragment. In contrast, there was no positive signal in either –Dox or non-transfected groups (Figure 17).

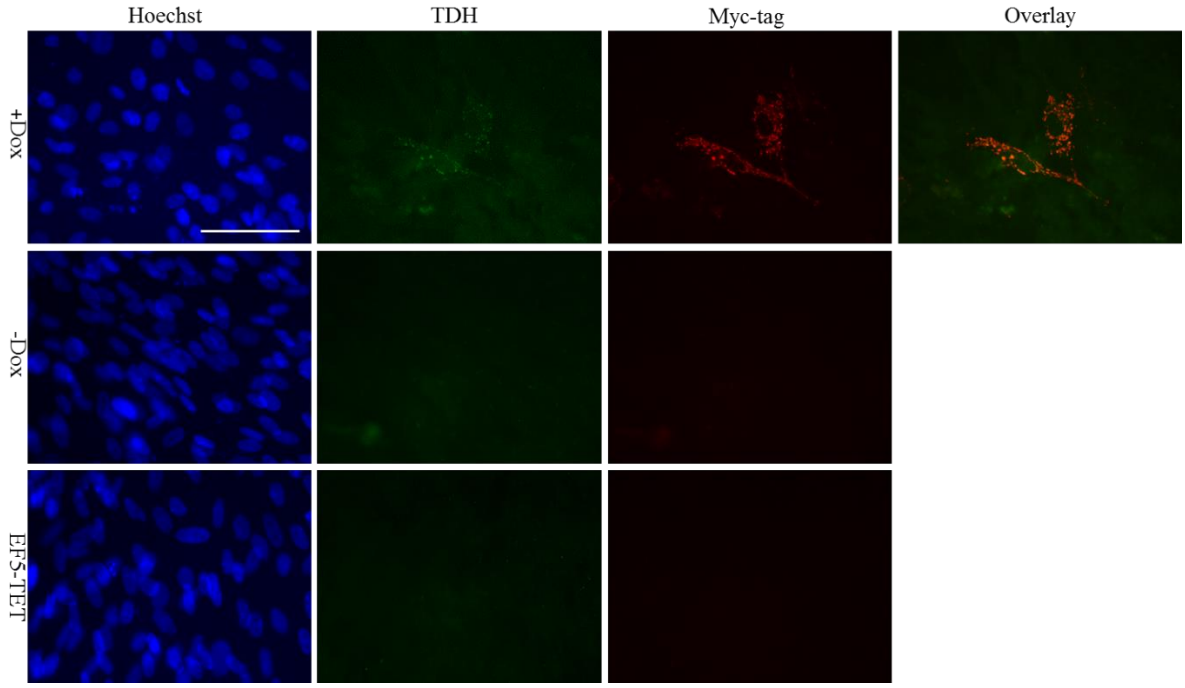

Figure 17. Immunostaining of TDH enzyme in the transient transfected bovine EF5-TET cell line.
Transfected cells in the presence of Dox express TDH protein after 48 h. TDH signal was co-localised with a Myc-tag protein attached to the C-terminus of TDH protein. Images were pseudo coloured using ImageJ software. The dilution for the polyclonal TDH antibody raised in rabbit was 1:500. Hoechst DNA stained blues, TDH stained with Alexa Fluor® 488 (green) and Myc-tag stained with Alexa Fluor® 568 (red). The merged image consists of green and red channels. Scale bar = 100 µm.

4.1.1.2.3.2. Making a PB-TET-TDH stable cell line

Along with the cells used for transient transfection, some more EF5-TET cells were transfected for generating a stable cell line. The groups, media, and components were identical to transient transfection described in section 4.1.1.2.3.1, however, 48 h post-transfection, base media and doxycycline were refreshed on all dishes and the selection antibiotic, puromycin was added at concentration of 1 µg/ml. The media was refreshed every 48 hours up to the second passage, ensuring that they were under puromycin selection for approximately two weeks. They were then either frozen for storage or collected for further analysis as below.

To confirm stable transfection of cells, EFT5-TET-TDH stable cells were seeded on coverslips for performing an IF against the TDH protein. To make sure this protein is localised to mitochondria, the cells were co-stained with anti-TDH antibody and a Mitotracker Red CMXRos (Molecular Probes M-7512, Oregon, USA). The results indicated specific staining of TDH protein, which was co-localised, with the mitochondrial staining, denoting that the protein is located in mitochondria (Figure 18). The TDH signal has a punctate and speckle-like

structure that spread across the cytoplasm, co-localised with the mitochondria. These results showed that EF5 cells had incorporated the TDH gene into their genomic content, and the TDH protein was being expressed. As expected, no positive signal was detected in the no primary antibody control group.

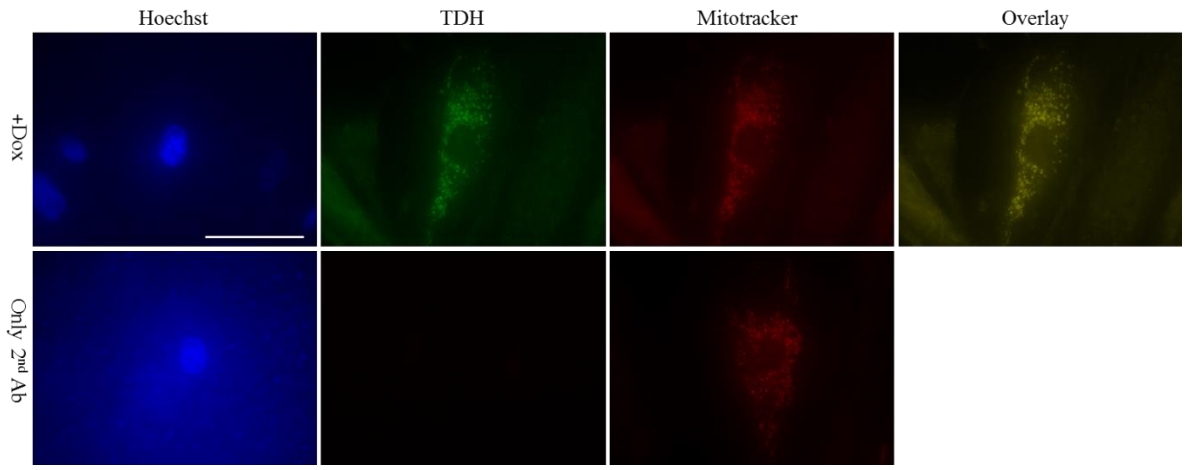

Figure 18. Immunostaining of TDH enzyme in the stably transfected bovine EF5-TET cell line.
Transfected cells in the presence of Dox express TDH after 14 days under puromycin selection. TDH signal was co-localized with a mitotracker indicating mitochondrial localisation of this protein. Images were pseudo coloured using ImageJ software. The dilution for the polyclonal TDH antibody raised in rabbit was 1:500. Hoechst DNA stained blue, TDH stained with Alexa Fluor® 488 (green) and mitotracker (red, Excitation⁄Emission= 579/599). The merged image consists of TDH and mitotracker channels. In the negative control, samples were incubated only with the secondary antibody. Scale bar = 200 μm.

To further confirm TDH protein expression in the stably transfected cell line, some samples including mouse ESCs, ± Dox (PB-TRE-TDH), and EF5-TET cells were collected for western blotting. Mouse ePSCs were used as positive control. As shown below (Figure 19) in the + Dox group there was a band appearing at 38 kilodaltons (kDa), whereas, the band in the positive control was slightly lower than + Dox band. This discrepancy is due to extra amino acids of Myc-Tag protein attached to the C-terminus of TDH protein. The –Dox group also showed a band that was not expected to be present since there was no Dox to trigger the protein expression. Nevertheless, this could be explained by the leaky expression of plasmid DNA [147]. In contrast, there was no expression of TDH protein in the non-transfected EF5-TET. Overall, these findings confirm that the mouse anti-TDH antibody specifically recognizes bovine mitochondrial TDH enzyme and therefore, in addition to the mouse, it cross-reacts with TDH in bovine cell types as well.

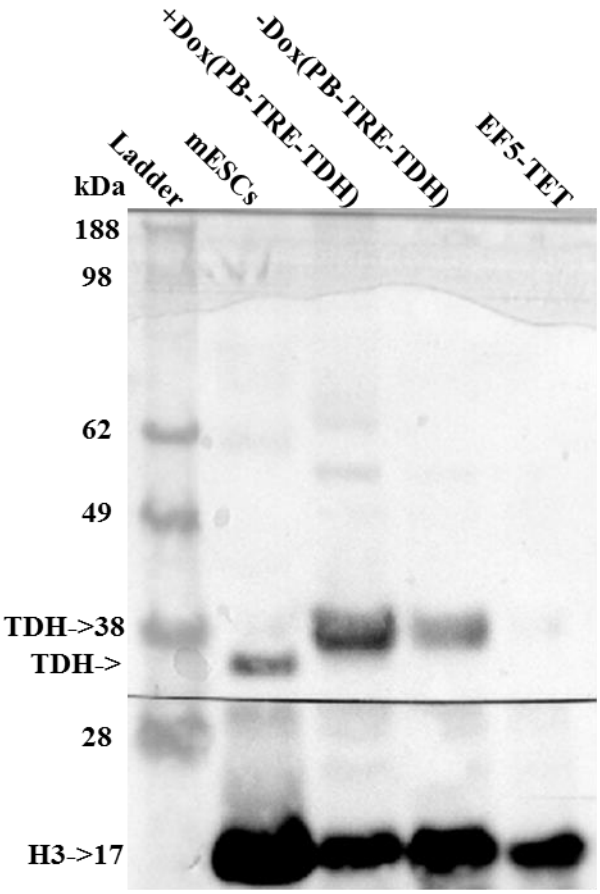

Figure 19. Representative western blot analysis of TDH for transfected EF5-TET cell line.
mESCs served as a positive control with the expected band at 37 kDa. The discrepancy between the positive control and other groups is due to extra amino acids of Myc-Tag protein attached to the C-terminus of bovine TDH protein. A non-transfected EF5-TET served as negative control. The exposure time was 10 seconds. n=3. kDa= kilodalton, TDH=threonine dehydrogenase, H3= histone 3.

4.1.2. Characterisation of ICM outgrowths and TE primary cultures

For cell culture experiments (pharmacological inhibitions), freshly isolated and cultured ICM and TE cells were required. Therefore, it was a prerequisite to characterise these cells before proceeding with any experimental work. This characterisation would help to determine the identity of cells undergoing the following experiments.

4.1.2.1. Isolation of bovine ICM via Triton X-100 and characterisation

The conventional method for ICM isolation involves immunosurgery in which antibodies are used against the trophectoderm cells which are subsequently supplemented with guinea pig complement to dissociate TE cells from ICM [142]. However, since cells are exposed to antibody and guinea pig complement for a relatively long period (approximately 3 h), the gene expression and metabolic profiles of the given samples may undergo some changes. Therefore,

we aimed to develop a technique, which was relatively faster and used fewer components. The TX technique was adopted from a paper published in 2013 [141]. In this procedure, there is no need for antibodies and complement. Instead, detergent TX was employed as described in methodology (see section 2.12.1). The gene expression profile of TX-isolated ICMs was studied and compared it to the gene expression profiles of IS-isolated ICMs and mechanically bisected TEs. ICM marker genes (*NANOG* and *PDGFRα*) and TE markers (*CDX2* and *SOX2*) were used for cell characterisation. Ribosomal *18s* RNA was used as an internal control and for normalising target genes expression data.

Epiblast marker, *NANOG* mRNA was not expressed in the TE group, whereas, both ICM (TX) and ICM (IS) groups expressed this gene at similar levels. This discrepancy was statistically significant ($P<0.05$). Hypoblast marker, *PDGFRα*, was not expressed in the TE group either, while, both ICM (TX) and ICM (IS) groups expressed this gene at similar levels, which was significant relative to the TE group ($P<0.005$).

With regards to TE markers, *CDX2* was expressed in the TE group and was not expressed in the ICM (TX) and ICM (IS) groups. This difference was statistically significant ($P<0.05$). *KRT8* was also expressed in abundance in the TE group and significantly reduced in the ICM (TX) and ICM (IS) groups when compared to TE group ($P<0.005$) (Figure 20).

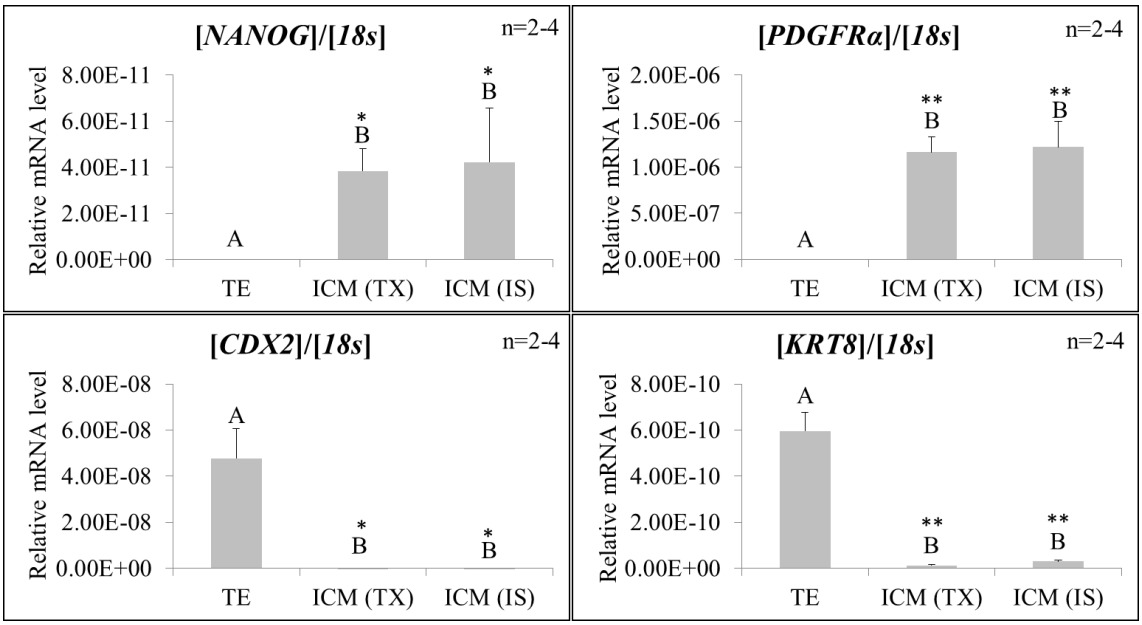

Figure 20. Relative gene expression of lineage-specific markers in the isolated TE and ICM samples.

Values were normalised against 18s internal control and then averaged. Error bars = SEM. Student′s t-test was used to measure significance. *, **= Group differs P<0.05 and P<0.005, respectively, from the TE group. Means with different letters are significantly different (P<0.05). n= no. of independent biological replicates. TX= Triton X-100, IS= immunosurgery.

To confirm the purity of the ICM (TX), it was immunostained against CDX2 and SOX2 markers. The result showed that it was negative to the TE marker, CDX2, while positive for ICM marker, SOX2 (Figure 21).

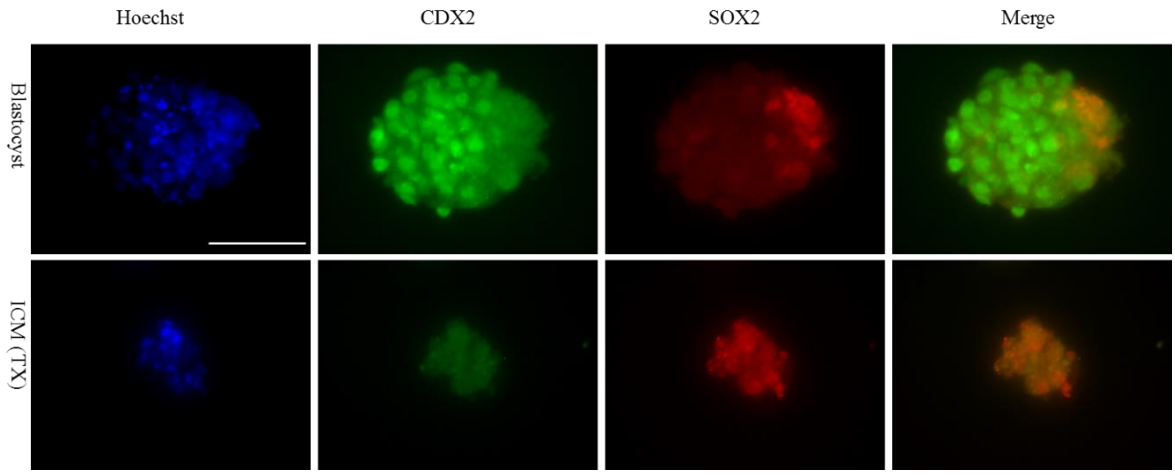

Figure 21. Immunostaining of TX-isolated ICM using CDX2 and SOX2 as TE and ICM markers, respectively. Images were pseudo coloured using ImageJ software. Hoechst DNA stain (blue), CDX2 immunostained with Alexa Fluor® 488 (green), and SOX2 stained with Alexa Fluor® 568 (red). Merged channels consist of green and red channels. TX-isolated ICM was negative for CDX2 and positive for SOX2. A D8 bovine blastocyst was used as a control. n = 3 (no. of biological replicates). N = 67 (no. of isolated ICMs for each group). Scale bar= 100 µm. TX= triton X-100.

TX-isolated ICMs were also cultured to see if they were capable of expanding and forming ICM outgrowths similar to IS-isolated ICMs. In order to do that, IS- and TX-isolated ICMs were cultured for 6 days under identical culture conditions (see Table 23). They were subsequently immunostained with anti -CDX2 and -SOX2 antibodies, for TE and ICM markers, respectively. Immunofluorescence analysis showed that a majority of cells within the TX-isolated ICM outgrowths were SOX2 positive similar to that of IS-isolated ICM outgrowths (Figure 22). Overall, these results indicate that the TX technique is a reliable, faster and cheaper technique than the IS-based method for isolating ICM.

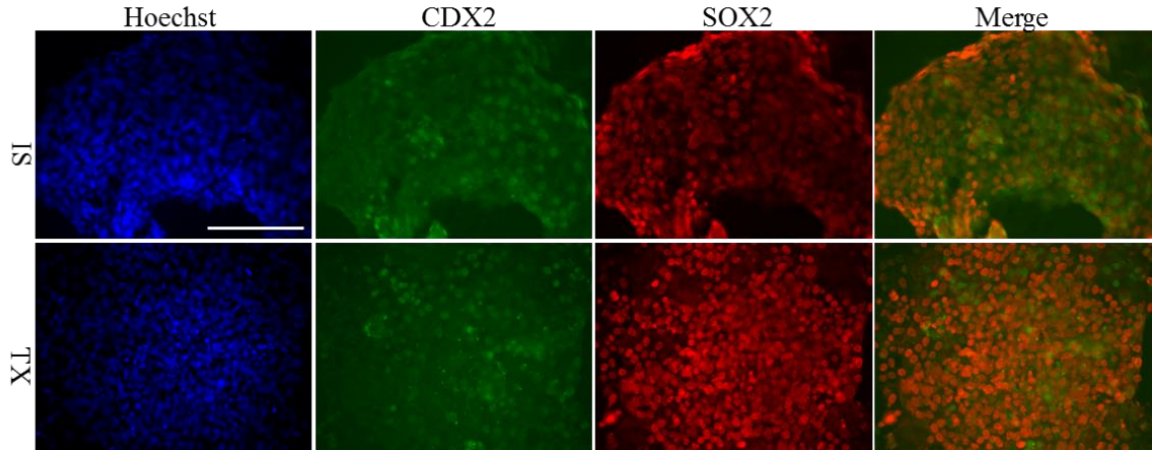

Figure 22. Immunostaining of TX- and IS-isolated ICM outgrowths using CDX2 and SOX2 as TE and ICM markers, respectively.
Isolated ICMs were cultured for 6 days in their conventional culture conditions (Table 23). Hoechst DNA stain (blue), CDX2 stained with Alexa Fluor® 488 (green), and SOX2 stained with Alexa Fluor® 568 (red), taken by an epifluorescent microscope. Merged channels consist of green and red channels. n = 3 (no. of biological replicates). N (no. of cultured ICM outgrowths for each group)= IS:100, TX: 120. Scale bar= 200 µm. IS= immunosurgery, TX= triton X-100.

4.1.2.2. Bovine trophectoderm primary culture and characterisation

The TE primary culture procedure was adopted from a study published in 2004 [148]. D8 bovine blastocysts were cultured in trophectoderm culture medium (see table E) for 6 days (see full detail in section 2.14). On day 6, they were characterised at the protein and lineage-specific gene levels. Phase contrast (PH) photography showed that primary cultures grew as a monolayer with relatively large round cells (Figure 23A). Immunostaining analysis showed that almost all cells within the primary culture stained positive for CDX2. Moreover, none of the cells within the culture stained positive for SOX2 (Figure 23B). Along with TE primary culture, an ICM outgrowth was also stained as a positive control for SOX2 staining.

A.

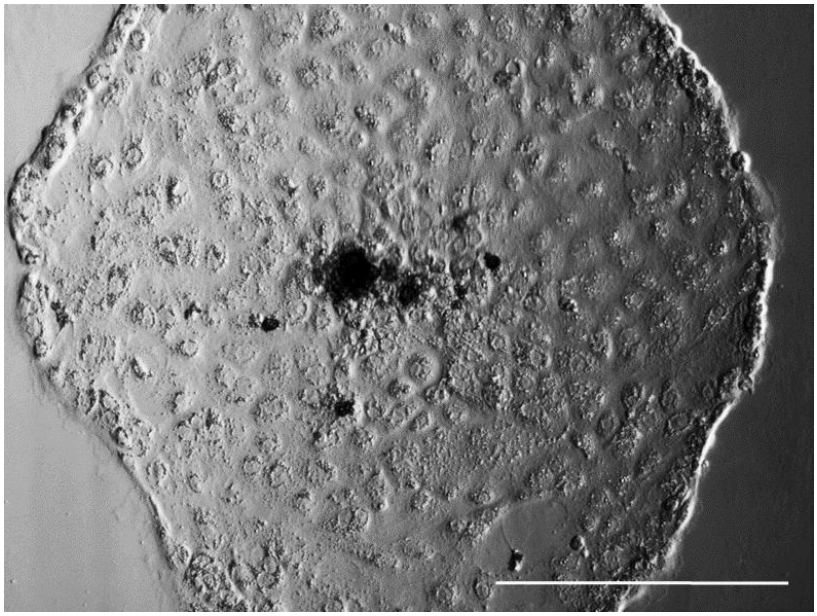

B.

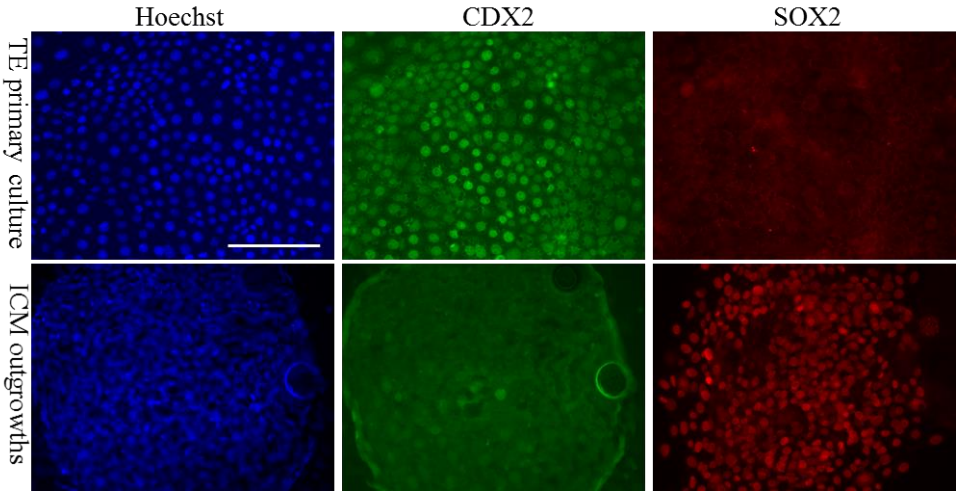

Figure 23. Characterisation of D6 bovine TE primary cultures. **A**) Phase contrast photograph of a D6 TE primary culture. The image was captured by Leica light microscope. Scale bar= 400 µm. **B**) Immunostaining of D6 TE primary culture using CDX2 and SOX2 as TE and ICM markers, respectively. While the TE cell population stained positive for CDX2, it showed no SOX2 positive signal. The ICM outgrowth was used for SOX2 antibody control with a majority of cells stained positive. Photos were taken via epifluorescent microscope. Hoechst DNA stain (blue), CDX2 stained with Alexa Fluor® 488 (green) and SOX2 stained with Alexa Fluor® 568 (red). n = 3 (no. of biological replicates). N = 70 (no. of cultured primary TEs). Scale bar= 200 µm.

In summary, a homogenous TE primary culture can be achieved with this technique (see section 2.14).

4.1.2.3. Chronological comparison of molecular changes in the ICM and TE cultures

Chronological comparison of the ICM- and TE-specific genes was performed to monitor changes in their expression pattern over time. Groups included ICM, D1 and D6 ICM outgrowths, TE, and D6 TE primary cultures. Marker genes consisted of epiblast (*FGF4* and *SOX2*), hypoblast (*PDGFRα* and *SOX17),* and trophectoderm (*CDX2* and *KRT8*) markers.

After 6 days of TE culture, *KRT8* was the only marker whose mRNA level decreased dramatically by 3.5-fold ($P<0.005$) (Figure 24). Upon one day of ICM culture, *SOX17* and *KRT8* mRNA expression changed significantly, whereby *SOX17* was reduced by 6.5-fold ($P<0.05$) and *KRT8* increased by 4-fold ($P<0.005$). When ICMs were cultured for 6 days, all tested mRNA levels changed except for *SOX17* that remained unchanged ($P>0.05$). *SOX2* mRNA expression decreased significantly by 12-fold ($P<0.005$). Likewise, *FGF4* level significantly declined by 5-fold ($P<0.05$). *PDGFRα* also showed a reduction by 5-fold ($P=0.05$). In contrast, *CDX2* and *KRT8* mRNA levels increased significantly by 7- and 13-fold, respectively ($P<0.005$ for both). To summarise, 6 days of TE culture only decreased *KRT8* mRNA level. On the other hand, one-day culture of ICM reduced *SOX17* and increased *KRT8* mRNA levels, while, 6 days of ICM culture reduced epiblast markers, *FGF4* and *SOX2*, hypoblast marker, *PDGFRα*, and increased TE markers, *CDX2* and *KRT8* mRNA levels. These findings indicate that over a 6 day culture, some CDX2- and KRT8- positive cells appear in the ICM culture (also confirmed by double staining of TX- and IS- isolated ICMs in Figure 22.) and the current culture condition is not able to sustain bovine pluripotency for a long time.

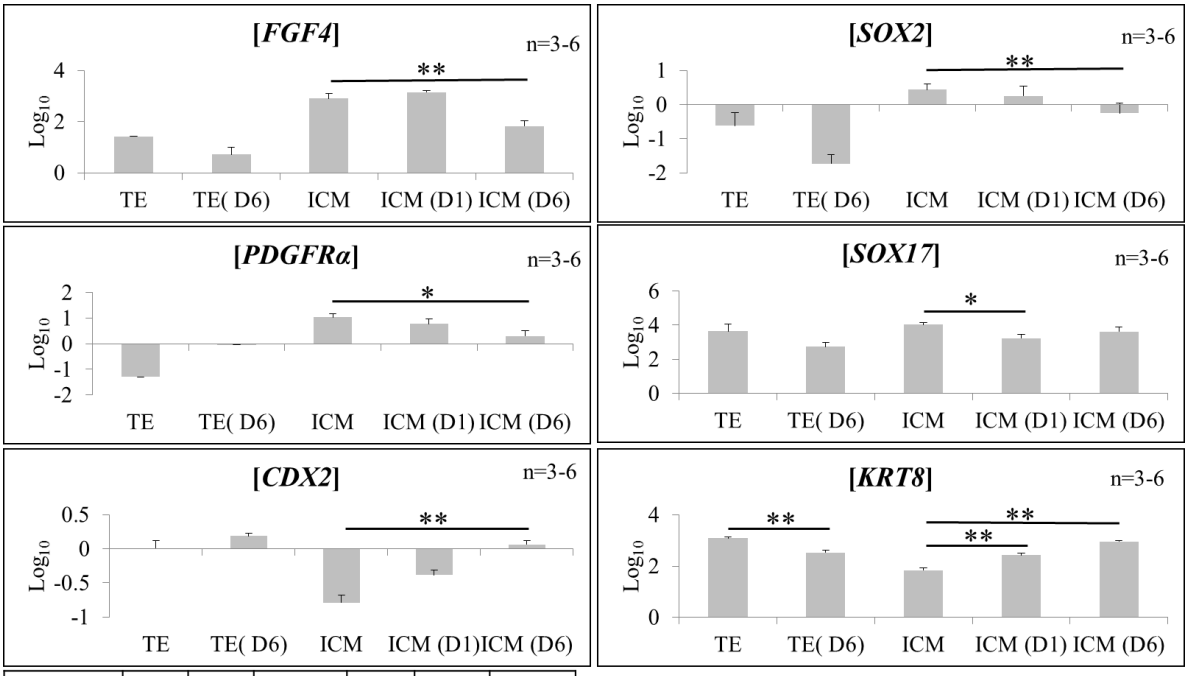

T-test	*FGF4*	*SOX2*	*PDGFRα*	*SOX17*	*CDX2*	*KRT8*
TE vs. TE(D6)	0.406	0.077	0.373	0.150	0.124	0.0006
ICM vs. ICM(D1)	0.424	0.580	0.404	0.033	0.067	0.0006
ICM vs. ICM(D6)	0.003	0.045	0.056	0.325	8.23E-05	1.26E-09

Figure 24. Relative gene expression of lineage-specific markers in bovine ICM and TE primary cultures.
Values were normalised against *18s* internal control, logged and then averaged. Error bars = SEM. *, **= P<0.05 and P<0.005, determined by Student′s t-tests. Red values = P<0.05 and P<0.005 in the table. n = no. of independent biological replicates.

4.1.3. TDH gene and protein expression levels in bovine and mouse cells

4.1.3.1. Relative *TDH* mRNA levels in bovine embryonic and adult tissues

Relative *TDH* mRNA level was measured in D8 bovine blastocyst, ICM, TE, ICM D6, TE D6, bovine muscle fibroblast (bMF), bovine embryonic fibroblast (BEF), liver, testis, brain, heart, kidney, muscle, spleen and skin fibroblasts (LJ801 cell line) as described in section 2.10.4. The results indicated no significant difference between the relative mRNA levels of the whole blastocyst, ICM (control) and TE (P>0.05). The BEF cells showed a 20-fold reduced *TDH* mRNA level in comparison to the ICM group (P<0.05). With regard to adult tissues, muscle fibroblasts, liver, and testis also expressed *TDH* gene. Liver (P>0.05), muscle fibroblasts (P>0.05) and testis (P>0.05) did not show any significant difference in *TDH* mRNA levels relative to the ICM control group. *TDH* mRNA was not detectable in bovine brain, heart, kidney, muscle, spleen and skin cells, which was significantly reduced compared with the ICM group (P<0.05) (Figure 25). In summary, these findings indicate that bovine ICM and TE cells

express *TDH* mRNA at similar levels. Moreover, adult tissues including testis, liver, and muscle fibroblasts also have similar *TDH* mRNA levels to that of ICM.

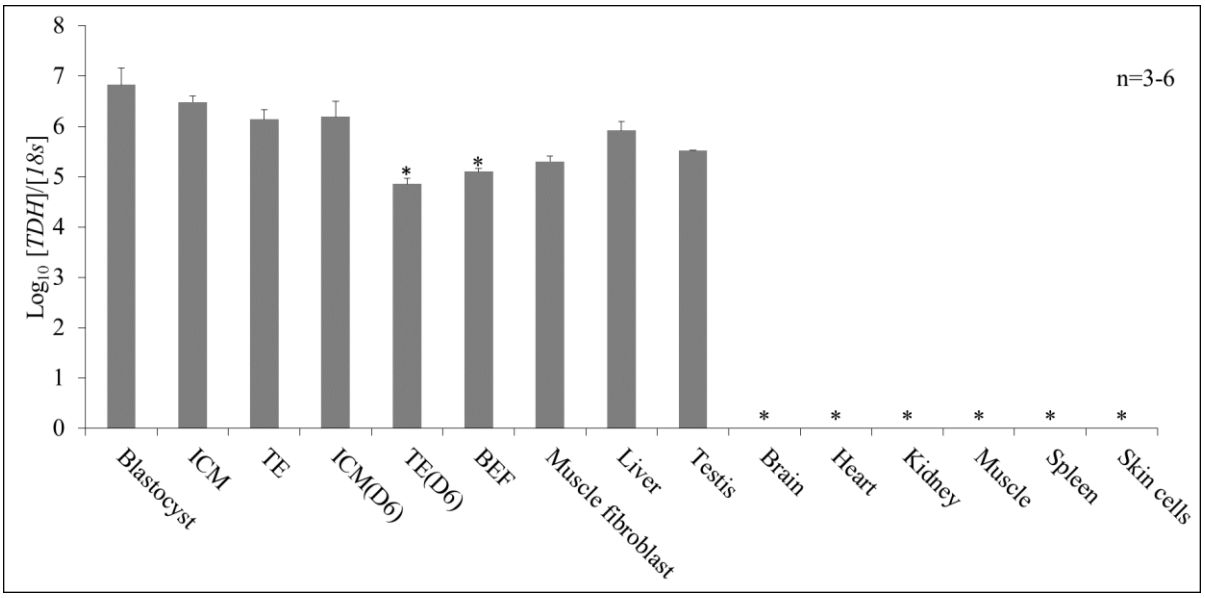

Figure 25. Relative *TDH* gene expression in bovine embryonic and adult tissues.
Values were normalised against *18s* internal control, logged and then averaged. Error bars = SEM. * = Groups differ P<0.05 from the ICM control group. n = no. of independent biological replicates.

4.1.3.2. TDH immunostaining of bovine cells and tissues

To determine if TDH protein was present in the tissues expressing *TDH* mRNA, they were stained with an anti-TDH polyclonal antibody raised in rabbit. Staining of mouse ESCs served as positive control, showed specific TDH signals which were speckle-like structures occupying the narrow cytoplasmic space around the nucleus (Figure 26). However, in the IVF-produced D8 bovine embryos, the signal appeared homogenous across the whole embryo rather than speckle structures observed in the positive control. Nonetheless, the signal was above the background in the negative control sample. The pattern in the bovine embryo resembles the pattern in the photograph published in the paper [8] even though it appears to be only one stack of an image. Regarding D6 ICM outgrowth, the specific signal was present which was also above the background with speckle-like structures occupying the cytoplasmic pre-nucleus space similar to the pattern observed in the mouse ESCs. D6 TE primary culture showed no positive signal compared to the positive control. Furthermore, it appeared to look like the background signal in the negative control. TDH staining in the BEF cells showed no positive signal when compared to the positive control, but rather it looked like the background signal in the negative control.

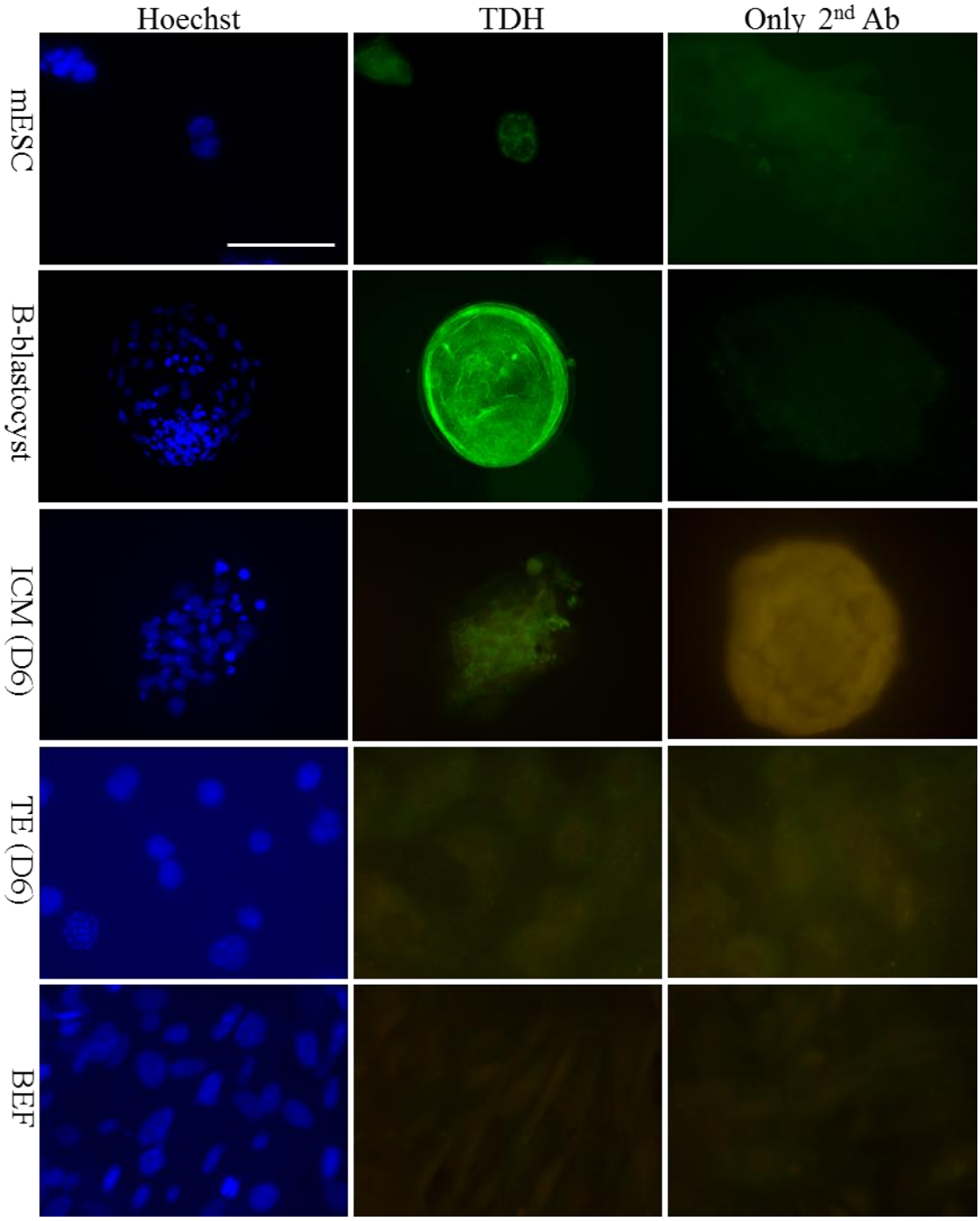

Figure 26. Immunostaining of TDH enzyme in embryonic and adult tissues of bovine and mouse.
Images were pseudo coloured using ImageJ software. Hoechst DNA stain (blue), TDH stained with Alexa Fluor® 488 (green). In the "only 2nd AB" panel, primary antibody incubation was omitted. mESC staining represents a positive control. Scale bar = 100 µm. B= bovine.

4.1.3.3. TDH immunoblotting of bovine cells

To confirm if TDH protein was indeed present in bovine embryonic cells, total cellular protein was extracted as described in section 2.9 from BEF, bMF cells, mouse ePSCs and iPSCs cells

and MEF cells and subjected to WB analysis. IF of mouse ESCs indicated a very strong TDH signal (Figure 26). WB analysis confirmed that both mouse ESCs and mouse iPSCs expressed this protein in abundance (Figure 27). As expected, no band was seen with MEF cells, as these cells do not express any *TDH* gene [8], and served as a negative control. Since it was not possible to collect a large number of bovine embryos for western blot analysis, we had to rely on TDH gene and protein expression (immunostaining) data. BEF and bMF cells were shown earlier to express *TDH* mRNA (Figure 25). BEF cells expressed *TDH* gene but at a significantly lower level than that of ICM (Figure 25). Immunostaining results for BEFs did not show any TDH protein signal (Figure 26). Consistent with this finding, no protein band was detected in the western blot analysis. bMF cells also expressed *TDH* mRNA almost as much as BEF cells, and likewise, they failed to show any TDH protein band with western blotting (Figure 27).

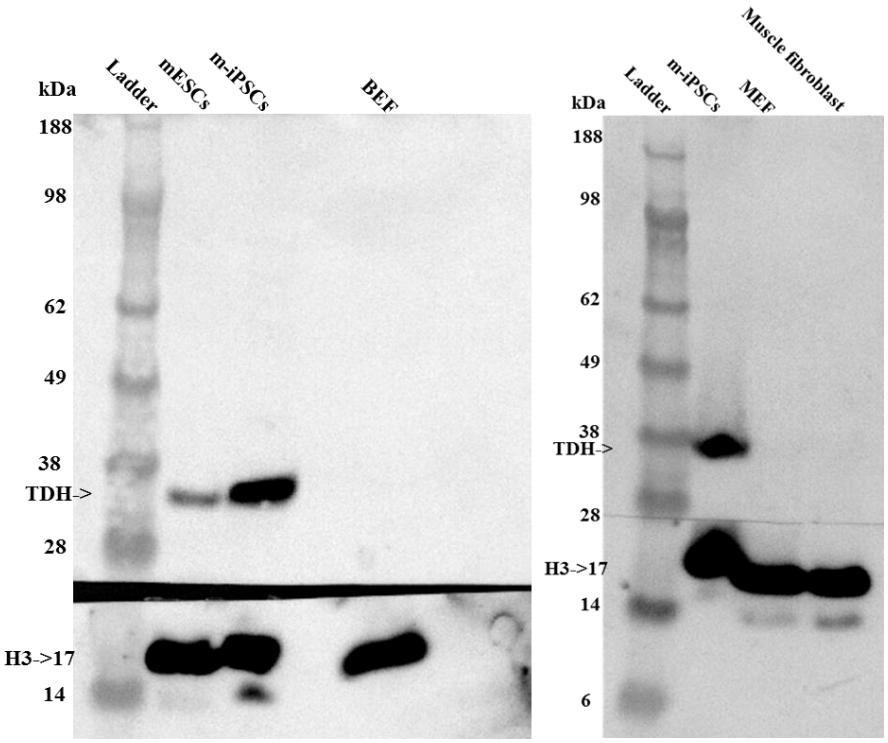

Figure 27.TDH immunoblot of embryonic and adult tissues in mouse and bovine cells.
The blot demonstrated TDH band at 37 kDa in the mESCs (V6.5 cell line, AgResearch, New Zealand) and mouse iPSCs (m-iPSCs) (JMJd2 MEFH1P4 cell line, AgResearch, New Zealand) serving as positive control. However, no TDH band was detectable in BEF and muscle fibroblast cells. Histone 3 (H3) was used as an internal control. The exposure time was 30 seconds.

Overall, findings from TDH gene and protein expression data suggest that TDH is present in D8 bovine blastocysts and D6 ICM outgrowths and disappears from trophectoderm upon

culture for six days. This may indicate that TDH is vital for early bovine embryonic development and bovine pluripotency *in vitro.*

4.1.3.4. *Tdh* mRNA levels in mouse cells

Since there were no published data comparing *Tdh* gene expression levels between mouse embryos and mESCs, *Tdh* gene expression analysis was performed on the cells above using qPCR and was compared with MEF cells, which did not express *Tdh* [8]. After collecting samples, RNA extraction was performed, as described in section 2.10, which was followed by cDNA synthesis and qPCR. After acquiring *Tdh* values, they were normalized against *Gapdh*, as an internal control. When comparing mESCs to mouse blastocysts, *Tdh* expression significantly reduced by 12 fold (P<0.005) (Figure 28). No *Tdh* mRNA was detected in MEF cells, which was significant with respect to the mESCs *Tdh* mRNA level (P<0.005). These findings indicate that *Tdh* mRNA level in mESCs is higher than mouse blastocysts, whereas, it is expressed at similar levels in bovine embryos and ICM.

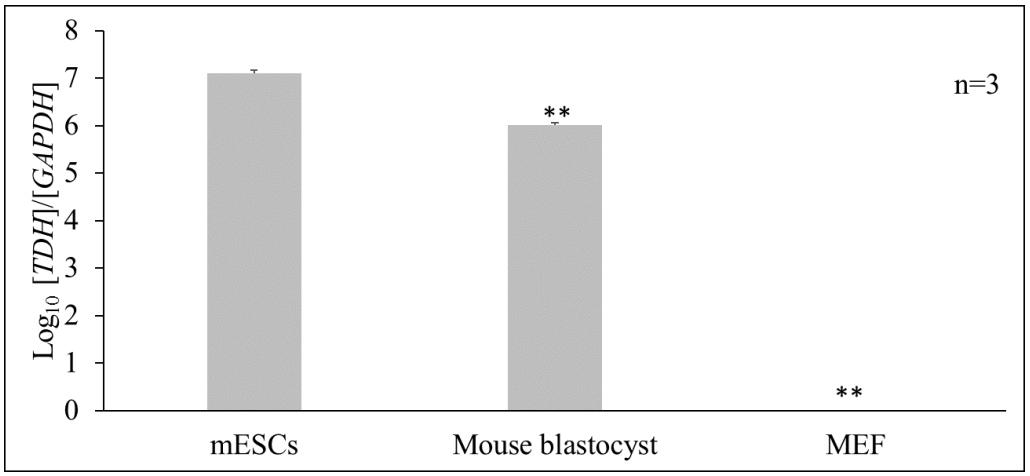

Figure 28. Relative *Tdh* mRNA levels in mouse embryonic tissues and cells.
Values were normalised against *Gapdh* internal control, logged, and then averaged. Error bars = SEM. ** = Group differs P<0.005 from mESCs, determined by Student′s t-test. n = no. of independent biological replicates.

Chapter 5

5. Chapter Five: Results- role of the threonine-SAM metabolic pathway in bovine ICM development and pluripotency (TDH functionality)

In chapter four, it was shown that TDH was detectable in the bovine ICM, D6 ICM in culture, and TE cells. In this chapter, the functionality of the enzyme was investigated using pharmacological inhibition and its effect on downstream intermediates.

5.1. Effect of Qc1 on the TDH-mediated threonine-SAM pathway

TDH enzyme in bovine embryos was knocked down using TDH inhibitor Qc1 and its effect on embryo development, average cell number, autophagy, epigenetic markers, and gene expression profile was measured. As a control experiment and in parallel, the effect of TDH inhibitor Qc1 on the mouse embryo development was also investigated. Finally, the inhibitory effect of Qc1 was probed in bovine cells particularly ICM and TE cultures to determine the role of this pathway in these cells.

5.1.1.1. Qc1 inhibitory effect on bovine embryos

5.1.1.1.1. Qc1 reduces bovine embryo development

Bovine embryos were produced via IVF and were cultured in their IVC culture medium for 5 days as described in section 2.2. On D5, compact morulae were randomly transferred to LSOF medium containing 50 µM Qc1 (according to the concentration used in the paper [8]) and cultured for three days. Grading was performed based on the criteria described in section E of the appendix. With regards to B^{1-3} development, the DMSO control group showed 37% development, whereas, the Qc1-treated group demonstrated 24% development, showing 13% reduction which was significant ($P<0.005$). B^{1-2} development in the DMSO and treatment groups was 19% and 8%, respectively, which was significant ($P<0.005$) (Figure 29). To confirm that the Qc1 effect was not due to general toxicity, a cell line that did not express any *TDH* mRNA, skin fibroblasts, was selected to be treated with Qc1. Skin fibroblast cells were seeded and subsequently treated with 50 µM Qc1 for 24 h. The following day, cell viability was assessed using Hoechst/PI staining as outlined in section 2.7.5.2. The result showed that around 5% of the cells were compromised in the Qc1-treated group, which was not statistically different from the number in the control group (4%; $P>0.05$) (Figure 43). This demonstrates that the inhibitory effect of Qc1 is not due to a general toxic effect.

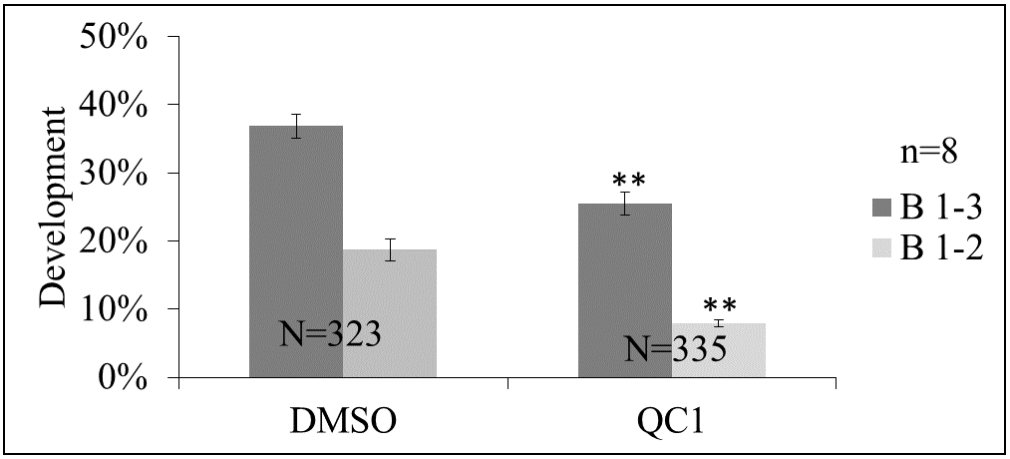

Figure 29. 50 µM Qc1 reduces bovine embryo development.
IVF-produced embryos were treated with Qc1 on D5 and graded on D8. Grading criteria from Appendix E. N= no. of fertilized embryos placed into IVC. n= no. of independent IVF experiments. Error bars = SEM. ** = Group differ P<0.005 from the DMSO control group, determined by Fisher`s Exact test.

5.1.1.1.2. Qc1 reduces ICM and TE cell number in bovine embryos

In this section, the effect of 50 µM Qc1 on the ICM and TE cell numbers was investigated. These cells both express *TDH* mRNA at similar levels. D8 bovine embryos were differentially stained with Hoechst and PI stains as described in section 2.7.5.1, photographed and then analysed using ImageJ software. The average number of ICM cells in the DMSO control group was 19 (±5), whereas, in the Qc1-treated group was 10 (±2), it being significant (P<0.005). In the TE group, the same reducing trend was observed wherein the DMSO control group the average number of cells was 67 (±16) to 37 (±8) in the Qc1 treatment group, which was significant (P<0.005) (Figure 30).

A.

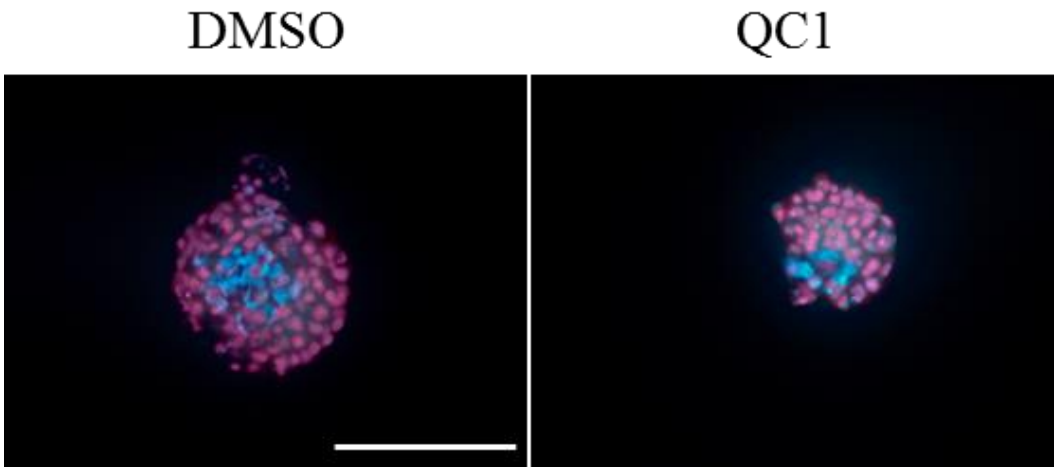

B.

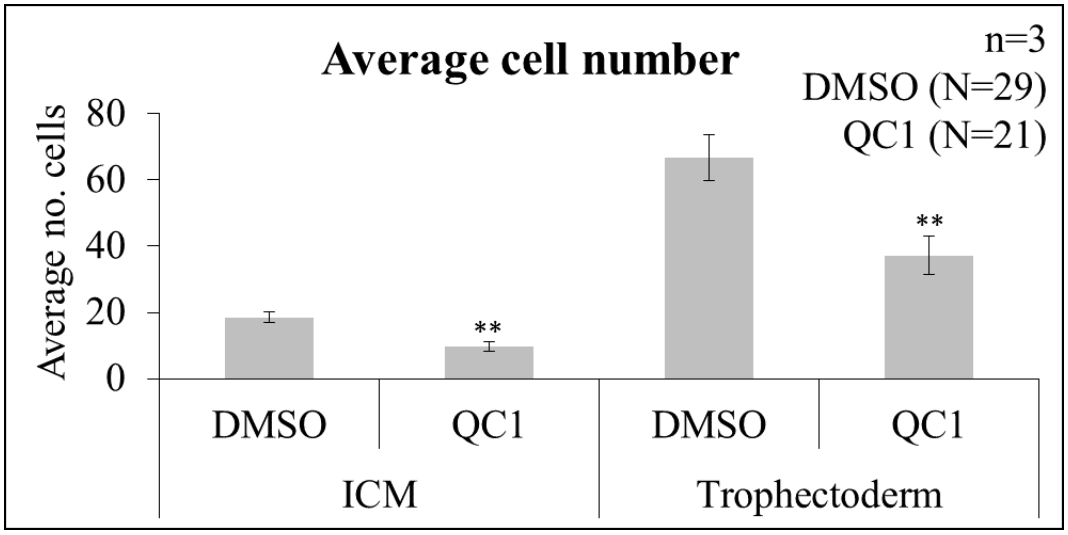

Figure 30. 50 µM Qc1 reduces cell number in both ICM and TE lineages. IVF-produced embryos were treated with Qc1 from D5-8. **A**) Differential staining photographs are representing D8 bovine embryos stained with Hoechst (blue) in ICM and Hoechst& Propidium iodide (PI) (pink) in TE cells. Since their cell membrane was compromised by immunosurgery antibody and the GP complement combination, TE cells were stained with both PI and Hoechst, appearing pink under the microscope, whereas ICM cell membrane remained intact and is only stained blue. Scale bar= 200 µm. **B**) Quantification of Hoechst/PI stained cells in D8 bovine embryos. N= no. embryos used in each treatment group. n= no. of biological replicates. Error bars = SEM. ** = Group differ P<0.005 from the DMSO control group, determined by Student′s t-test.

5.1.1.1.3. Qc1 stimulates autophagy in bovine embryos

It has been shown that inhibiting TDH enzyme led to the death of mouse ePSCs stimulated via autophagy, whereas this did not happen to the more differentiated embryoid bodies [11]. Autophagy is a process of self-cannibalism which provides an internal source of nutrients for generation of energy and thus survival during starvation [82]. Upon deprivation, large

organelles and bulk cytoplasmic proteins are degraded by lysosomes to maintain vital processes [11; 82]. It has been shown that mouse ePSCs underwent autophagy once exposed to Qc1, whereas, this did not happen to the more differentiated embryoid bodies [11]. In this study, the aim was to investigate whether Qc1 stimulates autophagic reactions in bovine embryos. Bovine embryos were incubated with 50 µM Qc1 on D5 and analysed for autophagy reaction on D8 using an Autophagy Detection Kit (Abcam (ab139484), USA). The immunofluorescence dye in the kit, which is a cationic amphiphilic tracer dye, acts by partitioning into cells via passive diffusion. It carefully selects and stains titratable moieties (a functional group of a molecule) preventing its accumulation when incorporated into pre-autophagosomes, autophagosomes, and autolysosomes. The dye is also pH clamped for pre-autophagosomes, autophagosomes and autophagolysosomes, which also means that lysosomes are too acidic and the cytosol too alkaline to accumulate the dye. It will only fluoresce at the specific pH found in the aforementioned vacuoles, but it does not bind to a specific vacuole structure or component.

The results showed that in the Qc1-treated group the signal associated with autophagic vacuoles increased significantly by 1.5 fold when comparing to the DMSO control group ($P<0.05$) (Figure 31). This finding explains why cells in the TE and ICM population disappear upon exposure to Qc1 (Figure 30).

A.

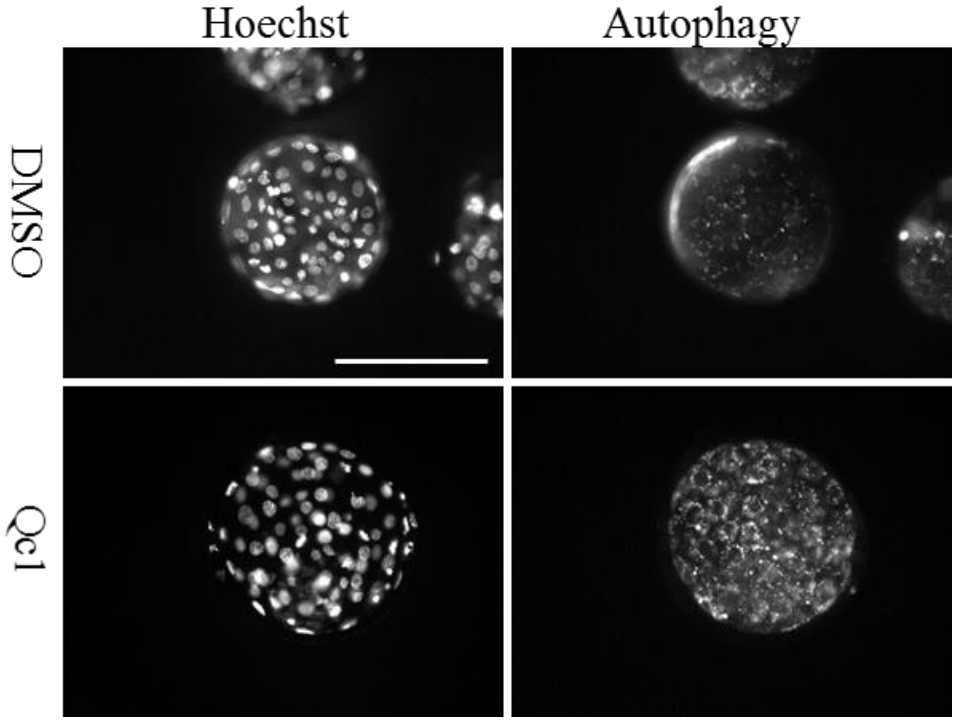

B.

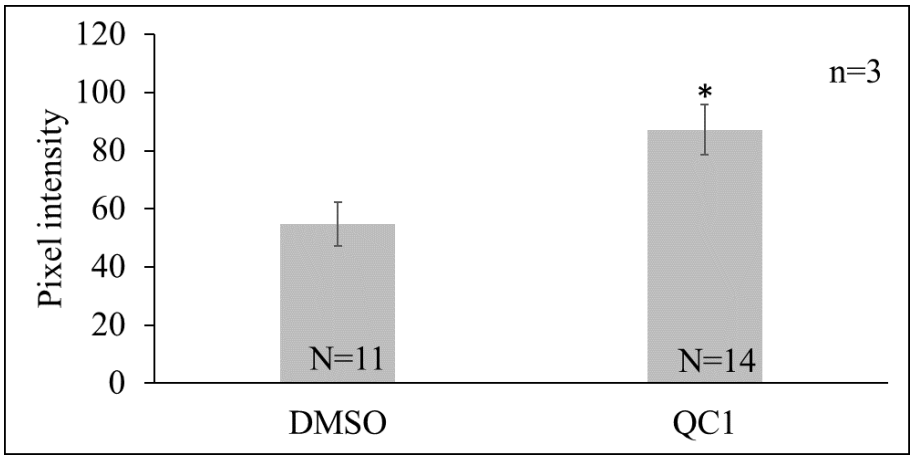

Figure 31. 50 µM Qc1 increases autophagy vacuoles in bovine embryos. IVF-produced embryos were treated with DMSO and Qc1 from D5 and analysed on D8. **A**) Microscopic immunofluorescent analysis showing nucleus (Hoechst) stain and autophagic vacuoles (detecting titratable moieties, a functional group of a molecule) in the Qc1-treated embryos and DMSO control group. The intensity of autophagy signal was enhanced relative to the DMSO control group. Scale bar= 200 µM. **B**) Quantification of immunofluorescence signals of autophagy vesicles in the Qc1 and DMSO control group. The autophagy signal was detected with the Autophagy Detection Kit (Abcam (ab139483), USA) on an epifluorescence microscope. After taking IF photographs, they were opened with ImageJ software and the autophagy signal intensity was quantified. n= no. of biological replicates. N= no. of quantified embryos. Error bars = SEM. * = Group differ $P<0.05$ from the DMSO control group, determined by Student′s t-test.

5.1.1.1.4. SAM/SAH detection is not feasible in bovine embryos

SAM/SAH ratio is a crucial regulator of the epigenetic state of mouse and human ESCs [9; 10]. SAM serves as a universal substrate for DNA and protein methylation. Once donated its methyl groups, it is converted to SAH. SAM/SAH ratio is imperative for regulating methylation levels since methyltransferases activities are inhibited by SAH [10]. Performing routine methods such as liquid or gas chromatography for identifying metabolites within a bovine embryo was not possible since the number of cells within an embryo is very low (150-200 cells) and collecting a large number of embryos is not an easy task. Thus, options were limited to do immunostaining with SAM and SAH antibodies obtained from Arthus Biosystems (USA) and then quantifying their pixel intensity using IF photographs through ImageJ software as described in section 2.8.22.8.2. After trying, it was noted that SAM and SAH molecules were not detectable even with antibodies (Table 2) even though SAM and SAH signals were detectable in the goat fetal fibroblast cells, serving as positive control (Figure 32). This may be explained by the very low abundance of this intermediate product which makes its detection extremely difficult.

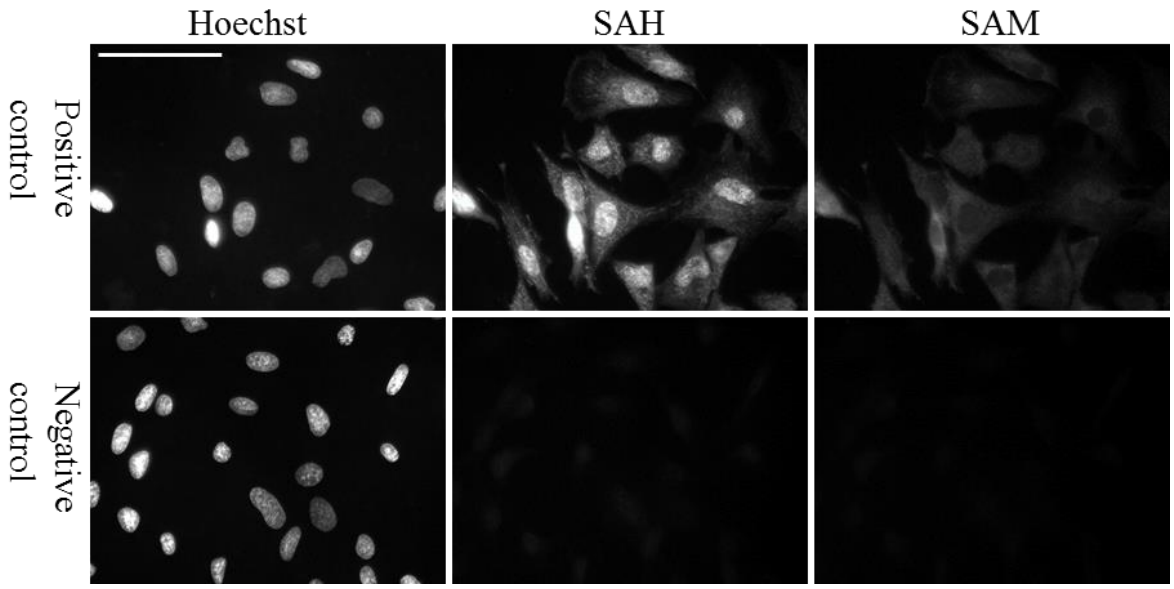

Figure 32. SAM and SAH were detectable in fetal goat fibroblasts. Immunostaining of SAM and SAH molecules in goat fetal fibroblast cells using antibodies from Arthus Biosystems (USA). Hoechst stains DNA. Upper panel represents a positive control with cells expressing both SAM and SAH. The lower panel depicts a negative control without using any SAM and SAH antibodies. Scale bar= 100 μm.

5.1.1.1.5. Qc1 enhances H3K4 trimethylation levels in bovine embryos

It has been shown that in mouse ePSCs threonine metabolism controls H3K4me3 levels via the regulation of SAM/SAH ratio levels [10]. Therefore, the Qc1 effect on the expression levels of epigenetically suppressive markers, H3K9me3 and H3K27me3 and activating marker, H3K4me3, in bovine embryos was investigated. This was determined by IF using anti -H3K4me3, -H3K9me3 and -H3K27me3 antibodies after incubation of bovine embryos with 50 μM Qc1 from D5-8.

IF results of ICM cells showed that H3K4me3 levels significantly increased by 2.3 fold in Qc1-treated embryos compared to the DMSO control group ($P<0.005$) (Figure 33). The intensity of H3K4me3 staining significantly increased in the TE population by 2-fold in response to Qc1 treatment relative to the DMSO control group ($P<0.005$). The H3K9me3 level in the Qc1-treated ICM and TE cells did not significantly affect with respect to the DMSO control groups ($P>0.05$) (Figure 34). H3K27me3 levels in either of ICM and TE cell populations did not show statistically significant increase/decrease in the Qc1-treated groups relative to the DMSO control groups ($P>0.05$) (Figure 35). Overall, these findings suggest that Qc1 increases H3K4me3 levels in the Qc1-treated group, whereas, it does not affect H3K9me3 and H3K27me3 levels. This may suggest that TDH inhibition affects early bovine embryo development via regulation of H3K4me3 level.

A.

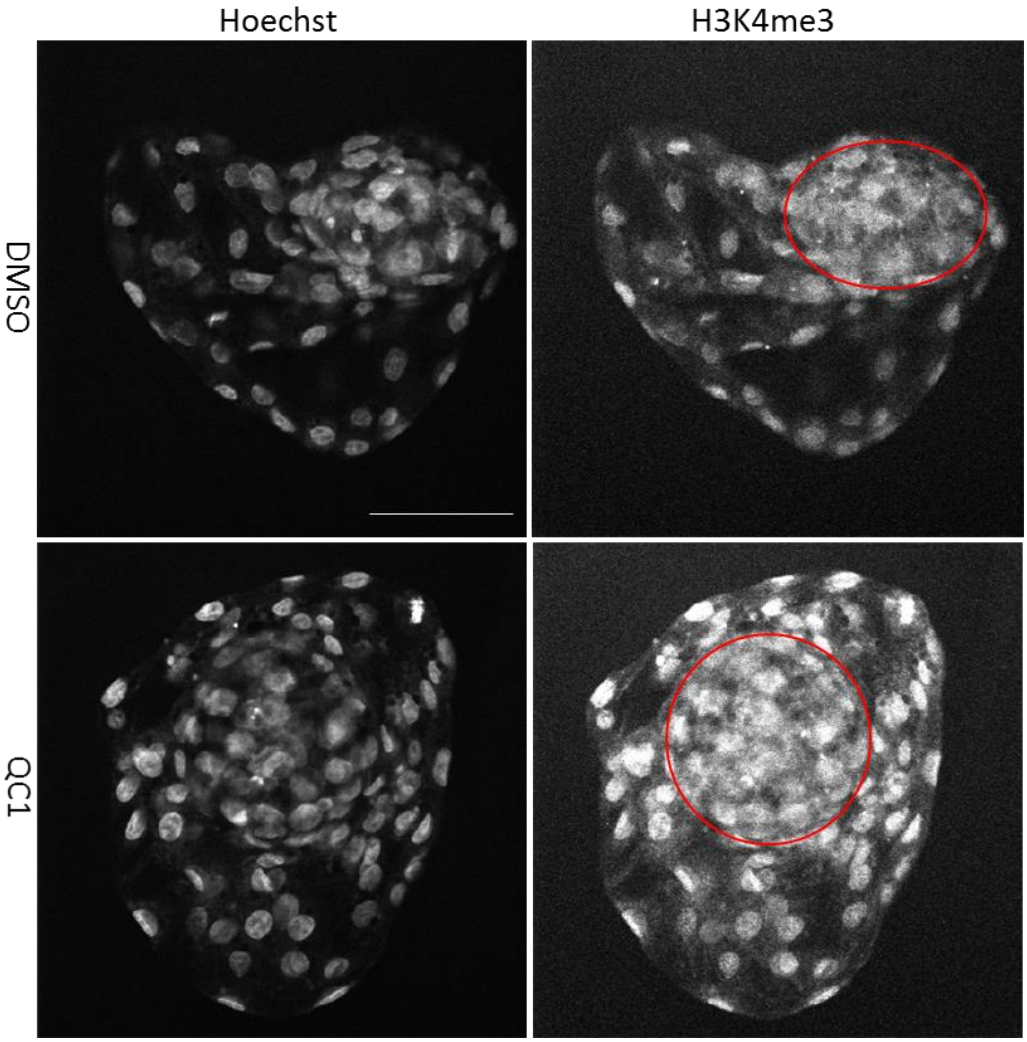
Hoechst
H3K4me3
DMSO
QC1

B.

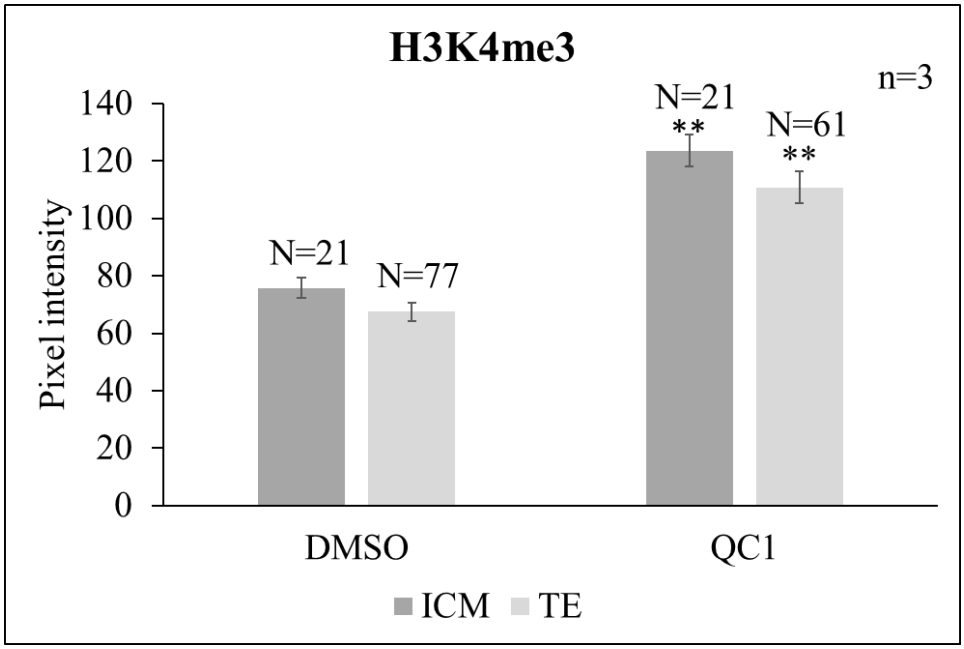
H3K4me3
n=3
Pixel intensity
140
120
100
80
60
40
20
0
N=21
N=77
N=21
**
N=61
**
DMSO
QC1
ICM
TE

Figure 33. Average pixel intensity of H3K4me3 levels in Qc1-treated D8 bovine blastocysts.
IVF-produced embryos were treated with 50 µM Qc1 on D5 and immunostained on D8. **A**) Embryos were immunostained with the H3K4me3 antibody. Hoechst stained DNA. Red circles indicate the approximate area of ICM which was identified by its small densely packed nuclei. Scale bar= 50 µm. **B**) Quantitative analysis of H3K4me3 levels via pixel intensity. N= no. of analysed nuclei. n= no. of independent biological replicates. Error bars = ±SEM. ** = Groups differ P<0.005, from the DMSO control group, determined by Student′s t-test.

A.

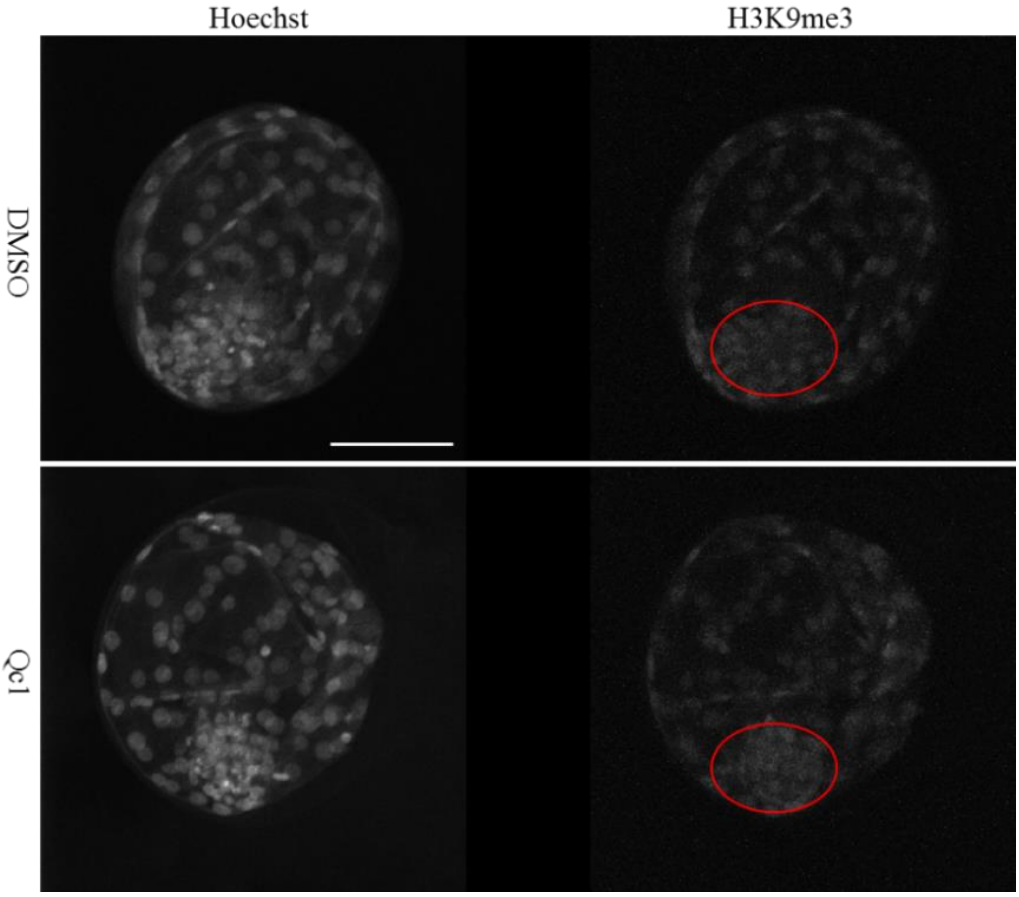

B.

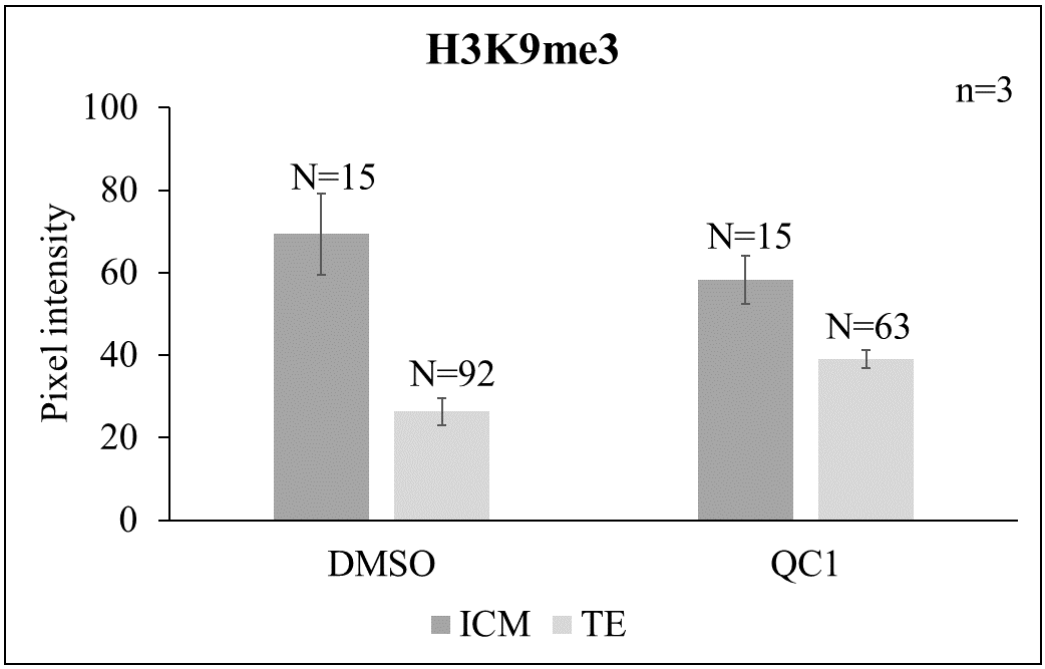

Figure 34. Average pixel intensity of H3K9me3 levels in Qc1-treated D8 bovine blastocysts.
IVF-produced embryos were treated with 50 µM Qc1 on D5 and immunostained on D8. **A**) Embryos were immunostained with the H3K9me3 antibody. Hoechst stained DNA. Red circles indicate the approximate area of ICM which was identified by its small densely packed nuclei. Scale bar= 50 µm. **B**) Quantitative analysis of H3K9me3 levels via pixel intensity. N= no. of analysed nuclei. n= no. of independent biological replicates. Error bars = ±SEM. Student′s t-test was used to measure significance.

A.

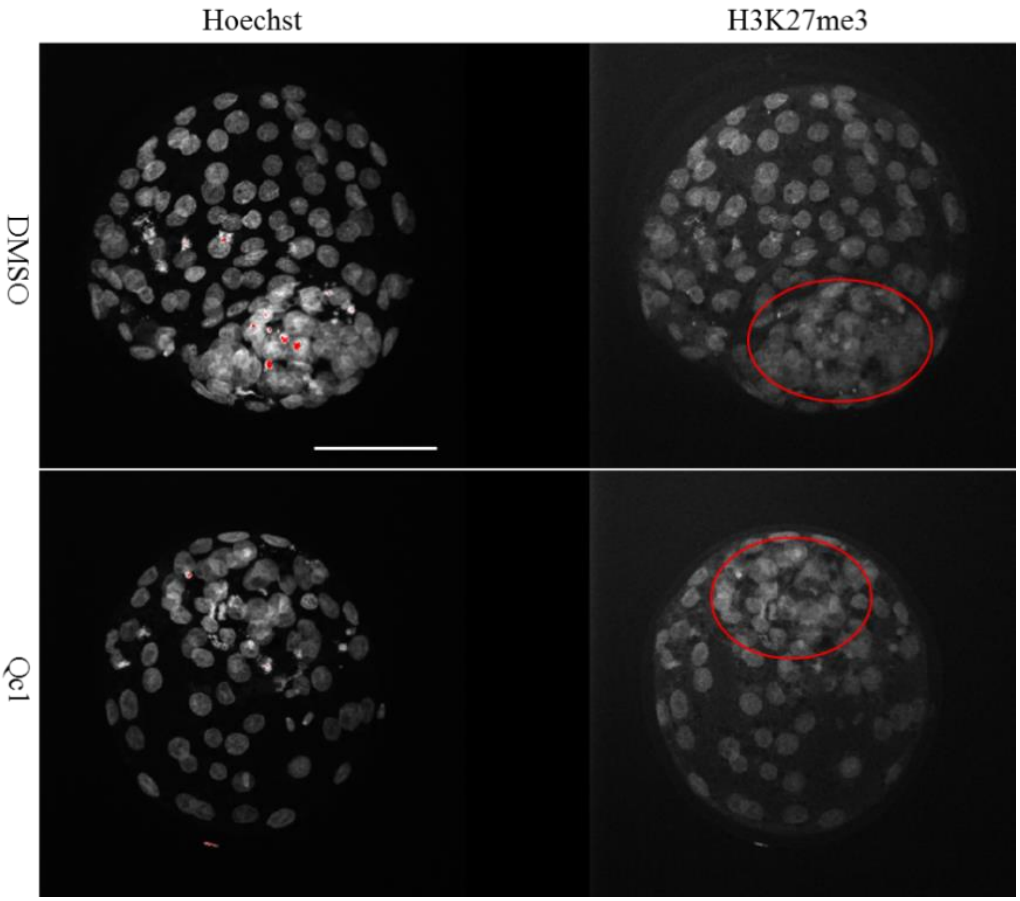
Hoechst
H3K27me3
DMSO
Qc1

B.

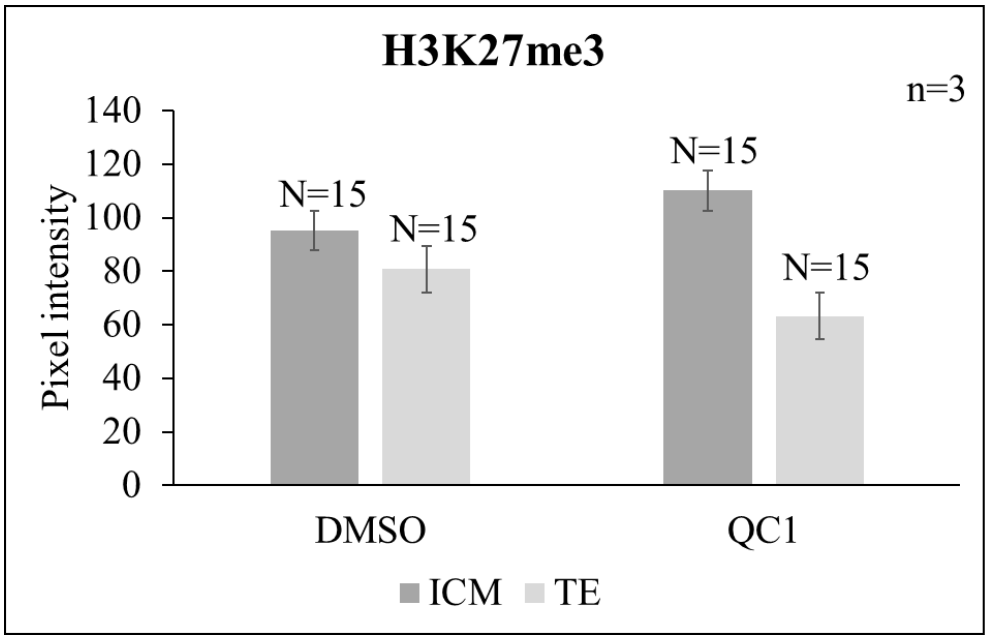
H3K27me3
n=3
Pixel intensity
140
120
100
80
60
40
20
0
N=15
N=15
N=15
N=15
DMSO
QC1
ICM
TE

Figure 35. Average pixel intensity of H3K27me3 levels in the Qc1-treated D8 bovine blastocysts.
IVF-produced embryos were treated with 50 µM Qc1 on D5 and immunostained on D8. **A**) Embryos were immunostained with the H3K27me3 antibody. Hoechst stained DNA. Red circles indicate the approximate area of ICM which was identified by its small densely packed nuclei. Scale bar= 50 µm. **B**) Quantitative analysis of H3K27me3 levels via pixel intensity. N= no. of analysed nuclei. n= no. of independent biological replicates. Error bars = ±SEM. Student′s t-test was used to measure significance.

5.1.1.1.6. Effect of Qc1 on the gene expression profile of lineage-specific markers in bovine embryos

Epigenetics changes determine chromatin dynamics which lead to regulation of gene expression patterns [149]. Therefore, in this section, the effect of Qc1 on the gene expression profiles of ICM and TE cells within D8 bovine embryos was investigated. Bovine embryos were treated with 50 µM Qc1 from D5. They were subsequently treated with RNAGEM™ reaction for cDNA synthesis on D8, followed by qPCR. The effect of Qc1 on the gene expression levels of epiblast (*NANOG*, *FGF4*, *and SOX2*), hypoblast (*PDGFRα*), trophectoderm (*CDX2*), and Thr-SAM (*TDH*) markers was investigated. The results demonstrated no significant changes in the three epiblast markers *NANOG*, *FGF4*, and *SOX2* in the treatment groups relative to the DMSO control group (P>0.05). Hypoblast marker, *PDGFRα,* showed no difference compared to the DMSO control group (P>0.05). Qc1 did not reduce the TE marker level, *CDX2* significantly in comparison to the control group (P>0.05). Thr-SAM marker, *TDH*, in the Qc1-treated group was not affected relative to the DMSO control group (P>0.05) (Figure 36). Overall, these findings indicate that TDH enzyme inhibition does not show any effect on lineage-specific gene markers in D8 bovine blastocysts.

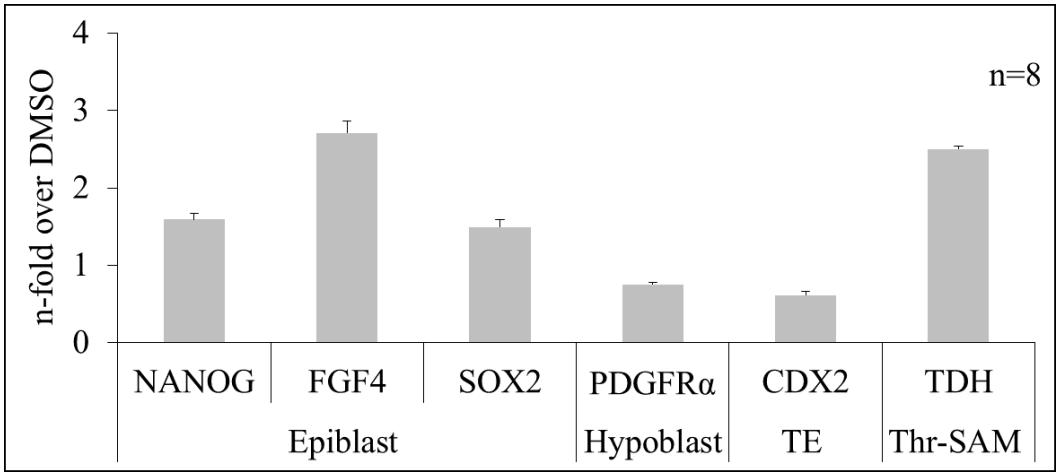

Figure 36. Log-fold changes of lineage-specific and Thr-SAM markers in D8 bovine blastocysts treated with 50 µM Qc1.
Values were normalised against *18s* internal control, logged, and then averaged. The averaged values of each mRNA transcript in the Qc1 treatment group were then subtracted from the averaged values of the corresponding mRNA transcript in the DMSO control to be demonstrated as n-fold. Error bars = SEM. Student′s t-test was used to measure significance. n = no. of independent biological replicates.

In summary, since TDH inhibition reduces bovine embryo development via increased H3K4me3 levels, these findings suggest that TDH-mediated Thr-SAM pathway regulates bovine embryonic development and survival through regulating H3K4me3 levels.

5.1.1.2. Effect of Qc1 on mouse embryo development

Regarding Qc1 effect, since a direct comparison of bovine embryos to mouse ePSCs was not possible, the effect of Qc1 on mouse embryos was studied. Mouse embryos were produced *in vitro* via parthenogenetic activation (see section 2.3). Following the next day (zygote stage), they were treated with 50 µM Qc1. After three days of incubation, they were graded and photographed. The results demonstrated that no mouse embryo developed beyond 2 cell stage with some having many fragmented cells in the Qc1-treated group, while the DMSO control group showed 42% mouse embryo development ($P<0.005$) (Figure 37A and B). This finding confirms the results documented earlier (Figure 29) which demonstrated that Qc1 effect led to a significant reduction in the development of bovine embryos.

A.

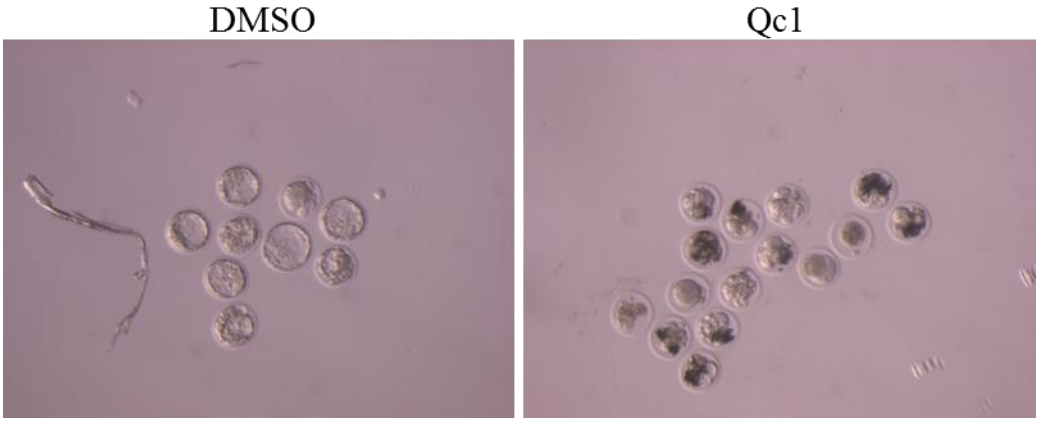

B.

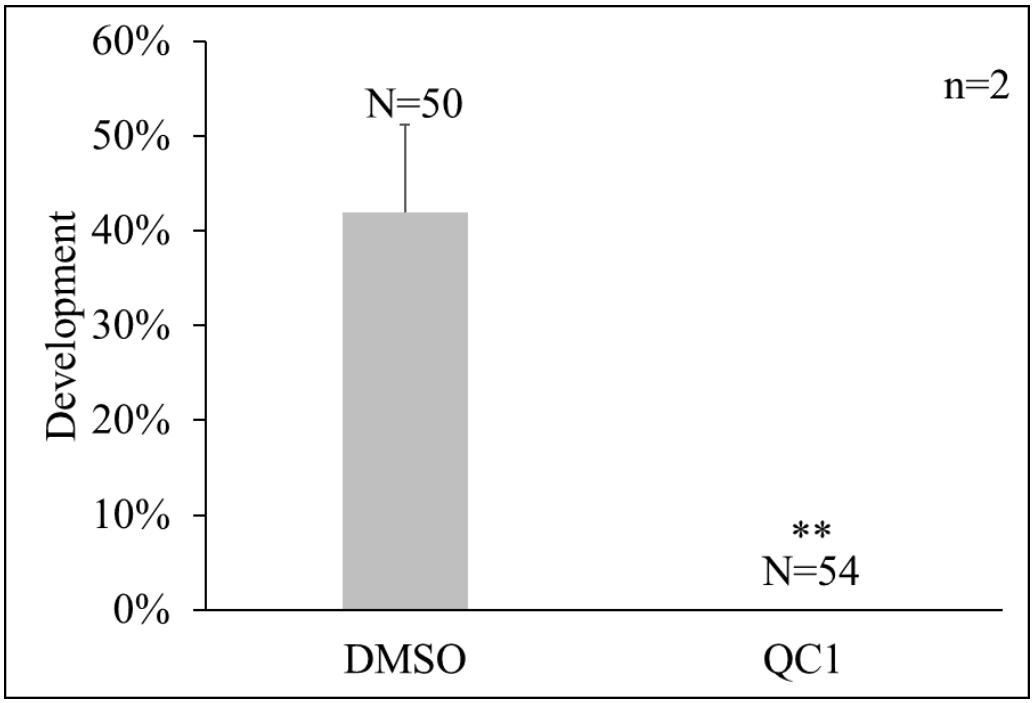

Figure 37. Effect of 50 µM Qc1 on mouse embryo development. Mouse embryos were produced via PG activation and exposed to Qc1 on day one while at the zygote stage. They were graded and subsequently photographed on day 4. **A**) Photographs of mouse embryos on day 4 taken by EVOS microscope. While the embryos in the DMSO control group developed to the blastocyst stage, all embryos in the Qc1 treatment group appeared to be compromised. **B**) The development rate of mouse embryos. N= no. of mouse embryos placed into treatment groups. n= no. of independent biological replicates. ** = Group differ P<0.005 from the DMSO control group.

5.1.1.3. Effect of Qc1 on bovine cells

The role of TDH-mediated Thr-SAM pathway was also investigated in ICM and TE cells *in situ*. This was to see if this pathway is still essential for these embryonic cells once isolated and cultured. To do that, ICM and TE cells were isolated (sections 2.12.1 and 2.13). Fresh and in

culture cells were subsequently treated with 50 µM Qc1 for 24 h. The following day, phase contrast photos were taken and followed by Hoechst, a blue DNA stain, and PI for detecting and quantifying compromised cells. PI is membrane impermeant and does not incorporate into the genomic content of viable cells. This red stain is commonly used for identifying dead cells and as a counterstain in multicolour fluorescent techniques [150]. Compromised cells stained with both Hoechst and PI appeared pink under the fluorescence microscope. Photos were subsequently taken and used for quantitative analysis using ImageJ software. The following sections present the results obtained from the different cell types investigated in this study.

5.1.1.3.1. Effect of Qc1 on bovine ICM cells

In this study bovine ICM cells were isolated using TX method developed during this study (section 2.12.1) followed by culturing in their appropriate culture medium (see Table 23). They were immediately treated with 50 µM Qc1 while still floating and left for 24 h in the 38°C and 5% CO_2 incubator. The following day they were photographed and their viability was measured using Hoechst/PI stains.

Phase contrast images showed that ICM outgrowths expanded and formed dome-shaped colonies within 24 h in their culture medium containing DMSO, whereas, in the Qc1 treatment group, ICM cells turned dark, and the structure of the cells were disintegrated. The ICM colony was no longer dome-shaped (Figure 38A).

Subsequently, the colonies were exposed to Hoechst/PI stains to measure cell death. Quantitative analysis indicated that the percentage of compromised cells in the DMSO control group was 11%, whereas, in the Qc1 treatment group it significantly increased up to 90% ($P<0.005$) (Figure 38B&C). These findings demonstrate that Qc1 severely compromises freshly isolated ICMs.

A.

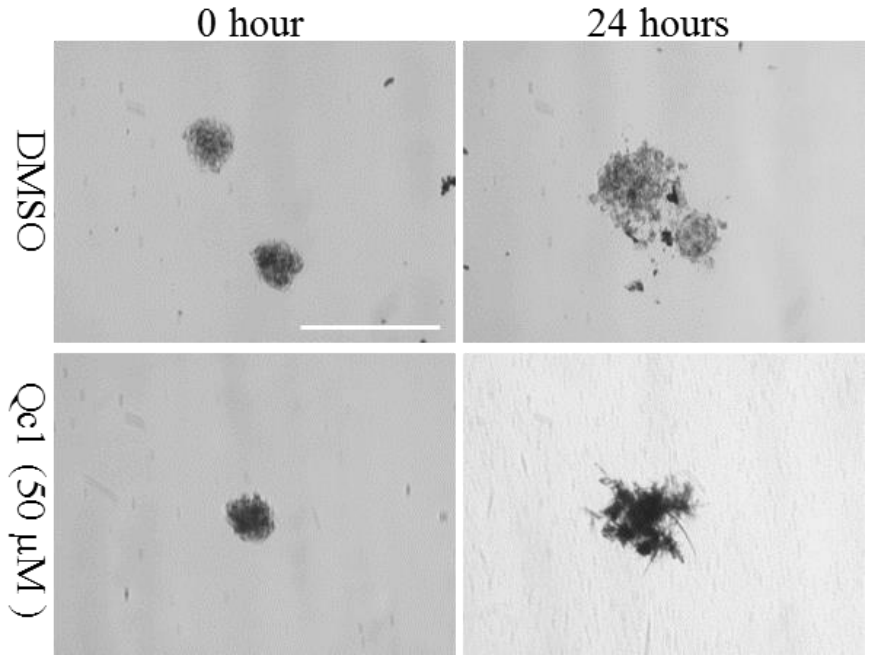
0 hour
24 hours
DMSO
QC1 (50 μM)

B.

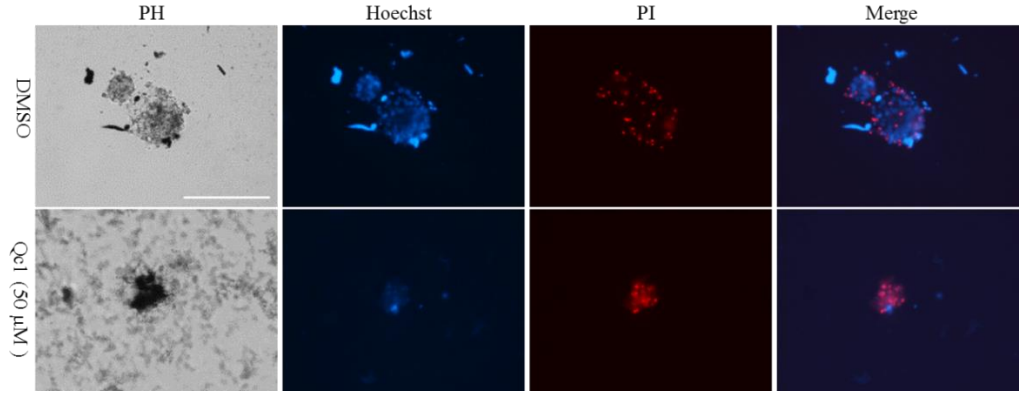
PH
Hoechst
PI
Merge
DMSO
QC1 (50 μM)

C.

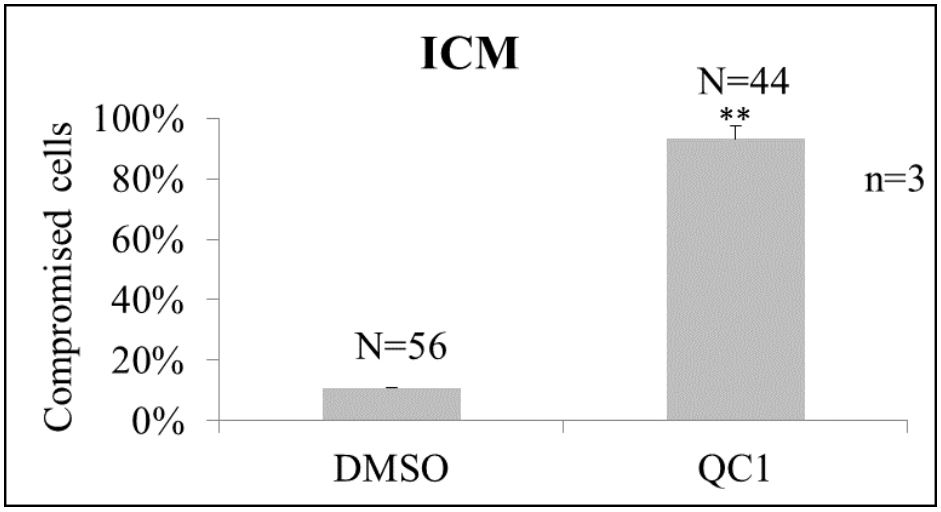
ICM
Compromised cells
100%
80%
60%
40%
20%
0%
N=56
N=44
**
n=3
DMSO
QC1

Figure 38. Freshly isolated ICMs exposed to 50 µM Qc1 for 24 h.
A) Phase contrast photographs of DMSO- and Qc1-treated ICMs 0 and 24 h after treatment, taken by EVOS microscope. Scale bar=200 µm. **B**) Hoechst (blue)/PI (red) staining of ICMs 24 h post-treatment. Merged channels consist of blue and red channels. PH= phase contrast. Scale bar=200 µm. **C**) Percentage of compromised cells in the treatment groups. Error bars = SEM. **= P<0.005 differ from the DMSO control group, determined by Student′s t-test. N= no. of analysed cells. n = no. of independent biological replicates.

5.1.1.3.2. Effect of Qc1 on D6 ICM outgrowths

TX-isolated ICMs were cultured in their appropriate culture medium (see Table 23) for 6 days. On day 6, they were then treated with 50 µM Qc1 for 24 h. The following day they were photographed and their viability was measured using Hoechst/PI stains.

Phase contrast pictures showed that ICM outgrowths in DMSO control group grew in size and cells within the colony looked healthy, whereas, when exposed to Qc1, the ICM colony stopped growing and some cells within the colony turned dark. Some spikey-like structures also appeared on the surface of the colony (Figure 39A). Once exposed to Hoechst/PI, quantitative analysis showed that cell death was significantly high in the Qc1 treatment group with 53% compared to 7% in the DMSO control group (P<0.005) (Figure 39B&C). These results suggest that Qc1 severely compromises D6 ICM outgrowths.

There was 90% cell death in Qc1-treated ICMs to around 50% in Qc1-treated D6 ICM outgrowths, which corresponded to about a 40% reduction in cell death (comparing Figure 38 & Figure 39). However, this decline was not statistically significant (P>0.05). This denotes that TDH enzyme is still active in a majority of cells within the ICM outgrowths.

A.

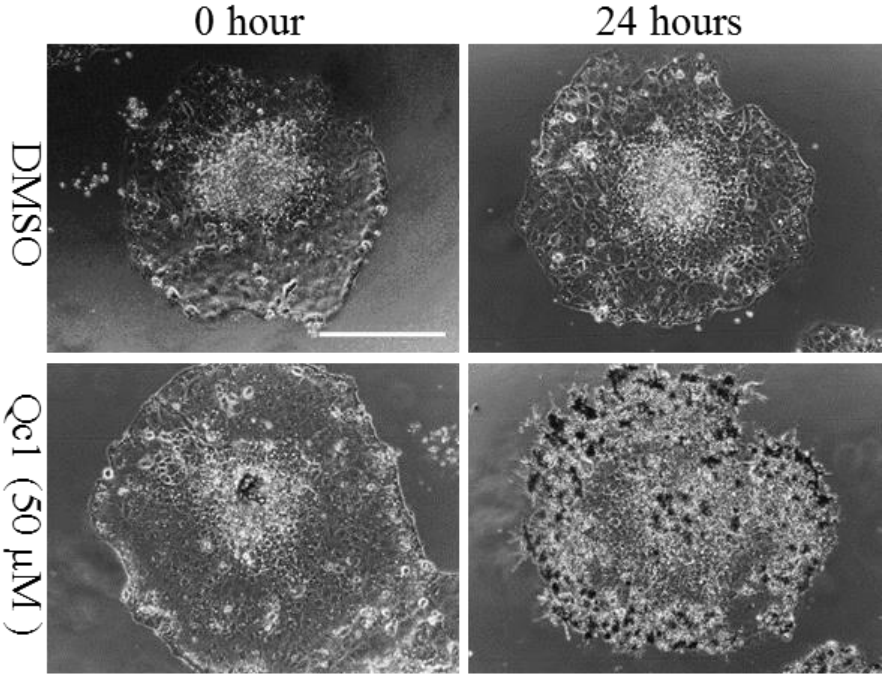
0 hour
24 hours
DMSO
QC1 (50 μM)

B.

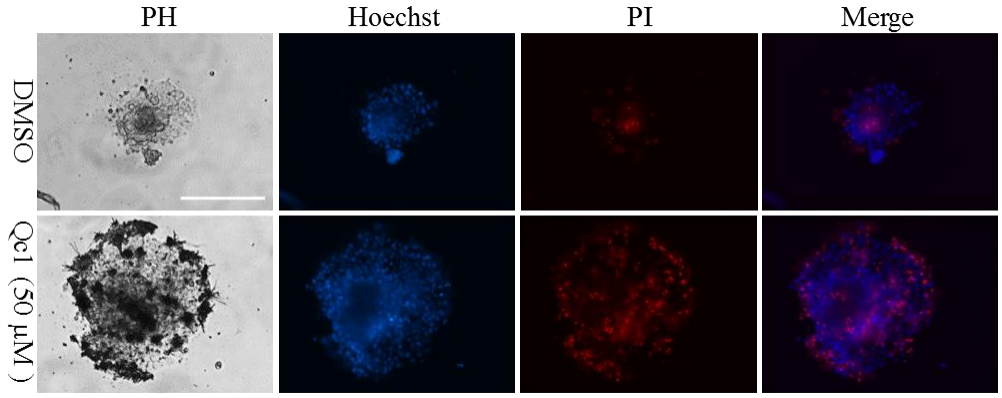
PH
Hoechst
PI
Merge
DMSO
QC1 (50 μM)

C.

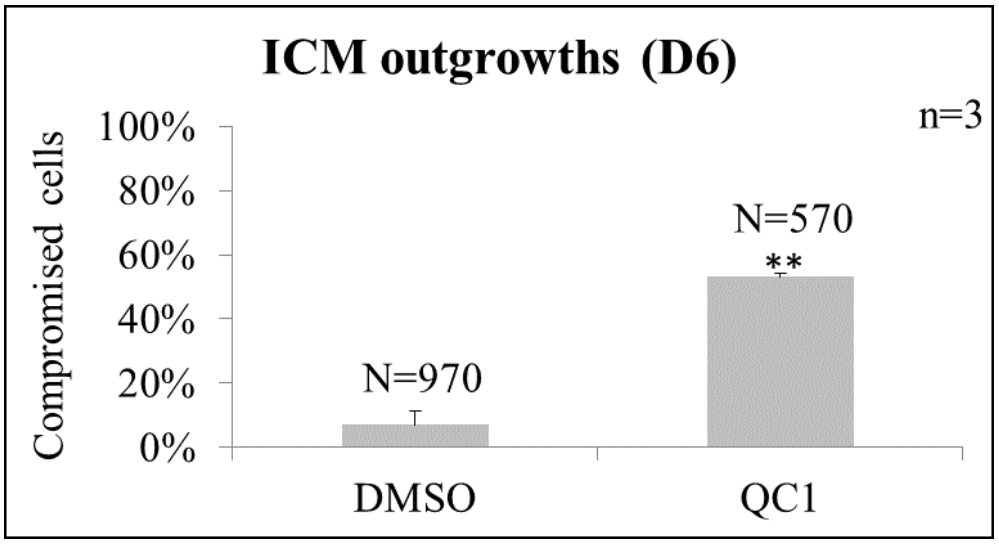
ICM outgrowths (D6)
n=3
Compromised cells
100%
80%
60%
40%
20%
0%
N=970
N=570
**
DMSO
QC1

Figure 39. Six days old ICM outgrowths exposed to 50 µM Qc1 for 24 h. **A**) Phase contrast photographs of DMSO- and Qc1-treated D6 ICM outgrowths 0 and 24 h after treatment, taken by EVOS microscope. Scale bar=400 µm. **B**) Hoechst(blue)/PI(red) staining of ICM outgrowths 24 h post-treatment. Merged Photographs consist of blue and red channels. PH= phase contrast. Scale bar=400 µm. **C**) Percentage of compromised cells in the treatment groups. Error bars = SEM. **= P<0.005 differ from the DMSO control group, determined by Student′s t-test. N= no. of analysed cells. n = no. of independent biological replicates.

5.1.1.3.3. Effect of Qc1 on TE cells

Mechanically isolated TEs were cultured in their appropriate culture medium (see Table 23) and were treated with 50 µM Qc1 for 24 h. The following day they were photographed and their viability was measured using Hoechst/PI stains.

Phase contrast pictures showed that TE dissections in DMSO control group looked healthy, containing many cells with bright cytoplasm over 24 h culture, however, when exposed to Qc1, the TE became a dark clump having the appearance of a disintegrating cell mass (Figure 40A).

Quantitative analysis of cell death indicated that QC1-treated TE exhibited significantly higher levels of cell death (91%), with respect to 20% in the DMSO control group, which was significant (P<0.005) (Figure 40B&C). These findings suggest that Qc1 severely compromises TE cell seeding after 24 h of culture.

A.

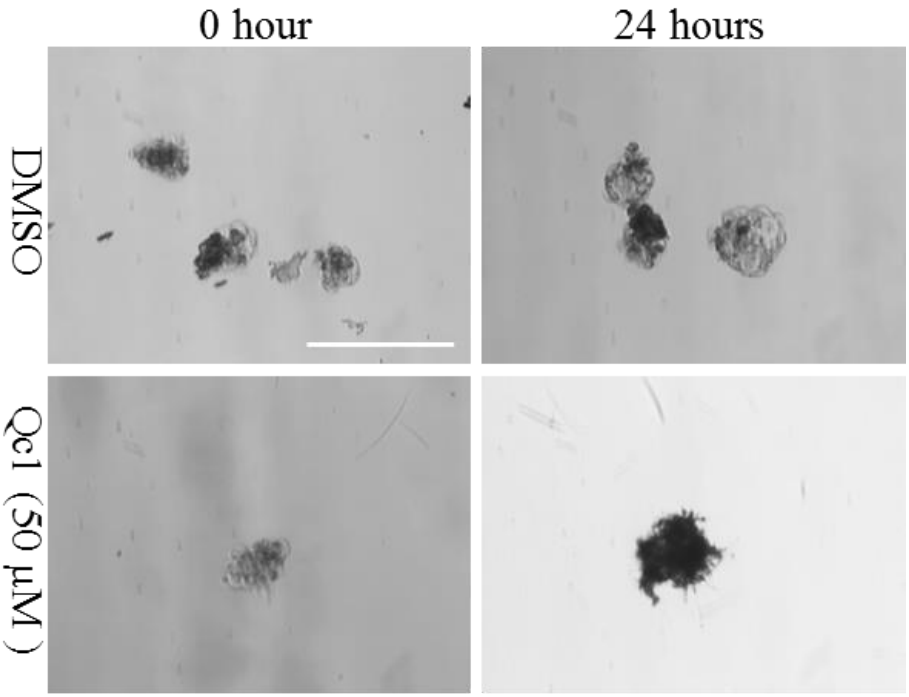

B.

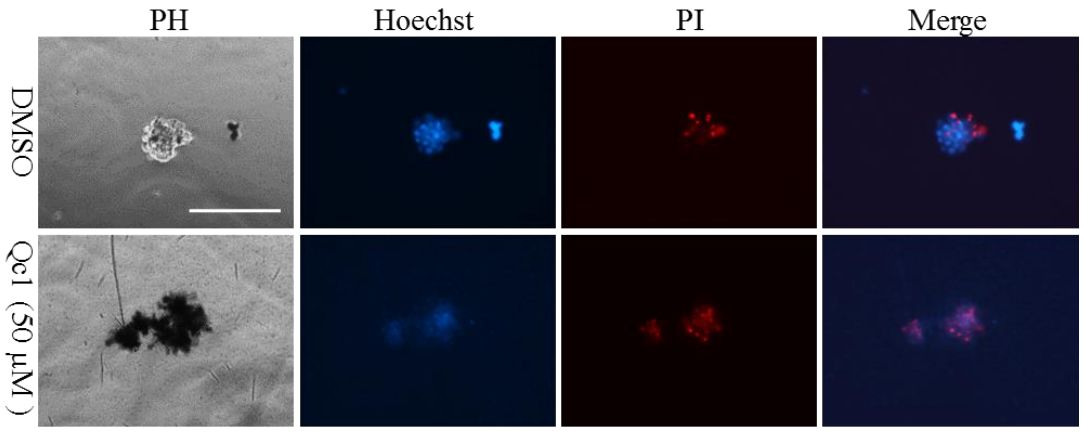

C.

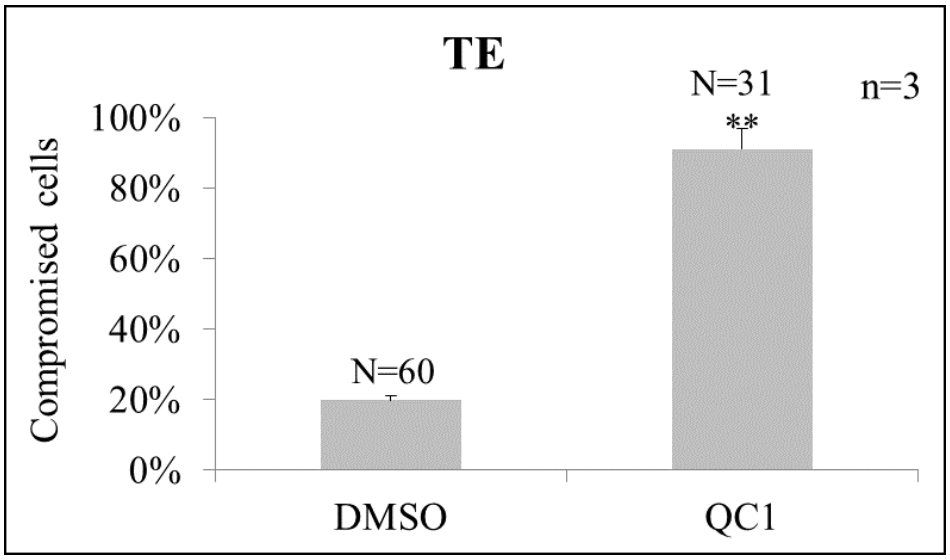

Figure 40. TE dissections exposed to 50 µM Qc1 for 24 h.A) Phase contrast photographs of DMSO- and Qc1-treated TEs 0 and 24 h after treatment, taken by EVOS microscope. Scale bar=200 µm. **B**) Hoechst (blue)/PI (red) staining of TEs 24 h post-treatment. Merged channels consist of blue and red channels. PH= phase contrast. Scale bar=200 µm. **C**) Percentage of compromised cells in the treatment groups. Error bars = SEM. **= P<0.005 differ from the DMSO control group, determined by Student′s t-test. N= no. of analysed cells. n = no. of independent biological replicates.

5.1.1.3.4. Effect of Qc1 on D6 TE primary cultures

Mechanically bisected TEs were cultured in their appropriate culture medium (see Table 23) for 6 days and were subsequently treated with 50 µM Qc1 for 24 h. The following day they were photographed and their viability was measured using Hoechst/PI stains.

Phase contrast images showed that TE primary cultures in DMSO control group appeared intact and without any morphological changes. Cells within the culture also appeared to have healthy and transparent cytoplasm. Likewise, the TE primary cultures exposed to Qc1 did not show

any morphological changes compared to the DMSO group. The cells inside the cultures appeared to have a transparent cytoplasm with a distinct plasma membrane (Figure 41A).

Once exposed to Hoechst/PI stains, the quantitative analysis indicated that the percentage of cell death in both DMSO control and treatment groups was 1% ($P>0.05$) (Figure 41B&C). These findings indicate that Qc1 does not compromise 6 days old TE primary cultures.

When comparing the percentage of cell death in the Qc1-treated fresh TEs to the Qc1-treated D6 TE primary cultures (Figure 40C and Figure 41C), there was an approximately 90% reduction in cell death that according to t-test analysis this discrepancy was significant ($P<0.005$; data not shown). This implies that TDH enzyme is no longer functional after 6 days of TE culture and its absence was confirmed by gene expression analysis and IF.

A.

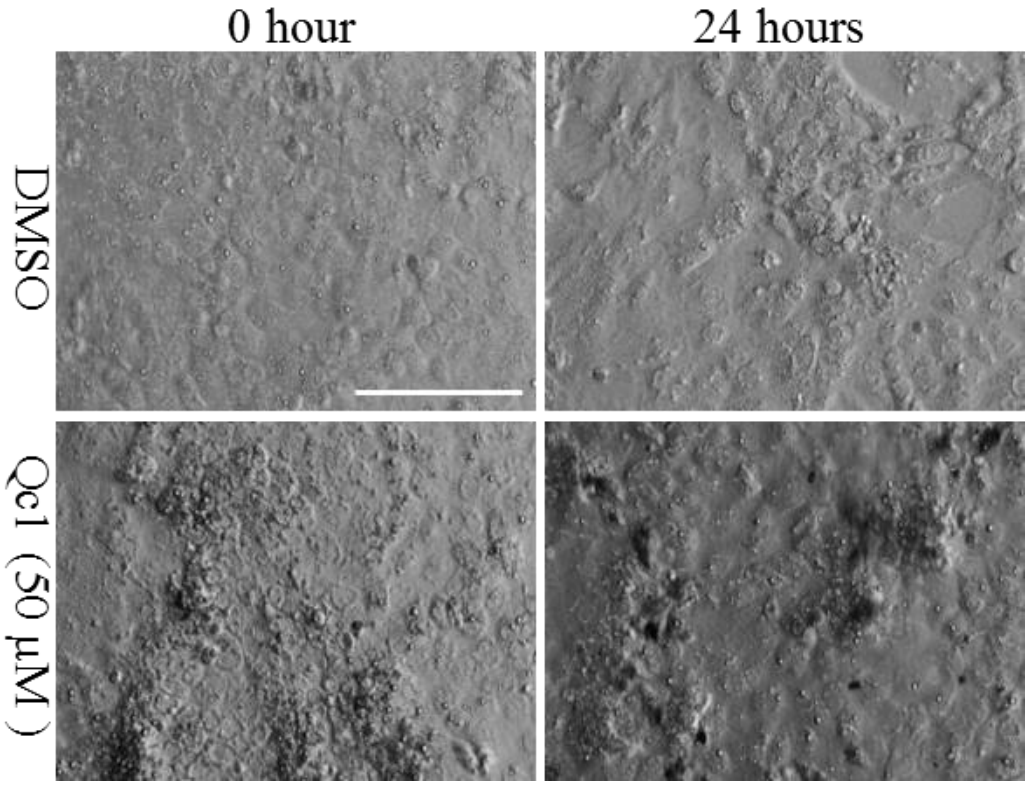

B.

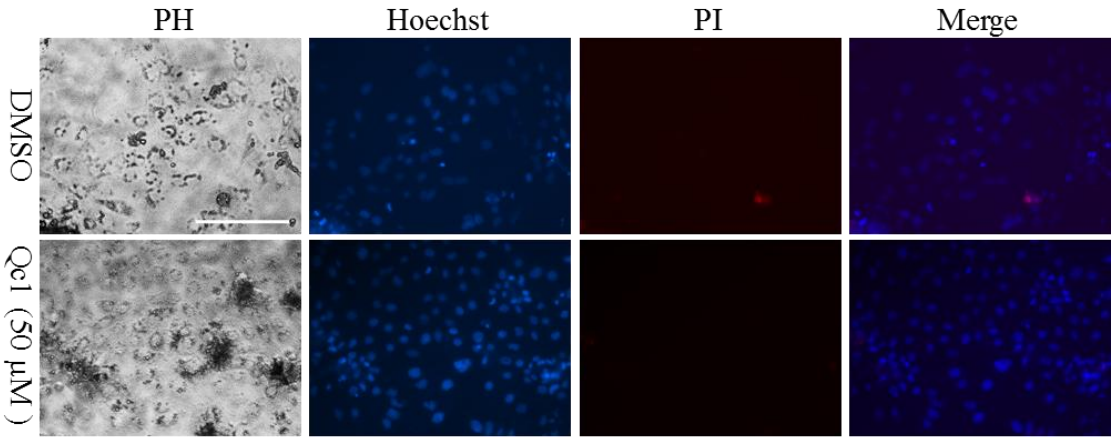

C.

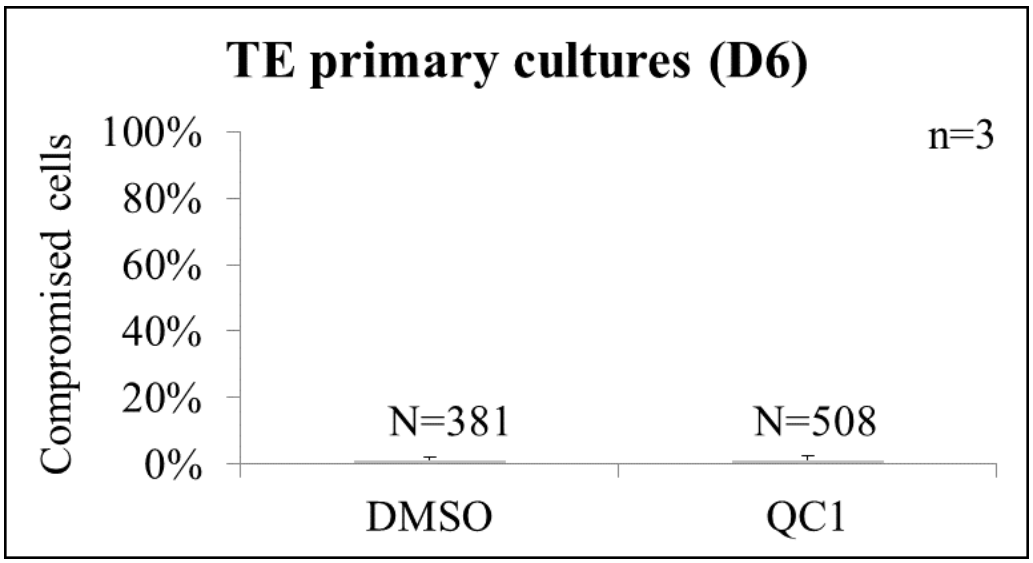

Figure 41. Six days old TE primary cultures exposed to 50 µM Qc1 for 24 h. **A**) Phase contrast photographs of DMSO- and Qc1-treated D6 TE primary cultures 0 and 24 h after treatment, taken by EVOS microscope. Scale bar=200 µm. **B**) Hoechst (blue) and PI (red) staining of TE primary cultures 24 h post-treatment. Merged channels consist of blue and red channels. PH= phase contrast. Scale bar=200 µm. **C**) Percentage of compromised cells in the treatment groups. Error bars = SEM. Student′s t-test was used to measure significance. N= no. of analysed cells. n = no. of independent biological replicates.

5.1.1.3.5. Effect of Qc1 on BEF cells

Since BEF cells expressed some level of *TDH* but lower than that of ICM cells (see Figure 25), they were exposed to Qc1 to see how they respond to it. BEF cells were cultured in culture medium for five hours (Table 23) and then treated with 50 µM Qc1 for 24 h. The following day they were photographed and their viability was measured using Hoechst/PI stains.

Phase contrast pictures showed both Qc1 treatment and DMSO control groups looked normal with cells having transparent cytoplasm with intact and distinct plasma membrane after 24 h (Figure 42A). Once exposed to Hoechst/PI, the quantitative analysis showed that cell death in the treatment group was significantly higher (20%) than the DMSO control group (3%) ($P<0.005$) (Figure 42B&C). This finding indicates that Qc1 compromises BEF cells.

A.

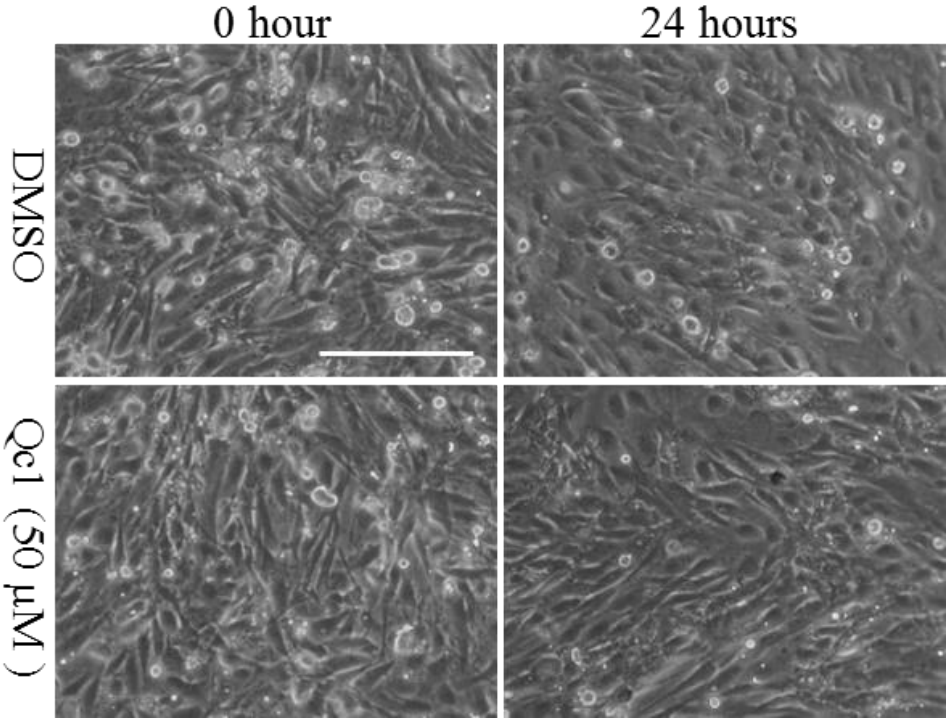
0 hour
24 hours
DMSO
Qc1 (50 μM)

B.

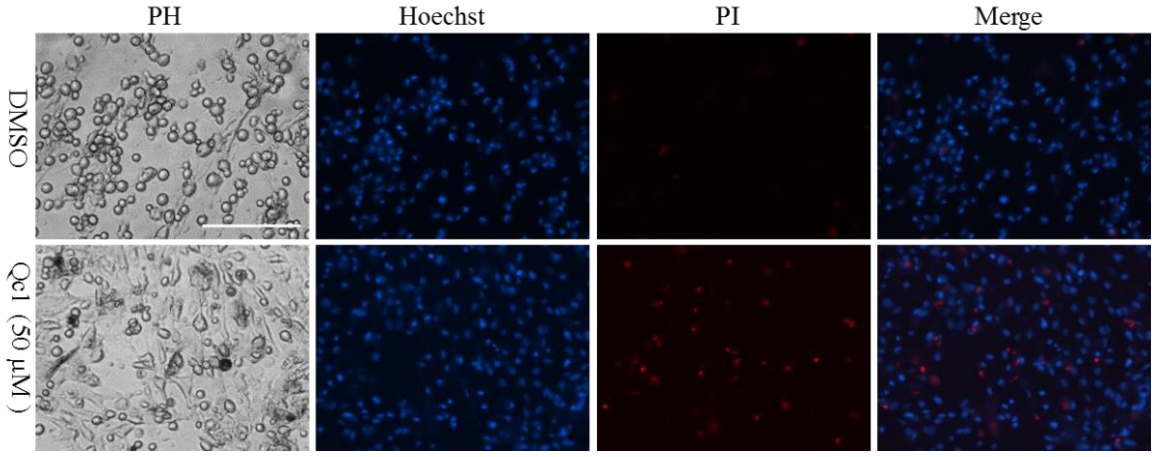
PH
Hoechst
PI
Merge
DMSO
Qc1 (50 μM)

C.

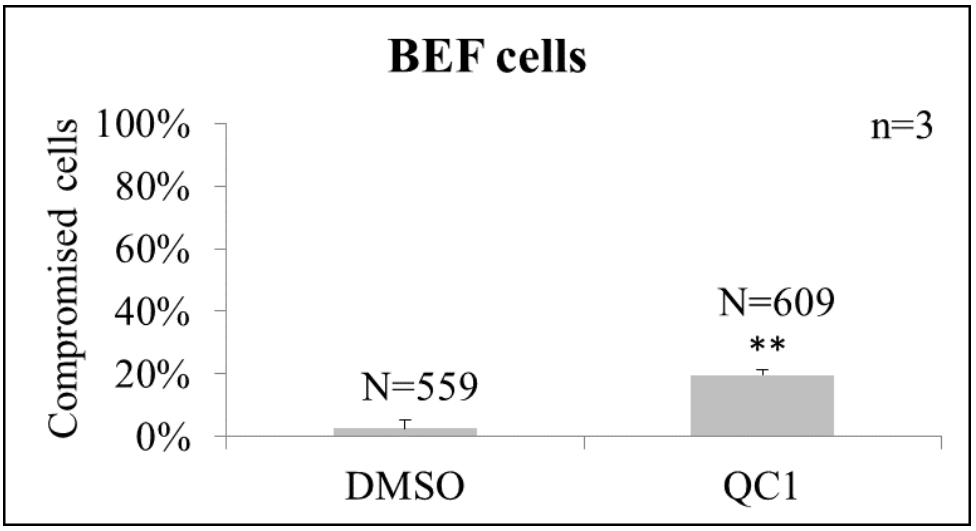
BEF cells
n=3
Compromised cells
100%
80%
60%
40%
20%
0%
N=559
N=609
**
DMSO
QC1

Figure 42. BEF cells exposed to 50 µM Qc1 for 24 h.
A) Phase contrast photographs of DMSO- and Qc1-treated BEF cells 0 and 24 h after treatment, taken by EVOS microscope. Scale bar =200 µm. **B**) Hoechst (blue) and PI (red) staining of BEF cells 24 h post-treatment. Merged channels consist of blue and red channels. PH= phase contrast. Scale bar=200 µm. **C**) Percentage of compromised cells in the treatment groups. Error bars = SEM. **= P<0.005 differ from the DMSO control group, determined by Student′s t-test. N= no. of analysed cells. n = no. of independent biological replicates.

5.1.1.3.6. Effect of Qc1 on skin fibroblast cells

To ensure that the effect of Qc1 on cells was not due to general toxicity, skin fibroblast line (LJ801 cell line), which did not express any *TDH* mRNA (see Figure 25) was exposed to Qc1. Skin fibroblast cells were cultured in their appropriate culture medium (see Table 23) containing 50 µM Qc1 for 24 h. The following day they were photographed and their viability was measured using Hoechst/PI stains.

Phase contrast pictures showed that the cells in both treatment and DMSO control groups looked healthy with transparent cytoplasm and distinct and intact borders after 24 h (Figure 43A).

Once exposed to Hoechst/PI, the quantitative analysis showed that cell death in the DMSO control and treatment group was 4% and 5%, respectively (P>0.05) (Figure 43B&C). Since the skin fibroblast cells did not express any *TDH* mRNA transcripts (Figure 25), they were used as a control for the Qc1 chemical. Qc1 specifically targets TDH enzyme in mouse ePSCs [11]. Since Qc1 did not compromise skin fibroblast cells, this suggests that Qc1 targets explicitly TDH enzyme in bovine cells and its effect is not due to general toxicity.

A.

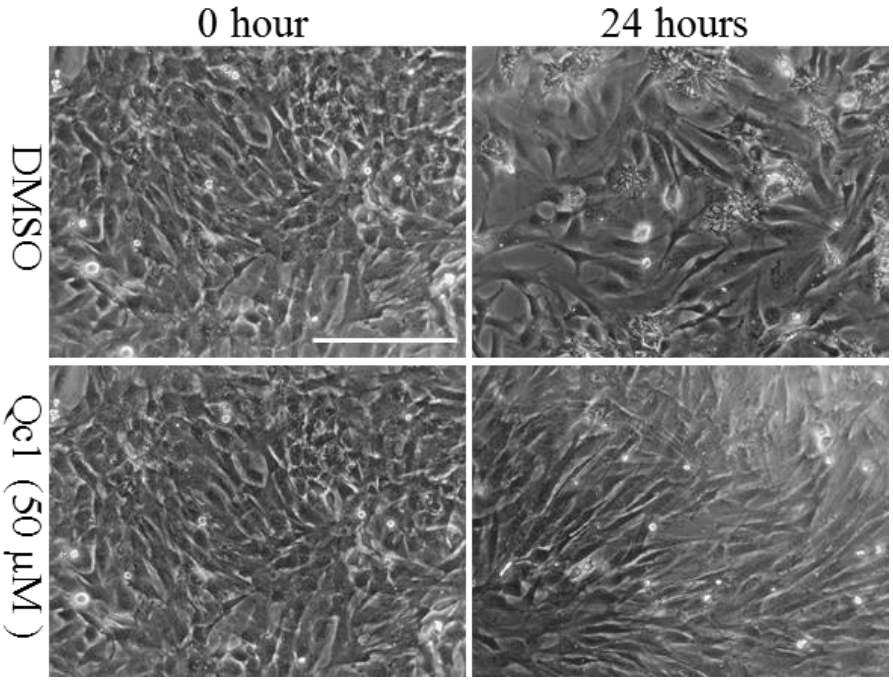
0 hour
24 hours
DMSO
QC1 (50 μM)

B.

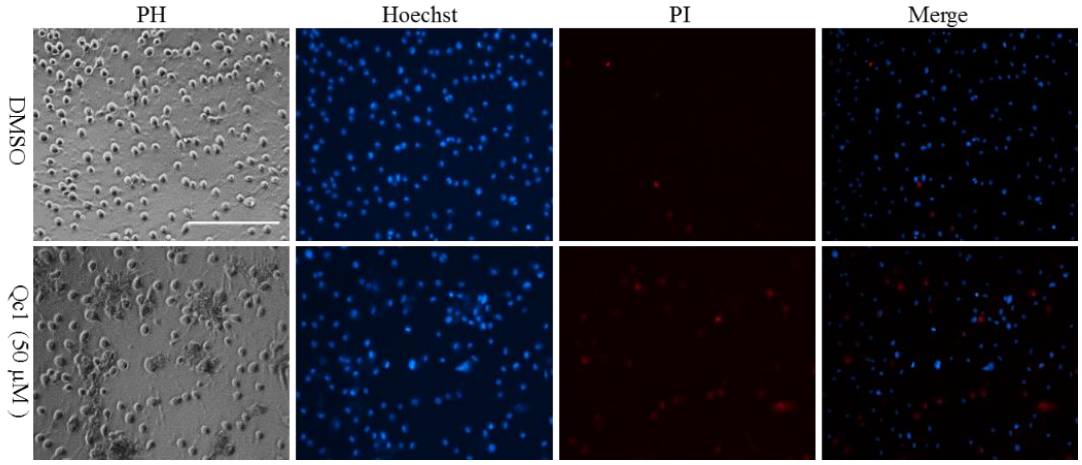
PH
Hoechst
PI
Merge
DMSO
QC1 (50 μM)

C.

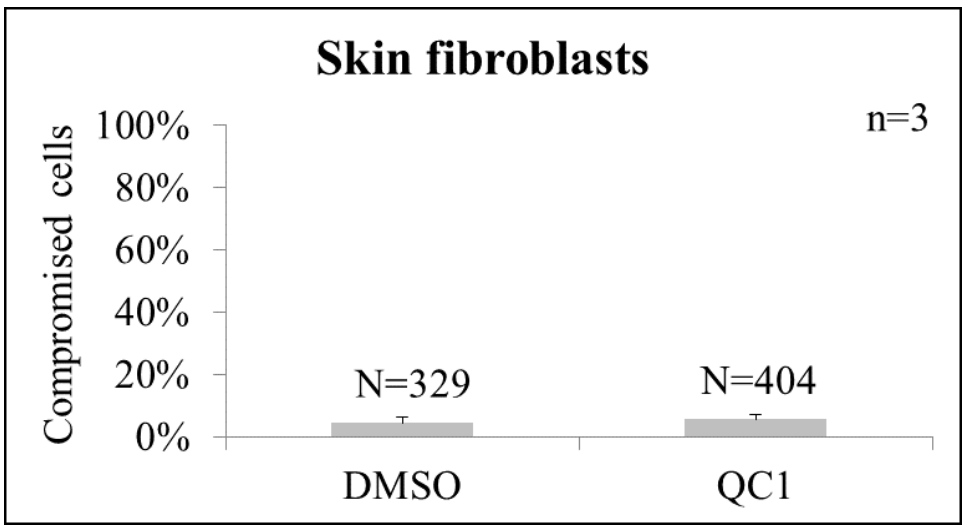
Skin fibroblasts
n=3
Compromised cells
100%
80%
60%
40%
20%
0%
N=329
N=404
DMSO
QC1

Figure 43. Skin fibroblast cells (LJ801 line) exposed to 50 µM Qc1 for 24 h.
A) Phase contrast photographs of DMSO- and Qc1-treated skin fibroblast cells 0 and 24 h after treatment, taken by EVOS microscope. Scale bar =200 µm. **B**) Hoechst (blue) and PI (red) staining of skin fibroblast cells 24 h post-treatment. Merged channels consist of blue and red channels. PH= phase contrast. Scale bar =200 µm. **C**) Percentage of compromised cells in the treatment groups. Error bars = SEM. Student′s t-test was used to measure significance. N= no. of analysed cells. n = no. of independent biological replicates.

5.1.1.3.7. Effect of Qc1 on bovine muscle fibroblasts

Since bovine muscle fibroblast cells expressed *TDH* mRNA at a lower level than ICM (see Figure 25), they were exposed to Qc1 to observe how they would respond to its effect. Bovine muscle fibroblast cells were cultured in their appropriate culture medium (see Table 23) with 50 µM Qc1 for 24 h. The following day they were photographed and their viability was measured using Hoechst/PI stains. Phase contrast images showed that the DMSO control group appeared normal after 24 h, whereas in the treatment group some cells appeared disintegrated and formed shrub-like structures in the culture medium (Figure 44A).

Once exposed to Hoechst/PI stains, the quantitative analysis showed that cell death in the DMSO control was 4%, whereas, in the treatment group it was 7%, which was statistically significant (P=0.05) (Figure 44C).

A.

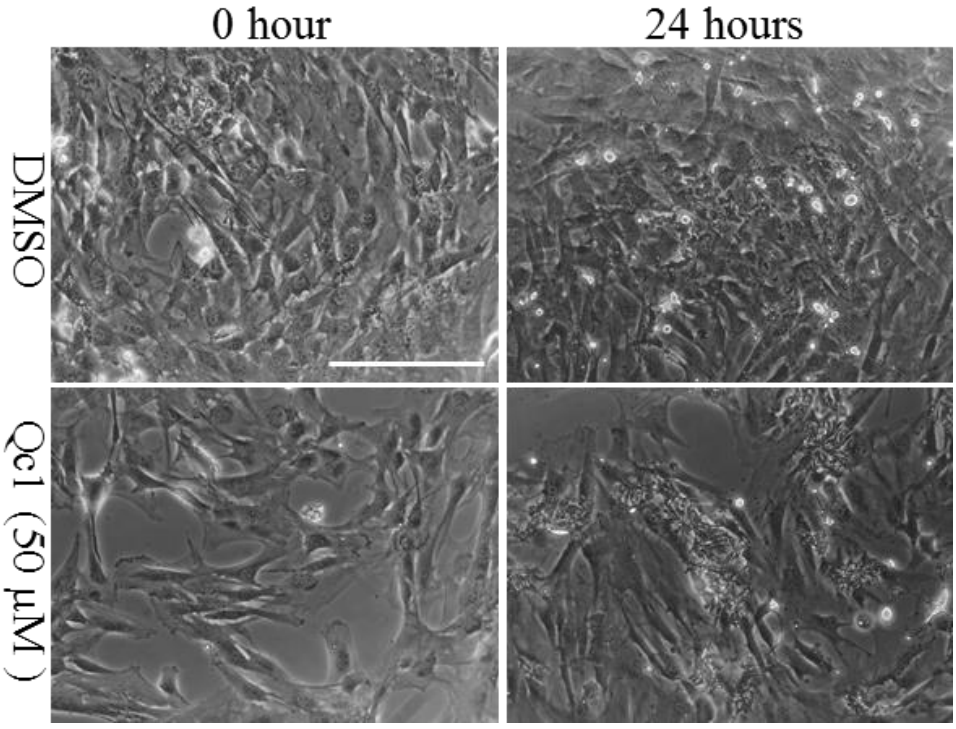

B.

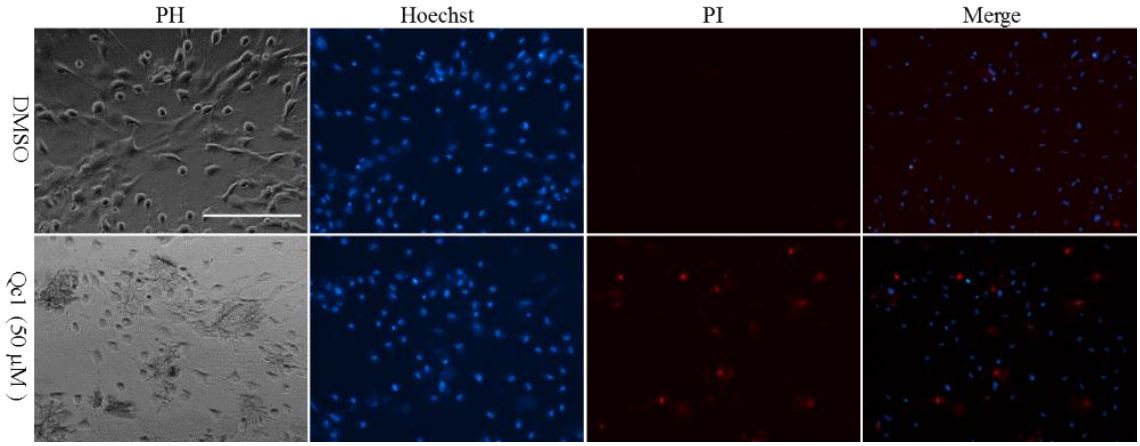

C.

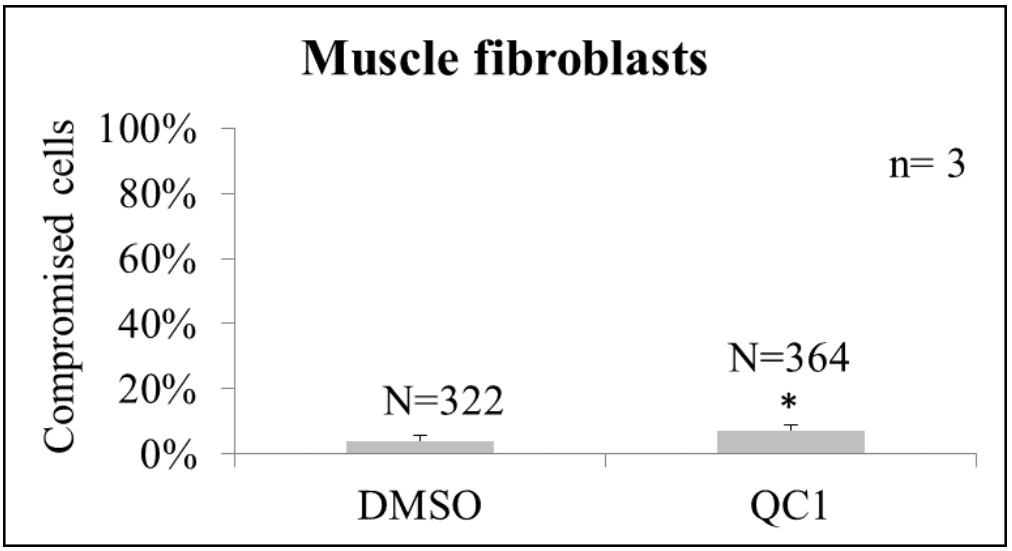

Figure 44. Bovine muscle fibroblast cells exposed to 50 µM Qc1 for 24 h. **A**) Phase contrast photographs of DMSO- and Qc1-treated muscle fibroblast cells 0 and 24 h after treatment, taken by EVOS microscope. Scale bar = 200 µm. **B**) Hoechst (blue) and PI (red) staining of muscle fibroblast cells 24 h post-treatment. Merged channels consist of blue and red channels. PH= phase contrast. Scale bar =200 µm. **C**) Percentage of compromised cells in the treatment groups. Error bars = SEM. *= $P<0.05$ differs from the DMSO control group, determined by Student′s t-test. N= no. of analysed cells. n = no. of independent biological replicates.

In summary, these findings demonstrate that Qc1 compromises ICM even after 6 days of culture, which may suggest that TDH-mediated threonine-SAM pathway still operates after 6 days of ICM culture. This corresponds to their TDH gene and protein profiles in which ICM cells still express TDH after 6 days in culture. In contrast, Qc1 impairs TE cells. However, it fails to compromise them after 6 days of culture. This also corresponds to the *TDH* gene and protein profiles of freshly isolated and D6 primary TE cultures since it is downregulated upon 6 days of TE *in vitro* culture (Table 9). This may indicate that TDH functionality is no longer needed in TE cells in later stages of embryonic development. These findings also imply the

discrepancy between mouse and bovine species as in the mouse TDH is restricted explicitly to ICM and ESCs [8], whereas in bovine both ICM and TE cells express it.

Table 9. Summary of the TDH expression profile of investigated bovine cell types and their response to Qc1 treatment.

Bovine cell type	TDH expression	Qc1 effect
ICM	Yes	Yes
D6 ICM	Yes	Yes
TE	Yes	Yes
D6 TE	No	No
BEF	No	No
Skin fibroblasts	No	No
Muscle fibroblasts	Yes	Yes

5.1.1.4. The effect of 3-HNV on the TDH-mediated threonine-SAM pathway

It has been suggested that 3-HNV is another specific inhibitor of the threonine-SAM pathway [8]. 3-HNV is a synthetic variant of threonine which has an extra carbon atom in its molecular structure. TDH enzyme can hydrolyse this chemical; however, instead of producing glycine and acetyl-CoA, it breaks it down to glycine and propionyl-CoA. Both glycine and acetyl-CoA are essential for mouse ESCs maintenance and ICM formation as glycine contributes to SAM production which consequently trimethylates H3K4 marker, while acetyl-CoA helps with adenosine triphosphate (ATP) production via the TCA cycle [8] as well as contributing to histone acetylation [151]. Therefore, when exposed to 3-HNV, mouse ePSCs and ICM in the embryo (both express TDH protein), will not be provided with acetyl-CoA, and as a result, they cease colony formation and development, respectively [8]. To further confirm that TDH plays a vital role in bovine embryonic development, 3-HNV was administered to the culture media of bovine embryos and cells.

5.1.1.5. Effect of 3-HNV on bovine embryo development

IVF-produced bovine embryos were treated with 300 µM 3-HNV (according to paper [8]) in bSOF_AAs_ΔThr on D5 and graded on D8. B^{1-3} development declined from 29% in the control group to 0% in the 3-HNV-treated group ($P<0.005$). Consequently, there was no B^{1-2} development in the treatment group compared to 13% development in the control group ($P<0.005$). Supplementation of culture medium with 4 mM Thr and 300 µM 3-HNV restored B^{1-3} development to normal levels of 29%, which was no different to the control group

(P>0.05). Likewise, B $^{1-2}$ development was restored to 10% in the presence of 4 mM Thr and 3-HNV, relative to 13% in the control group (P>0.05) (Figure 45). These results suggest a substantial adverse effect of 3-HNV on bovine embryo development.

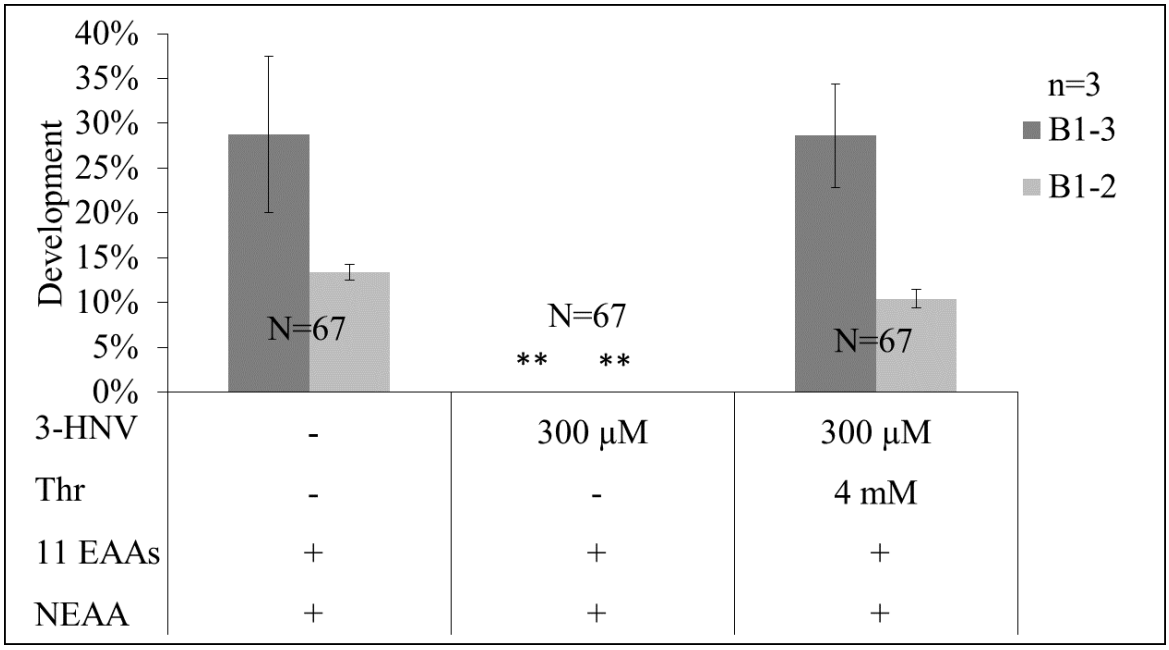

Figure 45. 300 µM 3-HNV severely compromises bovine embryo development.
IVF-produced embryos were treated with 3-HNV on D5 and graded on D8. Grading criteria from Appendix E. N= no. of fertilized embryos placed into IVC. n= no. of independent IVF experiments. Error bars = ±SEM. ** = Group differs P<0.005 from the DMSO control group, determined by Fisher`s Exact test. Thr= threonine, EAAs= essential amino acids, NEAAs= non-essential amino acids.

5.1.1.6. Effect of 3-HNV on bovine cells

5.1.1.6.1. Effect of 3-HNV on D1 ICM outgrowths

Similar to the experiment with bovine embryos, the effect of 3-HNV on ICM and TE cultures was also studied. ICMs were isolated from D8 bovine blastocysts using the developed TX technique. They were then cultured in an appropriate culture medium (see Table 23) for 24 h. ICM outgrowths were subsequently exposed to a variety of 3-HNV concentrations ranging from 1-4 mM for 48 h, according to paper [8]. As shown in the Figure 46, the ICM outgrowth in the vehicle control group was growing in size over the 48 h period. The colony exhibited a dome-shaped structure with a clear border. The ICM colony exposed to 1 mM 3-HNVseemed to be growing as much as the ICM outgrowth in the control group with distinct margins, however, some dark cells appeared on the surface of the colony. The colony looked integrated and dome-shaped. The ICMs in the 2 and 3 mM showed many dark cells while having smaller colonies than the control group. These colonies were also not as compact and dome-shaped as

the control group. The ICM in the 4 mM 3-HNV shrank in size with many dark cells in comparison to the control group. The colony also lost its entire integrity and dome shape (Figure 46A). Hoechst/PI staining of the control group indicated that the majority of cells within the colony were stained with Hoechst and not PI, denoting that most of the ICM cells were alive. ICMs in the 1 mM and 2 mM 3-HNV likewise demonstrated that the number of compromised cells was not more than that of the control group and a majority of cells remained alive. ICMs in 3 and 4 mM 3-HNV concentration seemed to have shrunken with relatively fewer live cells than the control group. (Figure 46B). This finding suggests that 3-HNV is most effective at concentrations of 3 and 4 mM on the one day old ICM outgrowths.

A.

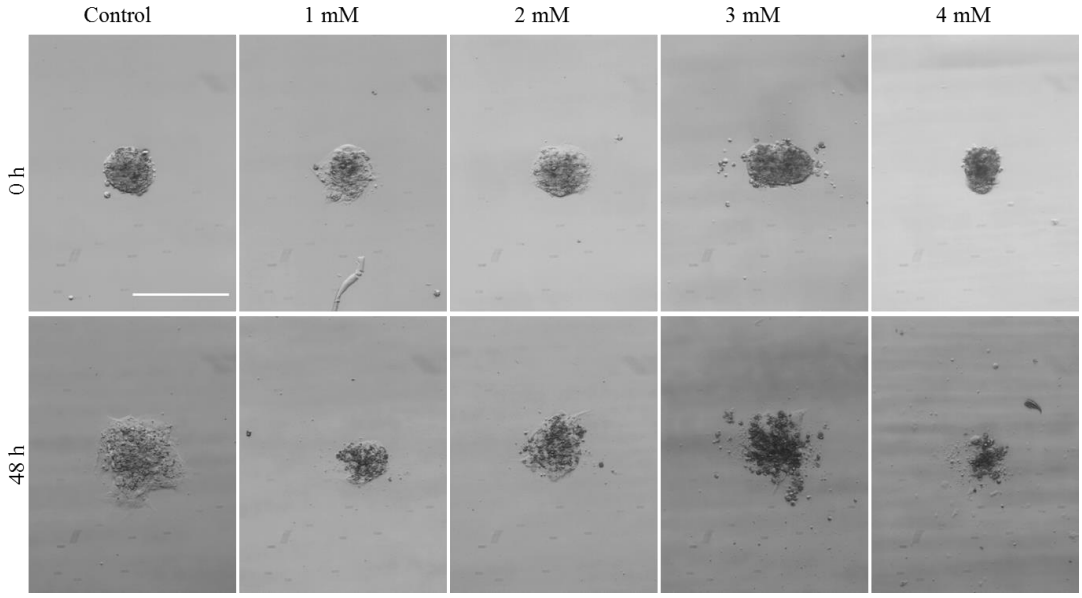

B.

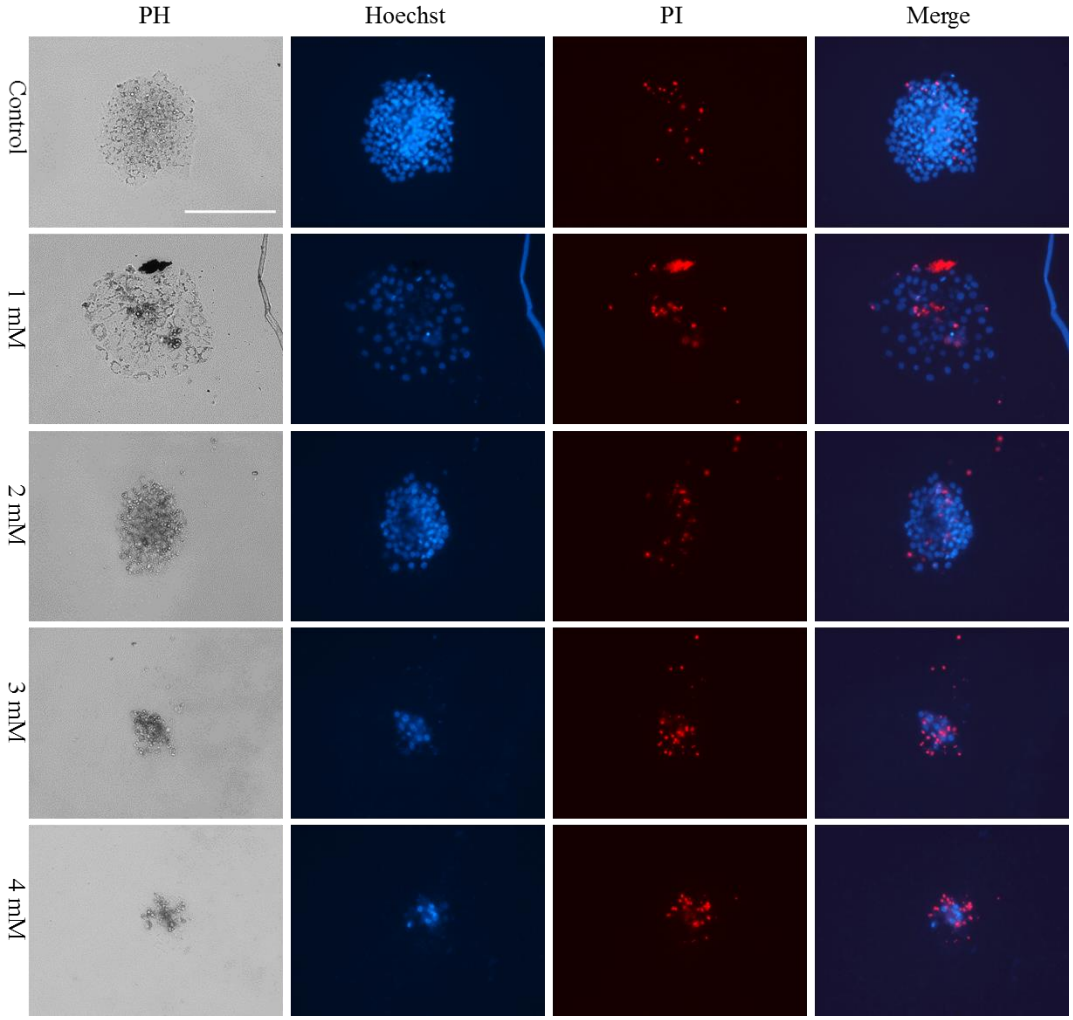

Figure 46. D1 ICM cells exposed to various concentrations of 3-HNV for 48 h.
A) Phase contrast photographs were taken at 0 and 48 h post-treatment using Leica microscope. Scale bar =200 µm. **B**) Hoechst/PI staining of one-day old ICM outgrowths. Hoechst DNA stain (blue) and PI (red). Merged channels consist of blue and red channels. The photos were taken on EVOS microscope. N (no. of colonies) = 30 for each treatment group. n (no. of independent biological replicates) = 3. PH= phase contrast. Scale bar =200 µm.

5.1.1.6.2. Effect of 3-HNV on D6 TE primary cultures

Mechanically bisected TEs were cultured in culture medium containing normal concentration of Thr (see Table 23) for 6 days. They were subsequently exposed to a variety of 3-HNV concentrations ranging from 1-4 mM for a period of 48 h. On day 8 of outgrowth, TE cells in the control group grew in number and size. TE cells in the 1 mM concentration also grew in size as much as the control group and the cells had clear cytoplasm with clear borders. At concentrations of above 2 mM 3-HNV, there was significant cell death in the TE primary cultures having lost their integrity as indicated by phase contrast microscopy (Figure 47A).

Once exposed to Hoechst/PI, the results showed tightly packed cells growing in monolayer with no PI (red) stained cells in the control group. 1 mM 3-HNV concentration did not show much effect on the TE cultures as it demonstrated many growing cells in the culture. However, from 2 mM concentration upwards, there was significant shrinkage in the cultures, so that monolayer cells lost their integrity. Although there were not many red cells appearing in the cultures, there was clear indication that the cultures had shrunken dramatically (Figure 47B).

A.

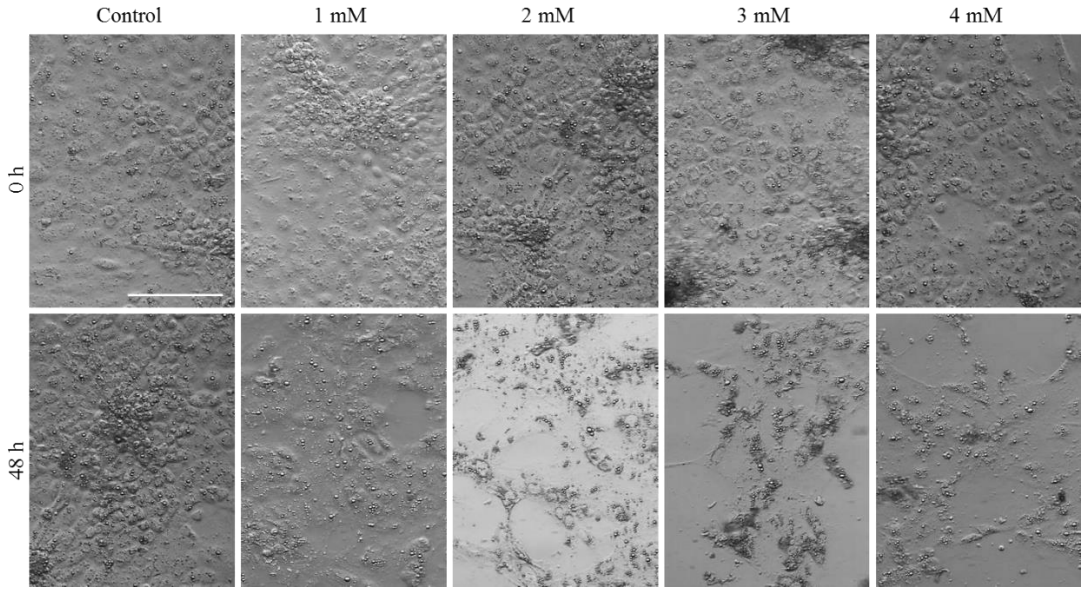

B.

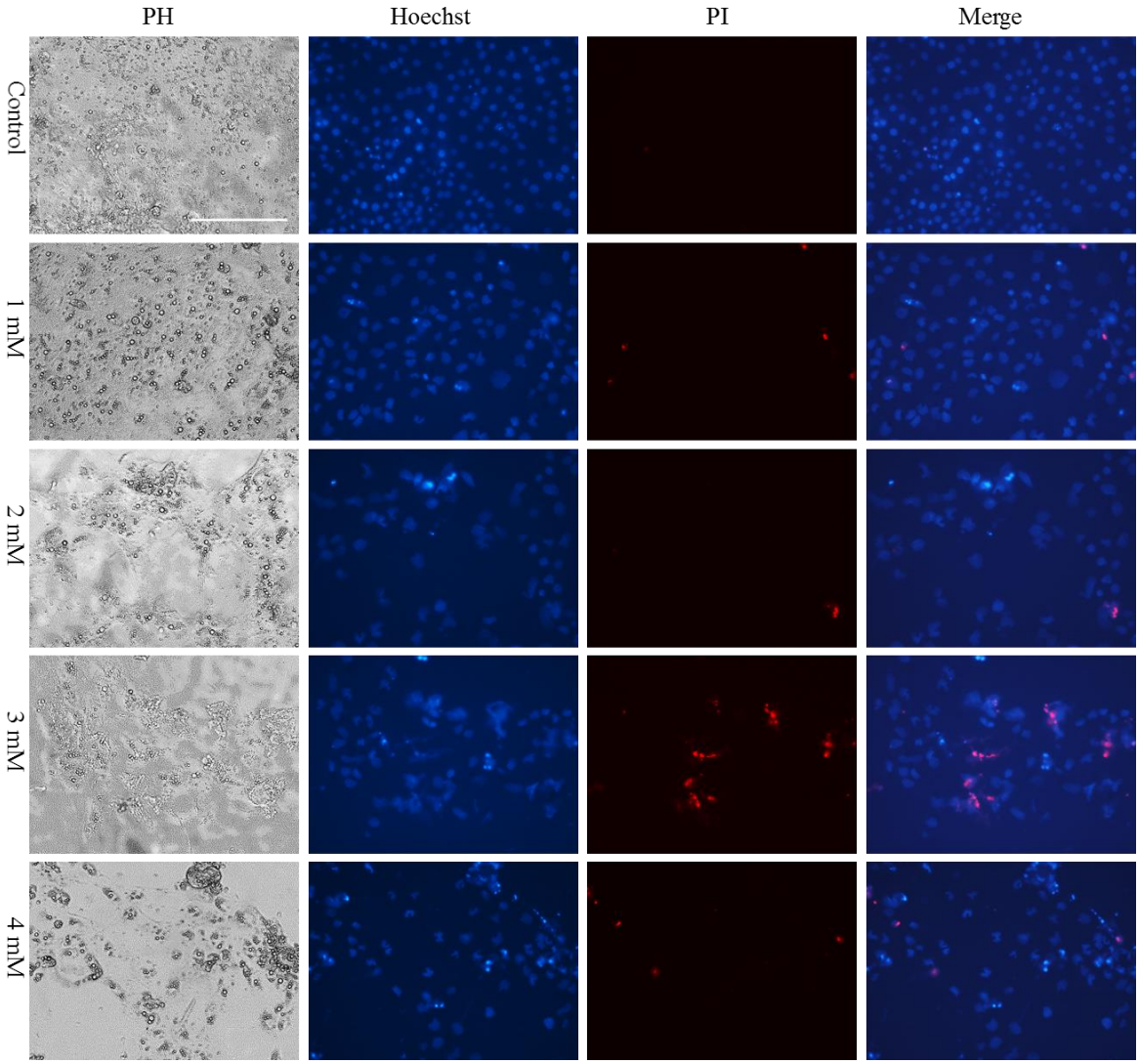

Figure 47. D6 TE primary cultures exposed to various concentrations of 3-HNV for 48 h. A) Phase contrast photographs were taken at 0 and 48 h post-treatment using Leica microscope. Scale bar =200 µm. **B**) Hoechst/PI staining of 6 days old TE primary cultures. Hoechst DNA stain (blue) and PI (red). Merged channels consist of blue and red channels. Photos were taken using EVOS microscope. N (no. of primary TE cultures) = 30 for each treatment group. n (no. of independent biological replicates) = 3. PH= phase contrast. Scale bar=200 µm.

5.1.1.6.3. Effect of 3-HNV on BEF cells

BEF cells were seeded in culture medium containing normal concentration of Thr (Table 23). They were subsequently treated with various concentrations of 3-HNV ranging from 1-4 mM for 48 h. Phase contrast images showed that BEF cells in the control group grew in number with cells demonstrating distinct plasma membrane. In all treatment groups, cells grew in monolayers as healthy as the control group with no sign of colony disintegration (Figure 48A). Once exposed to Hoechst/PI, the images showed that the cells in all treatment groups were

stained with Hoechst. However, no sign of red cells or culture shrinkage was observed in any of the treatment groups (Figure 48B).

A.

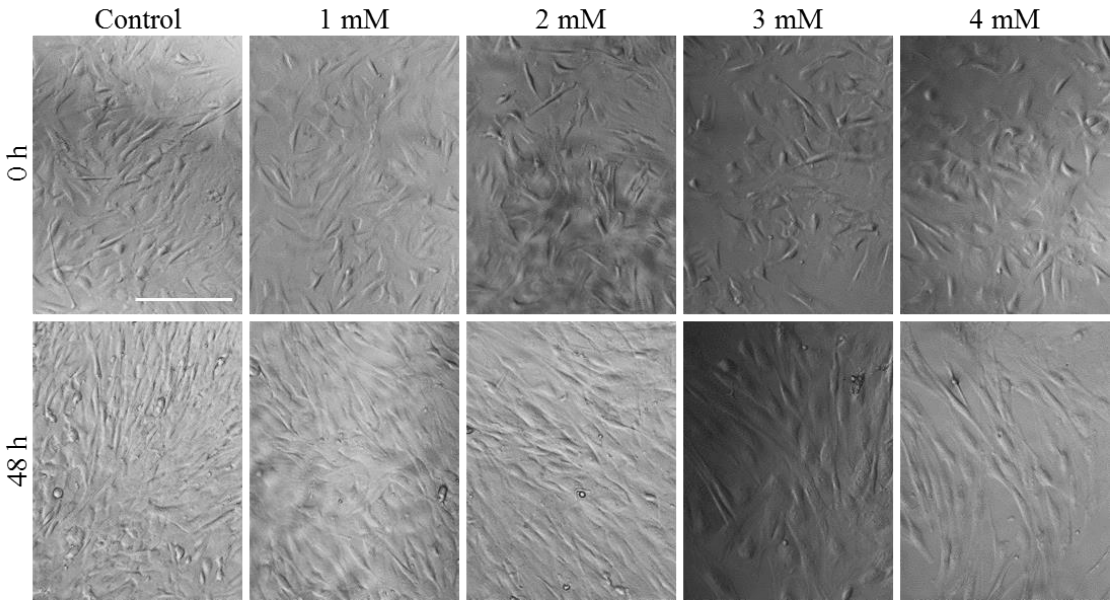

B.

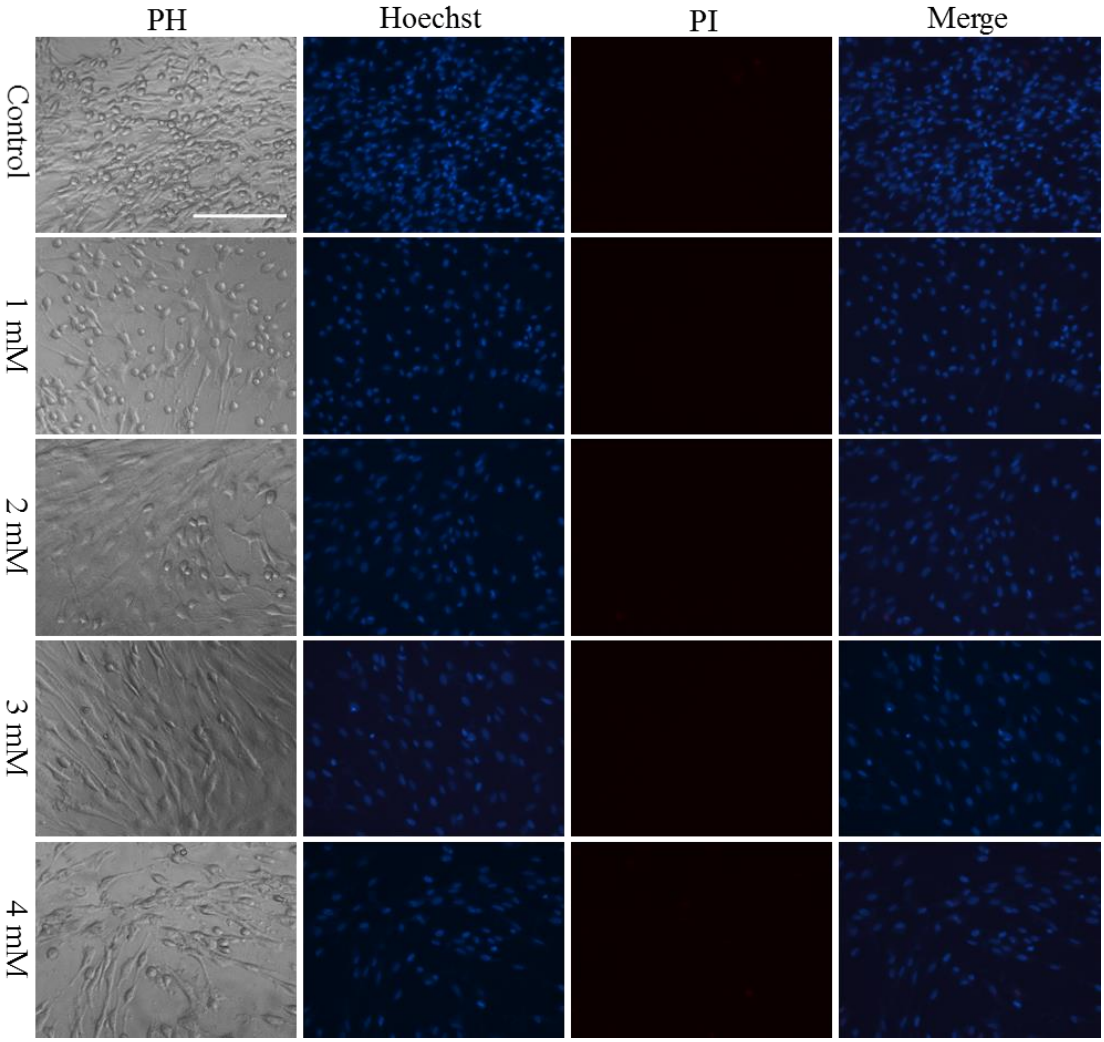

Figure 48. BEF cells exposed to various concentrations of 3-HNV for 48 h.
A) Phase contrast photographs were taken at 0 and 48 h post-treatment using Leica microscope.Scale bar=200 µm. **B**) Hoechst/PI staining of BEF cells. Hoechst DNA stain (blue) and PI (red). Merged channels consist of blue and red channels. Photos were taken using EVOS microscope. N (no. of wells cultured with cells) = 15 for each treatment group. n (no. of independent biological replicates) = 3. PH= phase contrast. Scale bar =200 µm.

It was hypothesized that since BEF cells do not express the TDH enzyme, they should not be affected by 3-HNV in a threonine-free culture condition. Therefore, BEF cells were cultured in a bSOF_AAs_ΔThr culture medium containing 300 µM 3-HNV. Phase contrast images demonstrated that 3-HNV produced significant cell death, whereas, in the bSOF_AAs_ΔThr control group, BEFs grew in number with cells having clear borders. Interestingly, 4 mM Thr masked the effect of 300 µM 3-HNV and BEF cells grew similar to that of the control group, therefore suggesting that BSA/protein available in the DMEM/F12 was able to mask the effect of the 3-HNV (Figure 49).

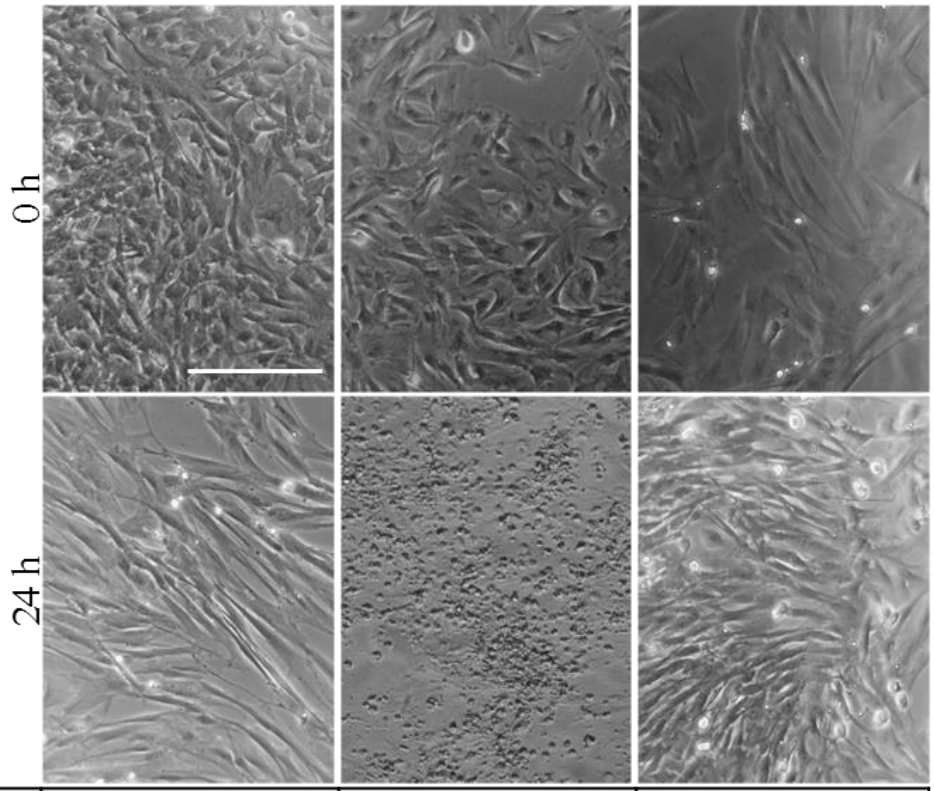

Threonine	-	-	4 mM
3-HNV	-	300 µM	300 µM
11 EAAs	+	+	+
NEAA	+	+	+

Figure 49. Phase contrast photographs of BEF cells exposed to 300 µM 3-HNV for 24 h.
300 µM 3-HNV compromises BEF cells in the bSOF_AAs_Δthr medium. Photos were taken at 0 and 24 h post-treatment, using Leica microscope. EAA= essential amino acids, NEAA= non-essential amino acids. N (no. of wells cultured with cells) = 20 for each treatment group. n (no. of independent biological replicates) = 3. Scale bar =200 µm.

Since BEF cells still expressed some level of *TDH* mRNA (see Figure 25) even though 20-fold lower than that of in ICM, this cell compromise could still be attributed to the inhibitory effect of 3-HNV on the TDH enzyme. To further validate these findings, the effect of 3-HNV on a cell line that did not express *TDH* gene was tested.

5.1.1.6.4. Effect of 3-HNV on skin fibroblast cells

In this study, the aim was to test the effect of 3-HNV on a cell line with no *TDH* gene expression. According to qPCR results, there was no *TDH* gene expression in the skin fibroblast cells (Figure 25). Therefore, this cell line was selected to test the effect of 3-HNV.

The skin fibroblast cells were cultured in a bSOF_AAs_ΔThr medium containing 300 µM 3-HNV. Phase contrast images indicated that the skin fibroblasts were severely compromised after 24 h incubation in this culture medium. However, skin cells in the bSOF_AAs_ΔThr control group grew in size with cells demonstrating clear borders. When seeding in a bSOF_AAs_ΔThr culture medium containing Thr and 3-HNV combined, the phase contrast images showed that skin cells grew as normal as the control group. This implies that 4 mM Thr masked the effect of 300 µM 3-HNV (Figure 50).

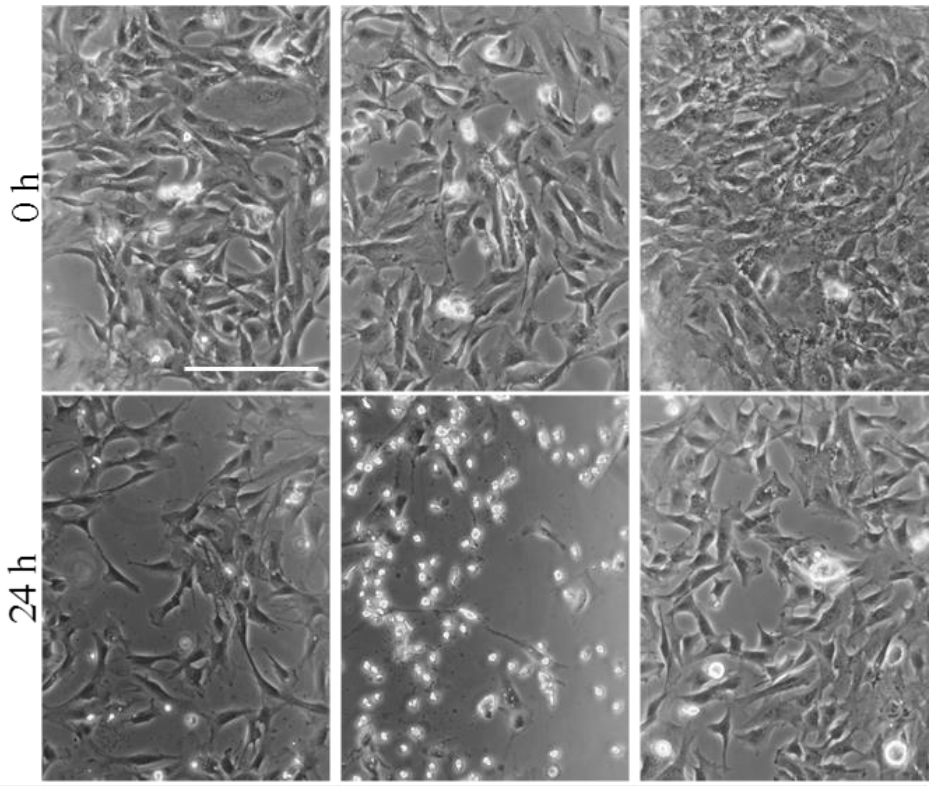

Threonine	-	-	4 mM
3-HNV	-	300 µM	300 µM
11 EAAs	+	+	+
NEAA	+	+	+

Figure 50. Phase contrast photographs of skin fibroblast cells exposed to 300 µM 3-HNV for 24 h.
300 µM 3-HNV compromises skin cells, which do not express any *TDH* mRNA, in a bSOF_AAs_ΔThr medium. Photos were taken at 0 and 24 h post-treatment, using Leica microscope. N (no. of wells cultured with cells) = 20 for each treatment group. n (no. of independent biological replicates) = 3. EAA= essential amino acids, NEAA= non-essential amino acids. Scale bar=200 µm.

In summary, these findings indicate that since skin fibroblasts do not express any TDH (Table 10), 3-HNV does not impair cellular function specifically via TDH inhibition in the threonine-SAM pathway as suggested by [8]. However, instead, the detrimental effect of this chemical, observed in both bovine cells and embryos, is attributed to the impairment of cellular function maybe via interfering with protein synthesis [152].

Table 10. Summary of the TDH expression profile of investigated bovine cell types and their response to 3-HNV treatment.

Bovine cell type	TDH expression	3-HNV effect
Embryos	Yes	Yes
D1 ICM	Yes	Yes
D6 TE	No	Yes
BEF	No	Yes
Skin fibroblasts (LJ801)	No	Yes

Chapter 6

6. Chapter Six: Discussion

The two primary objectives of this study were to: i) conduct an amino acid screen to determine if any particular amino acid(s) was essential for bovine ICM development and pluripotency, and ii) to investigate the role of the TDH-mediated threonine-SAM pathway in bovine ICM development and pluripotency. The following sections will discuss the results obtained under each objective.

6.1. Objective One: amino acid requirements of bovine ICM development

The primary goal of this objective was to screen for amino acid(s) whose metabolism is vital for bovine ICM development and pluripotency. To achieve this, experiments were performed on bovine embryos instead of ICM outgrowths for the following reasons; i) ICM cells do not propagate *in vitro* as much which is due to their culture conditions not being optimised yet. Therefore, drawing any conclusion based on a very limited number of ICM cells would not be convincing. ii) ICM culture medium consists of a combination of Dulbecco modified Eagle medium/F12 and Neurobasal medium both having their own set of amino acid mixture, which makes it almost impossible to drop out a single amino acid. In addition, compromising their culture conditions would make their limited growth even harder. Based on this, an amino acid depletion protocol was developed. After setting up the screening system, it was not surprising to find out that EAAs had a more substantial adverse effect on bovine embryo development than NEAAs. Therefore, EAAs were omitted from the bovine embryo culture media individually, in pairs, triplets or groups of six.

The findings indicate that bovine embryos can survive in the absence of up to 6 essential amino acids. This contrasts with an earlier study which showed that mouse ePSCs depend on threonine catabolism whose absence impedes mouse ePSC colony formation [8]. The study showed that when mouse ePSCs were cultured under a threonine-free culture condition, ePSCs ceased colony formation, whereas, in the other 19 culture conditions, each missing one amino acid, mouse ePSCs colony formation was comparable to that seen in the control group. Another study in 2014 [9] demonstrated that human ESCs rely on the EAA methionine. Even though their findings, measured by cell counting, indicated that individual absence of leucine, lysine and tryptophan and methionine compromised human ESC growth, the focus was only on methionine as its absence had the most detrimental effect. Even though these findings also contradict with the results presented in this study, it should be noted that this study investigated pluripotency via bovine embryos. Since there was no published information on amino acid requirement during embryo development, to validate the results obtained using bovine

embryos, a threonine starvation experiment on mouse embryos was also undertaken. The results indicate that threonine starvation does not affect mouse embryo development (Figure 12), which is in agreement with the findings of this study on bovine embryos. However, this is inconsistent with the study that showed mouse ESCs stop proliferating and forming colony formation upon threonine starvation [8]. The threonine starvation experiment on mouse embryos validates the protocol used for amino acid starvation studies on bovine embryos. These results indicate that the amino acid screening system on the embryos is not appropriate for measuring ICM development and pluripotency since the outcome of performing amino acid dropout on mouse ES cells and mouse embryos was not the same. There are fundamental differences between an ESC (as an individual cell) versus an embryo (as a multicellular diploid eukaryotic organism). In biology, an *in vitro* cultured ESC is defined as an individual living cell that can function and uptake nutrients individually and independently directly from the culture medium, whereas, a blastocyst is defined as an organism with a contiguous living system which is capable of responding to stimuli, reproduction, growth, development and homeostasis. This organism has three different cell types namely epiblast, hypoblast and trophectoderm each having different nutritional requirements [153]. Moreover, not all cells within the blastocyst can directly uptake their nutritional requirements from the culture medium, especially ICM cells that are surrounded by trophectoderm cells and fluid-filled blastocoel cavity. Metabolic interactions between ICM and TE cells may happen via paracrine regulations [153]. The blastocoel fluid also functions as a reservoir for transported glucose, pyruvate, amino acids, and proteins [153-158].

A study in 1983 [159] investigated the role of blastocoel in accumulating amino acids in the rabbit embryos. It was shown that rabbit embryos use this cavity as a reservoir and bulks of amino acids are accumulated in it. In another study [154] properties of uptake of amino acid methionine were examined in the mouse embryo. By mechanically collapsing the blastocyst, uptake of amino acid into the intact blastocyst was resolved into cellular and cavity components. It was found that about 70 % of the radiolabelled methionine was accumulated in the blastocyst cavity. Another study investigated the concentrations of amino acids in blastocyst cavity of bovine embryos [153]. Their findings showed that all amino acids were available in the blastocoel fluid at different concentrations. This cavity can serve as an amino acid reservoir for both the trophectoderm, which has an exchange system on its inner surface [160] and ICM to provide with the amino acids required for their growth and differentiation [154]. Transport systems on the membrane of the TE cells operate to maintain the amino acid content of the cavity pool [154]. Another study in 1995 investigated the effects of insulin on

the endocytic activity of mouse blastocysts in vitro [161]. Confocal studies showed that fluorescein isothiocyanate-labeled dextran and albumin were endocytosed by blastocysts and localized within vesicles in the outer trophectoderm cells. No labelled dextran and albumin was detected in the inner cell mass cells or the blastocoel cavity. In another study in 1998 [162] the protein content of day 7 blastocysts was measured in the cultures supplemented with either PVA, BSA and FCS or *in vivo*-derived day 7 blastocysts. The results indicated that the protein content was significantly lower in PVA-cultured embryos than other treatments. Incubation of bovine blastocysts with FITC-labelled BSA or β-casein and microscopic analysis also showed that protein in the extra-embryonic environment was actively taken up by the trophectoderm of day 7 blastocysts. These findings advocate that exogenous protein be essential for maintaining intracellular amino acid pools. Thus, building upon these studies, it is highly likely that amino acid-starved embryos benefit from the blastocoel reservoir and metabolic interactions between ICM and TE, and therefore, sustain a homeostasis state which results in embryo survival. Overall, these findings imply that the effect of amino acid deprivation on embryos is different from that of on cells.

6.2. Objective Two: the TDH-mediated threonine-SAM pathway

Even though threonine deprivation did not show any adverse impact on bovine embryo development, an investigation into the downstream of the threonine-SAM pathway was instigated on the rationale that this pathway had been documented to be vital for mouse ESC colony formation and survival [8]. In this pathway, mitochondrial TDH breaks down amino acid threonine into glycine and acetyl-CoA. Acetyl-CoA goes through the TCA cycle to contribute to providing ATP, while glycine contributes to the one-carbon metabolism pathway. This will lead to the production of SAM which is a universal substrate for donating its methyl groups to trimethylate H3K4 (Figure 4).

6.2.1. Presence of TDH enzyme in bovine cells and tissues

To investigate *TDH* expression at mRNA levels in bovine cells and tissues, quantitative PCR analysis was performed on bovine embryos, pure ICM, pure TE, D6 ICM, D6 TE, BEF, muscle fibroblasts, liver, testis, brain, heart, kidney, muscle, spleen, and skin cells. The results indicated that bovine *TDH* mRNA expression is not restricted to ICM and that TE cells also express it at similar levels to that of ICM. This is in contrast with what has been reported in the mouse where there was no TDH expression in TE cells being restricted to ICM, as shown by *in situ* hybridization and IF [8]. This is perhaps because *TDH* gene is important for the development of TE as much as ICM in the bovine embryo in the preimplantation phase. Of those bovine adult cells tested for *TDH* mRNA transcript, liver and testis express this gene at

similar levels to ICM (Figure 25). In contrast to these findings, in another study, *Tdh* mRNA level of mouse testis, with the highest amongst the other 6 mouse adult tissues tested, was one-thousand times less than that of mESCs [8]. In that paper [8], Wang and colleagues concluded that since they have not been able to find any mouse tissue expressing *Tdh* mRNA at similar levels to mESCs, *TDH* expression appears to be restricted to mouse ESCs.

When comparing mESCs to mouse blastocysts, *Tdh* mRNA level decreased by 12 fold (Figure 28), whereas, in bovine, *TDH* was expressed at similar levels between blastocyst and ICM (Figure 25). This indicates that the gene expression discrepancy that exists in mouse between ESCs and embryo is not observed in bovine between ICM and embryo, because in the mouse only ICM expresses *Tdh*, whereas in bovine both ICM and TE cells express this gene.

Subsequently, in order to detect TDH at protein levels in bovine cells, a rabbit polyclonal anti-TDH antibody (generously gifted by Dr McKnight laboratory, USA) was used in this study. The suitability of this antibody was initially confirmed by aligning TDH synthetic peptides [146], used for generating this antibody, against the bovine TDH protein sequence, where epitope 1 and 2 showed 2 and 4 mismatches, respectively, against the protein (see Figure 13). After verifying that this antibody specifically recognizes bovine TDH enzyme using a stably expressing bovine TDH cell line (Figure 18), an immunofluorescence staining on bovine cells was performed. This antibody also stained mouse ESCs further confirming the findings published by [8]. These results indicate that TDH enzyme is restricted to D8 bovine embryos, in both ICM and TE cells. Bovine blastocyst showed a homogenous TDH expression pattern, resembling the pattern in mouse blastocysts [8], in both ICM and TE cells. This staining also matches the blastocyst gene expression profile showing *TDH* being expressed in both ICM and TE population at similar levels. In the mouse embryo, however, TDH signal is restricted to ICM [8], which is inconsistent with the findings of this study. This is because perhaps TDH is required for early bovine embryonic development, preimplantation phase, and inhibition of this enzyme may result in compromising embryo development, whereas, in the mouse, TDH is only responsible for the unique metabolic state in the ICM cells [8]. The role of TDH in the context of mouse embryo development is not yet fully understood and investigations are still ongoing [8]. Six-day old ICM outgrowths also showed TDH signal which corresponded to its *TDH* mRNA level, being expressed at similar levels to pure ICM. These findings are in agreement with the results demonstrating TDH protein expression in mouse ESCs [8] and mouse iPSCs [163]. In contrast, TDH signal was not detectable in 6 days old TE primary culture, which corresponded to its mRNA level showing 19-fold reduction compared to *TDH* level in ICM. These findings confirm that TDH is not expressed in the D6 TE primary cultures. Bovine ICM

outgrowths express pluripotency markers including NANOG, SOX2, and OCT4. No pluripotency marker is expressed in the trophectoderm cells. Since TDH is only expressed in the ICM cultures and not in the TE cells, it implies a role between TDH and bovine pluripotency. TDH may be involved in sustaining pluripotency via regulation of SAM levels and subsequently methylation markers including H3K4me3, which may end up regulating pluripotency-associated markers including NANOG. This link has previously been established in mouse ePSCs [10].

TDH protein was not detectable in BEF cells either, which corresponded to its mRNA level that is 24-fold lower than that of in ICM. To confirm the presence of TDH enzyme in bovine cells, western blot analysis was undertaken. Unfortunately, due to limitations in collecting the required number of cells in bovine embryos and D6 ICM outgrowths, western blotting was unable to be performed for these cells. Therefore, the presence of TDH enzyme in these cells relied solely on the *TDH* gene expression profiles and immunostaining findings. Detecting TDH band in mouse ESCs and mouse iPSCs and its absence in MEF cells further confirmed previously published data [8; 163]. BEFs and muscle fibroblasts were selected for western blotting since they expressed some levels of *TDH* mRNA and harvesting lysates at required amounts was possible. These results showed that there were no detectable TDH bands in the BEF and bMF lysates, which were consistent with their *TDH* gene expression profile. This was also in agreement with the IF images for BEF cells demonstrating no TDH signal. In conclusion, the results from *TDH* gene and protein expression findings indicate that TDH protein is present in D8 bovine embryos, which may imply that TDH expression is essential for early bovine embryonic development. However, it becomes restricted to *in vitro* cultured ICM outgrowths. This may also indicate that TDH might be necessary for sustaining pluripotency in *in vitro* cultured ICMs.

6.2.2. The role of TDH enzyme in bovine embryonic development

To determine if TDH enzyme was crucial for bovine embryonic development, an approach to inhibit TDH enzyme using a TDH inhibitor, Qc1, was adopted. This chemical has been shown to specifically impede ePSCs growth and colony formation via the inhibition of TDH enzyme [11]. This chemical reversibly occupies the active site of TDH enzyme and blocks its activity. Subsequently, TDH fails to convert threonine into glycine and acetyl-CoA. Lack of glycine will then lead to ceasing SAM production and therefore inhibition of H3K4 trimethylation. Thus, this starvation stimulates the autophagy pathway, which results in degrading unnecessary organelles inside the cell to fuel the threonine-SAM pathway for survival. This starvation eventually leads to mouse ES cell death [10; 11]. The specificity effect of the Qc1 inhibitor on

bovine cells was confirmed by exposing a TDH-free cell line (bovine skin fibroblasts Lj801 cell line) to this chemical which showed no adverse effect of this inhibitor on the cells. These findings indicate that early bovine embryonic development relies on TDH enzyme. Qc1 severely reduced B^{1-3} and B^{1-2} bovine embryo development by 1.5 and 2.5 fold, respectively, compared to the DMSO control (Figure 29). This is the first documentation of the inhibitory effect of Qc1 on bovine embryos. Qc1 reduced the number of cells in both bovine ICM and TE populations via stimulating autophagy. An autophagy kit measuring signal intensity of autophagic vacuoles confirmed this. This finding is consistent with the results published by [11] that showed that Qc1 kills mouse ESCs via stimulating autophagy process. Interestingly, Qc1 was also shown to severely impair mouse embryo development (**Figure 37**), presumably via activating the autophagy cascade.

The effect of Qc1 was also studied on the SAM/SAH ratio in the bovine embryos. SAM/SAH ratio is key since SAH inhibits the activity of methyltransferases [10]. It has been shown that this ratio decreases when the Thr-SAM pathway is inhibited, resulting in inhibition of methyltransferases. This would then lead to ceasing trimethylation of H3K4 marker [10]. Unfortunately, measuring SAM/SAH ratio levels in bovine embryos is not as feasible. Since this study did not have access to platforms sensitive to the lower number of cells for quantitative analysis of SAM/SAH levels, antibodies against SAM and SAH molecules were tried. Unfortunately, neither of these antibodies were able to detect any SAM or SAH signal in the D8 bovine embryos, even though the antibodies worked on a positive control. This indicated that this approach was not suitable for measuring SAM/SAH ratio in bovine embryos. Since the antibodies worked on the positive control group, not detecting SAM/SAH in bovine embryos is likely due to very low production of these molecules in the ICM and TE cells. To date, there appears to be no published data on embryos detecting SAM/SAH with antibodies. Routine methods of measuring these molecules rely on using liquid/gas chromatography. There are some published data on mouse ESCs measuring their SAM/SAH levels [8; 10]. However, these platforms require relatively large numbers of cells (minimum 1×10^5 cells) and since it is not feasible to collect too many embryos, using these approaches on bovine embryos is not reasonable.

Next, the inhibitory effect of Qc1 on trimethylation markers H3K4me3, H3K9me3 and H3K27me3 in D8 bovine embryos was investigated. Generally, H3K4 trimethylation confers a relaxed state to chromatin, allowing genes to be transcribed, whereas, H3K9me3 and H3K27me are both repressive markers that condense the chromatin preventing genes from transcribing [10; 164]. The results indicate that Qc1 inhibition promotes H3K4 trimethylation

levels in both bovine ICM and TE cells, whereas, it does not affect H3K9me3 and H3K27me3 levels. In contrast to these findings, a study published in 2013 [10], showed that after threonine restriction for 24 h in mouse ESCs, H3K4me3 disappears, however, other tested methylation markers including H3K9me3 and H3K27me3 remained intact which were consistent with the findings of this study. Logically, there should not be a difference between approaches towards methyl group restriction as both Δthreonine culture condition and TDH inhibition by Qc1 limit the amount of SAM availability to methyl contribution. Therefore, in either case, trimethylation of H3K4 should disappear. One possible explanation for this could be considering a repressive role for H3K4me3 in the course of embryonic development. In a study in 2016 [165] it was shown that ICM cells of IVF-produced D7 bovine embryos were hypomethylated at H3K4me3 relative to their TE counterparts. Knowing that ICM is *in vivo* equivalent of ESCs, which sustain a naïve pluripotent state, it is sensible to keep it hypomethylated allowing transcription of genes associated with pluripotency and embryonic development. In another published study, overexpression of histone lysine demethylases 2A/B, which hypomethylate transcriptionally activating H3K36 and H3K4, led to increased efficiency of induced pluripotency [166]. In a study in 2010 [167] on zebrafish embryos, the investigators showed that many inactive genes were uniquely marked by H3K4me3. Despite this activating modification, these monovalent genes were neither expressed nor stably bound by RNA polymerase II. In another study in 2011 [168], the investigators suggested that genes that were marked with H3K4me3 at pre- and mid-blastula transition, were transcriptionally inactive. These studies lend support for a repressive role of H3K4me3 which could account for its increase upon TDH inhibition in bovine embryos. This increase might lead to downregulation of early embryonic developmental genes and subsequent compromised embryo development.

Next, the inhibitory effect of Qc1 on lineage-specific genes in D8 bovine blastocysts was investigated as they are under direct regulation of epigenetic markers [169; 170]. When epiblast (*NANOG*, *FGF4*, and *SOX2*), hypoblast (*PDGFRα*), trophectoderm (*CDX2*) and *TDH* mRNA levels were measured in bovine embryos, results indicated that Qc1 did not influence the gene expression levels of these markers, whereas a study published from mouse ESCs in 2013 [10] showed reduced expression of pluripotency markers *Oct4, Sox2, Nanog, Rex1,* and *Blimp1* and increased levels of differentiation markers. This gene expression discrepancy in pluripotency markers between mouse and bovine species is yet to be understood.

Overall, these findings show that early bovine embryonic development requires TDH enzyme to regulate H3K4me3 levels, suggesting connections between metabolism, epigenetics and embryonic development.

6.2.3. The role of TDH enzyme in bovine primary ICM cultures

The role and importance of TDH enzyme in cultured ICM cells was studied since the ultimate goal was to better understand the mechanisms underlying bovine pluripotency *in situ*. This will lead to optimization of their culture condition and finally triggering their proliferation capacity. The results indicated that upon 6 days of *in vitro* culture, TDH enzyme is still operating in ICM outgrowths, but disappears in TE primary cultures. Qc1 impaired freshly isolated ICMs, however, after 6 days of *in vitro* culture, some ICM cells within the outgrowth started differentiating (because the culture condition is not yet fully optimized which is due to the poor understanding of mechanisms underlying bovine pluripotency). The percentage of compromised cells declined approximately 40% from ICM to D6 ICM outgrowths, which was not statistically significant. These results correspond to their *TDH* mRNA levels where after 6 days of ICM culture *TDH* was still expressed at similar levels to that of the ICM. Furthermore, TDH protein was still detectable after 6 days of *in vitro* ICM culture, which matches the Qc1 findings. In agreement with these results, a published study in 2011 [11] inhibited TDH in mouse ESCs, which express *Tdh* gene at high abundance [8], with Qc1 and noted that this chemical impaired these cells. However, when differentiating embryoid bodies, which were losing the expression of *Tdh* gene and protein [8], were treated with even 90 µM Qc1, the cells remained intact, with respect to cell growth and morphology. Qc1 also failed to compromise HeLa cells even with 300-fold higher levels than that administered to impair mouse ES cells [11]. Even though Qc1 compromised TE cells, it did not impair them after 6 days of culture. This corresponds to their *TDH* mRNA profile which declines from TE cells to D6 TE primary culture. Qc1 results from this study also correspond to the TDH protein profile. This enzyme was detectable in TE cells, whereas, D6 TE primary cultures did not show any TDH signal. These findings suggest that TDH enzyme becomes restricted to ICM outgrowths after 6 days of *in vitro* culture, and disappears from the trophectoderm culture. This is perhaps because the TDH-mediated metabolic state observed in mouse ESCs [8] becomes restricted to the bovine cultured ICM cells. Indeed TDH may be imperative for sustaining bovine pluripotency *in vitro* as it is co-expressed with pluripotency markers NANOG, FGF4, and SOX2, and blocking this enzyme results in increased cell death, whereas TE primary cultures do not express any pluripotency marker and therefore do not need this TDH-mediated metabolic state.

6.2.4. 3-HNV effect on the threonine-SAM pathway

Next, 3-HNV, as an inhibitor of TDH enzyme, was investigated since an earlier study showed that this chemical specifically inhibited the TDH-mediated threonine-SAM pathway in mouse ESCs and embryos leading to cell death and impairment of embryo development [8]. This

chemical is a synthetic variant of threonine containing an extra carbon atom which TDH enzyme catabolizes it to glycine and propionyl-CoA instead of glycine and acetyl-CoA [8]. It was concluded that since mouse ESCs and ICMs need both glycine and acetyl- CoA, and 3-HNV does not give rise to acetyl-CoA, it leads to mouse ESC and ICM cell death [8]. The findings of this study indicate that the detrimental effect of 3-HNV is not exerted via the TDH-mediated Thr-SAM pathway. When this TDH inhibitor was tested on both bovine embryos and cells, an LSOF medium containing 300 µM 3-HNV impaired embryo development severely, while the group containing 4 mM threonine supplement and 3-HNV developed as normal since it was suggested that threonine provides both glycine and acetyl-CoA [8] to the embryos. These results are consistent with the findings on the effect of 3-HNV on mouse embryos, showing that 300 µM severely compromised mouse embryo development, whereas, 4 mM threonine supplement rescued development blockade [8]. When this chemical was tested on D1 ICM outgrowths and D6 primary cultures, both containing threonine, the findings showed that 3-HNV severely impaired both cell types. When exposing BEF cells (which do not express TDH) to 3-HNV in a medium containing protein/serum, the cells remained intact and alive after 48 h. Since these cells do not express any TDH to catabolize 3-HNV, it was hypothesized that 3-HNV should not affect BEF cells in a threonine-free culture medium. BEF cells were then cultured in a bSOF_AAs_ΔThr medium containing 300 µM 3-HNV. After only 24 h a significant cell death was observed, whereas, in the control group and the group containing 4mM Thr plus 300 µM 3-HNV, BEF cells grew in as normal. This suggested that 3-HNV might not impair cells via the TDH-mediated threonine-SAM pathway since there was no TDH enzyme present in the BEF cells to catabolize this chemical. As BEF cells had been shown to express some levels of *TDH* mRNA, this finding was not yet conclusive. Thus, next, skin fibroblast cells expressing no *TDH* mRNA at all were tried. The results demonstrate that the *TDH*-free skin fibroblast cells, cultured in bSOF_AAs_ΔThr medium containing 300 µM 3-HNV were severely compromised after 24 h, while in both control group and the group containing 4 mM Thr and 300 µM 3-HNV, BEF cells showed no sign of cell death. In a study in 2009 [8], the investigators incubated mouse embryos with 30 µM, 100 µM, 300 µM and 1 mM of 3-HNV and saw the inhibitory effect in 300 µM and 1 mM concentrations. However, when the embryos were incubated in a culture condition containing 4mM Thr plus 300 µM and 4mM Thr plus 1 mM 3-HNV, the embryos grew normally. mESCs were also treated with 3-HNV using culture media with or without threonine. Using standard culture medium, they found that 3-HNV inhibited ESC colony growth in the absence of Thr. This chemical was also tested on TDH-free MEFs, 3T3 (mouse embryonic fibroblasts), and HeLa (human cell line having a truncated TDH protein) cells and no inhibitory effect on these cell types was observed.

Therefore, it was concluded that 3-HNV inhibitory effect is specific to the threonine-SAM pathway and mESCs critically rely on the TDH-mediated production of both glycine and acetyl-CoA [8]. The problem with their experiment was that even though cells with no TDH expression were seeded, the culture medium for these cell types was inappropriate. Because it contained serum/BSA which provided cells with enough Thr residues. Hence, these Thr residues replaced 3-HNV and masked the nonspecific effect of this chemical. In a separate study published in 2013 [163], the investigators transfected MEF cells with TDH, OCT4, SOX2, C-MYC and KLF4 to produce mouse iPSCs. The iPSCs were subsequently incubated with varying amounts of 3-HNV ranging from 0-2 mM. It was stated that 3-HNV inhibited TDH-facilitated reprogramming efficiency in a dose-dependent manner. It was then concluded that acetyl-CoA produced from TDH-mediated threonine catabolism is essential for TDH in promoting reprogramming. Since this study failed to demonstrate an appropriate control group to monitor the non-specific effect of 3-HNV on the TDH-free MEF cells in a Δthreonine culture medium, their conclusion may not be valid. In agreement with the findings of this study, a group tested whether 3-HNV inhibits human embryonic stem cell proliferation [152]. Human cells produce a truncated TDH protein which is non-functional [146] (Figure 14). The study showed that 4 mM 3-HNV inhibited human ePSCs growth and the colonies lost their integrity. 4 mM threonine, however, rescued them from the 3-HNV effect. It was concluded that 3-HNV does not impair human ePSC colony formation via TDH inhibition. Overall, the findings of this study suggest that 3-HNV does not exert its inhibitory effect specifically via the TDH-mediated threonine-SAM pathway and indeed, it impairs cellular function via other ways. The likely explanation is that when there is not enough threonine for protein synthesis, it is replaced with 3-HNV leading to the alteration of protein structure which makes it non-functional [152].

6.3. Conclusion and future directions

6.3.1. Amino acid starvation experiments

It appears that amino acid starvation in embryos is not as straightforward as in ESCs. This is most likely due to their capability to store nutrients in their blastocoel cavity. Furthermore, metabolic interactions between ICM and TE may contribute to compensating for amino acid shortcomings. Moreover, an embryo is multicellular organisms with 3 different cell type each having their own nutritional requirements. As mentioned earlier, having limitations on ICM propagation and complex culture conditions are the constraints preventing meaningful data generation using amino acid dropout approaches on bovine ICM outgrowths. Hence, it would be better to first address as to why these isolated ICM cells do not propagate in vitro as mouse ESCs do, that this lies in optimizing their culture conditions. This consequently depends on

understanding the mechanisms underlying ICM formation and pluripotency regulation. So far this progress has led to the development of a chemically defined culture regime known as 2i, which is based on dual inhibition of two signalling pathways, mitogen-activated protein kinase (MAPK) signalling suppressed by PD0325901 inhibitor and GSK-3 suppressed by CHIR99021 inhibitor [4]. This regime has derived naïve ESCs from previously refractory mouse [4] and rat species [5]. In our lab, we have developed a more robust culture condition called $2i^+$ regime. This has improved *in vitro* bovine embryo development significantly and also enhanced pluripotency-associated gene expression profile of bovine ICM [118]. The $2i^+$ regime has also made *in vitro* short-term culture of ICM outgrowths possible, sustaining pluripotency markers in more cells relative to previous culture conditions [171]. However, their proliferation is very limited and some cells inside the colonies start differentiating. Progress has so far been slow but promising. A better understanding of mechanisms governing bovine pluripotency will lead to having a fully defined and optimized culture condition, which will enable indefinite proliferation of bovine ICM cells in culture. This would then make performing amino acid deprivation experiments on bovine ESCs possible.

6.3.2. TDH-mediated threonine-SAM pathway

This study suggests that the TDH-mediated Thr-SAM metabolic pathway is a crucial requirement for early embryonic development via regulating H3K4me3 levels. The findings also suggest that the TDH enzyme is vital for maintaining bovine ICM cells in culture. Unfortunately, it was not possible to confirm the presence of TDH enzyme in the bovine embryos and ICM cells via western blotting. This was due to the low number of cells (approximately 200 cells per embryo, and 400 cells per each D6 ICM outgrowth), given that western blotting requires a minimum of 5×10^5 cells. Recent advances in protein analysis have made it possible to detect proteins even at single cell levels. These technologies include single cell analysis by flow cytometry, microfluidics, and mass spectrometry [172]. It is hoped that using these approaches the presence of TDH in bovine embryos and cultured ICMs will be further confirmed. It was surprising that Qc1 did not affect the expression of the selected lineage-specific genes. Testing other genes including *OCT4*, *KLF4*, *SOX17*, and *KRT8* should be performed to determine which genes are influenced by the effect of TDH inhibition. Since SAM/SAH ratio directly regulates H3K4me3 levels, measuring SAM/SAH ratio will also be another experiment to do. Antibody staining was shown to not optimal. More cutting-edge technologies such as targeted metabolomics analysis using mass spectrometry on single cell level would be another alternative to use on embryos for determining the SAM/SAH ratio. Supplementing bovine embryos with downstream intermediates of TDH enzyme would be

another interesting approach to undertake. Providing bovine embryos with combinations of glycine plus acetyl-CoA or glycine plus pyruvate, or SAM alone while blocking TDH enzyme will indicate if these substances can sustain embryo development in the absence of TDH enzyme. This will further shed light on the role of TDH in bovine embryo development. Hypothesizing that TDH inhibition leads to the accumulation of threonine and depletion of acetyl-CoA and glycine, bovine embryos could be treated with TDH inhibitor and the fluctuation rate of these metabolites would be measured. This will again determine if the TDH enzyme is crucial for bovine embryonic development. Mapping the metabolic state of ICM cells would be another exciting objective to perform. Studies on the mouse and human have shown that ESCs are in an exceptional metabolic state that is different from that of in somatic cells [173; 174]. In our lab, a preliminary metabolomics study was performed on bovine embryos; however, since few numbers of cells were dealt with (maximum 2000 cells per each group) the outcome did not lead to any meaningful data. Recent advances in mass spectrometry, mass spectrometry imaging, capillary electrophoresis, optical spectroscopy, and fluorescence biosensors now enable us to determine hundreds of metabolites in a single cell simultaneously [175]. Using these technologies will enable us to better characterize bovine ICM cells metabolically, which this will then lead us to a better understanding of bovine pluripotency.

To verify if the gifted anti-TDH antibody works in bovine species, a stably TDH-expressing cell line was generated. It would be interesting to do some functional studies by performing nuclear transfer using these TDH overexpressing cells as donors and producing bovine embryos. This will give us more insight into TDH function in the context of bovine embryo development. It would also be intriguing to block the TDH enzyme in the TDH overexpressing bovine embryos and study its effect on ICM and TE development and cell number, SAM levels, methylation marker as well as lineage-specific gene expression levels in comparison to normal TDH expressing embryos.

TDH knockout bovine embryo would be another alternative. To do this, a TDH-null cell line first needs to be generated. CRISPR/Cas9 system is a relatively highly efficient genome-editing tool that site-specifically targets the gene of interest. To knock out the *TDH* gene, the Cas9 nuclease is directed to the gene location by a single guide RNA to introduce targeted double-strand breaks and subsequent gene deletion [176]. Once generated, TDH-null cells would subsequently be used to produce TDH-null bovine embryos. It would be of interest to investigate if these embryos lacking TDH enzyme can develop or not. If they do not, it will further confirm the findings of this study showing the dependence of embryonic cells on TDH. However, if these TDH-null embryos did develop, it would be informative to observe how ICM

and TE cells lacking TDH will develop and if its absence will affect them at all. Moreover, further down the development course, what would be the effect of TDH absence on the developing organs? Culturing TDH-null ICM outgrowths *in situ* will be another experiment to perform. It would be instructive to investigate if these TDH-null ICM cells will grow as good as normal ICM outgrowths, despite their insufficient growth.

References

1. Martin G. R. 1981. ***Isolation of a pluripotent cell line from early mouse embryos cultured in medium conditioned by teratocarcinoma stem cells***. Proceedings of the National Academy of Sciences 78(12):7634-7638.
2. Evans M. J., Kaufman M. H. 1981. ***Establishment in culture of pluripotential cells from mouse embryos***. Nature 292(5819):154-156.
3. Oback B., Huang B. 2014. ***Pluripotent stem cells from livestock***. Stem Cells: From Basic Research to Therapy, Volume Two: Tissue Homeostasis and Regeneration during Adulthood, Applications, Legislation and Ethics 2:304.
4. Silva J., Barrandon O., Nichols J., Kawaguchi J., Theunissen T. W., Smith A. 2008. ***Promotion of reprogramming to ground state pluripotency by signal inhibition***. PLoS Biol 6(10):e253.
5. Buehr M., Meek S., Blair K., Yang J., Ure J.et al. 2008. ***Capture of authentic embryonic stem cells from rat blastocysts***. Cell 135(7):1287-1298.
6. Buecker C., Chen H.-H., Polo J. M., Daheron L., Bu L.et al. 2010. ***A murine esc-like state facilitates transgenesis and homologous recombination in human pluripotent stem cells***. Cell Stem Cell 6(6):535-546.
7. Laible G. 2009. ***Enhancing livestock through genetic engineering—recent advances and future prospects***. Comparative immunology, microbiology and infectious diseases 32(2):123-137.
8. Wang J., Alexander P., Wu L., Hammer R., Cleaver O., McKnight S. L. 2009. ***Dependence of mouse embryonic stem cells on threonine catabolism***. Science 325(5939):435-439.
9. Shiraki N., Shiraki Y., Tsuyama T., Obata F., Miura M.et al. 2014. ***Methionine metabolism regulates maintenance and differentiation of human pluripotent stem cells***. Cell metabolism 19(5):780-794.
10. Shyh-Chang N., Locasale J. W., Lyssiotis C. A., Zheng Y., Teo R. Y.et al. 2013. ***Influence of threonine metabolism on s-adenosylmethionine and histone methylation***. Science 339(6116):222-226.
11. Alexander P. B., Wang J., McKnight S. L. 2011. ***Targeted killing of a mammalian cell based upon its specialized metabolic state***. Proceedings of the National Academy of Sciences 108(38):15828-15833.
12. Silva J., Smith A. 2008. ***Capturing pluripotency***. Cell 132(4):532-536.
13. De Miguel M. P., Fuentes-Julián S., Alcaina Y. 2010. ***Pluripotent stem cells: Origin, maintenance and induction***. Stem Cell Reviews and Reports 6(4):633-649.
14. Cockburn K., Rossant J. 2010. ***Making the blastocyst: Lessons from the mouse***. The Journal of clinical investigation 120(4):995-1003.
15. Takaoka K., Hamada H. 2012. ***Cell fate decisions and axis determination in the early mouse embryo***. Development 139(1):3-14.
16. Rossant J., Tam P. P. 2009. ***Blastocyst lineage formation, early embryonic asymmetries and axis patterning in the mouse***. Development 136(5):701-713.
17. Blair K., Wray J., Smith A. 2011. ***The liberation of embryonic stem cells***. PLoS Genet 7(4):e1002019.
18. Bazer F., Geisert R., Zavy M. 1993. ***Fertilization, cleavage, and implantation***. Reproduction in farm animals 6:88-212.
19. Guillomot M., Turbe A., Hue I., Renard J.-P. 2004. ***Staging of ovine embryos and expression of the t-box genes brachyury and eomesodermin around gastrulation***. Reproduction 127(4):491-501.

20. Stroband H., der Lende Van T. 1990. ***Embryonic and uterine development during early pregnancy in pigs***. Journal of reproduction and fertility Supplement 40:261-277.
21. Geisert R. D., Brookbank J. W., Michael Roberts R., Bazer F. W. 1982. ***Establishment of pregnancy in the pig: Ii. Cellular remodeling of the porcine blastocyst during elongation on day 12 of pregnancy***. Biology of Reproduction 27(4):941-955.
22. Hue I., Renard J.-P., Viebahn C. 2001. ***Brachyury is expressed in gastrulating bovine embryos well ahead of implantation***. Development Genes & Evolution 211(3).
23. Blomberg L., Hashizume K., Viebahn C. 2008. ***Blastocyst elongation, trophoblastic differentiation, and embryonic pattern formation***. Reproduction 135(2):181-195.
24. Vejlsted M., Du Y., Vajta G., Maddox-Hyttel P. 2006. ***Post-hatching development of the porcine and bovine embryo—defining criteria for expected development in vivo and in vitro***. Theriogenology 65(1):153-165.
25. Oback B., Huang B. 2012. ***Pluripotent stem cells in livestock***. Stem cells. in press: CRC Press/Taylor & Francis Group.
26. Takahashi K., Yamanaka S. 2006. ***Induction of pluripotent stem cells from mouse embryonic and adult fibroblast cultures by defined factors***. Cell 126(4):663-676.
27. Okita K., Ichisaka T., Yamanaka S. 2007. ***Generation of germline-competent induced pluripotent stem cells***. Nature 448(7151):313-317.
28. Takahashi K., Tanabe K., Ohnuki M., Narita M., Ichisaka T.et al. 2007. ***Induction of pluripotent stem cells from adult human fibroblasts by defined factors***. Cell 131(5):861-872.
29. Yu J., Vodyanik M. A., Smuga-Otto K., Antosiewicz-Bourget J., Frane J. L.et al. 2007. ***Induced pluripotent stem cell lines derived from human somatic cells***. Science 318(5858):1917-1920.
30. Park I.-H., Zhao R., West J. A., Yabuuchi A., Huo H.et al. 2008. ***Reprogramming of human somatic cells to pluripotency with defined factors***. Nature 451(7175):141-146.
31. Li W., Wei W., Zhu S., Zhu J., Shi Y.et al. 2009. ***Generation of rat and human induced pluripotent stem cells by combining genetic reprogramming and chemical inhibitors***. Cell Stem Cell 4(1):16-19.
32. Liu H., Zhu F., Yong J., Zhang P., Hou P.et al. 2008. ***Generation of induced pluripotent stem cells from adult rhesus monkey fibroblasts***. Cell Stem Cell 3(6):587-590.
33. Chambers I., Smith A. 2004. ***Self-renewal of teratocarcinoma and embryonic stem cells***. Oncogene 23(43):7150-7160.
34. Batlle-Morera L., Smith A., Nichols J. 2008. ***Parameters influencing derivation of embryonic stem cells from murine embryos***. Genesis 46(12):758-767.
35. Alberts B., Johnson A., Lewis J., Raff M., Roberts K., Walter P. 2010. ***Molecular biology of the cell, chapter 9. New york: Garland science; 2002***. Classic textbook now in its 5th Edition.
36. Smith A. G. 2001. ***Embryo-derived stem cells: Of mice and men***. Annual Review of Cell and Developmental Biology 17:435-462.
37. Palmieri S. L., Peter W., Hess H., Schöler H. R. 1994. ***Oct-4 transcription factor is differentially expressed in the mouse embryo during establishment of the first two extraembryonic cell lineages involved in implantation***. Developmental biology 166(1):259-267.
38. Nichols J., Zevnik B., Anastassiadis K., Niwa H., Klewe-Nebenius D.et al. 1998. ***Formation of pluripotent stem cells in the mammalian embryo depends on the pou transcription factor oct4***. Cell 95(3):379-391.
39. Niwa H., Miyazaki J.-i., Smith A. G. 2000. ***Quantitative expression of oct-3/4 defines differentiation, dedifferentiation or self-renewal of es cells***. Nature genetics 24(4):372-376.

40. Avilion A. A., Nicolis S. K., Pevny L. H., Perez L., Vivian N., Lovell-Badge R. 2003. ***Multipotent cell lineages in early mouse development depend on sox2 function***. Genes & development 17(1):126-140.
41. Mitsui K., Tokuzawa Y., Itoh H., Segawa K., Murakami M.et al. 2003. ***The homeoprotein nanog is required for maintenance of pluripotency in mouse epiblast and es cells***. Cell 113(5):631-642.
42. Chambers I., Colby D., Robertson M., Nichols J., Lee S.et al. 2003. ***Functional expression cloning of nanog, a pluripotency sustaining factor in embryonic stem cells***. Cell 113(5):643-655.
43. De Los Angeles A., Ferrari F., Xi R., Fujiwara Y., Benvenisty N.et al. 2015. ***Hallmarks of pluripotency***. Nature 525(7570):469-478.
44. Degrelle S. A., Campion E., Cabau C., Piumi F., Reinaud P.et al. 2005. ***Molecular evidence for a critical period in mural trophoblast development in bovine blastocysts***. Developmental biology 288(2):448-460.
45. Kuijk E. W., van Tol L. T., Van de Velde H., Wubbolts R., Welling M.et al. 2012. ***The roles of fgf and map kinase signaling in the segregation of the epiblast and hypoblast cell lineages in bovine and human embryos***. Development 139(5):871-882.
46. Khan D. R., Dubé D., Gall L., Peynot N., Ruffini S.et al. 2012. ***Expression of pluripotency master regulators during two key developmental transitions: Ega and early lineage specification in the bovine embryo***. PloS one 7(3):e34110.
47. Hall V. J., Jacobsen J. V., Rasmussen M. A., Hyttel P. 2010. ***Ultrastructural and molecular distinctions between the porcine inner cell mass and epiblast reveal unique pluripotent cell states***. Developmental Dynamics 239(11):2911-2920.
48. Norton A. T., Zehner O. 2008. ***Which half is mommy?: Tetragametic chimerism and trans-subjectivity***. WSQ: Women's Studies Quarterly 36(3):106-125.
49. Gardner R. 1978. ***Production of chimeras by injecting cells or tissue into the blastocyst***. Methods in Mammalian Reproduction:137-165.
50. Robertson E. J. 1986. ***Pluripotential stem cell lines as a route into the mouse germ line***. Trends in Genetics 2:9-13.
51. Rossant J. 2008. ***Stem cells and early lineage development***. Cell 132(4):527-531.
52. Beddington R., Robertson E. 1989. ***An assessment of the developmental potential of embryonic stem cells in the midgestation mouse embryo***. Development 105(4):733-737.
53. Tam P. P., Rossant J. 2003. ***Mouse embryonic chimeras: Tools for studying mammalian development***. Development 130(25):6155-6163.
54. Kaufman M., Webb S. 1990. ***Postimplantation development of tetraploid mouse embryos produced by electrofusion***. Development 110(4):1121-1132.
55. Rossant J. 1986. ***Development of extraembryonic cell lineages in the mouse embryo***. Experimental approaches to mammalian embryonic development:97-120.
56. Kleinsmith L. J., Pierce G. B. 1964. ***Multipotentiality of single embryonal carcinoma cells***. Cancer research 24(9):1544-1551.
57. Bradley A., Evans M., Kaufman M. H., Robertson E. 1984. ***Formation of germ-line chimaeras from embryo-derived teratocarcinoma cell lines***. Nature 309(5965):255-256.
58. Brinster R. L. 1974. ***The effect of cells transferred into the mouse blastocyst on subsequent development***. The Journal of experimental medicine 140(4):1049-1056.
59. Kawase E., Suemori H., Takahashi N., Okazaki K., Hashimoto K., Nakatsuji N. 1994. ***Strain difference in establishment of mouse embryonic stem (es) cell lines***. International Journal of Developmental Biology 38:385-385.
60. Ledermann B., Bürki K. 1991. ***Establishment of a germ-line competent c57bl/6 embryonic stem cell line***. Experimental cell research 197(2):254-258.

61. Smith A. G., Heath J. K., Donaldson D., Wong G., Moreau J.et al. 1988. ***Inhibition of pluripotential embryonic stem cell differentiation by purified polypeptides***. Nature 336:688-690.
62. Pease S., Braghetta P., Gearing D., Grail D., Williams R. L. 1990. ***Isolation of embryonic stem (es) cells in media supplemented with recombinant leukemia inhibitory factor (lif)***. Developmental biology 141(2):344-352.
63. Nichols J., Evans E. P., Smith A. G. 1990. ***Establishment of germ-line-competent embryonic stem (es) cells using differentiation inhibiting activity***. Development 110(4):1341-1348.
64. Niwa H., Burdon T., Chambers I., Smith A. 1998. ***Self-renewal of pluripotent embryonic stem cells is mediated via activation of stat3***. Genes & development 12(13):2048-2060.
65. Heinrich P. C., Behrmann I., Müller-Newen G., Schaper F., Graeve L. 1998. ***Interleukin-6-type cytokine signalling through the gp130/jak/stat pathway***. Biochemical Journal 334(2):297-314.
66. Ma Y.-G., Rosfjord E., Huebert C., Wilder P., Tiesman J.et al. 1992. ***Transcriptional regulation of the murine k-fgf gene in embryonic cell lines***. Developmental biology 154(1):45-54.
67. Wilson P. A., Hemmati-Brivanlou A. 1995. ***Induction of epidermis and inhibition of neural fate by bmp-4***. Nature 376(6538):331-333.
68. Ying Q.-L., Nichols J., Chambers I., Smith A. 2003. ***Bmp induction of id proteins suppresses differentiation and sustains embryonic stem cell self-renewal in collaboration with stat3***. Cell 115(3):281-292.
69. Ying Q. L., Wray J., Nichols J., Batlle-Morera L., Doble B.et al. 2008. ***The ground state of embryonic stem cell self-renewal***. Nature 453(7194):519-523.
70. Sato N., Meijer L., Skaltsounis L., Greengard P., Brivanlou A. H. 2004. ***Maintenance of pluripotency in human and mouse embryonic stem cells through activation of wnt signaling by a pharmacological gsk-3-specific inhibitor***. Nature medicine 10(1):55-63.
71. Hanna J., Markoulaki S., Mitalipova M., Cheng A. W., Cassady J. P.et al. 2009. ***Metastable pluripotent states in nod-mouse-derived escs***. Cell Stem Cell 4(6):513-524.
72. Kiyonari H., Kaneko M., Abe S. i., Aizawa S. 2010. ***Three inhibitors of fgf receptor, erk, and gsk3 establishes germline-competent embryonic stem cells of c57bl/6n mouse strain with high efficiency and stability***. Genesis 48(5):317-327.
73. Nichols J., Jones K., Phillips J. M., Newland S. A., Roode M.et al. 2009. ***Validated germline-competent embryonic stem cell lines from nonobese diabetic mice***. Nature medicine 15(7):814-818.
74. Vallier L., Alexander M., Pedersen R. A. 2005. ***Activin/nodal and fgf pathways cooperate to maintain pluripotency of human embryonic stem cells***. Journal of cell science 118(19):4495-4509.
75. Silva J., Smith A. 2008. ***Capturing pluripotency***. Cell 132(4):532-536.
76. Nichols J., Smith A. 2009. ***Naive and primed pluripotent states***. Cell Stem Cell 4(6):487-492.
77. Bertero A., Madrigal P., Galli A., Hubner N. C., Moreno I.et al. 2015. ***Activin/nodal signaling and nanog orchestrate human embryonic stem cell fate decisions by controlling the h3k4me3 chromatin mark***. Genes & development 29(7):702-717.
78. Nichols J., Smith A. 2009. ***Naive and primed pluripotent states***. Cell Stem Cell 4(6):487-492.
79. León Z., García-Cañaveras J. C., Donato M. T., Lahoz A. 2013. ***Mammalian cell metabolomics: Experimental design and sample preparation***. Electrophoresis.

80. Aoyama Y., Motokawa Y. 1981. ***L-threonine dehydrogenase of chicken liver. Purification, characterization, and physiological significance***. Journal of Biological Chemistry 256(23):12367-12373.
81. Dale R. A. 1978. ***Catabolism of threonine in mammals by coupling of l-threonine 3-dehydrogenase with 2-amino-3-oxobutyrate-coa ligase***. Biochimica et Biophysica Acta (BBA)-General Subjects 544(3):496-503.
82. Rabinowitz J. D., White E. 2010. ***Autophagy and metabolism***. Science 330(6009):1344-1348.
83. Roje S. 2006. ***S-adenosyl-l-methionine: Beyond the universal methyl group donor***. Phytochemistry 67(15):1686-1698.
84. Luka Z., Mudd S. H., Wagner C. 2009. ***Glycine n-methyltransferase and regulation of s-adenosylmethionine levels***. Journal of Biological Chemistry 284(34):22507-22511.
85. Gaspar-Maia A., Alajem A., Meshorer E., Ramalho-Santos M. 2011. ***Open chromatin in pluripotency and reprogramming***. Nature reviews Molecular cell biology 12(1):36-47.
86. Azuara V., Perry P., Sauer S., Spivakov M., Jørgensen H. F.et al. 2006. ***Chromatin signatures of pluripotent cell lines***. Nature cell biology 8(5):532-538.
87. Zhao X. D., Han X., Chew J. L., Liu J., Chiu K. P.et al. 2007. ***Whole-genome mapping of histone h3 lys4 and 27 trimethylations reveals distinct genomic compartments in human embryonic stem cells***. Cell Stem Cell 1(3):286-298.
88. Pan G., Tian S., Nie J., Yang C., Ruotti V.et al. 2007. ***Whole-genome analysis of histone h3 lysine 4 and lysine 27 methylation in human embryonic stem cells***. Cell Stem Cell 1(3):299-312.
89. Li P., Tong C., Mehrian-Shai R., Jia L., Wu N.et al. 2008. ***Germline competent embryonic stem cells derived from rat blastocysts***. Cell 135(7):1299-1310.
90. Thomson J. A., Itskovitz-Eldor J., Shapiro S. S., Waknitz M. A., Swiergiel J. J.et al. 1998. ***Embryonic stem cell lines derived from human blastocysts***. Science 282(5391):1145-1147.
91. Gafni O., Weinberger L., Mansour A. A., Manor Y. S., Chomsky E.et al. 2013. ***Derivation of novel human ground state naive pluripotent stem cells***. Nature 504(7479):282-286.
92. Ware C. B., Nelson A. M., Mecham B., Hesson J., Zhou W.et al. 2014. ***Derivation of naive human embryonic stem cells***. Proceedings of the National Academy of Sciences 111(12):4484-4489.
93. Pastor W. A., Chen D., Liu W., Kim R., Sahakyan A.et al. 2016. ***Naive human pluripotent cells feature a methylation landscape devoid of blastocyst or germline memory***. Cell Stem Cell 18(3):323-329.
94. Thornton P. K., Herrero M. 2014. ***Climate change adaptation in mixed crop–livestock systems in developing countries***. Global Food Security 3(2):99-107.
95. Saito S., Strelchenko N., Niemann H. 1992. ***Bovine embryonic stem cell-like cell lines cultured over several passages***. Roux's archives of developmental biology 201(3):134-141.
96. Stekelenburg-Hamers V., Annelies E., Van Achterberg T. A., Rebel H. G., Fléchon J. E.et al. 1995. ***Isolation and characterization of permanent cell lines from inner cell mass cells of bovine blastocysts***. Molecular reproduction and development 40(4):444-454.
97. Talbot N. C., Powell A. M., Rexroad C. E. 1995. ***In vitro pluripotency of epiblasts derived from bovine blastocysts***. Molecular reproduction and development 42(1):35-52.

98. Saito S., Sawai K., Ugai H., Moriyasu S., Minamihashi A.et al. 2003. ***Generation of cloned calves and transgenic chimeric embryos from bovine embryonic stem-like cells***. Biochemical and biophysical research communications 309(1):104-113.
99. Munoz M., Rodriguez A., De Frutos C., Caamaño J. N., Diez C.et al. 2008. ***Conventional pluripotency markers are unspecific for bovine embryonic-derived cell-lines***. Theriogenology 69(9):1159-1164.
100. Cao S., Wang F., Chen Z., Liu Z., Mei C.et al. 2009. ***Isolation and culture of primary bovine embryonic stem cell colonies by a novel method***. Journal of Experimental Zoology Part A: Ecological Genetics and Physiology 311(5):368-376.
101. Pant D., Keefer C. L. 2009. ***Expression of pluripotency-related genes during bovine inner cell mass explant culture***. Cloning and Stem Cells 11(3):355-365.
102. Gong G., Roach M. L., Jiang L., Yang X., Tian X. C. 2010. ***Culture conditions and enzymatic passaging of bovine esc-like cells***. Cellular Reprogramming (Formerly" Cloning and Stem Cells") 12(2):151-160.
103. Pashaiasl M., Khodadadi K., Holland M. K., Verma P. J. 2010. ***The efficient generation of cell lines from bovine parthenotes***. Cellular Reprogramming (Formerly" Cloning and Stem Cells") 12(5):571-579.
104. Lim M., Vassiliev I., Richings N., Firsova A., Zhang C., Verma P. 2011. ***A novel, efficient method to derive bovine and mouse embryonic stem cells with in vivo differentiation potential by treatment with 5-azacytidine***. Theriogenology 76(1):133-142.
105. Maruotti J., Muñoz M., Degrelle S. A., Gómez E., Louet C.et al. 2012. ***Efficient derivation of bovine embryonic stem cells needs more than active core pluripotency factors***. Molecular reproduction and development 79(7):461-477.
106. Strelchenko N., Mitalipova M., Stice S. 1995. ***Further characterization of bovine pluripotent stem cells***. Theriogenology 43(1):327-327.
107. Sims M., First N. 1993. ***Production of fetuses from totipotent cultured bovine inner cell mass cells***. Theriogenology 39(1):313.
108. Sims M., First N. 1994. ***Production of calves by transfer of nuclei from cultured inner cell mass cells***. Proceedings of the National Academy of Sciences 91(13):6143-6147.
109. First N., Sims M., Park S., Kent-First M. 1994. ***Systems for production of calves from cultured bovine embryonic cells***. Reproduction, fertility and development 6(5):553-562.
110. Stice S. L., Strelchenko N. S., Keefer C. L., Matthews L. 1996. ***Pluripotent bovine embryonic cell lines direct embryonic development following nuclear transfer***. Biology of reproduction 54(1):100-110.
111. Cibelli J. B., Stice S. L., Golueke P. J., Kane J. J., Jerry J.et al. 1998. ***Transgenic bovine chimeric offspring produced from somatic cell-derived stem-like cells***. Nature biotechnology 16(7):642-646.
112. Iwasaki S., Campbell K. H., Galli C., Akiyama K., Iwasaki S. 2000. ***Production of live calves derived from embryonic stem-like cells aggregated with tetraploid embryos***. Biology of reproduction 62(2):470-475.
113. Mitalipova M., Beyhan Z., First N. L. 2001. ***Pluripotency of bovine embryonic cell line derived from precompacting embryos***. Cloning 3(2):59-67.
114. Buehr M., Meek S., Blair K., Yang J., Ure J.et al. 2008. ***Capture of authentic embryonic stem cells from rat blastocysts***. Cell 135(7):1287-1298.
115. Harris D., Huang B., Oback B. 2013. ***Inhibition of map2k and gsk3 signaling promotes bovine blastocyst development and epiblast-associated expression of pluripotency factors***. Biology of Reproduction.
116. Verma V., Huang B., Kallingappa P. K., Oback B. 2013. ***Dual kinase inhibition promotes pluripotency in finite bovine embryonic cell lines***. Stem Cells Dev.

117. Huang B., Li T., Alonso-Gonzalez L., Gorre R., Keatley S.et al. 2011. ***A virus-free poly-promoter vector induces pluripotency in quiescent bovine cells under chemically defined conditions of dual kinase inhibition***. Plos One 6(9):e24501.
118. McLean Z., Meng F., Henderson H., Turner P., Oback B. 2014. ***Increased map kinase inhibition enhances epiblast-specific gene expression in bovine blastocysts***. Biology of reproduction:biolreprod. 114.120832.
119. Alberts B J. A., Lewis J, et al. 2002. ***Studying gene expression and function***.
120. Lloyd A. 2003. ***Vector construction for gene overexpression as a tool to elucidate gene function***. Plant Functional Genomics:329-344.
121. Wilson M. H., Coates C. J., George A. L. 2007. ***Piggybac transposon-mediated gene transfer in human cells***. Molecular therapy 15(1):139-145.
122. Zhao S., Jiang E., Chen S., Gu Y., Shangguan A. J.et al. 2016. ***Piggybac transposon vectors: The tools of the human gene encoding***. Translational lung cancer research 5(1):120.
123. Wang W., Lin C., Lu D., Ning Z., Cox T.et al. 2008. ***Chromosomal transposition of piggybac in mouse embryonic stem cells***. Proceedings of the National Academy of Sciences 105(27):9290-9295.
124. Li Z., Michael I. P., Zhou D., Nagy A., Rini J. M. 2013. ***Simple piggybac transposon-based mammalian cell expression system for inducible protein production***. Proceedings of the National Academy of Sciences 110(13):5004-5009.
125. Oback B., Wells D. 2003. ***Cloning cattle***. Cloning & Stem Cells 5(4):243-256.
126. Schurmann A., Wells D. N., Oback B. 2006. ***Early zygotes are suitable recipients for bovine somatic nuclear transfer and result in cloned offspring***. Reproduction 132(6):839-848.
127. Guan M., Bogani D., Marschall S., Raspa M., Takeo T.et al. 2014. ***In vitro fertilization in mice using the mbcd-gsh protocol***. Current protocols in mouse biology:67-83.
128. Steeves T., Gardner D. 1999. ***Temporal and differential effects of amino acids on bovine embryo development in culture***. Biology of Reproduction 61(3):731-740.
129. Phelan K., May K. M. 2007. ***Basic techniques in mammalian cell tissue culture***. Current protocols in cell biology:1.1. 1-1.1. 22.
130. Recillas-Targa F. 2006. ***Multiple strategies for gene transfer, expression, knockdown, and chromatin influence in mammalian cell lines and transgenic animals***. Molecular biotechnology 34(3):337-354.
131. Kim T. K., Eberwine J. H. 2010. ***Mammalian cell transfection: The present and the future***. Analytical and bioanalytical chemistry 397(8):3173-3178.
132. Chesnoy S., Huang L. 2000. ***Structure and function of lipid-DNA complexes for gene delivery***. Annual review of biophysics and biomolecular structure 29(1):27-47.
133. Van Soom A., Boerjan M., Hardy K. 2002. ***Differential staining of inner and outer cells to assess mammalian embryo quality***. Assessment of mammalian embryo quality: Springer.237-266.
134. Eslami A., Lujan J. 2010. ***Western blotting: Sample preparation to detection***. Journal of visualized experiments: JoVE(44).
135. Berg D. K., Li C., Asher G., Wells D. N., Oback B. 2007. ***Red deer cloned from antler stem cells and their differentiated progeny***. Biology of Reproduction 77(3):384-394.
136. Smith C., Berg D., Beaumont S., Standley N. T., Wells D. N., Pfeffer P. L. 2007. ***Simultaneous gene quantitation of multiple genes in individual bovine nuclear transfer blastocysts***. Reproduction 133(1):231-242.
137. Smith C. S., Berg D. K., Berg M., Pfeffer P. L. 2010. ***Nuclear transfer-specific defects are not apparent during the second week of embryogenesis in cattle***. Cell Reprogram 12(6):699-707.

138. Meng F., Forrester-Gauntlett B., Turner P., Henderson H., Oback B. 2015. ***Signal inhibition reveals jak/stat3 pathway as critical for bovine inner cell mass development***. Biology of reproduction 93(6):132, 131-139.
139. Theunissen T. W., Van Oosten A. L., Castelo-Branco G., Hall J., Smith A., Silva J. C. ***Supplemental information nanog overcomes reprogramming barriers and induces pluripotency in minimal conditions***.
140. Guhaniyogi J., Brewer G. 2001. ***Regulation of mrna stability in mammalian cells***. Gene 265(1):11-23.
141. Nagatomo H., Kagawa S., Kishi Y., Takuma T., Sada A.et al. 2013. ***Transcriptional wiring for establishing cell lineage specification at the blastocyst stage in cattle***. Biology of reproduction:biolreprod. 113.108993.
142. Solter D., Knowles B. B. 1975. ***Immunosurgery of mouse blastocyst***. Proceedings of the National Academy of Sciences 72(12):5099-5102.
143. Talbot N. C., Caperna T. J., Edwards J. L., Garrett W., Wells K. D., Ealy A. D. 2000. ***Bovine blastocyst-derived trophectoderm and endoderm cell cultures: Interferon tau and transferrin expression as respective in vitro markers***. Biology of reproduction 62(2):235-247.
144. Edgar A. J. 2002. ***Molecular cloning and tissue distribution of mammalian l-threonine 3-dehydrogenases***. BMC biochemistry 3(1):1.
145. Altschul S. F., Madden T. L., Schäffer A. A., Zhang J., Zhang Z.et al. 1997. ***Gapped blast and psi-blast: A new generation of protein database search programs***. Nucleic acids research 25(17):3389-3402.
146. Edgar A. J. 2002. ***The human l-threonine 3-dehydrogenase gene is an expressed pseudogene***. BMC genetics 3(1):18.
147. Zhu Z., Zheng T., Lee C. G., Homer R. J., Elias J. A. ***Tetracycline-controlled transcriptional regulation systems: Advances and application in transgenic animal modeling***; 2002. Elsevier.121-128.
148. Talbot N. C., Caperna T. J., Powell A. M., Garrett W. M., Ealy A. D. 2004. ***Isolation and characterization of a bovine trophectoderm cell line derived from a parthenogenetic blastocyst***. Molecular reproduction and development 69(2):164-173.
149. Li E. 2002. ***Chromatin modification and epigenetic reprogramming in mammalian development***. Nature Reviews Genetics 3(9):662-673.
150. Moore A., Donahue C. J., Bauer K. D., Mather J. P. 1998. ***Simultaneous measurement of cell cycle and apoptotic cell death***. Methods in cell biology 57:265-278.
151. Moussaieff A., Rouleau M., Kitsberg D., Cohen M., Levy G.et al. 2015. ***Glycolysis-mediated changes in acetyl-coa and histone acetylation control the early differentiation of embryonic stem cells***. Cell metabolism 21(3):392-402.
152. Van Winkle L. J., Galat V., Iannaccone P. M. 2014. ***Threonine appears to be essential for proliferation of human as well as mouse embryonic stem cells***. Frontiers in cell and developmental biology 2:18.
153. Gopichandran N., Leese H. 2003. ***Metabolic characterization of the bovine blastocyst, inner cell mass, trophectoderm and blastocoel fluid***. Reproduction 126(3):299-308.
154. Miller J., Schultz G. 1985. ***Amino acid transport in mouse blastocyst compartments***. Development 89(1):149-158.
155. Pantaleon M., Kaye P. L. 1998. ***Glucose transporters in preimplantation development***. Reviews of Reproduction 3(2):77-81.
156. Weingarten M., Akhavan N., Hanau J., Peter Y. 2015. ***A place to call home: Bioengineering pluripotential stem cell cultures***. AIMS Bioengineering 2(2):15-28.
157. Fleming T. P., Wilkins A., Mears A., Miller D. J., Thomas F.et al. 2004. ***Society for reproductive biology founders' lecture 2003. The making of an embryo: Short-term***

goals and long-term implications. Reproduction, Fertility and Development 16(3):325-337.

158. Brison D., Hewitson L., Leese H. 1993. ***Glucose, pyruvate, and lactate concentrations in the blastocoel cavity of rat and mouse embryos***. Molecular reproduction and development 35(3):227-232.
159. Miller J., Schultz G. 1983. ***Properties of amino acid transport in preimplantation rabbit embryos***. Journal of Experimental Zoology Part A: Ecological Genetics and Physiology 228(3):511-525.
160. Kaye P., Schultz G., Johnson M., Pratt H. P., Church R. 1982. ***Amino acid transport and exchange in preimplantation mouse embyros***. Journal of reproduction and fertility 65(2):367-380.
161. Dunglison G., Jane S., McCaul T., Chad J., Fleming T., Kaye P. 1995. ***Stimulation of endocytosis in mouse blastocysts by insulin: A quantitative morphological analysis***. Journal of reproduction and fertility 105(1):115-123.
162. Thompson J., Sherman A., Allen N., McGowan L., Tervit H. 1998. ***Total protein content and protein synthesis within pre-elongation stage bovine embryos***. Molecular reproduction and development 50(2):139-145.
163. Han C., Gu H., Wang J., Lu W., Mei Y., Wu M. 2013. ***Regulation of l-threonine dehydrogenase in somatic cell reprogramming***. Stem Cells 31(5):953-965.
164. Tee W.-W., Reinberg D. 2014. ***Chromatin features and the epigenetic regulation of pluripotency states in escs***. Development 141(12):2376-2390.
165. Kallingappa P. K., Turner P. M., Eichenlaub M. P., Green A. L., Oback F. C.et al. 2016. ***Quiescence loosens epigenetic constraints in bovine somatic cells and improves their reprogramming into totipotency 1***. Biology of reproduction 95(1):Article 16, 11-10.
166. Liang G., He J., Zhang Y. 2012. ***Kdm2b promotes induced pluripotent stem cell generation by facilitating gene activation early in reprogramming***. Nature cell biology 14(5):457-466.
167. Vastenhouw N. L., Zhang Y., Woods I. G., Imam F., Regev A.et al. 2010. ***Chromatin signature of embryonic pluripotency is established during genome activation***. Nature 464(7290):922-926.
168. Lindeman L. C., Andersen I. S., Reiner A. H., Li N., Aanes H.et al. 2011. ***Prepatterning of developmental gene expression by modified histones before zygotic genome activation***. Developmental cell 21(6):993-1004.
169. Gao Y., Hyttel P., Hall V. J. 2010. ***Regulation of h3k27me3 and h3k4me3 during early porcine embryonic development***. Mol Reprod Dev 77(6):540-549.
170. Gao Y., Hyttel P., Hall V. J. 2011. ***Dynamic changes in epigenetic marks and gene expression during porcine epiblast specification***. Cell Reprogram 13(4):345-360.
171. OBACK B., WELLS D. ***Pluripotent stem cells in cattle: Recent advances and applications***; 2014.75.
172. Wu M., Singh A. K. 2012. ***Single-cell protein analysis***. Current opinion in biotechnology 23(1):83-88.
173. Sperber H., Mathieu J., Wang Y., Ferreccio A., Hesson J.et al. 2015. ***The metabolome regulates the epigenetic landscape during naive-to-primed human embryonic stem cell transition***. Nature cell biology 17(12):1523-1535.
174. Panopoulos A. D., Yanes O., Ruiz S., Kida Y. S., Diep D.et al. 2012. ***The metabolome of induced pluripotent stem cells reveals metabolic changes occurring in somatic cell reprogramming***. Cell research 22(1):168-177.
175. Zenobi R. 2013. ***Single-cell metabolomics: Analytical and biological perspectives***. Science 342(6163):1243259.

176. Ran F. A., Hsu P. D., Lin C.-Y., Gootenberg J. S., Konermann S.et al. 2013. ***Double nicking by rna-guided crispr cas9 for enhanced genome editing specificity***. Cell 154(6):1380-1389.
177. Stringfellow D. A., Seidel S. M. 1998. ***Manual of the international embryo transfer society***: The Society.

Appendix

A. Molecular biology reagents and stocks

Table 11. DNA and mRNA analysis reagents.

Reagent	Source
1x TAE buffer; 40 mM Tris base, 20 mM acetic acid, 1 mM EGTA in Milli-Q H2O	
1 Kb+ DNA Ladder™ (1 µg/µl)	Invitrogen (USA)
5x DNA loading buffer; 30% glycerol, 1% orange G dye in Milli-Q H2O	
5x First-Strand Buffer [250 mM Tris-HCl, 375m MKCl, 15 mM $MgCl_2$]	Invitrogen (USA)
Agarose UltraPure™ Powder	Invitrogen (USA)
dATPs (10 mM)	Invitrogen (USA)
dNTP mix (10 mM)	Invitrogen (USA)
FastStart 10x buffer	Roche (Germany)
FastStart Taq DNA polymerase	Roche (Germany)
$MgCl_2$ (25 mM)	Roche (Germany)
Random hexamer primers (50 µM)	Roche (Germany)
RNaseOUT™ Recombinant Ribonuclease Inhibitor (40 U/µl)	Invitrogen (USA)
SuperScriptTM III Reverse Transcriptase (200 U/µl)	Invitrogen (USA)
SYBR® Safe DNA Gel Stain	Invitrogen (USA)
T4 DNA ligase	Invitrogen (USA)
T4 DNA ligase buffer	Invitrogen (USA)
Takara Bio SYBR® Premix Ex Taq™ (Tli RNaseHPlus)	Clontech Laboratories Inc. (USA)

Table 12. Immunofluorescence reagents.

Reagents	Source
Blocking solution	5% goat, donkey, or serum (all Invitrogen, USA) in PBS
Hoechst 33342 nuclear stain	Sigma-Aldrich
Quench solution	50 mM NH_4Cl
PFA fixing solution, pH 7; 4% depolymerised (w/v) PFA, 4% (w/v) sucrose, in PBS with phenol red indicator	
ProLong® Diamond Antifade Mountant	Life Technologies (USA)

Table 13. Western blotting reagents.

Reagent	Source
RIPA buffer; 50 mM TRIS-HCl pH 7.4, 150 mM NaCl, 1 mM EDTA, 1% Triton X-100, 1% Sodiumdeoxycholate, 0.1% SDS	(all Invitrogen)
pre-cast 4-12% Bis-Tris gradient polyacrylamide gel	ThermoFisher Scientific
NuPAGE running buffer	ThermoFisher Scientific
electro-blot chamber	Bio-Rad, USA
Ponceau S	Sigma, USA
Tris-buffered saline+ tween 20 (TBST)	Home-made
5% skim milk	
Western Lightning Plus ECL kit	Perkin Elmer, USA
ImageQuant LAS 4000	GE Healthcare Life Sciences, UK

Table 14. Stock reagents.

Reagent	Source
Acetic acid	ThermoFisher Scientific (USA)
Deoxycholic acid	Sigma-Aldrich (Switzerland)
Donkey Serum	GIBCO, Life Technologies (USA)
DMSO	Sigma-Aldrich (Switzerland)
EDTA	Invitrogen (USA)
EGTA	Sigma-Aldrich (Switzerland)
Ethanol	ThermoFisher Scientific (USA)
FCS	GIBCO, Life Technologies (USA)
Gelatin	Sigma-Aldrich (Switzerland)
Goat Serum	GIBCO, Life Technologies (USA)
Glycerol	J.T. Baker® Chemicals (USA)
Isopropanol	LabServ (Ireland)
KCl	Sigma-Aldrich (Switzerland)
$K_3Fe(CN)_6$	BDH Ltd. (UK)
$K_4Fe(CN)_6$	Sigma-Aldrich (Switzerland)
KH_2PO_4	Sigma-Aldrich (Switzerland)
Methanol	ThermoFisher Scientific (USA)
$MgCl_2$	J.T. Baker® Chemicals (USA)
$MgSO_4$	Sigma-Aldrich (Switzerland)
Nonidet® P-40 detergent	Sigma-Aldrich (Switzerland)
Na_2HPO_4	Sigma-Aldrich (Switzerland)
NaCl	J.T. Baker® Chemicals (USA)
NP-40 detergent	Sigma-Aldrich (Switzerland)

Orange G dye	Sigma-Aldrich (Switzerland)
Ponceau-S	Sigma-Aldrich (Switzerland)
SDS	Sigma-Aldrich (Switzerland)
Tris base	J.T. Baker® Chemicals (USA)
Triton X-100	Sigma-Aldrich (Switzerland)
Tween	Bio-Rad (USA)

B. Commercial kits, and equipment

Table 15. Commercial kits

Kit	Source
Lipofectamine® LTX with PLUS™ reagent	Invitrogen (USA)
PureLink® HiPure Plasmid Filter Maxiprep Kit	Invitrogen (USA)
PureLink® HiPure Plasmid Filter Miniprep Kit	Invitrogen (USA)
RNAGEM	ZyGEM (NZ)
Wizard® SV Gel & PCR Clean-Up System	Promega (USA)
Autophagy Detection Kit (ab139484)	Abcam (UK)

Table 16. Equipment.

Equipment	Manufacturer
Biofuge fresco centrifuge	Heraeus (Germany)
Biofuge primo centrifuge	Heraeus (Germany)
Clean bench fume hood	Pall Corporation (USA)
Dual-intensity transilluminator	UVP (USA)
Eppendorf centrifuge 5417C	Eppendorf (Germany)
Eppendorf Mastercycler gradient PCR machine	Eppendorf (Germany)
EVOS fluorescence microscope	AMG (USA)
Gel Doc 2000	Bio-Rad (USA)
Infors HT Ecotron incubator (Bacterial culture)	Infors HT (Switzerland)
LC carousel centrifuge 2.0	Roche (Germany)
Leica DFC290 light microscope	Leica (Germany)
LightCycler 2.0	Roche (Germany)
Minispin plus centrifuge	Eppendorf (Germany)
Nanodrop ND-1000	ThermoFisher Scientific (USA)
Neon™ transfection system	Invitrogen (USA)
Nikon TMS light microscope	Nikon (Japan)
Olympus BX50 fluorescent microscope	Olympus (Japan)
Sanyo incubator (Transformation plates)	Sanyo (Japan)
Sorvall RC5C Plus centrifuge	Thermo Scientific (USA)
Spot RT3 camera	Spot Imaging Solutions (USA)
Sub-cell gel tank	Bio-Rad (USA)
Thermo Forma series II water jacketed CO_2 incubator	Thermo Scientific (USA)

C. Nucleotide sequences

Table 17. Bovine TDH fragment that was cloned into a PB-TRE3G plasmid.

Full Sequence of TDH fragment (with SalI and NotI cut sites)
CATGTCGACGCCACCATGCCTGTCGTCAGGGTGCTGAGAAGAGTGGCCTGTTG GATGCTGCAGTCTCCTGCCTGTGGATGCAGAGCACCTGTGCTGCCTTCTAGATT CCTGGGCACAAGCCCCAGGCAGATCCCTATGGATGCCAACTTCCACAGCACCA GCTTCAGCGAGGCCGACCAGCAGAGAGTGCTGATTACAGGCGGACTGGGACA GCTCGGAGTTGGCCTGGCAAGCTTCCTGAGGAAGAGATTCGGCAAGGACAACG TGATCCTGAGCGACATCAGAAAGCCTCCAGAGCACGTGTTCCTCAGCGGCCCC TTCATCTACAGCGACATCCTGGACTACAAGAACCTGCGCGAGATCGTGGTCAA CAACAGGATCACCTGGCTGTTCCACTACAGCGCCCTGCTGTCTGCTGTGGGAG AAGCCAATGTGTCCCTGGCCAGAGCCGTGAACATCACCGGACTGCACAACGTG CTGGATGTGGCCGCTGAACACGGCCTGAGACTGTTCGTGCCTTCTACCATCGGC GCCTTCGGACCCACCTCTCCTAGAAACCCTACACCTGACCTGTGCATCCAGAGG CCTAGGACCATCTACGGCGTGTCCAAAGTGCACGCCGAGCTGATGGGCGAGTA CTACTACTACAGATACGGCCTGGACTTCAGATGCCTGAGATACCCCGGCATCA TCAGCGCCGATTCTCAACCTGGCGGAGGCACCACAGATTACGCCGTGCAGATC TTTCACGAGGCCGTGAAGAACGGCAGATTCGAGTGCAACCTGAAGCCTGACAC CAGGCTGCCCATGATGTATATCGACGACTGCCTGAGGGCCACACTGGAAGTGA TGGAAGCCCCTGCCGAGAGCCTGAGCATGAGGACCTACAACATCTCCGCCATG AGCTTCACCCCTGAGGAACTGGCTCAAGAGGTGCTGAAGCACGTGCCCGAGCT GCAAGTGACCTACAATGTGGATCCTGTGCGCCAGGCCATTGCCGACTCTTGGC CTATGAACTTCGACGACAGCAACGCCAGAAAGGACTGGGGCTGGAAGCACGA CTTTGACCTGCCTGAGCTGGTCACCACCATGCTGAACTTCCACGGCAGCGAGTC TAGAGTGGCCCAGGCCAATGAGCAGAAGCTGATCTCCGAAGAGGACCTCTGAG CGGCCGCCCT

D. Bacterial and cell culture information

Table 18. Bacterial cell culture reagents.

Reagent	Source
Luria-Bertani (LB) broth (25g/L)	Invitrogen (USA)
LB agar	Invitrogen (USA)
SOC medium	Invitrogen (USA)

Table 19. Mammalian cell lines.

Cell line	Source
BEF cells	AgResearch Ruakura
Mouse embryonic stem cells (V6.5)	AgResearch Ruakura
Mouse IPSCs (JMJd2 MEFH1P4)	AgResearch Ruakura
MEF cells	AgResearch Ruakura
bovine liver cells (EF61V)	AgResearch Ruakura
Skin fibroblast cells (LJ801 line)	AgResearch Ruakura
Bovine muscle fibroblast cells	AgResearch Ruakura
EF5-TET cells	AgResearch Ruakura

Table 20. Mammalian cell culture reagents.

Reagent	Details	Source
Cryoprotectant Solution	FCS + 20% DMSO	Homemade
Doxycycline Hyclate	2 mg/ml stock	Sigma-Aldrich (Switzerland)
10x PBS	80g NaCl, 2g KCl, 14.4g Na_2HPO_4, 2.4g KH_2PO_4 in 1L Milli-Q H_2O	Homemade
Trypsin-EDTA (0.25%), phenol red	Used for lifting off epithelial cells	GIBCO, Life Technologies (USA)

Table 21. Cell seeding density and media volume for various size tissue culture dishes.

Tissue culture dish	Area (cm^2)	Seeding density	Volume of media
96-well	0.3	0.1×10^5	200 µl
48-well	0.7	0.3×10^5	400 µl
4-well/24-well	2	0.5×10^5	500 µl
12-well	4	1×10^5	1 ml
3cm/6-well	9.6	2×10^5	2 ml
6cm	28	5×10^5	5 ml
10cm	78.5	1×10^6	10 ml

E. Media

Table 22. The M16 recipe used for mouse embryo threonine dropout.

Ingredients	Cat no (Sigma)	mM
Calcium chloride ($CaCl_2.2H_2O$)	C7902	2.26
Magnesium sulfate (anhydrous)($MgSO_4$)	M7506	1.374
Potassium chloride (KCl)	P5405	4.75
Potassium dehydrogen orthophosphate(KH_2PO_4)	P5655	1.19
Sodium bicarbonate ($NaHCO_3$)	S5761	25
Sodium chloride (NaCl)	S5886	95.38
D(+)-glucose	G6152	5.551
Pyruvic acid – Na	P2256	0.408
DL-Lactic acid – Na	L7900	7.12

Table 23. Tissue and embryo culture media composition

Media	Ingredients
B199	M199 with 25 mM $NaHCO_3$, 0.2 mM Pyruvate and 0.086 mM kanamycin monosulfate
ESOF	1.71 mM $CaCl_2$:$2H_2O$, 25 mM $NaHCO_3$, 107.7 mM NaCl, 3.32 mM sodium lactate, 7.15 mM KCl, 0.30 mM KH_2PO_4, 0.15 mM D-Glucose, 0.33 mM pyruvate, 0.04 mM kanamycin monosulfate, and 0.081 g/L non-essential amino acids, 8 mg/ml fatty acid free BSA and 1 mM GlutaMAX™
H199	M199 with 15 mM HEPES, 5 mM $NaHCO_3$ and 0.086 mM kanamycin monosulfate
HSOF	Hepes-buffered synthetic oviduct fluid (SOF) with 1.71 mM $CaCl_2.2H_2O$, 5 mM $NaHCO_3$, 107.7 mM NaCl, 3.32 mM sodium lactate, 7.15 mM KCl, 20 mM Hepes, 0.3 mM KH_2PO_4, 0.069 mM kanamycin monosulfate, 0.33 mM pyruvate and 3 mg/ml fatty acid free BSA
IVF media	25 mM $NaHCO_3$, 107.7 mM NaCl, sodium lactate, 7.15 mM KCl, 3.32 mM 0.3 mM KH_2PO_4, 0.04 mM kanamycin monosulfate, 1.71 mM $CaCl_2.2H_2O$, 0.33 mM pyruvate, 8 mg/ml fatty acid free bovine albumin, supplemented with 0.2 mM Penicillamine, 0.1 mM hypotaurine and 0.001 mM heparin
IVM media	B199 with 10% FCS, 1 µg/ml ovine LH (Ovagen; ImmunoChemicals Products (ICP), New Zealand), 10 µg/ml ovine FSH (ICP, New Zealand), 1 µg/ml 17-b-estradiol and 0.1 mM cysteamine
LSOF	1.71 mM $CaCl_2$:$2H_2O$, 0.49 mM $MgCl_2$:$6H_2O$, 25 mM $NaHCO_3$, 107.7 mM NaCl, 3.32 mM sodium lactate, 7.15 mM KCl, 0.30 mM KH_2PO_4, 1 µM DNP (2-, 4dinitrophenol), 1.5 mM D-Glucose, 0.33 mM pyruvate, 0.04 mM kanamycin monosulfate, and 0.081 g/L non-essential amino acids, 0.22 g/L essential amino acids, 8 mg/ml fatty acid free BSA and 1 mM GlutaMAX ™
Oocyte aspiration medium	H199 + 925 IU/ml heparin, 20 µl/ml 20% albumin

Fibroblast medium	DMEM/F12 + 1mM GlutaMAX ™, 10% FCS
ICM outgrowths medium	DMEM/F12- Hepes (Invitrogen 12400-024), N_2 (Invitrogen 17502-048) 100X stock, Neurobasal (Invitrogen 21103-049), B27 (Invitrogen 17504-044), 200 mM L-Glutamine, 3 µM CHIR (Sigma), 10 µM PD0325901 (Sigma), 2000 units of LIF/ml.
TE primary culture medium	DMEM/F12, 10% FCS, 50 µM 2ME, 10 µl/ml penicillin/Streptomycin
Parthenogenetic medium (calcium-free)	162 mg/L KH_2PO_4, 293 mg/L $MgSO_4{\cdot}7H_2O$, 5680 mg/L NaCl, 356 mg/L KCl, 36 mg/L Na-Pyruvate, 5.5 ml Lactic Acid 60%, 1000 mg/L D-Glucose, 37 mg/L EDTA (disodium) , 2101 mg/L $NaHCO_3$, 25 mg/L (500µl) Gentamycin, Milli-Q H20 Up to 1L.

E. Embryo grading guidelines

Images were taken from "Manual of the International Embryo Transfer Society" (3rd edition) [177]. When applied for the purposes of this research stages were numbered as follows: 4= Tight Morula (TM), 5= Early blastocyst (EM), 6= Blastocyst (B), 7= expanded blastocyst (EB) and 8= hatched blastocyst (HB). The cycle day is the equivalent day at which the stage code would develop after fertilisation. Quality code or grade (1-3) is based on morphological characteristics depicted in each corresponding image. Clarifications about reasoning of morphological grade identified by the manual are presented as stated below.

Clarifications:

d) Single or small blastomeres comprise less than 15% of the total cellular material and the embryo is consistent with the expected stage of development.

e) Sperm on zona pellucida.

f) Embryos with many extruded cells or debris must be carefully rolled over to determine the presence and quality of any viable embryo mass.

g) Quality code 3 embryos have an embryo mass that is less than 50% of all cellular material within the zona pellucida.

h) This embryo has a nice but very small mass. If the embryo mass is less than 25% of all cellular material, it should be given a code 4 (non-viable).

i) Irregular shape is a common variation in blastocoel development.

j) Collapsing of the blastocoel is considered a normal physiological process that does not lower the quality grade.

k) Extruded cells in stage 6, 7, and 8 embryos are often pressed against the zona pellucida and not obvious unless the embryo has collapsed due to normal physiological processes or when cryoprotective additive is introduced.

l) This embryo has a flat (even concave) surface of the zona pellucida that can cause the embryo to stick to the petri dish or straw. This defect alone keeps the embryo from being classified as quality grade 1 and should not be utilised in international commerce unless agreements allow for other than quality code 1 embryos.

m) Cellular debris on the surface of the zona pellucida shows that this embryo has not been washed by proper procedures.

n) This embryo has a cracked zona pellucida at the top of the picture. Embryos that do not have an intact zona pellucida should not be utilised in international commerce.

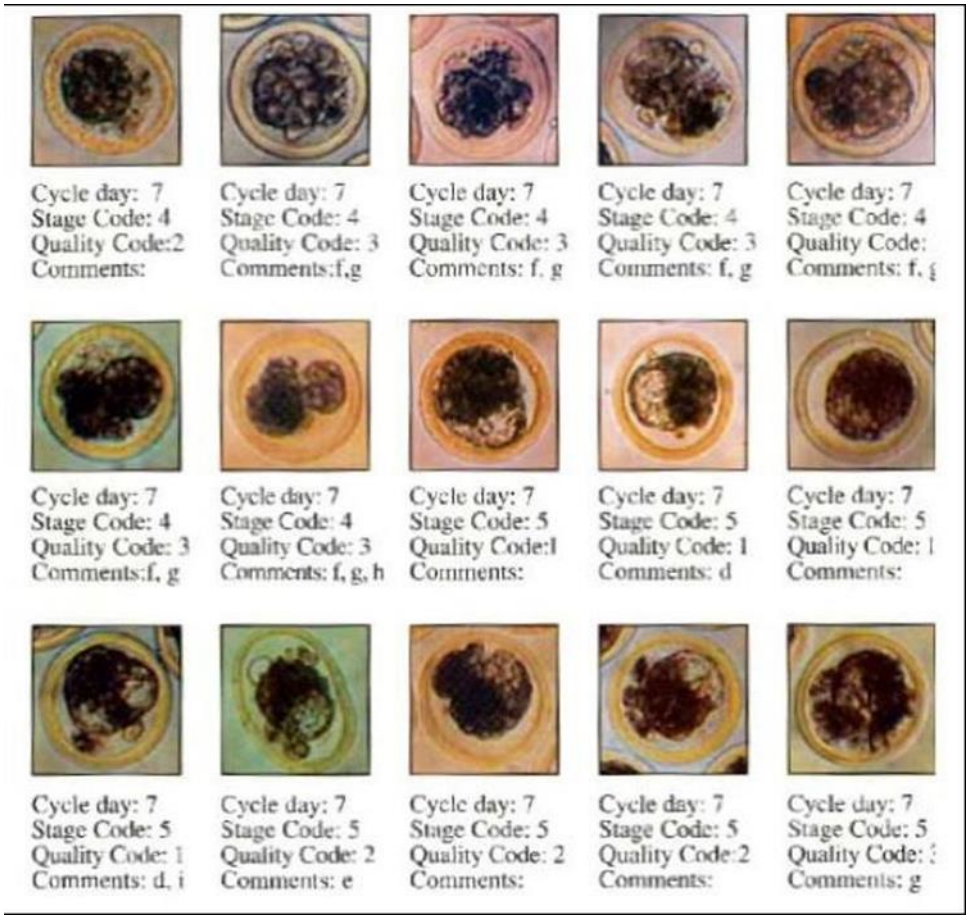
Cycle day: 7
Stage Code: 4
Quality Code:2
Comments:
Cycle day: 7
Stage Code: 4
Quality Code: 3
Comments:f,g
Cycle day: 7
Stage Code: 4
Quality Code: 3
Comments: f, g
Cycle day: 7
Stage Code: 4
Quality Code: 3
Comments: f, g
Cycle day: 7
Stage Code: 4
Quality Code:
Comments: f, g
Cycle day: 7
Stage Code: 4
Quality Code: 3
Comments:f, g
Cycle day: 7
Stage Code: 4
Quality Code: 3
Comments: f, g, h
Cycle day: 7
Stage Code: 5
Quality Code:1
Comments:
Cycle day: 7
Stage Code: 5
Quality Code: 1
Comments: d
Cycle day: 7
Stage Code: 5
Quality Code: 1
Comments:
Cycle day: 7
Stage Code: 5
Quality Code: 1
Comments: d, i
Cycle day: 7
Stage Code: 5
Quality Code: 2
Comments: e
Cycle day: 7
Stage Code: 5
Quality Code: 2
Comments:
Cycle day: 7
Stage Code: 5
Quality Code:2
Comments:
Cycle day: 7
Stage Code: 5
Quality Code:
Comments: g

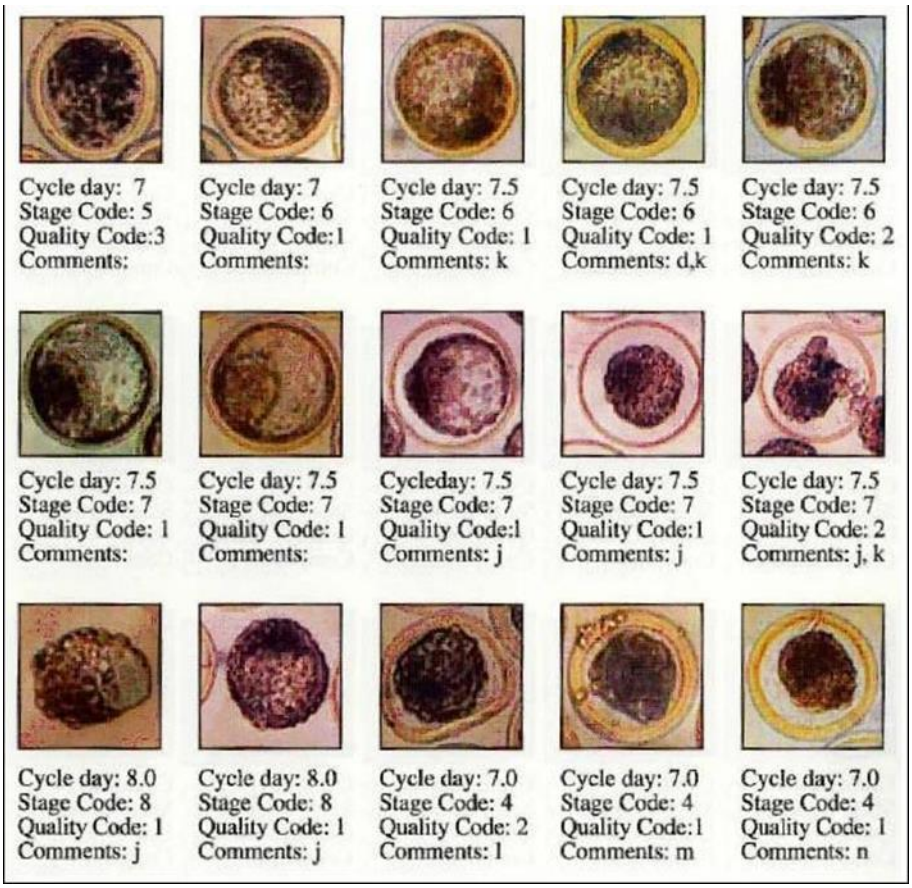
Cycle day: 7
Stage Code: 5
Quality Code:3
Comments:
Cycle day: 7
Stage Code: 6
Quality Code:1
Comments:
Cycle day: 7.5
Stage Code: 6
Quality Code: 1
Comments: k
Cycle day: 7.5
Stage Code: 6
Quality Code: 1
Comments: d,k
Cycle day: 7.5
Stage Code: 6
Quality Code: 2
Comments: k
Cycle day: 7.5
Stage Code: 7
Quality Code: 1
Comments:
Cycle day: 7.5
Stage Code: 7
Quality Code: 1
Comments:
Cycleday: 7.5
Stage Code: 7
Quality Code:1
Comments: j
Cycle day: 7.5
Stage Code: 7
Quality Code:1
Comments: j
Cycle day: 7.5
Stage Code: 7
Quality Code: 2
Comments: j, k
Cycle day: 8.0
Stage Code: 8
Quality Code: 1
Comments: j
Cycle day: 8.0
Stage Code: 8
Quality Code: 1
Comments: j
Cycle day: 7.0
Stage Code: 4
Quality Code: 2
Comments: l
Cycle day: 7.0
Stage Code: 4
Quality Code:1
Comments: m
Cycle day: 7.0
Stage Code: 4
Quality Code: 1
Comments: n